



TECHNISCHE
UNIVERSITÄT
DARMSTADT

*Many-Body Perturbation Theory for Ab
Initio Nuclear Structure*

Vielteilchenstörtheorie in der Ab Initio Kernstrukturphysik

VOM FACHBEREICH PHYSIK
DER TECHNISCHEN UNIVERSITÄT DARMSTADT

ZUR ERLANGUNG DES GRADES
EINES DOKTORS DER NATURWISSENSCHAFTEN
(DR. RER. NAT.)

GENEHMIGTE DISSERTATION VON
ALEXANDER TICHAI, M.SC.
GEBOREN IN DARMSTADT

DARMSTADT 2017
D17

Many-Body Perturbation Theory for *Ab Initio* Nuclear Structure

Vielteilchenstörtheorie in der *Ab Initio* Kernstrukturphysik

Genehmigte Dissertation von Alexander Tichai, geboren in Darmstadt.

Referent: Prof. Dr. Robert Roth

Korreferent: Prof. Dr. Jens Braun

Tag der Einreichung: 18.07.2017

Tag der Prüfung: 30.10.2017

2017 – Darmstadt – D17

Please cite this work as:

URN: urn:nbn:de:tuda-tuprints-69424

URL: <http://tuprints.ulb.tu-darmstadt.de/69424>

This document is provided by tuprints,

<http://tuprints.ulb.tu-darmstadt.de/>



This work is licensed under a Creative Commons [BY-NC-ND 4.0 International](https://creativecommons.org/licenses/by-nc-nd/4.0/) license.

Visit <https://creativecommons.org/licenses/> for more information.

© 2017 - *Alexander Tichai*

ALL RIGHTS RESERVED.

Many-Body Perturbation Theory for *Ab Initio* Nuclear Structure

ABSTRACT

The solution of the quantum many-body problem for medium-mass nuclei using realistic nuclear interactions poses a superbe challenge for nuclear structure research. Because an exact solution can only be provided for the lightest nuclei, one has to rely on approximate solutions when proceeding to heavier systems. Over the past years, tremendous progress has been made in the development and application of systematically improvable expansion methods and an accurate description of nuclear observables has become viable up to mass number $A \approx 100$. While closed-shell systems are consistently described via a plethora of different many-body methods, the extension to genuine open-shell systems still remains a major challenge and up to now there is no *ab initio* many-body method which applies equally well to systems with even and odd mass numbers.

The goal of this thesis is the development and implementation of innovative perturbative approaches with genuine open-shell capabilities. This requires the extension of well-known single-reference approaches to more general vacua. In this work we choose two complementary routes for the usage of generalized reference states.

First, we derive a new *ab initio* approach based on multi-configurational reference states that are conveniently derived from a prior no-core shell model calculation. Perturbative corrections are derived via second-order many-body perturbation theory, thus, merging configuration interaction and many-body perturbation theory. The generality of this ansatz enables for a treatment of medium-mass systems with arbitrary mass number, as well as the extension to low-lying excited states such that ground and excited states are treated on an equal footing.

In a complementary approach, we use reference states that break a symmetry of the underlying Hamiltonian. In the simplest case this corresponds to the expansion around a particle-number-broken Hartree-Fock-Bogoliubov vacuum which is obtained from a mean-field calculation. Pairing correlations are already absorbed in the reference state. The mild scaling allows for investigations up to tin isotopic chains.

All benchmarks were performed using state-of-the-art chiral two- plus three-nucleon interactions thus allowing for a universal description of nuclear observables in the medium-mass regime.

Vielteilchenstörtheorie in der Ab Initio Kernstrukturphysik

ZUSAMMENFASSUNG

Die Lösung des quantenmechanischen Vielteilchenproblems für mittelschwere Kerne mittels realistischer nuklearer Wechselwirkungen stellt die moderne Kernstrukturphysik vor eine große Herausforderung. Da eine exakte Lösung nur für sehr leichte Systeme möglich ist, werden für schwerere Systeme approximate Lösungsverfahren angewandt. Innerhalb der letzten Jahre sind große Fortschritte in der Entwicklung solcher Näherungsverfahren erzielt worden und eine präzise Beschreibung von Kernstrukturobservablen bis hin zu Massenzahlen $A = 100$ wurde ermöglicht. Obwohl für Kerne mit Schalenabschlüssen eine Vielzahl verschiedener Vielteilchenmethoden existieren, ist die Erweiterung solcher Methoden auf Systeme fernab von Schalenabschlüssen noch immer eine große Herausforderung. Insbesondere existiert keine *ab initio* Methode, die auf mittelschwere Systeme mit gerader und ungerader Massenzahl angewendet werden kann.

Das Ziel dieser Arbeit ist die Entwicklung und Implementierung innovativer störungstheoretischer Methoden, die auf beliebige mittelschwere Kerne angewendet werden können. Dies setzt insbesondere die Erweiterung auf allgemeinere Referenzzustände voraus, die keine einfachen Slaterdeterminanten sind. In dieser Arbeit zeigen wir zwei verschiedene Lösungsansätze auf.

Wir führen eine neuartige *ab initio* Methode ein, bei welcher störungstheoretische Korrekturen bezüglich eines Multi-Determinanten-Zustands bestimmt werden. Solche Referenzzustände können mit Hilfe des No-Core Schalenmodells konstruiert werden. Dies erlaubt die Bestimmung von korrelierten Grundzustands- und Anregungsenergien für Systeme mit gerader und ungerader Massenzahl.

Ein ergänzender Ansatz besteht in der Verwendung Symmetrie-gebrochener Referenzzustände. Im einfachsten Fall führt das auf Teilchenzahl-gebrochene Hartree-Fock-Bogoliubov-Vakua, die aus einer vorherigen Lösung eines effektiven Einteilchenproblems bestimmt werden. Dabei werden Pairing-Korrelationen bereits in den Referenzzustand absorbiert. Aufgrund des moderaten Skalierungsverhaltens können hierbei Grundzustandsenergien bis hin zu schweren Zinn-Isotopen berechnet werden.

Alle Berechnungen in dieser Arbeit wurden mit modernen chiralen Zwei- plus Drei-Nukleonen-Wechselwirkungen durchgeführt. Dies erlaubt eine universelle Beschreibung von Kernstrukturobservablen bis hin zu mittelschweren Kernen.

Contents

INTRODUCTION	v
I Basics	1
1 PRELIMINARIES	3
1.1 Single-particle basis and model-space truncations	3
1.2 Angular-momentum coupling	4
1.3 Particle-hole formalism	8
1.4 Normal ordering	8
2 THE NUCLEAR HAMILTONIAN	15
2.1 Empirical properties	15
2.2 Phenomenological potentials	16
2.3 Chiral effective field theory	16
3 SIMILARITY RENORMALIZATION GROUP	19
3.1 Flow equation	19
3.2 Choice of generator	20
3.3 Cluster decomposition	21
3.4 Types of interactions	23
II Single-Configurational Many-Body Perturbation Theory	25
4 HARTREE-FOCK THEORY	29
4.1 Variational principle and testspace	29
4.2 Derivation of the Hartree-Fock equations	30
4.3 Brillouin's theorem	33
5 FORMAL PERTURBATION THEORY	35
5.1 The perturbative ansatz	35
5.2 Derivation of the resolvent expansion	38
5.3 Partitioning of the Hamiltonian	42
5.4 The normal-product Schrödinger equation	43

5.5	Diagrammatic representation	44
5.6	Remarks and further reading	48
6	SINGLE-CONFIGURATIONAL MANY-BODY PERTURBATION THEORY	51
6.1	Derivation of low-order formulas	51
6.2	Angular-momentum coupling	53
6.3	Computational considerations	56
6.4	Limitations of single-reference theories	59
7	COUPLED CLUSTER THEORY	61
7.1	The Exponential Ansatz	61
7.2	Similarity-Transformed Hamiltonian	62
7.3	Truncation of the Cluster Operator	64
7.4	Connections to perturbation theory	64
8	GROUND-STATE ENERGIES OF CLOSED-SHELL SYSTEMS	67
8.1	Impact of partitioning	67
8.2	SRG dependence	70
8.3	Low-order energy corrections	73
8.4	Anatomy of the third-order energy correction	76
III	Perturbatively-Enhanced No-Core Shell Model	79
9	CONFIGURATION INTERACTION	83
9.1	Full Configuration Interaction	83
9.2	Truncated Configuration Interaction	84
9.3	No-Core Shell Model	86
9.4	Importance-Truncated No-Core Shell Model	87
10	MULTI-CONFIGURATIONAL PERTURBATION THEORY	89
10.1	Definition of Partitioning	89
10.2	Derivation of low-order corrections	92
10.3	Merging MCPT and NCSM	103
11	AUTOMATED CODE GENERATION	105
11.1	Encoding diagrams as graphs	105
11.2	Derivation of perturbative formulas	110
11.3	Further Extensions	113

12	OPEN-SHELL GROUND STATES AND SPECTRA	115
12.1	Convergence behavior in NCSM-PT	115
12.2	Second-order NCSM-PT for ground-state energies of isotopic chains	116
12.3	Excitation spectra	119
12.4	C_{\min}^2 truncation	121
12.5	Dependence on the oscillator frequency	123
12.6	NCSM-PT with Hartree-Fock basis	125
IV	Symmetry-Broken Many-Body Perturbation Theory	129
13	HARTREE-FOCK-BOGOLIUBOV THEORY	133
13.1	Bogoliubov algebra	133
13.2	The Hartree-Fock-Bogoliubov equations	135
13.3	The canonical basis	136
13.4	The intrinsic Hamiltonian	138
14	BOGOLIUBOV MANY-BODY PERTURBATION THEORY	139
14.1	The symmetry group $U(1)$	140
14.2	Time-dependent formalism	141
14.3	Normal-ordering with respect to the HFB vacuum	144
14.4	Unperturbed system	146
14.5	Perturbative expansion of operator kernels	147
14.6	Extraction of diagrammatic rules	150
14.7	Diagrammatic treatment	154
14.8	Exponentiation of connected diagrams	155
14.9	Second-order correction to the norm kernel	156
14.10	Norm kernel and correlation energy	156
14.11	Perturbative expansion of generic operator kernels	157
14.12	Monitoring symmetry breaking	160
14.13	Implementation	162
14.14	Spherical symmetry	163
15	TOWARDS CORRELATED ENERGY DENSITY FUNCTIONAL KERNELS	165
15.1	Basic elements of group theory	165
15.2	Off-diagonal kernels	166
15.3	Effective-Hamiltonian kernels	168
15.4	Single-reference EDF	168
15.5	Multi-reference EDF	170
15.6	Pathologies in MR applications	171

15.7	EDF kernels from <i>ab initio</i> theory	172
16	MEDIUM-MASS SEMI-MAGIC ISOTOPIC CHAINS	175
16.1	Oxygen isotopes	175
16.2	Calcium isotopes	177
16.3	Nickel isotopes	178
16.4	Tin isotopes	179
16.5	Pairing properties	181
16.6	Computational scaling	181
	SUMMARY AND OUTLOOK	183
	Appendices	191
A	SPHERICAL HARTREE-FOCK MANY-BODY PERTURBATION THEORY	193
A.1	The particle-particle channel	193
A.2	The hole-hole channel	194
A.3	The particle-hole channel	194
B	INTEGRAL IDENTITIES	199
C	NORMAL-ORDERED MATRIX ELEMENTS	201
C.1	Generic operator \hat{O}	201
C.2	Grand canonical potential $\hat{\Omega}$	203
C.3	Hamiltonian operator \hat{H}	204
C.4	Particle-number operator \hat{A}	204
C.5	\hat{A}^2 operator	205
D	UNPERTURBED PROPAGATOR	207
E	SPHERICAL BOGOLIUBOV MANY-BODY PERTURBATION THEORY	211
E.1	Spherical Hartree-Fock-Bogoliubov theory	211
E.2	Angular-momentum coupling of quasiparticle operators	213
E.3	Cross coupling of matrix elements	215
E.4	Particle-number operator	236
E.5	Particle-number variance operator	237
E.6	Second-order corrections for operators	237
E.7	Third-order particle-number correction	238

LIST OF ACRONYMS

Introduction

Quantum Chromodynamics (QCD) is the fundamental theory of the strong interaction within the Standard Model of Particle Physics. QCD describes the interaction of quarks and gluons. Due to asymptotic freedom QCD can be handled by means of perturbation theory at high energies. The validity of a perturbative treatment breaks down in the low-energy regime of nuclear structure physics requiring a non-perturbative approach. Moreover, it is well established that physical bound states only consists of color-neutral objects—the baryons and mesons. Thus the lightest particles, being nucleons and pions are the relevant degrees of freedom for an *effective theory* of the strong interaction valid in the regime of nuclear structure. Over the past 20 years the development of *chiral effective field theory* (EFT) established the most consistent approach for the formulation of an effective theory of the strong interaction [EM03; EHM09].

When solving the quantum many-body problem, i.e., solving the stationary Schrödinger equation for a realistic nuclear Hamiltonian using basis-expansion methods, one faces the problem that these interactions exhibit very slow convergence with respect to model-space size. This effect is due to the strong short-range repulsion and tensor interactions. Such interactions induce a strong coupling between high and low momenta, yielding a strongly off-diagonal matrix in momentum representation of the Hamiltonian. Even though converged results can be obtained for the lightest nuclei up to mass number $A \approx 12$, e.g., in a No-Core Shell Model (NCSM) framework [Nav⁺09; Rot⁺11; BNV13], medium-mass systems require the use of different approaches.

In the past, several schemes have been proposed to overcome this difficulties by deriving 'softened' effective interactions, which preserve the low-energy phase shift and deuteron properties the initial interaction was fitted to. The presently most commonly used approach is the Similarity Renormalization Group (SRG) which uses a unitary transformation to tame the strong short-range repulsion and tensor correlation parts [BFP07; HR07; RRH08]. Unitarity of the transformation formally guarantees preservation of physical quantities. It is has been shown in numerous investigations that the use of SRG-transformed Hamiltonians strongly improves model-space convergence and gives a suppression of the aforementioned coupling of low- and high-momentum states.

The use of these renormalized interactions enables for the solution of the stationary Schrödinger equation for heavier systems. For the solution of the quantum many-body problem in a controllable way one desires the following key property:

An *ab initio* many-body method has a systematically improvable expansion

which—given a fixed Hamiltonian—reproduces the exact nuclear observable in a well-defined limit.

Fifteen years ago, *ab initio* calculations were limited to very light nuclei using diagonalization techniques, such as the NCSM, or Green’s function Monte Carlo techniques (GFMC) [Pud⁺97; PW01]. In the NCSM, for example, one builds from a given single-particle basis all many-body states up to a given model-space size and diagonalizes the matrix representation of the Hamiltonian via Lanczos techniques. Other than working with a finite basis set, the method is exact in the sense that the exact eigensystem is obtained in the limit where N_{\max} tends to infinity. A common feature of exact many-body methods is the *curse of dimensionality*, which reflects the fact that the size of the corresponding many-body basis grows factorially with the size of the single-particle basis. The range of applicability is limited to rather light nuclei, even though there exist extensions that enable calculations up to the oxygen dripline, e.g., the Importance-Truncated No-Core Shell Model (IT-NCSM). However, when proceeding to heavier systems one must adapt a different strategy.

The first investigations of medium-mass nuclei made use of independent-particle models such as the HF approximation and were restricted to ground-state energies of *closed-shell nuclei*, where all shells are either fully occupied or unoccupied. Typically, ground-state wave functions of closed-shell nuclei are dominated by a single Slater determinant such that the HF model constitutes a good initial approximation. In more sophisticated many-body approaches, the HF determinant is, therefore, used as a reference state for a properly designed correlation expansion, e.g., via many-body perturbation theory or coupled-cluster theory. A key feature of these methods is a *systematic expansion* of correlation effects available with a well-defined limit in which the expansion becomes exact. In actual applications these expansions are truncated, inducing a systematic error that can be *controlled* and systematically improved in accord with the *ab initio* philosophy. However, improved the accuracy simultaneously requires larger computational effort.

Such many-body techniques have a long history in nuclear structure and quantum chemistry but are also applied in other areas of physics such as solid state physics. In particular, in quantum chemistry Many-Body Perturbation Theory (MBPT) [Sch26; SB09; SO82] and Coupled-Cluster (CC) theory have been successfully applied for almost 60 years. A decade ago CC theory has been applied to the calculation of ground-state energy of closed-shell nuclei by using a HF reference determinant [DH04; BM07; Hag⁺10; Kow⁺04; PGW09; Bin⁺14; Bin14]. In the following years other alternatives such as Self-Consistent Green’s function (SCGF) [DB04; CBN13] and In-Medium Similarity Renormalization Group (IM-SRG) [Her⁺13; TBS11; MPB15; Her14; Her⁺16] were developed. The *ab initio* community started to create a versatile toolbox of different many-body approaches that consistently describe medium-mass systems with $20 \lesssim A \lesssim 100$.

From experiment, we know of roughly 3000 nuclei today. However, only a few ten of them are closed-shell nuclei and can be described by the techniques mentioned above. The vast majority are so-called *open-shell* nuclei. First attempts to extend the range of many-body techniques into the open-shell region made use of equation-of-motion (EOM) techniques. Here one starts with a correlated wave function of a neighboring closed-shell nucleus and describes the target system via the action of particle creators/annihilators with respect to a state of different particle number. This has been successfully applied in the CC context to the calculation of open-shell system in the vicinity of shell closures [PGW09]. An EOM-extension of IM-SRG for the description of spectra of closed-shell nuclei was proposed very recently [PMB16]. However, the complexity of the formalism as well as computational considerations restrict their use to targeting systems which differ at most by two particles from the closed-shell reference. Thus, it does not provide a universal approach for solving the many-body problem for open-shell systems.

Another attempt for describing open-shell nuclei made use of effective interactions, where single-particle states are classified into core, valence and virtual states. The core states define the reference determinant which typically is a HF determinant with lower particle number than the target system. One then defines a valence space where correlation effects of virtual states are summed into the effective interaction. Subsequently the effective Hamiltonian is diagonalized in the valence space thus yielding the low-lying spectrum. This defines the *shell model*. Initially, shell-model interactions were developed in MBPT, but non-perturbative approaches for deriving valence-space interactions followed in the CC [Jan⁺14] and IM-SRG [Bog⁺14] frameworks. This enabled, for the first time, to calculate spectra of open-shell medium-mass nuclei. There are, however, several questions which need to be addressed. First of all, one always assumes an inert core. In nuclei which have a complicated structure this choice might be inappropriate. Furthermore, opening up large shells leads to a very large valence spaces which makes the subsequent diagonalization computationally demanding. Additionally, in the past years significant effort was spent in the derivation of effective interactions which include several major shells (so-called multi-shell approaches). The inclusion of several major shells yields a pronounced shell gap within the valence space which lead to results that heavily depend on the particular orbits which are included in the valence space. Till now this problem has not been solved in a satisfactory way.

The aforementioned approaches provide solutions to the open-shell many-body problem in a certain regime, where either the target system is near a shell closure or a properly designed valence space can be identified with a pronounced shell gap between core, valence and virtual single-particle states. Both frameworks, however, yield no generic solution for an arbitrary open-shell systems far away from shell closures and high degrees of degeneracy. It has been recognized that more general reference states, other than a HF determinant, are necessary to describe genuine open-shell systems, where the corresponding wave function

is not dominated by a single many-body configuration. In general, correlation effects can be distinguished into *static correlations* and *dynamic correlations*. Static correlations are a collective phenomenon, that is related to the fact that several determinants contribute significantly to an eigenvector of the Hamiltonian. Dynamic correlations, on the other hand, are related to the formation of nucleonic pairs, triplets, quadruplets and so on. Typically, dynamic correlations are accounted for via the correlation expansion, e.g., perturbative corrections in MBPT or the solution of the amplitude equations in CC. Static correlation effects require high excitation rank in a particle-hole picture, which is the natural framework for single-reference many-body methods. However, the appearance of these highly-excited states is strongly-suppressed in the correlation expansion and one has to include high-order effects, which typically are computationally too demanding. Therefore, one aims at incorporating static-correlation effects already at the level of the reference state. If the wave function of a target system is not dominated by a single Slater determinant, static correlations play an important role. Since by construction the HF approximation does not include correlations, a single-reference treatment either fails or requires a high degree of sophistication, i.e., relaxation of the truncation parameter in the many-body method.

The extension to more general reference states can be performed in two directions: either one uses reference states of *multi-configurational* character, i.e., the reference state itself is a superposition of several Slater determinants or one uses a *symmetry-broken* reference state, i.e., the reference states breaks a symmetry of the underlying Hamiltonian. The aim of this thesis is the extension of many-body perturbation theory to genuine open-shell systems. Both of the above options are investigated.

Multi-configurational reference states can be obtained from NCSM calculations in small model spaces. In particular this allows for describing complex collective effects at the zeroth-order description [RSS03; SSK04]. Multi-configurational states have successfully been incorporated in the multi-reference version of IM-SRG (MR-IM-SRG) which enabled, for the first, time the investigation of long isotopic chains up to the driplines from an *ab initio* perspective [Her14]. Analogously, one can extend the MBPT treatment also to NCSM reference states defining a novel *ab initio* approach which uses systematically improvable reference states and incorporates residual correlation effects perturbatively [TGR17]. The generality of this ansatz allows—for the first time in *ab initio* nuclear structure theory—to treat even and odd nuclei on equal footing in a medium-mass no-core approach.

While the concept of symmetry-breaking has a long tradition in other fields, e.g., energy density functional theory (EDF) or condensed matter physics, it has only scarcely been applied in the *ab initio* context. The basic idea is to let the reference state break a symmetry of the underlying Hamiltonian. In the simplest case this corresponds to using a particle-number non-conserving reference state, which can for example arise from the solution of the Hartree-Fock-Bogoliubov (HFB) equation and, therefore, corresponds to a violation of global

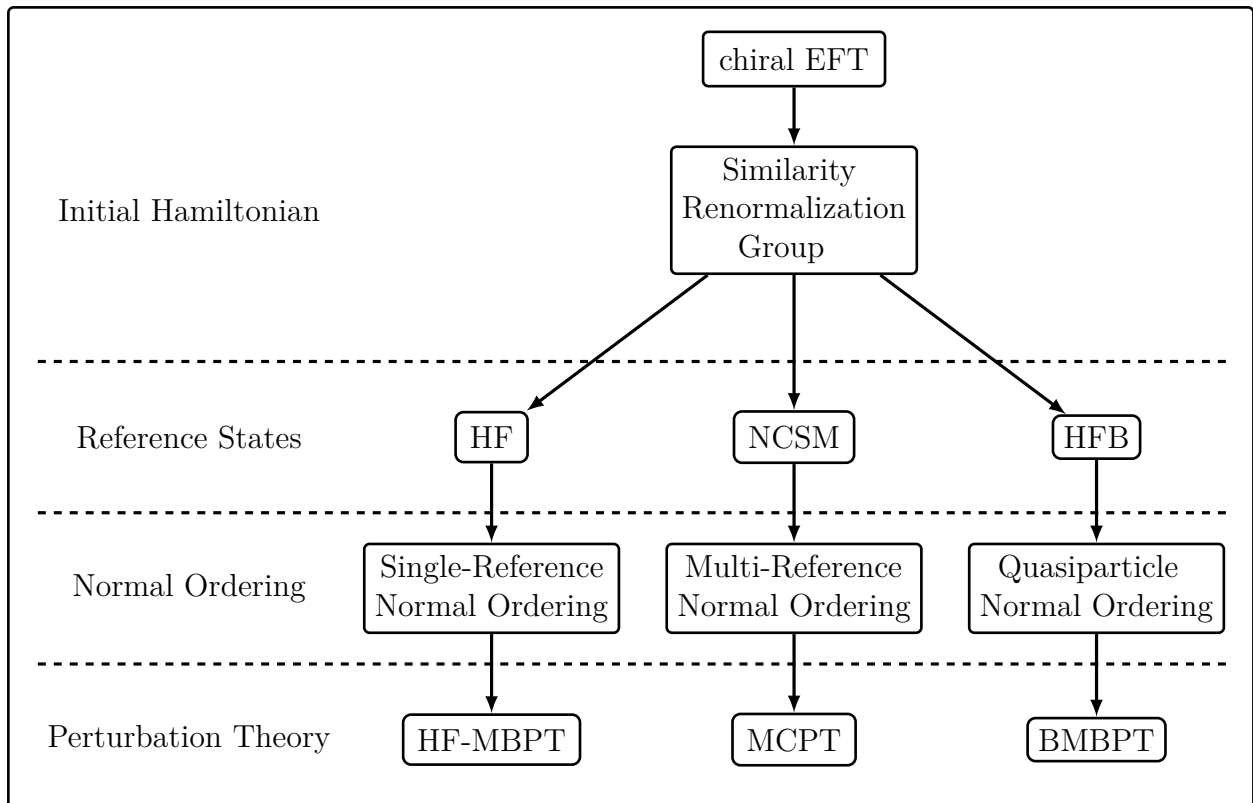


Figure 1: Schematic overview over the methods used for the solution of the quantum many-body problem.

$U(1)$ gauge symmetry. In the HFB scheme one can explicitly account for pairing correlations by going to a quasiparticle description, where particle-particle, hole-hole and particle-hole excitations are treated equally. Such reference states have only recently been adopted in the CC framework [Dug14]. The application to other—possibly non-abelian—symmetry groups, e.g., the breaking of $SU(2)$ and the corresponding violation of angular-momentum conservation, are under investigation.

For finite nuclei, the restoration of the broken symmetry is mandatory. This step, however, needs to be postponed to the future and to our knowledge there has been no implementation of a symmetry-broken many-body method that consistently restores the symmetry beyond the mean-field level, even though the theory is worked out on a formal level [DS16].

Although the entire work of this thesis is dedicated to the development and extension of innovative *ab initio* many-body techniques, one should keep in mind that plenty of additional work is necessary for the solution of the many-body problem for medium-mass nuclei. Figure 1 serves as a reminder of the individual aspects this thesis.

The structure of this work is as follows. This thesis is divided into four major parts. Part I is dedicated to the introduction of the nuclear Hamiltonian and the presentation of supplementary material needed later. In Part II we discuss single-configurational MBPT and its application to closed-shell nuclei. In Part III we introduce a multi-configurational

version of MBPT capable of describing genuine medium-mass open-shell systems via using NCSM reference states as zero-order input. Part IV is dedicated to symmetry-broken MBPT, where a particle-number-broken HFB vacuum is used as reference state for the correlation expansion. Parts II, III and IV have an introductory section, respectively, which displays the structure of the individual parts.

A number of technical derivations necessary for the implementations are gathered in the appendix.

Figure 1 gives a schematic overview of the content of this thesis and the workflow starting from chiral EFT to the approximate solution of the Schrödinger equation in a many-body framework.

PART I



BASICS

1

Preliminaries

The goal of the section is to provide the basic material that is necessary to follow the later derivations as well as to fix notations. This section includes a discussion of the single-particle basis used in the implementation as well as the different model-space truncation schemes, which will be applied subsequently. Furthermore, we introduce definitions of angular-momentum coupled quantities, the particle-hole formalism, and give an introduction to normal-ordering.

1.1 SINGLE-PARTICLE BASIS AND MODEL-SPACE TRUNCATIONS

We start with the definition of the single-particle basis. A general basis state $|k\rangle$ is written as

$$|k\rangle \equiv |n_k, j_k, l_k, t_k, m_k\rangle \equiv |n_k(l_k \frac{1}{2})j_k m_k, (\frac{1}{2}t_k)\rangle \quad (1.1)$$

where n_k denotes the radial quantum number, j_k the total angular momentum quantum number, l_k orbital angular momentum quantum number, t_k the isospin projection and m_k the total angular momentum projection. Furthermore, nucleons have spin $s_k = \frac{1}{2}$ and isospin quantum number $\tau_k = \frac{1}{2}$ which will be suppressed in the following.

In typical calculations the reference basis is constructed from the eigenstates of the spherical harmonic-oscillator (HO) Hamiltonian

$$\hat{H}_{\text{HO}} = \frac{\hat{p}^2}{2m} + \frac{1}{2}m\Omega^2 \hat{r}^2 \quad (1.2)$$

with m being the nucleon mass and Ω the *oscillator frequency* fixing the width of the HO potential. The eigenenergies, characterized by the n_k and l_k quantum numbers,

$$\epsilon_k = \left(2n_k + l_k + \frac{3}{2}\right) \hbar\Omega \quad (1.3)$$

coincide for proton and neutrons single-particle states. We further introduce the *principal quantum number*

$$e_k = (2n_k + l_k), \quad (1.4)$$

which fully defines the energy eigenvalue.

In actual applications the single-particle basis must be truncated to finite size for computational reasons. We define the *e_{\max} -truncated single-particle space*

$$V_{e_{\max}} \equiv \{|k\rangle \in \mathcal{H}_1 : e_k \leq e_{\max}\}, \quad (1.5)$$

that contains all single-particle states with principal quantum numbers up to e_{\max} , where \mathcal{H}_1 denotes the infinite-dimensional one-body Hilbert space.

When including three-body forces the typical number of matrix elements becomes intractable when using a single-particle truncation only. Therefore, one introduces a collective three-body truncation $E_{3\max}$ defined by

$$e_1 + e_2 + e_3 \leq E_{3\max} \quad (1.6)$$

and discards all three-body matrix elements where the sum of the principal quantum numbers of bra or ket states exceeds $E_{3\max}$.

For many-body methods such as the no-core shell model a mere single-particle truncation is prohibitive. Therefore, one introduces the so-called *N_{\max} -truncation scheme*. Given an A -body Slater determinant (SD) $|\psi\rangle$ one includes all many-body configurations $|\psi_I\rangle$ in the many-body basis for which the sum of HO excitation quanta does not exceed a given value of N_{\max} . We note that the number of single-particle orbitals in e_{\max} -truncated model spaces is independent of the considered nucleus while the number of many-body configurations in an N_{\max} -truncated model space does depend on the target system.

1.2 ANGULAR-MOMENTUM COUPLING

Even though large parts of this work are implemented in an m -scheme basis, it can be important to make use of symmetry properties of the Hamiltonian and transfer the implementation to an angular-momentum-coupled scheme.

Consider two different particles with corresponding angular-momentum vectors $\hat{\mathbf{J}}_1$ and $\hat{\mathbf{J}}_2$.¹ Then

¹A quantity $\hat{\mathbf{J}}$ is called *angular-momentum vector* if its components satisfy

$$[\hat{J}_{1k}, \hat{J}_{2l}] = 0 \text{ for all } k, l = 1, 2, 3, \quad (1.8)$$

where the indices k, l refer to the Cartesian coordinates. The angular-momentum operators have eigenstates satisfying

$$\hat{\mathbf{J}}_n^2 |j_n m_n\rangle = j_n(j_n + 1)\hbar^2 |j_n m_n\rangle, \quad (1.9)$$

$$\hat{J}_{nz} |j_n m_n\rangle = m_n \hbar |j_n m_n\rangle. \quad (1.10)$$

The corresponding eigenvector of $\hat{\mathbf{J}}_1 + \hat{\mathbf{J}}_2$ is given by the product of the eigenvectors of $\hat{\mathbf{J}}_1$ and $\hat{\mathbf{J}}_2$, respectively,

$$|j_1 m_1 j_2 m_2\rangle \equiv |j_1 m_1\rangle \otimes |j_2 m_2\rangle, \quad (1.11)$$

where \otimes denotes the tensor product of two single-particle states.

The states defined in (1.11) are eigenstates of the maximum set of commuting operators

$$\{\hat{\mathbf{J}}_1^2, \hat{J}_{1z}, \hat{\mathbf{J}}_2^2, \hat{J}_{2z}\}. \quad (1.12)$$

We call the set of states $\{|j_1 m_1 j_2 m_2\rangle\}$ the *uncoupled basis*. We further define *anti-symmetrized two-body states* by

$$|j_1 m_1 j_2 m_2\rangle_a \equiv \frac{1}{\sqrt{2}}(|j_1 m_1 j_2 m_2\rangle - |j_2 m_2 j_1 m_1\rangle). \quad (1.13)$$

For the exchange of the two-particle state we get

$$|j_1 m_1 j_2 m_2\rangle_a = -|j_2 m_2 j_1 m_1\rangle_a, \quad (1.14)$$

according to the Pauli principle.

One can show that the sum $\hat{\mathbf{J}} = \hat{\mathbf{J}}_1 + \hat{\mathbf{J}}_2$ also is an angular-momentum vector in the above sense. Equally, one can couple the angular momenta of the two particles. The coupled momentum $\hat{\mathbf{J}}^2$ is contained in the complete set of pairwise commuting operators

$$\{\hat{\mathbf{J}}_1^2, \hat{\mathbf{J}}_2^2, \hat{\mathbf{J}}^2, \hat{J}_z\}. \quad (1.15)$$

The complete set of states $\{|j_1 j_2 JM\rangle\}$ defines the *coupled basis*. We get for exchanging the total angular momenta

$$\hat{J}_k^\dagger = \hat{J}_k, \quad \text{for } k = 1, 2, 3 \quad \text{and} \quad [\hat{J}_i, \hat{J}_j] = i\hbar \sum_k \epsilon_{ijk} \hat{J}_k, \quad (1.7)$$

where ϵ_{ijk} denotes the totally anti-symmetric Levi-Civita tensor.

$$|(j_1 j_2) JM\rangle_a = (-1)^{j_1+j_2-J} |(j_2 j_1) JM\rangle_a. \quad (1.16)$$

COUPLING SYMBOLS

Since, both, the coupled and uncoupled basis form a complete set of states one can transform one basis into the other. Inserting a resolution of the identity with respect to the uncoupled basis gives

$$|(j_1 j_2) JM\rangle = \sum_{m_1 m_2} |j_1 m_1 j_2 m_2\rangle \langle j_1 m_1 j_2 m_2 | (j_1 j_2) JM\rangle. \quad (1.17)$$

The overlap

$$\begin{pmatrix} j_1 & j_2 & J \\ m_1 & m_2 & M \end{pmatrix} \equiv \langle j_1 m_1 j_2 m_2 | (j_1 j_2) JM\rangle \quad (1.18)$$

defines the so-called *Clebsch-Gordan (CG) coefficient*.

There are several important relations for the CGs. The most important ones being the *orthogonality* and *completeness relations*

$$\sum_{m_1 m_2} \begin{pmatrix} j_1 & j_2 & J \\ m_1 & m_2 & M \end{pmatrix} \begin{pmatrix} j_1 & j_2 & J' \\ m_1 & m_2 & M' \end{pmatrix} = \delta_{JJ'} \delta_{MM'}, \quad (1.19)$$

$$\sum_{JM} \begin{pmatrix} j_1 & j_2 & J \\ m_1 & m_2 & M \end{pmatrix} \begin{pmatrix} j_1 & j_2 & J \\ m_1' & m_2' & M \end{pmatrix} = \delta_{m_1 m_1'} \delta_{m_2 m_2'}. \quad (1.20)$$

Sometimes it is more convenient to use the so-called *Wigner 3j-symbol*

$$\begin{pmatrix} j_1 & j_2 & J \\ m_1 & m_2 & M \end{pmatrix} \equiv (-1)^{j_1-j_2-M} \hat{j}^{-1} \begin{pmatrix} j_1 & j_2 & J \\ m_1 & m_2 & M \end{pmatrix}_{\mathbf{3j}}, \quad (1.21)$$

where we introduced the *hat-symbol*²

$$\hat{J} \equiv \sqrt{2J+1}. \quad (1.22)$$

By means of the above Wigner 3j-symbols we further define the so-called *Wigner 6j-symbol*

$$\begin{aligned} \begin{Bmatrix} j_1 & j_2 & j_{12} \\ j_3 & j & j_{23} \end{Bmatrix} &\equiv \sum_{\substack{m_1 m_2 m_3 \\ m_{12} m_{23}}} (-1)^{j_3+j+j_{23}-m_3-m-m_{23}} \begin{pmatrix} j_1 & j_2 & j_{12} \\ m_1 & m_2 & m_{12} \end{pmatrix}_{\mathbf{3j}} \\ &\times \begin{pmatrix} j_1 & j & j_{23} \\ m_1 & -m & m_{23} \end{pmatrix}_{\mathbf{3j}} \begin{pmatrix} j_3 & j_2 & j_{23} \\ m_3 & m_2 & -m_{23} \end{pmatrix}_{\mathbf{3j}} \begin{pmatrix} j_3 & j & j_{12} \\ -m_3 & m & m_{12} \end{pmatrix}_{\mathbf{3j}} \end{aligned} \quad (1.23)$$

²The hat does *not* indicate an operator in this context.

which arises naturally in the coupling of three angular momenta and will be needed frequently in the coupling of matrix elements in appendix E.

For a discussion of symmetries and additional relations of the above introduced coupling symbols see, e.g., the extensive treatment in the book of Varshalovic, Moskalev and Khersonskii [VMK88].

MATRIX ELEMENTS

We define *anti-symmetrized matrix elements* of a generic Hermitian two-body operator \hat{O} written in m -scheme as

$$O_{k_1 k_2 k_3 k_4} \equiv {}_a \langle n_{k_1} l_{k_1} j_{k_1} t_{k_1} m_{k_1} n_{k_2} l_{k_2} j_{k_2} t_{k_2} m_{k_2} | \hat{O} | n_{k_3} l_{k_3} j_{k_3} t_{k_3} m_{k_3} n_{k_4} l_{k_4} j_{k_4} t_{k_4} m_{k_4} \rangle_a. \quad (1.24)$$

Note that, by Hermiticity, matrix elements are anti-symmetric with respect to exchange of bra single-particle states as well

$$\bar{O}_{k_1 k_2 k_3 k_4} = \bar{O}_{k_3 k_4 k_1 k_2} = -\bar{O}_{k_3 k_4 k_2 k_1} = -\bar{O}_{k_2 k_1 k_3 k_4}. \quad (1.25)$$

Using the definition of the two-body states in coupled basis we define

$$O_{\tilde{k}_1 \tilde{k}_2 J M; \tilde{k}_3 \tilde{k}_4 J' M'} \equiv \sum_{\substack{m_{k_1} m_{k_2} \\ m_{k_3} m_{k_4}}} \begin{pmatrix} j_{k_1} & j_{k_2} \\ m_{k_1} & m_{k_2} \end{pmatrix} \begin{pmatrix} J \\ M \end{pmatrix} \begin{pmatrix} j_{k_3} & j_{k_4} \\ m_{k_3} & m_{k_4} \end{pmatrix} \begin{pmatrix} J' \\ M' \end{pmatrix} \bar{O}_{k_1 k_2 k_3 k_4}, \quad (1.26)$$

where we introduce the *Baranger notation*

$$\tilde{k} \equiv (n_k, l_k, j_k, t_k) \quad (1.27)$$

which keeps all quantum numbers other than the angular momentum projection m_k . The above normalization constants are due to using anti-symmetrized two-particle states.

Conversely, we get for the transformation from the coupled to the uncoupled basis

$$\bar{O}_{k_1 k_2 k_3 k_4} = \sum_{J J'} \sum_{M M'} \begin{pmatrix} j_{k_1} & j_{k_2} \\ m_{k_1} & m_{k_2} \end{pmatrix} \begin{pmatrix} J \\ M \end{pmatrix} \begin{pmatrix} j_{k_3} & j_{k_4} \\ m_{k_3} & m_{k_4} \end{pmatrix} \begin{pmatrix} J' \\ M' \end{pmatrix} O_{\tilde{k}_1 \tilde{k}_2 J M; \tilde{k}_3 \tilde{k}_4 J' M'}. \quad (1.28)$$

We note that both (1.26) and (1.28) carry an additional prefactor that accounts for the correct normalization. However, since both prefactors cancel each other when performing the angular-momentum coupling, we will suppress them for the sake of simplicity.

Since nuclear potentials are rotationally invariant they do not depend on M or M' and are non-zero only if $J = J'$. Therefore, if the operator \hat{O} corresponds to the nuclear Hamiltonian $\hat{H}^{[2]}$ we get the J -coupled matrix elements

$$H_{\tilde{k}_1\tilde{k}_2JM;\tilde{k}_3\tilde{k}_4J'M'}^{[2]} \equiv \delta_{JJ'}\delta_{MM'}^J H_{\tilde{k}_1\tilde{k}_2\tilde{k}_3\tilde{k}_4}^{[2]}. \quad (1.29)$$

1.3 PARTICLE-HOLE FORMALISM

Several many-body approaches are conveniently formulated with respect to a reference Slater determinant $|\Phi\rangle$ instead of the physical vacuum $|0\rangle$,

$$|\Phi\rangle = |k_1k_2\cdots k_N\rangle_a \equiv \hat{c}_{k_1}^\dagger \hat{c}_{k_2}^\dagger \cdots \hat{c}_{k_N}^\dagger |0\rangle. \quad (1.30)$$

where \hat{c}_k^\dagger denotes a *single-particle creation operator*. Analogously we define *single-particle annihilation operators* \hat{c}_k by

$$\hat{c}_k |0\rangle = 0 \quad (1.31)$$

Other Slater determinants are then constructed with respect to the reference $|\Phi\rangle$ via the action of particle creation and annihilation operators

$$\begin{aligned} |\Phi_{i_1}^{a_1}\rangle &= \hat{c}_{a_1}^\dagger \hat{c}_{i_1} |\Phi\rangle, & (\text{single excitation}) \\ |\Phi_{i_1 i_2}^{a_1 a_2}\rangle &= \hat{c}_{a_1}^\dagger \hat{c}_{a_2}^\dagger \hat{c}_{i_2} \hat{c}_{i_1} |\Phi\rangle, & (\text{double excitation}) \\ &\vdots & \vdots \\ |\Phi_{i_1 \dots i_p}^{a_1 \dots a_p}\rangle &= \hat{c}_{a_1}^\dagger \dots \hat{c}_{a_p}^\dagger \hat{c}_{i_p} \dots \hat{c}_{i_1} |\Phi\rangle. & (p\text{-fold excitation}) \end{aligned} \quad (1.32)$$

The reference determinant $|\Phi\rangle$ is conveniently called *Fermi vacuum*. This allows for a classification of single-particle states. In the remainder of this work single-particle states which are occupied in the Fermi vacuum are called *holes* and single-particle states that are unoccupied in the reference state are called *particles*. We further fix the following index convention:

Holes	(i, j, k, \dots)
Particles	(a, b, c, \dots)
General	(p, q, r, \dots)

We note that there is no general convention on naming single-particle indices. The convention used here is consistent with the one used in Ref. [SB09]. However, other sources use different notation, e.g., [SO82].

1.4 NORMAL ORDERING

For the derivation of working formulas of many-body methods the evaluation of matrix elements containing products of second-quantized operators is inevitable. In this section we

introduce supplementary notations and techniques and ultimately formulate the Standard Wick's theorem which is of central importance when dealing with a diagrammatic representation of operator strings. The following treatment follows roughly the discussion in [SB09].

NORMAL ORDERING WITH RESPECT TO THE PHYSICAL VACUUM

Let $\hat{A}, \hat{B}, \hat{C}, \dots$ be various creation or annihilation operators. Then we define the *normal-ordered product* of such operators relative to the physical vacuum $|0\rangle$ to be the rearranged product of operators such that all creation operators are left to the annihilation operators. The normal-ordered product is denoted by

$$n[\hat{A}\hat{B}\hat{C}\dots]. \tag{1.33}$$

The normal-ordered product gathers a relative phase coming from the permutation of creation and annihilation operators.³ The usefulness of the normal-ordered form of a operator-string comes from its vanishing vacuum expectation value

$$\langle 0|n[\hat{A}\hat{B}\hat{C}\dots]|0\rangle = 0, \tag{1.34}$$

if $[\hat{A}\hat{B}\hat{C}\dots]$ is not empty. We define the *contraction* of two operators by

$$\hat{\underset{\square}{A}}\hat{B} \equiv \hat{A}\hat{B} - n[\hat{A}\hat{B}]. \tag{1.35}$$

For stating Wick's theorem we need to define a *normal product with contractions*

$$n[\hat{A}\hat{B}\hat{C}\dots\hat{\underset{\square}{R}}\dots\hat{\underset{\square}{S}}\dots\hat{\underset{\square}{T}}\dots\hat{\underset{\square}{U}}\dots] = (-1)^\sigma \hat{\underset{\square}{R}}\hat{\underset{\square}{T}}\hat{\underset{\square}{S}}\hat{\underset{\square}{U}}\dots n[\hat{A}\hat{B}\hat{C}\dots] \tag{1.36}$$

where σ is the parity of the permutation

$$\begin{pmatrix} \hat{A}\hat{B}\hat{C}\dots\hat{R}\dots\hat{S}\dots\hat{T}\dots\hat{U}\dots \\ \hat{R}\hat{T}\hat{S}\hat{U}\dots\hat{A}\hat{B}\hat{C}\dots \end{pmatrix}. \tag{1.37}$$

where the original order of \hat{R}, \hat{T} and \hat{S}, \hat{U} must be maintained. With this Wick's theorem states:

Theorem 1 (Time-independent Wick's theorem, [Wic50]). *A product of a string of creation and annihilation operators is equal to their normal product plus the sum of all possible normal products with contractions.*

³We note that the definition is not unique since permutation among the creators/annihilators yields an operator string in normal-ordered form but is the permutation would give an additional phase factor.

NORMAL ORDERING WITH RESPECT TO A SLATER DETERMINANT

As already mentioned, many-body theories are commonly formulated with respect to a Fermi vacuum that is not the physical vacuum. Therefore, it is useful to extend the notion of normal order to an arbitrary Slater determinant $|\Phi\rangle$. We define a product of creation and annihilation operators to be in *normal order relative to* $|\Phi\rangle$ if all pseudo-creation operators are left of all pseudo-annihilation operators. We introduce the notation

$$\hat{b}_i^\dagger \equiv \hat{c}_i, \quad (1.38a)$$

$$\hat{b}_i \equiv \hat{c}_i^\dagger, \quad (1.38b)$$

$$\hat{b}_a^\dagger \equiv \hat{c}_a^\dagger, \quad (1.38c)$$

$$\hat{b}_a \equiv \hat{c}_a. \quad (1.38d)$$

where i and a denote hole and particle indices, respectively. Then again it holds that the (Fermi-vacuum) expectation value of a normal-ordered product vanishes, since

$$\hat{b}_p|\Phi\rangle = 0 \quad \text{and} \quad \langle\Phi|\hat{b}_p^\dagger = 0, \quad (1.39)$$

where p is a general single-particle index. In order to distinguish the normal ordering with respect to a Fermi vacuum from normal-ordering with respect to the physical vacuum, we introduce ⁴

$$\{\hat{A}\hat{B}\hat{C}\dots\}_{|\Phi\rangle} = (-1)^\sigma \hat{b}_{p_1}^\dagger \hat{b}_{p_2}^\dagger \dots \hat{b}_{q_2} \hat{b}_{q_1}, \quad (1.40)$$

instead of using $n[\dots]$.⁵ Here σ denotes the parity of permutation from $\hat{A}\hat{B}\hat{C}\dots$ to $\hat{b}_{p_1}^\dagger \hat{b}_{p_2}^\dagger \dots \hat{b}_{q_2} \hat{b}_{q_1}$ and the particular nature of the pseudo-creator and pseudo-annihilators depends on the index type of the corresponding operator $\hat{A}, \hat{B}, \hat{C}, \dots$, i.e., if they correspond to creators or annihilators and if they correspond to particle or holes.

Analogously to the case of a physical vacuum we introduce the notion of a contraction (with respect to the Fermi vacuum) by

$$\overline{\hat{A}\hat{B}} \equiv \hat{A}\hat{B} - \{\hat{A}\hat{B}\}, \quad (1.41)$$

where we put brackets above the expression in order to distinguish from the contraction with respect to a physical vacuum. With this the only nonzero contractions are given by

$$\overline{\hat{c}_i^\dagger \hat{c}_j} = \delta_{ij}, \quad \overline{\hat{c}_a \hat{c}_b^\dagger} = \delta_{ab}. \quad (1.42)$$

⁴In the following we often discard the lower index which specifies the Fermi vacuum since it is clear from context which state is meant.

⁵It is also common to denote the normal-ordered operators with respect to the Fermi vacuum by $N[\dots]$.

Again a *normal product with contractions with respect to a reference state* $|\Phi\rangle$ is defined by

$$\{\hat{A}\hat{B}\hat{C}\cdots\hat{R}\cdots\hat{S}\cdots\hat{T}\cdots\hat{U}\cdots\}_{|\Phi\rangle} = (-1)^\sigma \overbrace{\hat{R}\hat{T}}^{\overbrace{\hat{S}\hat{U}}} \cdots \{\hat{A}\hat{B}\hat{C}\cdots\}_{|\Phi\rangle}. \quad (1.43)$$

With this the Wick theorem for an arbitrary Slater determinant reads

Theorem 2. *A product of a string of creation and annihilation operators is equal to their normal product with respect to a Fermi vacuum $|\Phi\rangle$ plus the sum of all possible normal products with contractions with respect to the Fermi vacuum $|\Phi\rangle$,*

$$\hat{A}\hat{B}\hat{C}\hat{D}\cdots = \{\hat{A}\hat{B}\hat{C}\hat{D}\cdots\} + \sum_{\substack{\text{all} \\ \text{contractions}}} \{\hat{A}\hat{B}\hat{C}\hat{D}\cdots\}. \quad (1.44)$$

STANDARD WICK'S THEOREM

For the evaluation of matrix elements and the use of diagrammatic techniques an additional extension of Wick's theorem is necessary that allows for the computation of products of normal-ordered operators.

In the context of many-body methods one typically evaluates expression between various SDs, and not just the reference state, i.e.,

$$\langle \Phi_{i_1 i_2 \dots}^{a_1 a_2 \dots} | \hat{O} | \Phi_{j_1 j_2 \dots}^{b_1 b_2 \dots} \rangle = \langle \Phi | \hat{c}_{i_1}^\dagger \hat{c}_{i_2}^\dagger \cdots \hat{c}_{a_2} \hat{c}_{a_1} \hat{O} \hat{c}_{b_1}^\dagger \hat{c}_{b_2}^\dagger \cdots \hat{c}_{j_2} \hat{c}_{j_1} | \Phi \rangle, \quad (1.45)$$

for some operator \hat{O} . The Standard Wick's theorem states which contractions need to be considered:

Theorem 3 (Standard Wick's theorem). *A general product of operators which are in normal-ordered form is given by the overall normal product plus the sum of all overall normal products with contractions between operators that were not in the same original normal product.*

$$\begin{aligned} & \{\hat{A}_1 \hat{A}_2 \cdots\} \{\hat{B}_1 \hat{B}_2 \cdots\} \{\hat{C}_1 \hat{C}_2 \cdots\} \\ &= \{\hat{A}_1 \hat{A}_2 \cdots \hat{B}_1 \hat{B}_2 \cdots \hat{C}_1 \hat{C}_2 \cdots\} + \sum_{\substack{\text{all external} \\ \text{contractions}}} \{\hat{A}_1 \hat{A}_2 \cdots \hat{B}_1 \hat{B}_2 \cdots \hat{C}_1 \hat{C}_2 \cdots\}. \end{aligned} \quad (1.46)$$

Contractions are called external if both operators belong to different normal products.

We emphasize that there is confusion on the naming of the version of Wick's theorem. The above Standard Wick's theorem is called 'generalized Wick's theorem' (GWT) in the book of Bartlett and Shavitt [SB09]. However, the naming GWT is commonly also used when defining contractions with respect to a symmetry-broken reference state [BB69]. In this

thesis when working with Slater determinants with ordinary single-particle states we refer to Standard Wick's theorem, and in the context of symmetry-breaking we use the term GWT.

We also note that there is a formalism of normal-ordering with respect to an arbitrary multi-determinantal reference state [KM97]. This is also often called 'generalized Wick theorem' and arises naturally in several many-body methods. However, it will not be used in this work.

NORMAL-ORDERED FORM OF THE HAMILTONIAN

The Standard Wick's theorem allows us to derive the normal-ordered form of the Hamiltonian. Let \hat{H} be a general three-body Hamiltonian

$$\begin{aligned}\hat{H} &= \hat{H}^{[0]} + \hat{H}^{[1]} + \hat{H}^{[2]} + \hat{H}^{[3]} \\ &= H^{[0]} + \sum_{pq} H_{pq}^{[1]} \hat{c}_p^\dagger \hat{c}_q + \frac{1}{4} \sum_{pqrs} \bar{H}_{pqrs}^{[2]} \hat{c}_p^\dagger \hat{c}_q^\dagger \hat{c}_s \hat{c}_r + \frac{1}{36} \sum_{pqrstu} \bar{H}_{pqrstu}^{[3]} \hat{c}_p^\dagger \hat{c}_q^\dagger \hat{c}_r^\dagger \hat{c}_u \hat{c}_t \hat{c}_s,\end{aligned}$$

with anti-symmetrized two- and three-body matrix elements.

In normal-ordered form the operator reads

$$\begin{aligned}\hat{H} &= \hat{H}^{[0]} + \sum_i H_{ii}^{[1]} + \frac{1}{2} \sum_{ij} \bar{H}_{ijij}^{[2]} + \frac{1}{6} \sum_{ijk} \bar{H}_{ijkijk}^{[3]} \\ &+ \sum_{pq} H_{pq}^{[1]} \{\hat{c}_p^\dagger \hat{c}_q\} + \sum_{pqi} \bar{H}_{piqi}^{[2]} \{\hat{c}_p^\dagger \hat{c}_q\} + \sum_{pqij} \bar{H}_{pijqij}^{[3]} \{\hat{c}_p^\dagger \hat{c}_q\} \\ &+ \frac{1}{4} \sum_{pqrs} \bar{H}_{pqrs}^{[2]} \{\hat{c}_p^\dagger \hat{c}_q^\dagger \hat{c}_s \hat{c}_r\} + \sum_{pqirsi} \bar{H}_{pqirsi}^{[3]} \{\hat{c}_p^\dagger \hat{c}_q^\dagger \hat{c}_s \hat{c}_r\} \\ &+ \frac{1}{36} \sum_{pqrstu} \bar{H}_{pqrstu}^{[3]} \{\hat{c}_p^\dagger \hat{c}_q^\dagger \hat{c}_r^\dagger \hat{c}_u \hat{c}_t \hat{c}_s\}\end{aligned}\tag{1.47}$$

$$\tag{1.48}$$

where we identify the zero-body part of \hat{H} in normal-ordered form with the reference expectation value $\langle \Phi | \hat{H} | \Phi \rangle$

$$\langle \Phi | \hat{H} | \Phi \rangle = \hat{H}^{[0]} + \sum_i H_{ii}^{[1]} + \frac{1}{2} \sum_{ij} \bar{H}_{ijij}^{[2]} + \frac{1}{6} \sum_{ijk} \bar{H}_{ijkijk}^{[3]},\tag{1.49}$$

as well as the one-, two- and three-body parts of the normal-ordered Hamiltonian

$$\hat{H}_N^{[1]} \equiv \sum_{pq} \langle p | \hat{H}_N^{[1]} | q \rangle \{\hat{c}_p^\dagger \hat{c}_q\},\tag{1.50a}$$

$$\hat{H}_N^{[2]} \equiv \frac{1}{4} \sum_{pqrs} \langle pq | \hat{H}_N^{[2]} | rs \rangle \{\hat{c}_p^\dagger \hat{c}_q^\dagger \hat{c}_s \hat{c}_r\},\tag{1.50b}$$

$$\hat{H}_N^{[3]} \equiv \frac{1}{36} \sum_{pqrstu} \langle pqr | \hat{H}_N^{[3]} | stu \rangle \{ \hat{c}_p^\dagger \hat{c}_q^\dagger \hat{c}_r^\dagger \hat{c}_u \hat{c}_t \hat{c}_s \}, \quad (1.50c)$$

with matrix elements

$$\langle p | \hat{H}_N^{[1]} | q \rangle = H_{pq}^{[1]} + \sum_i \bar{H}_{piqi}^{[2]} + \sum_{ij} \bar{H}_{pijqij}^{[3]}, \quad (1.51a)$$

$$\langle pq | \hat{H}_N^{[2]} | rs \rangle = \bar{H}_{pqrs}^{[2]} + 4 \sum_i \bar{H}_{pqirsi}^{[3]}, \quad (1.51b)$$

$$\langle pqr | \hat{H}_N^{[3]} | stu \rangle = \bar{H}_{pqrstu}^{[3]}. \quad (1.51c)$$

Note that the matrix elements of the normal-ordered zero-, one- and two-body part implicitly depend on the choice of the Fermi vacuum. With this the Hamiltonian can be written by

$$\hat{H} = \langle \Phi | \hat{H} | \Phi \rangle + \hat{H}_N^{[1]} + \hat{H}_N^{[2]} + \hat{H}_N^{[3]} \quad (1.52)$$

and we introduce

$$\hat{H}_N \equiv \hat{H} - \langle \Phi | \hat{H} | \Phi \rangle. \quad (1.53)$$

Starting from the Schrödinger equation of \hat{H} , we obtain

$$\hat{H}_N |\psi\rangle = \Delta E |\psi\rangle, \quad (1.54)$$

where

$$\Delta E \equiv E - \langle \Phi | \hat{H} | \Phi \rangle. \quad (1.55)$$

THE NORMAL-ORDER N -BODY APPROXIMATION

We have seen how to cast a general three-body Hamiltonian into normal-ordered form. The normal ordering is nothing but a reordering of creation and annihilation operators and transfers information about the three-body force into the normal-ordered zero-, one- and two-body parts.

However, as already mentioned the explicit treatment of three-body operators in many-body theories is complicated due to the increasing complexity of the underlying theory and the computational effort that is needed to solve the many-body problem.

Therefore, we define the *Hamiltonian in normal-ordered N -body approximation* via

$$\hat{H}^{\text{NONB}} \equiv \sum_{i=1}^N \hat{H}_N^{[i]}. \quad (1.56)$$

Of particular importance is the *Hamiltonian in normal-ordered two-body approximation* (NO2B)

$$\hat{H}^{\text{NO2B}} = \hat{H}_N^{[0]} + \hat{H}_N^{[1]} + \hat{H}_N^{[2]} \quad (1.57)$$

where the effect of three-body forces is included in the matrix elements of the normal-order parts of lower particle-rank. The residual three-body force is discarded.

EXTENSION TO MULTI-DETERMINANTAL REFERENCE STATES

The framework of contractions and normal ordering can be extended to arbitrary multi-determinantal reference states [KM97]. This allows extending normal-ordering to genuine open-shell nuclei, since a single Slater determinant is not a proper reference state for open-shell systems.

In particular the multi-configurational version of perturbation theory—to be discussed in Part III of this thesis—makes extensive use of the so-called *Hamiltonian in multi-reference normal-ordered two-body approximation*

$$\hat{H}^{\text{MR-NO2B}} \equiv \hat{H}_N^{\text{MR}[0]} + \hat{H}_N^{\text{MR}[1]} + \hat{H}_N^{\text{MR}[2]}, \quad (1.58)$$

where—similar to the single-determinantal case—the matrix elements are given by

$$H_N^{\text{MR}[0]} = \frac{1}{36} \sum_{pqrst} \bar{H}_{pqrst}^{[3]} (\gamma_{prtqsu} - 18\gamma_{pq}\gamma_{rtsu} + 36\gamma_{pq}\gamma_{rs}\gamma_{tu}), \quad (1.59a)$$

$$\langle p | \hat{H}_N^{\text{MR}[1]} | q \rangle = H_{pq}^{[1]} + \sum_{rs} \bar{H}_{prqs}^{[2]} \gamma_{rs} + \sum_{rstu} \bar{H}_{prtqsu}^{[3]} (\gamma_{rtsu} - 4\gamma_{rs}\gamma_{tu}), \quad (1.59b)$$

$$\langle pq | \hat{H}_N^{\text{MR}[2]} | rs \rangle = \bar{H}_{pqrs}^{[2]} + \sum_{tu} \bar{H}_{prtqsu}^{[3]} \gamma_{tu}, \quad (1.59c)$$

where

$$\gamma_{pq} = \langle \psi | \hat{c}_p^\dagger \hat{c}_q | \psi \rangle, \quad (1.60)$$

$$\gamma_{pqrs} = \langle \psi | \hat{c}_p^\dagger \hat{c}_q^\dagger \hat{c}_s \hat{c}_r | \psi \rangle, \quad (1.61)$$

$$\gamma_{pqrst} = \langle \psi | \hat{c}_p^\dagger \hat{c}_q^\dagger \hat{c}_r^\dagger \hat{c}_t \hat{c}_s | \psi \rangle, \quad (1.62)$$

are the one-, two- and three-body density matrices of the reference state $|\psi\rangle$. Contractions involve density matrices instead of simple delta constraints. For a discussion of multi-reference normal ordering in the context of nuclear Hamiltonians see Refs. [Geb13; GCR16].

Unless stated otherwise when referring to the Hamiltonian \hat{H} we always mean the nuclear Hamiltonian in (multi-reference) NO2B approximation with respect to a specified reference state.

2

The Nuclear Hamiltonian

In the history of physics the determination of the nuclear interaction is a long-standing problem. Even though it is clear from the Standard model of particle physics that the underlying theory of the strong interaction is quantum chromodynamics (QCD), the non-perturbative character prohibits a direct construction of the nuclear Hamiltonian that serves as input for subsequent many-body calculations.

2.1 EMPIRICAL PROPERTIES

Before constructing realistic nuclear potentials a few empirical properties obtained from experiments on finite nuclear systems as well as two-nucleon scattering phase shifts can be addressed.

An important property of finite nuclei is the saturation of nuclear binding energies, i.e., one empirically obtains a binding energy per nucleon of about 8MeV per nucleon. This is a direct hint for the finite-range character of the nuclear force. In the case that every single nucleon interacts with all other nucleon the overall binding energy will scale as $\sim A(A-1)/2$, which contradicts nuclear saturation properties. Instead nucleons tend to interact only with their nearest neighbors, thus, the displaying short-range behavior of the nuclear Hamiltonian.

Since nuclei are selfbound systems, the nuclear interaction must have a attractive component at intermediate distances. From nuclear matter calculations one obtains a nuclear saturation density of about 0.17 fm^{-3} , thus, leading to a mean distance of $1 - 2 \text{ fm}$ between nucleons. More precise statements about the sign of the interaction can be deduced from experimental scattering phase shifts. One obtains strong repulsion at short distances and attraction at long distances.

For the accurate reproduction of nuclear properties a mere central potential is insufficient.

It was, thus, recognized that for the description of magic numbers, the HO single-particle shell model fails to reproduce experimentally observed shell closures beyond $A = 20$. The corresponding spin-orbit splitting can be achieved by adding an additional *spin-orbit force* to the nuclear interaction.

Furthermore, when investigating deuteron properties one obtains a non-vanishing quadrupole moment due to an admixture of an $L = 2$ component to the ground-state wave function which does not occur when restricting to central potentials only. This motivates the existence of an additional *tensor force* in the nuclear interaction.

2.2 PHENOMENOLOGICAL POTENTIALS

From the above observations nuclear researchers started constructing realistic nuclear interactions with the additional constraint of being in agreement with fundamental symmetries observed in nature. Examples of such symmetries are Galilean, time-reversal or parity invariance.

While in the 1960s nuclear potentials were designed via mere parametrizations of radial dependences, e.g., the *Reid potential* [Rei68], later attempts, performed in the context of the *Argonne V₄* potential, used a Wood-Saxon form as ansatz for the short-range part and an additional spin-orbit coupling and isospin-dependent term were added to reproduce magic numbers. Later on other operator structures were obtained in the context of Argonne V14 and V18 potentials by enriching the simple V4 potential with additional higher-order polynomial dependencies of the momenta [WSA84; Vee11]. Alternatives to the Argonne interaction were later introduced by the *Nijmegen* and *Bonn* potentials [Mac89]. Such elaborate potentials yield highly accurate reproduction of NN phase shifts.

It is well known that three-body effects play a crucial role in deriving observables to high accuracy [Rot⁺11; Hag⁺12; Hol⁺12]. When following the same strategy and building a phenomenological three-body potential, the tremendous amount of possible operator structures makes it extremely challenging to derive a phenomenological three-body interaction consistently to the two-body sector [PG90].

2.3 CHIRAL EFFECTIVE FIELD THEORY

In order to systematically proceed one needs physical guidance on how to choose the operator structures in the NN, 3N and multi-nucleon sector, that may be important for the description of the atomic nucleus. In particular the construction of phenomenological interactions does not yield a systematically improvable way to deal with this problem.

One way for the construction of a systematically improvable interaction is *chiral effective field theory* (EFT), where one writes down the most general Lagrangian consistent with the symmetries of QCD, thus, having a sound connection with the underlying quantum field

theory of the strong interaction. In chiral EFT quark degrees are frozen and pions mediate the strong force as Goldstone bosons. Therefore, pions and nucleons are the effective degrees of freedom instead of quarks and gluons.

In the seminal work from the 1990s Steven Weinberg introduced a *power counting scheme* which allows for a systematic ordering of the importance of operator structures in terms of powers of Q/Λ , where Q denotes the typical momentum scale inside the nucleus and $\Lambda \approx 1 \text{ GeV}$ is the chiral breakdown scale [Wei90; Wei91; Wei92]. In particular, within this scheme higher particle-rank operators appear naturally at higher orders in the chiral expansion implying a hierarchy of the importance of many-body forces of higher particle rank.

Following, a strict *ab initio* route, the chiral interaction is ultimately fitted to two- and three-body properties such as the deuteron and ^3He binding energies, respectively. However, in recent years several chiral Hamiltonians were designed, that were fitted to A -body observables, e.g., the charge radius of ^{16}O . The corresponding interactions often yield better agreement with experimental data up to medium-mass nickel isotopes. The most prominent example of such an interaction is the N^2LO_{sat} interaction [Eks⁺13], where both two- and three-nucleon forces are consistently truncated at next-to-next-to leading order in the chiral power counting.

Chiral EFT is an overwhelming topic which is extensively covered in the literature. Therefore, we do not aim on giving a more detailed introduction here but rather refer the interested reader to the corresponding literature. Excellent modern reviews are given by Entem and Machleidt [ME11] as well as Epelbaum [Epe09]. A discussion of three-body operators can be found in [Epe⁺02; Heb12] and with particular focus on neutron-matter calculations [HS10]. For the extension to four-nucleon forces see [Epe06].

For a recent overview of the status of addressing theoretical uncertainties in the chiral Hamiltonian see the LENPIC proceedings [GS17].

In this thesis we work with several different Hamiltonians which we will introduce in the following. One choice is the use of a chiral two-body Hamiltonian constructed at next-to-next-to-next-to leading-order (N³LO) with a cutoff parameter of $\Lambda_{2N} = 500 \text{ MeV}$ with a non-local regularization scheme [EM03]. If we restrict ourselves to a two-nucleon interaction this yields the *NN-only interaction*, denoted by NN_{500}^4 . For the incorporation of three-body effects we use a N²LO three-body Hamiltonian with cutoff parameter $\Lambda_{3N} = 400 \text{ MeV}$ with a local regularization scheme [Nav07]. This defines the *NN+3N-full interaction*, denoted by $\text{NN}_{500}^4 + 3\text{N}_{400}^3$. Note that this induces a source of inconsistency since two-body and three-body operators are included up to different orders in the chiral expansion.

3

Similarity Renormalization Group

Nuclear structure calculations are severely complicated due to correlation effects coming from the strong repulsion of the nuclear force at short distances, leading to a coupling of high- and low-momentum many-body states. Therefore, we introduce a renormalization-group (RG) approach, which will be used subsequently to tame these correlation effects. Additionally, this greatly improves model-space convergence, thus, enabling converged results even for medium-mass systems.

3.1 FLOW EQUATION

In the (free-space) Similarity-Renormalization-Group (SRG) approach one uses a unitary transformation \hat{U}_α to transform the initial nuclear Hamiltonian \hat{H}_0 leaving the spectrum unchanged [SP00; BFP07; HR07; RRH08; Rot⁺11; Jur⁺13].¹

The transformed Hamiltonian is given by

$$\hat{H}_\alpha = \hat{U}_\alpha^\dagger \hat{H}_0 \hat{U}_\alpha, \quad (3.1)$$

where α defines the so-called *SRG flow parameter*. Differentiation of (3.1) with respect to α yields according to the product rule

$$\frac{d\hat{H}_\alpha}{d\alpha} = \frac{d\hat{U}_\alpha^\dagger}{d\alpha} \hat{H}_0 \hat{U}_\alpha + \hat{U}_\alpha^\dagger \hat{H}_0 \frac{d\hat{U}_\alpha}{d\alpha}. \quad (3.2)$$

¹We added the term 'free-space' in order to clearly distinguish the method from the In-Medium Similarity Renormalization Group. Even though both approaches share many formal similarities, (free-space) SRG is used for the renormalization of an operator whereas the in-medium SRG defines a many-body method which solves the quantum many-body problem.

Since by unitarity $\hat{U}_\alpha^\dagger \hat{U}_\alpha = 1$, it follows that

$$\frac{d\hat{U}_\alpha^\dagger}{d\alpha} \hat{U}_\alpha = -\hat{U}_\alpha^\dagger \frac{d\hat{U}_\alpha}{d\alpha}. \quad (3.3)$$

Solving for the derivatives of \hat{U}_α and \hat{U}_α^\dagger gives

$$\frac{d\hat{U}_\alpha^\dagger}{d\alpha} = -\hat{U}_\alpha^\dagger \frac{d\hat{U}_\alpha}{d\alpha} \hat{U}_\alpha^\dagger, \quad (3.4)$$

$$\frac{d\hat{U}_\alpha}{d\alpha} = -\hat{U}_\alpha \frac{d\hat{U}_\alpha^\dagger}{d\alpha} \hat{U}_\alpha. \quad (3.5)$$

In the following it will be convenient to define a *generator* of the SRG transformation

$$\hat{\eta}_\alpha \equiv -\frac{d\hat{U}_\alpha^\dagger}{d\alpha} \hat{U}_\alpha. \quad (3.6)$$

By (3.5) it follows the anti-Hermiticity of $\hat{\eta}_\alpha$,

$$\hat{\eta}_\alpha = -\hat{\eta}_\alpha^\dagger. \quad (3.7)$$

Substitution of (3.5) into (3.2) finally yields ²

$$\frac{d}{d\alpha} \hat{H}_\alpha = [\hat{\eta}_\alpha, \hat{H}_\alpha]. \quad (3.8)$$

Equation (3.8) is called the *SRG flow equation* and shares formal similarities with an equation of motion in the Heisenberg picture, i.e., an ordinary differential equation (ODE) for the Hamiltonian.

3.2 CHOICE OF GENERATOR

Up to now the discussion of the SRG is completely general. In an actual physical application the particular choice of the generator $\hat{\eta}_\alpha$ specifies the decoupling pattern. Assume we write the generator $\hat{\eta}_\alpha$ as

$$\hat{\eta}_\alpha = [\hat{G}_\alpha, \hat{H}_\alpha] \quad (3.9)$$

for some Hermitian operator \hat{G}_α such that anti-Hermiticity of $\hat{\eta}_\alpha$ is satisfied. As a first obvious choice we might take

²Even though all the discussion is based on the Hamiltonian, the flow equation holds for any operator \hat{O}

$$\frac{d}{d\alpha} \hat{O}_\alpha = [\hat{\eta}_\alpha, \hat{O}_\alpha].$$

$$\hat{G}_\alpha \equiv \hat{H}_\alpha^{\text{diag}} = \sum_I \langle \Phi | \hat{H}_\alpha | \Phi_I \rangle | \Phi_I \rangle \langle \Phi_I |, \quad (3.10)$$

i.e., as the diagonal part of \hat{H}_α in a given many-body basis. The advantage of this form is that by setting

$$\hat{\eta}_\alpha = [\hat{H}_\alpha^{\text{diag}}, \hat{H}_\alpha] \quad (3.11)$$

the generator $\hat{\eta}_\alpha$ will vanish as soon as \hat{H}_α becomes diagonal. In this way, we achieve a pre-diagonalization of \hat{H}_α , and since the generator is zero, this yields a stationary point of the SRG flow. However, building the generator $\hat{\eta}_\alpha$ from a general reference basis $\{|\Phi_I\rangle\}$ in which the Hamiltonian is represented may lead to an undesired suppression of certain parts of the Hamiltonian, since the reference basis may not have much in common with the eigenbasis of \hat{H}_α . In modern applications a convenient choice is given by

$$\hat{\eta}_\alpha = (2\mu)^2 [\hat{T}_{\text{int}}, \hat{H}_\alpha], \quad (3.12)$$

where μ is the reduced mass of the nucleon and $\hat{T}_{\text{int}} = \hat{T} - \hat{T}_{\text{cm}}$ the intrinsic kinetic-energy operator. In the approximation of equal proton and neutron masses the intrinsic kinetic-energy operator is defined as

$$\hat{T}_{\text{int}} \equiv \frac{1}{A\mu} \sum_{i<j} \hat{q}_{ij}^2, \quad (3.13)$$

with the relative-momentum operator $\hat{q}_{ij} = \frac{\hat{p}_i - \hat{p}_j}{2}$. However, in recent years several other possibilities for the definition of $\hat{\eta}_\alpha$ have been examined.

A schematic view on the effect of the SRG evolution can be seen in Figure 3.1. Initially, the Hamilton matrix representation is dense. Performing SRG evolution drives the Hamiltonian to a band diagonal structure and yields large blocks with vanishing matrix elements indicated by the blank white space. There are also other renormalization approaches like $V_{\text{low-k}}$ or the Unitary Correlation Operator Method (UCOM) [Fel+98; NF04; HR07; RRH08] which have been used in the past but follow different strategies to improve model-space convergence.

3.3 CLUSTER DECOMPOSITION

The major drawback of the SRG method are higher particle-rank many-body forces which are induced during the flow [BFP07; JNF09]. Typically (3.8) is solved by means of multi-step ODE solvers. When evaluating the commutator of, e.g., two two-body operators \hat{A} and

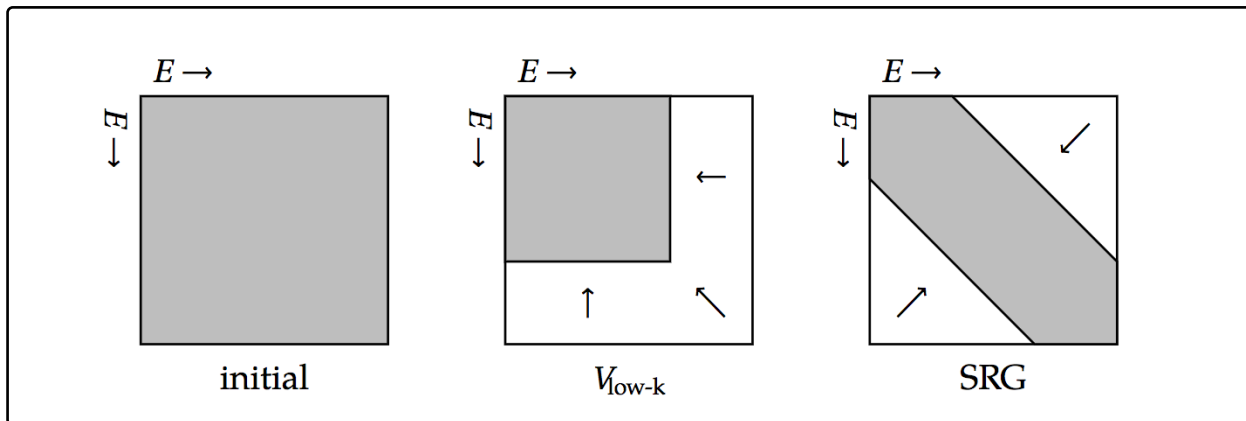


Figure 3.1: Schematic representation of several renormalization approaches. The picture is taken from [Bin14].

\hat{B} it holds that $[\hat{A}, \hat{B}]$ contains up to three-body operators.³ Therefore, the consecutive evaluation of the commutator in the flow-equation raises the particle rank of the evolved Hamiltonian, thus leading to induced many-body contributions up to the A -body level

$$\hat{H}_\alpha = \hat{H}_\alpha^{(1)} + \hat{H}_\alpha^{(2)} + \hat{H}_\alpha^{(3)} + \hat{H}_\alpha^{(4)} + \dots + \hat{H}_\alpha^{(A)}, \quad (3.14)$$

where the subscript corresponds to the flow parameter α and the superscripts in brackets indicate the irreducible particle rank of the corresponding operator. Irreducibility means that the operator can not be decomposed into operators of lower particle rank.

In subsequent many-body calculations the incorporation of higher particle-rank operators becomes challenging both conceptually and computationally. Therefore, contributions in (3.14) beyond the three-body level are typically discarded. This approximation step formally violates the unitarity of the SRG transformation in A -body space and leads to a dependence of the results on the SRG flow parameter α .

Therefore, even though the SRG transformation improves model-space convergence, the limit $\alpha \rightarrow \infty$ is undesirable since the amount of induced many-body forces strongly depends on α . In actual applications one must find a reasonable trade-off between convergence and the amount of induced many-body contributions.

The above choice for the generator in (3.12) is the standard choice in nuclear structure applications. While convergence with respect to model-space size is improved significantly it yields significant induced many-body contributions. Investigation of other choice for the generator have been explored recently with the aim of lowering the induced higher-particle rank contributions.

³Let $\text{rank}(\hat{A}) = m$ and $\text{rank}(\hat{B}) = n$ then $\text{rank}([\hat{A}, \hat{B}]) = m + n - 1$.

3.4 TYPES OF INTERACTIONS

In the following we will briefly define the different types of truncations of the cluster expansion used throughout this thesis and fix the nomenclature for later applications. They differ in the particle-rank of the initial Hamiltonian and the space which is used for the SRG evolution:

NN-only: Use an initial two-body force and perform evolution in two-body space

NN+3N-induced: Use an initial two-body force and perform evolution in two-body and three-body space

NN+3N-full: Use an initial two-body and three-body force and perform evolution in two-body and three-body space

We note that there have been studies on the impact of the evolution of two- and three-body operators in four-body space [Sch13; Cal14]. Due to large computational requirements and the incapability of reaching model-space convergence four-body forces (and beyond) are currently neglected in the description of medium-mass systems.

PART II

SINGLE-CONFIGURATIONAL MANY-BODY PERTURBATION THEORY

Introduction to Part II

The description of closed-shell systems constitutes the simplest case for the solution of the quantum many-body problem. The reason for this is that such nuclei are adequately described in an independent-particle model, e.g., the *Hartree-Fock* approximation. In particular all quantum numbers are correctly reproduced such that mean-field wave function has the same symmetry properties as the exact ground-state wave function. Furthermore, a large part of the overall binding energy can be described via the solution of an effective one-body problem. Residual correlation effects are comparably small such that they can be treated in a perturbative way.

For a long time it was argued that the hard core of the nuclear potential makes a non-perturbative description necessary, since the perturbation series was expected to diverge. Traditionally, G -matrix methods were used to renormalize the interaction. The advent of softened nuclear potentials incited a renaissance of perturbative approaches and lead to new insights, which will be presented at the end of this part of the thesis.

We give a self-contained introduction to many-body perturbation theory based on a single-configurational vacuum starting with a brief introduction of Hartree-Fock theory as a convenient way to obtain an optimized mean-field reference function. We proceed with the introduction of perturbation theory based on a formal derivation of the resolvent expansion in the case of a non-degenerate reference state. From this the many-body perspective is developed with particular focus on the use of diagrammatic techniques for the evaluation of expectation values of second-quantized operators by means of Wick's theorem. Finally, we derive second- and third-order energy corrections in the case of a single-determinantal reference state and discuss intrinsic scaling properties of low-order many-body perturbation theory. Furthermore, we emphasize the role of angular-momentum coupling techniques for the efficient evaluation of the occurring sums. We conclude with a qualitative discussion on the limitations of single-reference theories when proceeding to open-shell systems.

In our investigations, coupled-cluster methods will serve as benchmark calculations. Therefore, we briefly discuss the main concepts of single-reference coupled-cluster theory and introduce nomenclature used in the discussion of the results.

In the last chapter we present extensive benchmark studies of single-configurational many-body perturbation theory with respect to a canonical Hartree-Fock vacuum. We present a detailed analysis of the impact of the partitioning on the convergence behavior. Additionally, the role of renormalization, i.e., the Similarity Renormalization Group, is discussed and its impact on convergence rates of perturbation series of light nuclei. We proceed with a detailed

analysis of third-order many-body perturbation theory and state-of-the-art coupled-cluster calculations for selected closed-shell nuclei up to the heavy tin region. Furthermore, we present a detailed discussion of the individual diagrammatic contributions at third-order and question the reliability of approximations that neglect certain terms of the perturbative expansion at a given order.

4

Hartree-Fock Theory

A simple approach for the description of nuclear systems are the so-called *independent-particle models*, where one assumes the exact wavefunction to be given by a single Slater determinant. In this scenario, correlation effects are neglected and the individual particles move independently in an effective one-body potential.

The most commonly used model is the *Hartree-Fock (HF) approximation*, where the single-particle orbitals and energies are obtained from a self-consistent solution of a variational problem. The use of HF theory has a long history in nuclear structure and quantum chemistry and has successfully been applied to a vast variety of quantum systems. Most commonly, the HF approximation is not used as a standalone approach, but rather as a starting point for the construction of reference states for more advanced techniques, which explicitly construct correlations on top of the optimized HF reference state. Examples of such methods are many-body perturbation theory, coupled-cluster theory or the in-medium similarity renormalization group approach.

4.1 VARIATIONAL PRINCIPLE AND TESTSPACE

In the following we briefly discuss the fundamentals of HF theory. For an extensive treatment of HF theory and its extensions to open-shell systems see [\[SO82\]](#).

We start the derivation from the time-independent Schrödinger equation

$$\hat{H}|\psi\rangle = E|\psi\rangle. \quad (4.1)$$

The solution of (4.1) is equivalent to the solution of the variational equation

$$\delta E[\psi] = 0, \quad (4.2)$$

where the energy functional $E[\psi]$ is given by

$$E[\psi] = \frac{\langle \psi | \hat{H} | \psi \rangle}{\langle \psi | \psi \rangle}. \quad (4.3)$$

However, this equivalence breaks down if the test space is restricted. In HF theory the space of test functions \mathcal{H}_{var} consists of all Slater determinants and is, therefore, a proper subspace of the entire Hilbert space \mathcal{H} we work in,

$$\mathcal{H}_{\text{var}} \subset \mathcal{H}. \quad (4.4)$$

In case the lowest eigenvalue for a given Hamilton operator corresponds to an eigenvector which is a single Slater determinant, the HF method is exact. Otherwise it yields an approximation to the exact solution. However, by the Ritz variational principle it holds for $|\psi_{\text{var}}\rangle \in \mathcal{H}_{\text{var}}$

$$E[\psi_{\text{var}}] \geq E_0, \quad (4.5)$$

where E_0 denotes the exact ground-state energy such that the HF energy provides an upper bound.

4.2 DERIVATION OF THE HARTREE-FOCK EQUATIONS

To derive the HF equations the trial state is written in second quantization

$$|\text{HF}\rangle = |\varphi_1, \dots, \varphi_A\rangle, \quad (4.6)$$

$$= \prod_{i=1}^A \hat{a}_i^\dagger |0\rangle, \quad (4.7)$$

where $\{|\varphi_i\rangle\}$ denotes the set of HF single-particle states with corresponding creation operators $\{\hat{a}_i^\dagger\}$.

We expand the single-particle states and creation operators with respect to a fixed reference basis ¹

$$|\varphi_i\rangle = \sum_p D_{ip} |\chi_p\rangle, \quad (4.8)$$

$$\hat{a}_i^\dagger = \sum_p D_{ip} \hat{c}_p^\dagger, \quad (4.9)$$

where the overlap $D_{ia} = \langle \chi_a | \varphi_i \rangle$ denotes the matrix elements of the unitary transformation

¹In typical applications this is a spherical harmonic oscillator single-particle basis.

and $|\chi_a\rangle$ and \hat{c}_a^\dagger denote the single-particle states and creation operators in the reference basis, respectively. We define the one-body density matrix of the trial state with respect to the reference basis

$$\rho_{pq}^{(1)} = \langle \text{HF} | \hat{c}_q^\dagger \hat{c}_p | \text{HF} \rangle = \sum_{ij} D_{pi} D_{qj}^* \langle \text{HF} | \hat{a}_j^\dagger \hat{a}_i | \text{HF} \rangle = \sum_i^A D_{ip} D_{ji}^*. \quad (4.10)$$

Further we define the corresponding *density operator* by

$$\hat{\rho} \equiv \sum_{pq} \rho_{pq}^{(1)} |\chi_p\rangle \langle \chi_q|. \quad (4.11)$$

We must impose additional restrictions to ensure that the many-body state is still a single Slater determinant after the variation has been performed. We enforce this by requiring idempotency and hermiticity of the one-body density matrix

$$\sum_r \rho_{pr}^{(1)} \rho_{rq}^{(1)} = \rho_{pq}^{(1)}, \quad (4.12)$$

$$\rho_{pq}^{(1)*} = \rho_{qp}^{(1)}. \quad (4.13)$$

In the following we assume a general two-body Hamiltonian in second-quantized form with respect to the reference basis ²

$$\hat{H} = \sum_{pq} H_{pq}^{[1]} \hat{c}_p^\dagger \hat{c}_q + \frac{1}{4} \sum_{pqrs} \bar{H}_{pqrs}^{[2]} \hat{c}_p^\dagger \hat{c}_q^\dagger \hat{c}_s \hat{c}_r. \quad (4.14)$$

where t_{pq} denotes the matrix elements of the kinetic energy operator and v_{pqrs} the anti-symmetric matrix elements of the two-body potential. Since the state $|\text{HF}\rangle$, is normalized the energy functional reads

$$E[|\text{HF}\rangle] = \sum_{pq} H_{pq}^{[1]} \langle \text{HF} | \hat{c}_p^\dagger \hat{c}_q | \text{HF} \rangle + \frac{1}{4} \sum_{pqrs} \bar{H}_{pqrs}^{[2]} \langle \text{HF} | \hat{c}_p^\dagger \hat{c}_q^\dagger \hat{c}_s \hat{c}_r | \text{HF} \rangle. \quad (4.15)$$

We additionally introduce the two-body density matrix

$$\rho_{pqrs}^{(2)} = \langle \text{HF} | \hat{c}_p^\dagger \hat{c}_q^\dagger \hat{c}_s \hat{c}_r | \text{HF} \rangle, \quad (4.16)$$

and write (4.15) as

²The discussion can be extended to three-body operators by adding

$$\hat{H}_{3N} = \frac{1}{6} \sum_{p_1 p_2 p_3 q_1 q_2 q_3} \bar{H}_{p_1 p_2 p_3 q_1 q_2 q_3}^{[3]} \hat{c}_{p_1}^\dagger \hat{c}_{p_2}^\dagger \hat{c}_{p_3}^\dagger \hat{c}_{q_3} \hat{c}_{q_2} \hat{c}_{q_1}$$

in the following derivation.

$$E[|\text{HF}\rangle] = \sum_{pq} H_{pq}^{[1]} \rho_{qp}^{(1)} + \frac{1}{4} \sum_{pqrs} \bar{H}_{pqrs}^{[2]} \rho_{rspq}^{(2)}. \quad (4.17)$$

In the case of a single Slater determinant the two-body density matrix factorizes into its one-body components

$$\rho_{pqrs}^{(2)} = \rho_{ps}^{(1)} \rho_{qr}^{(1)} - \rho_{pr}^{(1)} \rho_{qs}^{(1)}. \quad (4.18)$$

Substituting (4.18) into (4.17) yields

$$E[\rho^{(1)}] = \sum_{pq} H_{pq}^{[1]} \rho_{qp}^{(1)} + \frac{1}{2} \sum_{pqrs} \bar{H}_{pqrs}^{[2]} \rho_{ps}^{(1)} \rho_{qr}^{(1)}. \quad (4.19)$$

We now perform a variation of the above expression neglecting terms, which are quadratic or higher in $\delta\rho^{(1)}$,

$$\delta E[\rho^{(1)}] = \sum_{pq} H_{pq}^{[1]} \delta\rho_{qp}^{(1)} + \frac{1}{2} \sum_{pqrs} \bar{H}_{pqrs}^{[2]} (\delta\rho_{ps}^{(1)} \rho_{qr}^{(1)} - \rho_{ps}^{(1)} \delta\rho_{qr}^{(1)}), \quad (4.20)$$

$$= \sum_{pq} (H_{pq}^{[1]} + \sum_{rs} \bar{H}_{pqrs}^{[2]} \rho_{rs}^{(1)}) \delta\rho_{qp}^{(1)}. \quad (4.21)$$

By defining an auxiliary mean-field Hamiltonian

$$h_{pq}[\rho^{(1)}] = H_{pq}^{[1]} + u_{pq}[\rho^{(1)}], \quad (4.22)$$

$$u_{pq}[\rho^{(1)}] = \sum_{rs} \bar{H}_{pqrs}^{[2]} \rho_{rs}^{(1)}, \quad (4.23)$$

the stationarity condition for the energy functional can be written

$$\sum_{ik} h_{ik}[\rho^{(1)}] \delta\rho_{ki}^{(1)} = 0. \quad (4.24)$$

Since for any variations $\rho^{(1)} + \delta\rho^{(1)}$ idempotency and Hermiticity must be fulfilled we get

$$\rho^{(1)} \delta\rho^{(1)} \rho^{(1)} = 0, \quad (4.25)$$

$$(1 - \rho^{(1)}) \delta\rho^{(1)} (1 - \rho^{(1)}) = 0. \quad (4.26)$$

Therefore, variations can only be performed between particle and hole states. From the stationarity condition (4.24) we know that the commutator between the mean-field Hamiltonian \hat{h} and the one-body density $\hat{\rho}^{(1)}$ vanishes,

$$[\hat{h}[\rho^{(1)}], \hat{\rho}^{(1)}] = 0. \quad (4.27)$$

thus, there exists a common eigenbasis of $\hat{h}[\rho^{(1)}]$ and $\hat{\rho}^{(1)}$. The operator-valued expression (4.27) can be cast into an eigenvalue equation for the mean-field Hamiltonian $\hat{h}[\rho^{(1)}]$,

$$\hat{h}[\rho^{(1)}]|\varphi_n\rangle = \epsilon_n|\varphi_n\rangle, \quad (4.28)$$

where the $\{\epsilon_n\}$ usually emerge as Lagrange multipliers for the normalization condition of single-particle states. The eigenvalues ϵ_n are the so-called *Hartree-Fock single-particle energies* and will play an important role in the development of many-body perturbation theory.

The transformation of the eigenvalue equation (4.28) to the reference basis yields

$$\sum_r h_{pr}[\rho^{(1)}]D_{ir} = \epsilon_i D_{ip}. \quad (4.29)$$

Substitution of the mean-field Hamiltonian gives

$$\sum_r (H_{pr}^{[1]} + \sum_{qs} \sum_j \bar{H}_{pqrs}^{[2]} D_{js}^* D_{jq}) D_{ir} = \epsilon_i D_{ip} \quad (4.30)$$

The above equation (4.30) is the *Hartree-Fock equation* and constitutes a non-linear equation for the solution of the eigensystem of \hat{h} . The non-linearity requires the use of iterative procedures.

For a given A -body system the lowest single-particle energies are used to define the occupied states in the Hartree-Fock ground state with corresponding ground-state energy

$$E[|\text{HF}\rangle] = \langle \text{HF} | \hat{H} | \text{HF} \rangle \quad (4.31)$$

$$= \sum_i \epsilon_i - \frac{1}{2} \sum_{ij} \bar{H}_{ijij}^{[2]}, \quad (4.32)$$

where obviously the HF energy is not just the sum of single-particle energies.

4.3 BRILLOUIN'S THEOREM

Of central importance in applications of HF theory in perturbation theory is *Brillouin's theorem*. Assume we have solved the HF equation and obtained a set of single-particle states $\{|\varphi_i\rangle\}$ and the corresponding HF determinant $|\text{HF}\rangle$ containing the single-particle states with the lowest single-particle energies. *A priori* one might expect that the leading corrections to this mean-field wave function come from singly-excited determinants $|\text{HF}_i^a\rangle$. However, the matrix elements of the HF reference state with singly-excited determinants

$$\langle \text{HF} | \hat{H} | \text{HF}_i^a \rangle = H_{ia+}^{[1]} \sum_j \bar{H}_{ajij}^{[2]}. \quad (4.33)$$

is an off-diagonal matrix element of the Fock operator. By construction, the solution of the HF eigenvalue problem requires the off-diagonal matrix elements to satisfy

$$h_{ia} = 0. \tag{4.34}$$

Equivalently, solving the HF equation is the same as ensuring that the HF vacuum does not mix with singly-excited determinants. Note that Brillouin's theorem prevents the HF vacuum from *direct* mixing with singly-excited determinants. This does not mean that there are no singly-excited states in the exact ground-state wave function. Mixing can still appear indirectly via matrix elements of the type $\langle \Phi_i^a | \hat{H} | \Phi_{ij}^{ab} \rangle$.

The above statement has several important consequences—in particular for many-body perturbation theory. For example it follows that, when using Hartree-Fock single-particle states, there are no diagrams containing one-body vertices in Hartree-Fock many-body perturbation theory. This significantly reduces the number of diagrams and the implementational effort decreases considerably.

5

Formal Perturbation Theory

This section is devoted to the discussion of general aspects of perturbation theory [Sch26; SB09; SO82]. Perturbation theory (PT) can be separated into a *formal* part, which is concerned with the general ansatz and the development in terms of many-body states and operators. The complementary, *many-body part* of PT, which makes use of properties of a particular reference state and a choice of the unperturbed Hamiltonian, is postponed to the next section. It is possible to derive very deep results, such as the resolvent expansion, without making use of any second-quantization techniques.

We start with the introduction of the PT ansatz and derive working formulae for energy corrections in terms of the unperturbed many-body quantities. By further making use of projection operators we introduce the Rayleigh-Schrödinger resolvent and derive the resolvent expansion for the exact ground-state energy and wave function. We proceed with a discussion of general aspects of the choice of partitioning and the relation to the zero-order energies. After introducing the normal-product Schrödinger equation we make the connection to the many-body part of PT and introduce the diagrammatic notation for the evaluation of matrix elements of second-quantized operators. At the end, aspects which are not covered in this work are summarized and referenced for further reading.

5.1 THE PERTURBATIVE ANSATZ

We divide the nuclear Hamiltonian \hat{H} into a zero-order or unperturbed part \hat{H}_0 and a perturbation \hat{W} ,

$$\hat{H} = \hat{H}_0 + \hat{W}, \quad (5.1)$$

thus formally defining the perturbation by $\hat{W} = \hat{H} - \hat{H}_0$. The additive splitting of the perturbation operator is the so-called *partitioning*.

Introducing an auxiliary parameter λ yields a one-parameter family of operators

$$\hat{H}_\lambda = \hat{H}_0 + \lambda\hat{W}, \quad (5.2)$$

where the unperturbed problem is obtained by setting $\lambda = 0$. We write the exact solution as

$$\hat{H}|\Psi_n\rangle = E_n|\Psi_n\rangle, \quad (5.3)$$

the zero-order solution as

$$\hat{H}_0|\Phi_n\rangle = E_n^{(0)}|\Phi_n\rangle, \quad (5.4)$$

and we assume orthonormality of the unperturbed states,

$$\langle\Phi_m|\Phi_n\rangle = \delta_{mn}. \quad (5.5)$$

As ansatz for the exact energy and state solutions of (5.3) we write

$$E_n = \sum_{p=0}^{\infty} E_n^{(p)}\lambda^p, \quad (5.6)$$

$$|\Psi_n\rangle = \sum_{p=0}^{\infty} |\Psi_n^{(p)}\rangle\lambda^p. \quad (5.7)$$

In the following derivation we always work in *intermediate normalization*

$$\langle\Psi_m^{(0)}|\Psi_n\rangle = \delta_{mn}, \quad (5.8)$$

and, furthermore, assume the zero-order solution to be non-degenerate. From now on we will denote the unperturbed basis functions by

$$|\Psi_n^{(0)}\rangle = |\Phi_n\rangle, \quad (5.9)$$

to make the dependence of the perturbation order explicit. Substitution of the above power-series ansatz into the Schrödinger equation yields

$$\hat{H}_0|\Psi_n^{(0)}\rangle + \sum_{p=1}^{\infty} \lambda^p \left(\hat{W}|\Psi_n^{(p-1)}\rangle + \hat{H}_0|\Psi_n^{(p)}\rangle \right) = E_n^{(0)}|\Psi_n^{(0)}\rangle + \sum_{p=1}^{\infty} \lambda^p \left(\sum_{j=0}^p E_n^{(j)}|\Psi_n^{(p-j)}\rangle \right). \quad (5.10)$$

Multiplication from the left with $\langle \Psi_n^{(0)} |$ gives

$$\begin{aligned} \langle \Psi_n^{(0)} | \hat{H}_0 | \Psi_n^{(0)} \rangle + \sum_{p=1}^{\infty} \lambda^p \left(\langle \Psi_n^{(0)} | \hat{W} | \Psi_n^{(p-1)} \rangle + \langle \Psi_n^{(0)} | \hat{H}_0 | \Psi_n^{(p)} \rangle \right) \\ = E_n^{(0)} + \sum_{p=1}^{\infty} \lambda^p \left(\sum_{j=0}^p E_n^{(j)} \langle \Psi_n^{(0)} | \Psi_n^{(p-j)} \rangle \right). \end{aligned} \quad (5.11)$$

Using the eigenvalue relation of the unperturbed Hamiltonian \hat{H}_0 gives

$$\langle \Psi_n^{(0)} | \hat{W} | \Psi_n^{(p-1)} \rangle = E_n^{(p)}, \quad (5.12)$$

which shows that the p -th order energy correction can be calculated from the $(p-1)$ -th order state correction.

In order to derive expressions for the corresponding state corrections we note that by completeness of the unperturbed basis

$$| \Psi_n^{(p)} \rangle = \sum_m | \Psi_m^{(0)} \rangle \langle \Psi_m^{(0)} | \Psi_n^{(p)} \rangle. \quad (5.13)$$

Multiplication of (5.10) from the left with $\langle \Psi_m^{(0)} |$ for $m \neq n$,

$$\sum_{p=1}^{\infty} \lambda^p \left(\langle \Psi_m^{(0)} | \hat{W} | \Psi_m^{(p-1)} \rangle + \langle \Psi_m^{(0)} | \hat{H}_0 | \Psi_m^{(p)} \rangle \right) = \sum_{p=1}^{\infty} \lambda^p \left(\sum_{j=0}^p E_m^{(j)} \langle \Psi_m^{(0)} | \Psi_m^{(p-j)} \rangle \right), \quad (5.14)$$

where we used orthogonality of the unperturbed basis states. By uniqueness of the power series expansion, (5.14) must hold for arbitrary λ ,

$$\langle \Psi_m^{(0)} | \hat{W} | \Psi_m^{(p-1)} \rangle + \langle \Psi_m^{(0)} | \hat{H}_0 | \Psi_m^{(p)} \rangle = E_m^{(0)} \langle \Psi_m^{(0)} | \Psi_m^{(p)} \rangle + \sum_{j=1}^p E_m^{(j)} \langle \Psi_m^{(0)} | \Psi_m^{(p-j)} \rangle, \quad (5.15)$$

where we split the sum on the right-hand-side of the last equation. Solving for $\langle \Psi_m^{(0)} | \Psi_m^{(p)} \rangle$ gives

$$\langle \Psi_m^{(0)} | \Psi_m^{(p)} \rangle = \frac{1}{E_m^{(0)} - E_m^{(0)}} \cdot \left(\langle \Psi_m^{(0)} | \hat{W} | \Psi_m^{(p-1)} \rangle - \sum_{j=1}^p E_m^{(j)} \langle \Psi_m^{(0)} | \Psi_m^{(p-j)} \rangle \right). \quad (5.16)$$

To further simplify the above equations we expand the energy and state corrections in terms of zero-order states,

$$\langle \Psi_m^{(0)} | \Psi_m^{(p)} \rangle = \frac{1}{E_m^{(0)} - E_m^{(0)}} \cdot \left(\langle \Psi_m^{(0)} | \hat{W} | \Psi_m^{(p-1)} \rangle - \sum_{j=1}^p E_m^{(j)} \langle \Psi_m^{(0)} | \Psi_m^{(p-j)} \rangle \right),$$

$$= \frac{1}{E_n^{(0)} - E_m^{(0)}} \cdot \left(\sum_{m'} \langle \Psi_m^{(0)} | \hat{W} | \Psi_{m'}^{(0)} \rangle \langle \Psi_{m'}^{(0)} | \Psi_n^{(p-1)} \rangle - \sum_{j=1}^p E_n^{(j)} \langle \Psi_m^{(0)} | \Psi_n^{(p-j)} \rangle \right). \quad (5.17)$$

In the following we make use of the short-hand notation

$$C_{m,n}^{(p)} \equiv \langle \Psi_m^{(0)} | \Psi_n^{(p)} \rangle, \quad (5.18)$$

such that the energy corrections read

$$E_n^{(p)} = \sum_m \langle \Psi_n^{(0)} | \hat{W} | \Psi_m^{(0)} \rangle \cdot C_{m,n}^{(p-1)}. \quad (5.19)$$

With this we can expand the corresponding energy corrections explicitly. For the first-order state correction we get

$$|\Psi_n^{(1)}\rangle = \sum_m' \frac{\langle \Psi_n^{(0)} | \hat{W} | \Psi_m^{(0)} \rangle}{E_n^{(0)} - E_m^{(0)}} |\Psi_m^{(0)}\rangle, \quad (5.20)$$

where the prime at the summation sign indicates that the reference state has to be excluded from the summation. Plugging (5.20) into (5.19) gives the well-known form of the second-order energy correction

$$E_n^{(2)} = \langle \Psi_n^{(0)} | \hat{W} | \Psi_n^{(1)} \rangle = \sum_m' \frac{\langle \Psi_n^{(0)} | \hat{W} | \Psi_m^{(0)} \rangle \langle \Psi_m^{(0)} | \hat{W} | \Psi_n^{(0)} \rangle}{E_n^{(0)} - E_m^{(0)}} = \sum_m' \frac{|\langle \Psi_m^{(0)} | \hat{W} | \Psi_n^{(0)} \rangle|^2}{E_n^{(0)} - E_m^{(0)}}, \quad (5.21)$$

where all matrix elements are taken with respect to the unperturbed basis states.

5.2 DERIVATION OF THE RESOLVENT EXPANSION

In this section we derive a formal expression of the exact ground-state energy in terms of a resolvent operator. In the following we will omit the index n and always use the index 0 regardless whether this corresponds to the ground state or some excited state. We start again from the Schrödinger equation

$$(\hat{H}_0 + \hat{W})|\Psi\rangle = E|\Psi\rangle, \quad (5.22)$$

with a given zero-order solution

$$\hat{H}_0|\Phi_0\rangle = E_0^{(0)}|\Phi_0\rangle. \quad (5.23)$$

For the following discussion it is convenient to define *projection operators*

$$\hat{P} = |\Phi_0\rangle\langle\Phi_0|, \quad \hat{Q} = \sum_I' |\Phi_I\rangle\langle\Phi_I|. \quad (5.24)$$

Adding $E_0^{(0)}|\Psi\rangle$ to both sides of (5.22) gives

$$(E_0^{(0)} - \hat{H}_0)|\Psi\rangle = (\hat{W} - E + E_0^{(0)})|\Psi\rangle. \quad (5.25)$$

Applying \hat{Q} to both sides yields

$$\hat{Q}(E_0^{(0)} - \hat{H}_0)|\Psi\rangle = \hat{Q}(\hat{W} - E - E_0^{(0)})|\Psi\rangle, \quad (5.26)$$

and since \hat{H}_0 commutes with \hat{Q} and by idempotency we get

$$\hat{Q}(E_0^{(0)} - \hat{H}_0)|\Psi\rangle = \hat{Q}(E_0^{(0)} - \hat{H}_0)\hat{Q}|\Psi\rangle. \quad (5.27)$$

Expanding the operator $\hat{Q}(E_0^{(0)} - \hat{H}_0)\hat{Q}$ in terms of zero-order functions gives

$$\hat{Q}(E_0^{(0)} - \hat{H}_0)\hat{Q} = \sum_{ij}' |\Phi_i\rangle\langle\Phi_i|(E_0^{(0)} - \hat{H}_0)|\Phi_j\rangle\langle\Phi_j|. \quad (5.28)$$

We then define the inverse of the operator $\hat{Q}(E_0^{(0)} - \hat{H}_0)\hat{Q}$

$$\hat{R} = \frac{\hat{Q}}{E_0^{(0)} - \hat{H}_0} \equiv \sum_{ij}' |\Phi_i\rangle\langle\Phi_i|(E_0^{(0)} - \hat{H}_0)^{-1}|\Phi_j\rangle\langle\Phi_j|, \quad (5.29)$$

to be the (*Rayleigh-Schrödinger*) *resolvent* of \hat{H}_0 .

Since all solutions are expanded with respect to (orthonormal) eigenfunctions of \hat{H}_0 , the resolvent can be expressed as

$$\hat{R} = \sum_i' \frac{|\Phi_i\rangle\langle\Phi_i|}{E_0^{(0)} - E_i^{(0)}}. \quad (5.30)$$

Equation (5.26) can be reexpressed via

$$\hat{Q}(E_0^{(0)} - \hat{H}_0)\hat{Q}|\Psi\rangle = \hat{Q}(\hat{W} - E + E_0^{(0)})|\Psi\rangle. \quad (5.31)$$

Multiplication with \hat{R} yields

$$\hat{Q}|\Psi\rangle = \hat{R}(\hat{W} - E + E_0^{(0)})|\Psi\rangle. \quad (5.32)$$

By adding $|\Phi_0\rangle$ and substituting $|\Psi\rangle = |\Phi_0\rangle + \hat{Q}|\Psi\rangle$ on the left-hand side, we get an implicit equation for $|\Psi\rangle$:

$$|\Psi\rangle = |\Phi_0\rangle + \hat{R}(\hat{W} - E + E_0^{(0)})|\Psi\rangle. \quad (5.33)$$

Iteratively plugging (5.33) into (5.32) yields the *resolvent expansion*

$$|\Psi\rangle = \sum_{n=0}^{\infty} [\hat{R}(\hat{W} - E + E_0^{(0)})]^n |\Phi_0\rangle. \quad (5.34)$$

Equation (5.34) constitutes the central equation of the perturbation problem and is subsequently used to derive explicit expressions for low-order energy corrections in the Rayleigh-Schrödinger framework.

By left-projecting eq. (5.34) on $\langle\Phi_0|$ and using again that $\Delta E = E - E_0^{(0)}$, we obtain the Rayleigh-Schrödinger correlation expansion for the ground-state energy

$$\Delta E = \sum_{n=0}^{\infty} \langle\Phi_0|\hat{W}[\hat{R}(\hat{W} - \Delta E)]^n|\Phi_0\rangle. \quad (5.35)$$

However, due to the presence of the term $-E + E_0^{(0)}$ we do not have a true expansion in powers of the perturbation operator \hat{W} (but rather in powers of $(\hat{W} - \Delta E)$).

Expanding the first few powers gives

$$\begin{aligned} \Delta E &= \langle\Phi_0|\hat{W}|\Phi_0\rangle + \langle\Phi_0|\hat{W}\hat{R}(\hat{W} - \Delta E)|\Phi_0\rangle + \\ &+ \langle\Phi_0|\hat{W}\hat{R}(\hat{W} - \Delta E)\hat{R}(\hat{W} - \Delta E)|\Phi_0\rangle + \dots \end{aligned} \quad (5.36)$$

Since ΔE is just a number it commutes with \hat{R} yielding

$$\hat{R}\Delta E|\Phi_0\rangle = 0, \quad (5.37)$$

i.e., the action of the resolvent on the reference gives zero. Equation (5.36) takes the simpler form

$$\Delta E = \langle\Phi_0|\hat{W}|\Phi_0\rangle + \langle\Phi_0|\hat{W}\hat{R}\hat{W}|\Phi_0\rangle + \langle\Phi_0|\hat{W}\hat{R}(\hat{W} - \Delta E)\hat{R}\hat{W}|\Phi_0\rangle + \dots \quad (5.38)$$

Insertion of (5.36) and rearranging (5.38) according to the number of \hat{W} factors yields

$$\begin{aligned} \Delta E &= \langle\Phi_0|\hat{W}|\Phi_0\rangle + \langle\Phi_0|\hat{W}\hat{R}\hat{W}|\Phi_0\rangle \\ &+ \langle\Phi_0|\hat{W}\hat{R}\hat{W}\hat{R}\hat{W}|\Phi_0\rangle - \langle\Phi_0|\hat{W}|\Phi_0\rangle\langle\Phi_0|\hat{W}\hat{R}^2\hat{W}|\Phi_0\rangle + \dots \end{aligned} \quad (5.39)$$

Explicitly the lowest orders read

$$E^{(1)} = \langle\Phi_0|\hat{W}|\Phi_0\rangle,$$

$$\begin{aligned}
 E^{(2)} &= \langle \Phi_0 | \hat{W} \hat{R} \hat{W} | \Phi_0 \rangle, \\
 E^{(3)} &= \langle \Phi_0 | \hat{W} \hat{R} (\hat{W} - \langle \Phi_0 | \hat{W} | \Phi_0 \rangle) \hat{R} \hat{W} | \Phi_0 \rangle, \\
 E^{(4)} &= \langle \Phi_0 | \hat{W} \hat{R} (\hat{W} - \langle \Phi_0 | \hat{W} | \Phi_0 \rangle) \hat{R} (\hat{W} - \langle \Phi_0 | \hat{W} | \Phi_0 \rangle) \hat{R} \hat{W} | \Phi_0 \rangle - E^{(2)} \langle \Phi_0 | \hat{W} \hat{R}^2 \hat{W} | \Phi_0 \rangle.
 \end{aligned} \tag{5.40}$$

Due to the frequent appearance of

$$\hat{W} - \langle \Phi_0 | \hat{W} | \Phi_0 \rangle \tag{5.41}$$

we define the *shifted perturbation operator* $\hat{\tilde{W}}$

$$\hat{\tilde{W}}_{ij} = \hat{W}_{ij} - \delta_{ij} E^{(1)}, \tag{5.42}$$

which allows for the more compact expressions

$$\begin{aligned}
 E^{(1)} &= \langle \Phi_0 | \hat{W} | \Phi_0 \rangle, \\
 E^{(2)} &= \langle \Phi_0 | \hat{W} \hat{R} \hat{W} | \Phi_0 \rangle, \\
 E^{(3)} &= \langle \Phi_0 | \hat{W} \hat{R} \hat{\tilde{W}} \hat{R} \hat{W} | \Phi_0 \rangle, \\
 E^{(4)} &= \langle \Phi_0 | \hat{W} \hat{R} \hat{\tilde{W}} \hat{R} \hat{\tilde{W}} \hat{R} \hat{W} | \Phi_0 \rangle - E^{(2)} \langle \Phi_0 | \hat{W} \hat{R}^2 \hat{W} | \Phi_0 \rangle.
 \end{aligned} \tag{5.43}$$

The above equations will be the starting point for the many-body development of perturbation theory using diagrammatic techniques.

We note that another possibility is the use of the *Brillouin-Wigner resolvent*

$$\hat{R}_{BW} = \sum_i' \frac{|\Phi_i\rangle\langle\Phi_i|}{E - E_i^{(0)}}. \tag{5.44}$$

Since the exact eigenvalue appears implicitly in the denominator, the corresponding energy corrections have to be solved for iteratively. The advantage of this choice is that the resolvent expression reads

$$|\Psi\rangle = \sum_{m=0}^{\infty} [\hat{R} \hat{W}]^m |\Phi_0\rangle, \tag{5.45}$$

which defines a true expansion in powers of the perturbation \hat{W} . The simplification in the resolvent expansion, however, yields a perturbation theory that is not size-extensive when truncated at finite orders. Therefore, this choice is only scarcely used in actual applications. Low-order working formulae must be solved iteratively due to the appearance of E in the denominators.

5.3 PARTITIONING OF THE HAMILTONIAN

Up to now we did not specify the particular form of the perturbation operator \hat{W} . Most importantly, the specific choice of \hat{H}_0 remains to be fixed. Commonly, \hat{H}_0 is chosen as a diagonal one-body operator, which can be expanded in its eigenbasis $\{\hat{p}^\dagger\}$ according to

$$\hat{H}_0 = \sum_p \epsilon_p \hat{p}^\dagger \hat{p}, \quad (5.46)$$

where the quantities ϵ_p are called *single-particle energies* or sometimes *orbital energies*. In most applications single-particle energies are chosen as diagonal elements

$$\epsilon_p = f_{pp} \quad (5.47)$$

of a suitably chosen *Fock operator*

$$\hat{F} = \sum_{pq} f_{pq} \hat{p}^\dagger \hat{q}. \quad (5.48)$$

With this, the perturbation operator $\hat{W} = \hat{H} - \hat{H}_0$ consists of one- and two-body parts

$$\hat{W} = \hat{W}^{[1B]} + \hat{W}^{[2B]}, \quad (5.49)$$

written in second-quantized form

$$\hat{W} = \sum_{pq} (h_{pq} - \epsilon_p \delta_{pq}) \hat{c}_p^\dagger \hat{c}_q + \frac{1}{4} \sum_{pqrs} \bar{H}_{pqrs}^{[2]} \hat{c}_p^\dagger \hat{c}_q^\dagger \hat{c}_s \hat{c}_r. \quad (5.50)$$

The advantage of using a diagonal zero-order Hamiltonian comes from knowing a complete set of eigenfunctions of \hat{H}_0 . This is the case of *diagonal perturbation theory* and all our investigations are based on choosing a diagonal zero-order Hamiltonian. When using a set of orthonormal single-particle states $\{|\varphi_i\rangle\}$ to construct the many-body SDs one finds that

$$\hat{H}_0 |\varphi_1, \dots, \varphi_A\rangle = \sum_i^A \epsilon_i |\varphi_1, \dots, \varphi_A\rangle \quad (5.51)$$

such that the zero-order energies of the SDs are given by

$$E_0^{(0)} = \sum_i \epsilon_i, \quad (5.52)$$

where the sum runs over all hole states of the corresponding SD. Furthermore, for the zero-order energy of a particle-hole excitation holds

$$\hat{H}_0|\Phi_{i_1 \dots i_p}^{a_1 \dots a_p}\rangle = \left(E_0^{(0)} + \epsilon_{a_1} + \dots + \epsilon_{a_p} - \epsilon_{i_1} + \dots + \epsilon_{i_p}\right)|\Phi_{i_1 \dots i_p}^{a_1 \dots a_p}\rangle. \quad (5.53)$$

The above choice of \hat{H}_0 and the unperturbed energies defines the *Møller-Plesset* (MP) *partitioning*.

Starting from the Rayleigh-Schrödinger resolvent expansion other partitionings of the Hamiltonian can be used. Alternatively, the diagonal part of the many-body Hamiltonian with respect to a fixed basis representation is used for \hat{H}_0

$$\begin{aligned} \hat{H}_0 &= \sum_i |\Phi_i\rangle\langle\Phi_i|\hat{H}|\Phi_i\rangle\langle\Phi_i| \\ &= \sum_i |\Phi_i\rangle E_i \langle\Phi_i|. \end{aligned} \quad (5.54)$$

The many-body states $\{|\Phi_i\rangle\}$ constitute eigenstates of \hat{H}_0 according to

$$\hat{H}_0|\Phi_i\rangle = E_i|\Phi_i\rangle. \quad (5.55)$$

This type of partitioning is called *Epstein-Nesbet* (EN) *partitioning* and results in shifted denominators due to the appearance of $\hat{H}_0 - E_i$ in the Rayleigh-Schrödinger resolvent. However, in the following we will not investigate this type of partitioning.

5.4 THE NORMAL-PRODUCT SCHRÖDINGER EQUATION

After discussing general aspects of MBPT and the partitioning we will cast the stationary Schrödinger equation into a form that is more convenient for the diagrammatic analysis that follows. In particular, this will allow for elimination of the first-order energy correction from our analysis. We start again from

$$(\hat{H}_0 + \hat{W})|\Psi\rangle = E|\Psi\rangle \quad (5.56)$$

and subtract

$$\langle\Phi|\hat{H}|\Phi\rangle = \langle\Phi|\hat{H}_0|\Phi\rangle + \langle\Phi|\hat{W}|\Phi\rangle \quad (5.57)$$

giving

$$\begin{aligned} \hat{H} - \langle\Phi|\hat{H}|\Phi\rangle &= (\hat{H}_0 - \langle\Phi|\hat{H}_0|\Phi\rangle) + (\hat{W} - \langle\Phi|\hat{W}|\Phi\rangle) \\ (\hat{H} - E_{\text{ref}}) &= (\hat{H}_0 - E^{(0)}) + \hat{W}_N. \end{aligned} \quad (5.58)$$

where $E^{(0)}$ is the unperturbed eigenvalue and E_{ref} the expectation value of the reference state with respect to the full Hamiltonian, i.e., $E^{(0)} + E^{(1)}$. In this scheme we define a new

zero-order Hamiltonian $\hat{H}_0 - E^{(0)} = (\hat{H}_0)_N$ leaving \hat{W} as the perturbation operator and $\hat{H} - E_{\text{ref}}$ as the full Hamiltonian. This yields the *normal-product Schrödinger equation*

$$\hat{H}_N|\Psi\rangle = \Delta E|\Psi\rangle, \quad (5.59)$$

with energy eigenvalue

$$\Delta E = E - E_{\text{ref}}. \quad (5.60)$$

The quantity ΔE captures corrections beyond the reference-state description. When using a HF reference state ΔE corresponds to the *correlation energy*.

5.5 DIAGRAMMATIC REPRESENTATION

The aim of this section is to develop tools for the evaluation of low-order energy corrections. For example the second-order energy correction can be written as

$$E^{(2)} = \sum_I' \frac{\langle \Phi | \hat{W} | \Phi_I \rangle \langle \Phi_I | \hat{W} | \Phi \rangle}{E_0^{(0)} - E_I^{(0)}} \quad (5.61)$$

where $|\Phi_I\rangle$ denote excited SD with respect to $|\Phi\rangle$. When using up to two-body interactions, we can rewrite (5.61) as

$$E^{(2)} = \sum_{ai} \frac{\langle \Phi | \hat{W} | \Phi_i^a \rangle \langle \Phi_i^a | \hat{W} | \Phi \rangle}{E_0^{(0)} - E^{(0)}(|\Phi_i^a\rangle)} + \sum_{abij} \frac{\langle \Phi | \hat{W} | \Phi_{ij}^{ab} \rangle \langle \Phi_{ij}^{ab} | \hat{W} | \Phi \rangle}{E_0^{(0)} - E^{(0)}(|\Phi_{ij}^{ab}\rangle)} \quad (5.62)$$

and evaluate the matrix elements in the numerator, e.g., via Wick's theorem. However, when going beyond second-order the derivation becomes very tedious due to the large number of contractions to be considered. For example consider the evaluation of the following matrix element that appears at third-order PT,

$$\langle \Phi_i^a | \hat{W} | \Phi_j^b \rangle = \frac{1}{4} \sum_{pqrs} \bar{H}_{pqrs}^{[2]} \langle \Phi | \{ \hat{c}_i^\dagger \hat{c}_a \} \{ \hat{c}_p^\dagger \hat{c}_q^\dagger \hat{c}_s \hat{c}_r \} \{ \hat{c}_b^\dagger \hat{c}_j \} | \Phi \rangle. \quad (5.63)$$

which yields according to Wick's theorem

$$\begin{aligned} \langle \Phi_i^a | \hat{W} | \Phi_j^b \rangle &= \frac{1}{4} \sum_{pqrs} \bar{H}_{pqrs}^{[2]} \langle \Phi | \{ \hat{c}_i^\dagger \hat{c}_a \} \{ \hat{c}_p^\dagger \hat{c}_q^\dagger \hat{c}_s \hat{c}_r \} \{ \hat{c}_b^\dagger \hat{c}_j \} | \Phi \rangle \\ &= \frac{1}{4} \sum_{pqrs} \bar{H}_{pqrs}^{[2]} \left(\langle \Phi | \{ \hat{c}_i^\dagger \hat{c}_a \} \{ \hat{c}_p^\dagger \hat{c}_q^\dagger \hat{c}_s \hat{c}_r \} \{ \hat{c}_b^\dagger \hat{c}_j \} | \Phi \rangle + \langle \Phi | \{ \hat{c}_i^\dagger \hat{c}_a \} \{ \hat{c}_p^\dagger \hat{c}_q^\dagger \hat{c}_s \hat{c}_r \} \{ \hat{c}_b^\dagger \hat{c}_j \} | \Phi \rangle \right) \end{aligned}$$

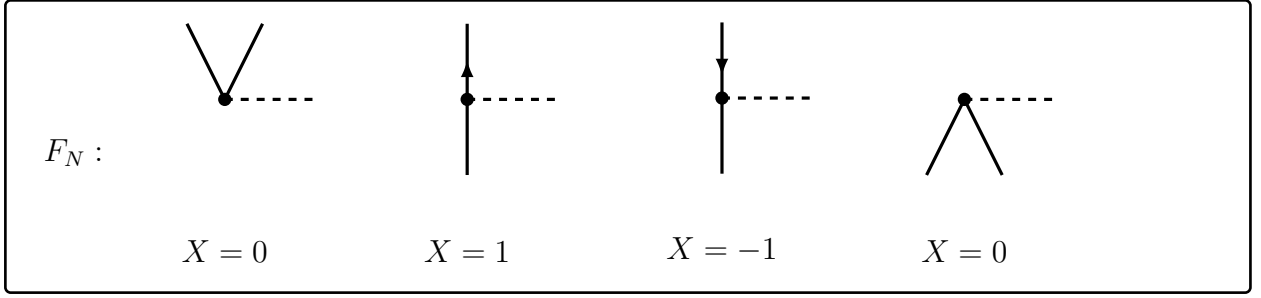


Figure 5.1: Goldstone diagrams representing the Fock operator \hat{F}_N .

$$\begin{aligned}
 & + \langle \Phi | \{ \hat{c}_i^\dagger \hat{c}_a \} \{ \hat{c}_p^\dagger \hat{c}_q^\dagger \hat{c}_s \hat{c}_r \} \{ \hat{c}_b^\dagger \hat{c}_j \} | \Phi \rangle + \langle \Phi | \{ \hat{c}_i^\dagger \hat{c}_a \} \{ \hat{c}_p^\dagger \hat{c}_q^\dagger \hat{c}_s \hat{c}_r \} \{ \hat{c}_b^\dagger \hat{c}_j \} | \Phi \rangle \\
 & = \frac{1}{4} \left[-\bar{H}_{ajbi}^{[2]} + \bar{H}_{ajib}^{[2]} + \bar{H}_{jab i}^{[2]} - \bar{H}_{jaib}^{[2]} \right] \\
 & = \bar{H}_{ajib}^{[2]}. \tag{5.64}
 \end{aligned}$$

where we made use of the Standard Wick theorem as stated in chapter 1. We note that equally the above matrix element could have been evaluated by means of Slater rules [Sla29; Con30].

It is clear that the evaluation of matrix elements of SDs with higher excitation rank becomes increasingly more cumbersome and a more systematic way of evaluating such expressions is desirable. The diagrammatic approach outlined below considerably lowers the effort of deriving MBPT formulae. We will not go into too much detail but only introduce the notation necessary for the derivation of energy corrections in Hartree-Fock MBPT and Multi-Configurational MBPT. The interested reader is referred to [SB09] for more information and an introduction to the application of diagrams in Coupled-Cluster theory.

The diagrammatic representation of the normal-ordered perturbation operator is displayed in Figure 5.1 and Figure 5.2. For every topology there exist an excitation rank X depending on the number of upgoing and downgoing lines. Consider now that we want to evaluate an expectation value with respect to the reference state $|\Phi\rangle$ of a product of two two-body operators

$$\langle \Phi | \hat{W} \hat{W} | \Phi \rangle. \tag{5.65}$$

Since the formula is closed from the left and right by the reference state the corresponding diagrams will be closed from above and below, i.e., the excitation rank X of the left operator must be -2 and the excitation rank of the right operator must be $+2$. There exists in each case only one topology. In the following picture vertical dotted lines correspond to contractions of single-particle indices:

We refer to the object on the right-hand side as an *anti-symmetrized Goldstone* (ASG)

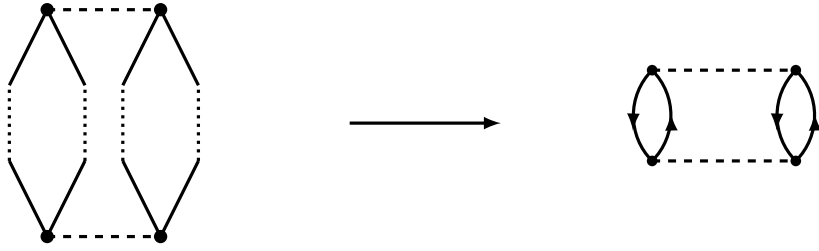
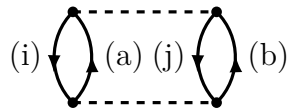


diagram. To complete the description of the diagrams the edges must be labelled by single-particle indices. Downgoing lines are labeled with hole indices, whereas upgoing lines are labelled by particle indices. The fully labelled ASG diagram reads



The rules for the evaluation are as follows:

Diagrammatic Rules for the Evaluation of Matrix Elements

1. Every vertex corresponds to an anti-symmetric matrix element, where the corresponding single-particle indices are read from left to right:

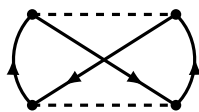
$$\langle \text{1st incoming line, 2nd incoming line} | \dots | \text{1st outgoing line, 2nd outgoing line} \rangle.$$

2. Add a prefactor $\frac{1}{2}$ for every pair of equivalent lines, i.e., lines connecting the same vertices.
3. The sign of the expression is given by $(-1)^{h+l}$ where h is given by the number of hole lines and l the number of closed loops.
4. Sum over all internal single-particle indices.

With this the above diagram evaluates to

$$\frac{1}{4} \sum_{abij} \bar{H}_{abij}^{[2]} \bar{H}_{ijab}^{[2]} \tag{5.66}$$

Note that we could have equally well contracted in the following way



leading to the expression

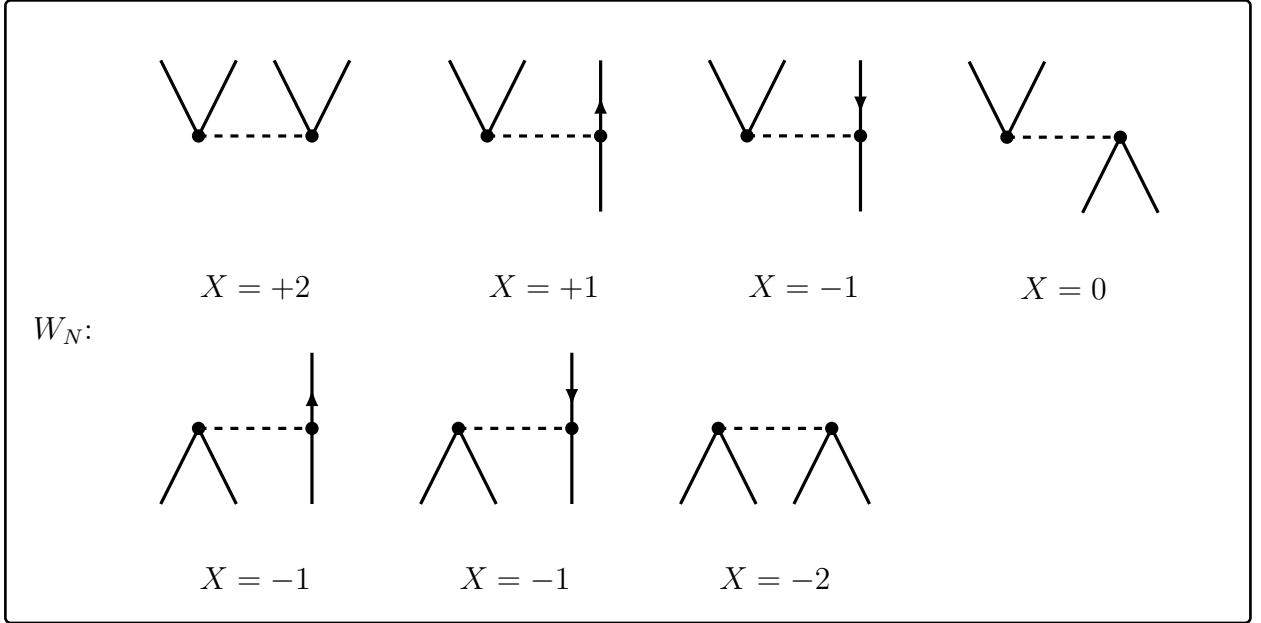


Figure 5.2: Anti-symmetrized Goldstone diagrams representing the 2B-part of the perturbation operator \hat{W}_N .

$$-\frac{1}{4} \sum_{abij} \bar{H}_{abij}^{[2]} \bar{H}_{ijba}^{[2]}, \quad (5.67)$$

which is by anti-symmetry of the matrix elements equivalent to (5.66). Therefore, one only needs to take one of the possible contraction schemes into account since all give the same contribution. More complex expressions, e.g.,

$$\langle \Phi | \hat{W}^3 | \Phi \rangle \quad (5.68)$$

can be evaluated by drawing all of the corresponding diagrams and summing up their individual contributions.

From the resolvent expansion we see that—in addition to higher powers of the perturbation operator—(5.35) contains the resolvent operator \hat{R} . Therefore, working formulae require the evaluation of

$$\langle \Phi | \hat{W} \hat{R} \hat{W} | \Phi \rangle \quad (5.69)$$

rather than $\langle \Phi | \hat{W}^2 | \Phi \rangle$. We, therefore, need a diagrammatic expansion of the resolvent operators

$$\hat{R} = \sum_I' \frac{|\Phi_I\rangle \langle \Phi_I|}{E_0^{(0)} - E_I^{(0)}} \quad (5.70)$$

where the sum is taken over all many-body states other than the reference state.¹ The operation of \hat{R} on a many-body SD $|\Phi_J\rangle$ gives

$$\begin{aligned}\hat{R}|\Phi_J\rangle &= \sum_I \frac{|\Phi_I\rangle\langle\Phi_I|\Phi_J\rangle}{E_0^{(0)} - E_I^{(0)}} \\ &= \sum_I |\Phi_I\rangle \frac{\delta_{IJ}}{E_0^{(0)} - E_I^{(0)}} \\ &= |\Phi_J\rangle \frac{1}{E_0^{(0)} - E_J^{(0)}}\end{aligned}\tag{5.71}$$

In the case of a single-configurational reference state the energy denominator reads

$$\epsilon_{i_1 \dots i_p}^{a_1 \dots a_p} = E^{(0)} - E_J^{(0)} = \epsilon_{i_1} + \dots + \epsilon_{i_p} - \epsilon_{a_1} + \dots + \epsilon_{a_p},\tag{5.72}$$

where $|J\rangle = |\Phi_{i_1 \dots i_p}^{a_1 \dots a_p}\rangle$. This concludes the formal development of MBPT.

5.6 REMARKS AND FURTHER READING

We covered an introduction of the formal aspects of MBPT. There are, however, many interesting features that we did not cover at all or only briefly mentioned in a side remark. One big topic is the use of MBPT formulations other than the Rayleigh-Schrödinger framework. The most important alternative is the Brillouin-Wigner perturbation theory as well as their relation to Coupled-Cluster theory. Even though not being size-extensive at finite order, there exist *a-posteriori* corrections to account for the lack of size-extensivity making it still a viable approach which is simpler due to the missing renormalization terms in the corresponding resolvent expansion. A discussion of the advantages and disadvantages can be found for example in the monograph by Hubac and Wilson [HW10].

Furthermore, all MBPT variants employed in this work are of single-reference type, meaning that we use one reference state for each individual calculation. There is a vast literature on *multi-reference many-body perturbation theory*, where n different SDs are taken as reference states. One constructs an *effective Hamiltonian* of dimension $n \times n$ which captures correlation effects by resumming Q-space effects into the effective Hamiltonian. A subsequent diagonalization yields the associated spectrum. For application in nuclear physics see for example [Hol⁺12]. There have also been extensive studies in the quantum chemistry literature on how to construct the Hamiltonian and which SDs to include in the construction. Typically, one includes all many-body states that can be formed from a fixed valence space of single-particle states leading to so-called *complete active space* (CAS) formulation of multi-reference MBPT. More general frameworks, where only a selected number of many-

¹Note we restrict ourselves to the case of a diagonal resolvent as already mentioned before. Equation (5.70) can be seen as the spectral resolution of \hat{R} in Q-space.

body configurations is included in the unperturbed basis yield the more advanced *incomplete active space* (IAS) methods, which can overcome some of the limitations of CAS approaches, but are conceptually more complicated. For an overview and present status of multi-reference MBPT in quantum chemistry see for example [Cha⁺16].

We remark that the term *multi-reference* specifies the number of reference states and not whether the reference states are single Slater determinants or more complex objects. Typically multi-reference approaches use several SDs as reference. However, there are also investigations of multi-reference MBPT with reference state which themselves are superpositions of SDs, see for example [Nak93]. Contrary, the term *multi-configurational* (or rarely *multi-determinantal*) specifies the structure of the reference state, i.e., if the reference state is a single SD or a superposition of SDs.

The development so far used an time-independent formalism. Another important variant are *time-dependent* approaches [Bru55; Gol57]. These were originally used to derive the linked-cluster expansion in terms of the time-evolution operator. In Part IV of this thesis, we will go into the details that are necessary for the use of symmetry-broken reference states.

Other than that, there are several more exotic variants of MBPT that get rid of the restriction to diagonal resolvent operators. The evaluation of energy corrections requires the inversion and, therefore, diagonalization of the many-body resolvent which is computationally demanding, but yields the additional freedom of using zero-order Hamiltonians which are non-diagonal one-body operators. Further, one is not restricted to using one-body operators as the unperturbed part of the Hamiltonian but can choose a more general ansatz.

6

Single-Configurational Many-Body Perturbation Theory

In the previous chapter we presented the fundamentals of many-body perturbation theory without specifying a particular reference state. In the simplest version, MBPT is performed on top of single Slater determinant. In such an approach we can efficiently investigate closed-shell nuclei. Additionally, the restriction to closed-shell systems allows for the use of angular-momentum coupling techniques, which enable for an efficient evaluation of MBPT formulas in a J -coupled framework. We further discuss computational details of the implementation that allow us to proceed to the heavy-mass regime. We conclude with a qualitative discussion of limitations of single-configurational perturbation theories and the reasons for their possible failure in actual applications in open-shell systems.

6.1 DERIVATION OF LOW-ORDER FORMULAS

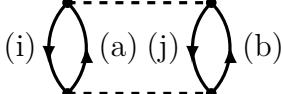
The resolvent expansion (5.35) derived in the previous chapter is the starting point for the diagrammatic treatment. We will explicitly derive all second- and third-order diagrams for an arbitrary reference determinant.

6.1.1 SECOND-ORDER ENERGY

From the resolvent expansion (5.35) we get for the second-order energy correction

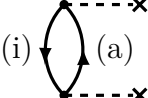
$$E^{(2)} = \langle \Phi | \hat{W} \hat{R} \hat{W} | \Phi \rangle. \quad (6.1)$$

The only two-body contribution appearing at second-order is given



$$\frac{1}{4} \sum_{abij} \frac{\langle ab | \hat{H}^{[2]} | ij \rangle \langle ij | \hat{H}^{[2]} | ab \rangle}{\epsilon_{ij}^{ab}}$$

where it is clear from the denominator that this diagrams corresponds to double-excited intermediate states. Additionally, we get a one-body contribution from the normal-ordered one-body part of the perturbation operator



$$\sum_{ai} \frac{\langle a | \hat{H}^{[1]} | i \rangle \langle i | \hat{H}^{[1]} | a \rangle}{\epsilon_i^a}$$

The last diagram corresponds to a singly-excited intermediate state. When using canonical HF single-particle states the last diagram does not contribute due to Brillouins theorem and we are left with the two-body contribution only. We also note that the second-order energy correction in the HF case is always negative since the expression in numerator is a square of a real quantity and the energy denominator ϵ_{ij}^{ab} is always negative by the construction of the hole states.¹

6.1.2 THIRD-ORDER ENERGY

From (5.35) we obtain for the third-order energy correction

$$E^{(3)} = \langle \Phi | \hat{W} \hat{R} \hat{W} \hat{R} \hat{W} | \Phi \rangle. \quad (6.2)$$

Instead of two matrix elements and one resolvent line we now have three matrix elements and two resolvent lines. When a HF single-particle basis is used, the only contributions come from diagrams containing two-body operators. One-body contribution vanish since intermediate states are eigenstates of the one-body part of the Hamiltonian. The corresponding diagrams and their algebraic expressions are displayed in Figure 6.1. When using a reference determinant that is not written in HF single-particle basis Brillouins theorem does not hold and we get additional contributions from diagrams containing a one-body operator. The additional eleven diagrams are shown in Figures 6.2 and 6.3, respectively.

From the third-order energy correction it is immediately clear that the use of HF orbitals simplifies the diagrammatic treatment significantly and the number of non-HF diagrams increases rapidly. Since we do not go beyond third-order in the calculations of medium-mass nuclei we do not show the fourth-order energy diagrams. The interested reader is referred to [SB09] for a complete list of HF and non-HF diagrams appearing at fourth-order MBPT.

¹We defined the hole states to be the single-particle states with the lowest single-particle energies.

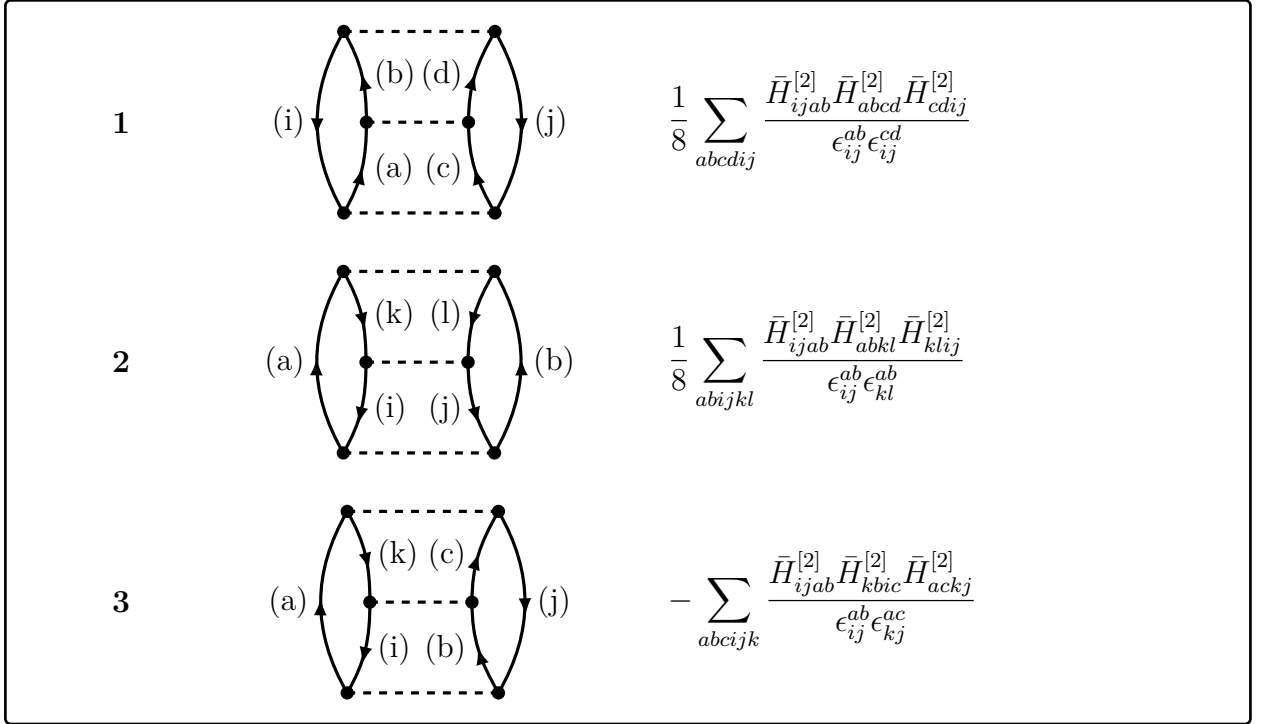


Figure 6.1: Anti-symmetrized Goldstone diagrams appearing at third-order MBPT when using a canonical HF reference state.

In summary, the second and third-order energy corrections for a HF reference determinant are given by

$$E^{(2)} = \frac{1}{4} \sum_{abij} \frac{\bar{H}_{abij}^{[2]} \bar{H}_{ijab}^{[2]}}{\epsilon_{ij}^{ab}} \quad (6.3)$$

$$E^{(3)} = \frac{1}{8} \sum_{abcdij} \frac{\bar{H}_{ijab}^{[2]} \bar{H}_{abcd}^{[2]} \bar{H}_{cdij}^{[2]}}{\epsilon_{ij}^{ab} \epsilon_{ij}^{cd}} \quad (6.4)$$

$$+ \frac{1}{8} \sum_{abijkl} \frac{\bar{H}_{ijab}^{[2]} \bar{H}_{abkl}^{[2]} \bar{H}_{kl ij}^{[2]}}{\epsilon_{ij}^{ab} \epsilon_{kl}^{ab}} \quad (6.5)$$

$$- \sum_{abcijk} \frac{\bar{H}_{ijab}^{[2]} \bar{H}_{kbic}^{[2]} \bar{H}_{ackj}^{[2]}}{\epsilon_{ij}^{ab} \epsilon_{kj}^{ac}}. \quad (6.6)$$

The above formula are implemented for the calculation of ground-state energies of medium-mass closed-subshell nuclei.

6.2 ANGULAR-MOMENTUM COUPLING

When proceeding to larger model spaces, the dimension of the single-particle basis becomes very large and calculations beyond second-order become impractical for heavy systems.

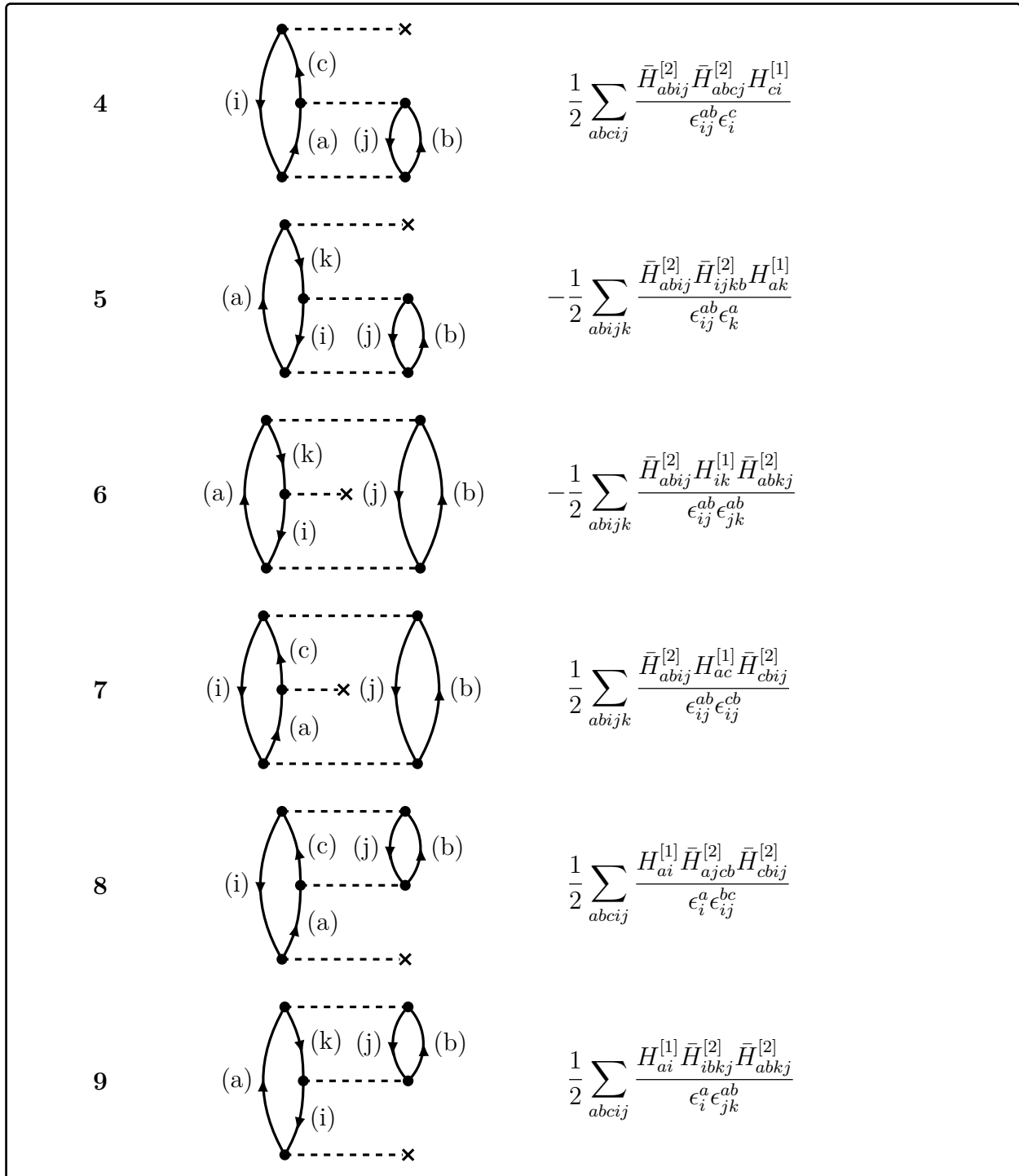


Figure 6.2: Hugenholtz diagrams appearing at third-order MBPT when using a non-canonical HF reference state.

Therefore, we use angular-momentum coupling techniques to cast the expressions for the energy corrections into spherical form. In the following we make use of the Baranger notation

$$k = (n_k, l_k, j_k, t_k, m_k) = (\tilde{k}, m_k), \quad (6.7)$$

where a collective single-particle index k is split into a spherical (i.e. m -independent) part \tilde{k} and its total angular-momentum projection m_k . The index \tilde{k} contains all information on the radial quantum number k_n , the orbital angular momentum n_l , total angular momentum j_k and isospin projection t_k .

We write the second-order energy correction by

$$\begin{aligned} E^{(2)} &= \frac{1}{4} \sum_{abij} \frac{\bar{H}_{abij}^{[2]} \bar{H}_{ijab}^{[2]}}{\epsilon_{ij}^{ab}} \\ &= \frac{1}{4} \sum_{\tilde{a}\tilde{b}\tilde{i}\tilde{j}} \sum_{m_a m_b} \sum_{\substack{J J' \\ M M'}} \frac{J H_{\tilde{a}\tilde{b}\tilde{i}\tilde{j}}^{[2]} J' H_{\tilde{i}\tilde{j}\tilde{a}\tilde{b}}^{[2]}}{\epsilon_{\tilde{i}\tilde{j}}^{\tilde{a}\tilde{b}}} \begin{pmatrix} j_a & j_b & J \\ m_a & m_b & M \end{pmatrix} \begin{pmatrix} j_a & j_b & J' \\ m_a & m_b & M' \end{pmatrix} \begin{pmatrix} j_i & j_j & J \\ m_i & m_j & M \end{pmatrix} \begin{pmatrix} j_i & j_j & J' \\ m_i & m_j & M' \end{pmatrix} \\ &= \frac{1}{4} \sum_{\tilde{a}\tilde{b}\tilde{i}\tilde{j}} \sum_{\substack{J J' \\ M M'}} \frac{J H_{\tilde{a}\tilde{b}\tilde{i}\tilde{j}}^{[2]} J' H_{\tilde{i}\tilde{j}\tilde{a}\tilde{b}}^{[2]}}{\epsilon_{\tilde{i}\tilde{j}}^{\tilde{a}\tilde{b}}} \delta_{J J'} \delta_{M M'} \\ &= \frac{1}{4} \sum_{\tilde{a}\tilde{b}\tilde{i}\tilde{j}} \sum_J \hat{j}^2 \frac{J H_{\tilde{a}\tilde{b}\tilde{i}\tilde{j}}^{[2]} J H_{\tilde{i}\tilde{j}\tilde{a}\tilde{b}}^{[2]}}{\epsilon_{\tilde{i}\tilde{j}}^{\tilde{a}\tilde{b}}}, \end{aligned} \quad (6.8)$$

where we used the definition of J -coupled matrix elements $J H_{\tilde{a}\tilde{b}\tilde{i}\tilde{j}}^{[2]}$ according to (1.28) and the orthogonality relation of the Clebsch-Gordan coefficients, as well as the notion of the hat-symbol $\hat{J} = \sqrt{2J+1}$ to account for the correct multiplicities. Note that for a closed-shell nucleus the HF single-particle energies are independent of the total angular-momentum projection, i.e., $\epsilon_{\tilde{i}\tilde{j}}^{\tilde{a}\tilde{b}} = \epsilon_{ij}^{ab}$.

COUPLING OF THE THIRD-ORDER ENERGY

Two of the three HF diagrams at third-order MBPT can coupled analogously to the second-order case. For the particle-hole channel, however, additional effort is needed. We define the so-called *generalized Pandya transformation* of a two-body operator by

$$J H_{abcd}^{XC} \equiv - \sum_{J'} \hat{j}^2 \begin{Bmatrix} j_a & j_b & J \\ j_c & j_d & J' \end{Bmatrix} J' H_{adcb}^{[2]}, \quad (6.9)$$

which allows for a recoupling of bra and ket indices [Suh07]. With this the J -coupled expressions of the third-order HF-MBPT energy correction are synthesized as follows:

$$\begin{aligned}
 E^{(3)} = & \frac{1}{8} \sum_{\tilde{a}\tilde{b}\tilde{c}\tilde{d}\tilde{i}\tilde{j}} \sum_J \hat{j}^2 \frac{J H_{\tilde{a}\tilde{b}\tilde{i}\tilde{j}}^{[2]} J H_{\tilde{i}\tilde{j}\tilde{c}\tilde{d}}^{[2]} J H_{\tilde{c}\tilde{d}\tilde{a}\tilde{b}}^{[2]}}{\epsilon_{\tilde{i}\tilde{j}}^{\tilde{a}\tilde{b}} \epsilon_{\tilde{i}\tilde{j}}^{\tilde{c}\tilde{d}}} \\
 & + \frac{1}{8} \sum_{\tilde{a}\tilde{b}\tilde{i}\tilde{j}\tilde{k}\tilde{l}} \sum_J \hat{j}^2 \frac{J H_{\tilde{i}\tilde{j}\tilde{a}\tilde{b}}^{[2]} J H_{\tilde{a}\tilde{b}\tilde{k}\tilde{l}}^{[2]} J H_{\tilde{k}\tilde{l}\tilde{i}\tilde{j}}^{[2]}}{\epsilon_{\tilde{i}\tilde{j}}^{\tilde{a}\tilde{b}} \epsilon_{\tilde{k}\tilde{l}}^{\tilde{a}\tilde{b}}} \\
 & - \sum_{\tilde{a}\tilde{b}\tilde{c}\tilde{i}\tilde{j}\tilde{k}} \sum_J \hat{j}^2 \frac{J H_{\tilde{a}\tilde{r}\tilde{s}\tilde{b}}^{XC} J H_{\tilde{s}\tilde{b}\tilde{t}\tilde{c}}^{XC} J H_{\tilde{t}\tilde{c}\tilde{a}\tilde{r}}^{XC}}{\epsilon_{\tilde{i}\tilde{j}}^{\tilde{a}\tilde{b}} \epsilon_{\tilde{k}\tilde{j}}^{\tilde{a}\tilde{c}}}
 \end{aligned}$$

The derivations of the J -coupled matrix energy expressions can be found in Appendix A.

6.3 COMPUTATIONAL CONSIDERATIONS

After deriving the m -scheme and J -scheme expressions we want to investigate some of the computational consequences and scaling properties. The second-order energy correction in HF-MBPT contains two particle summations and two hole summations. We will denote the computational scaling by

$$\text{HF-MBPT}(2) \sim n_p^2 \cdot n_h^2, \quad (6.11)$$

where n_p denotes the number of particle states and n_h denotes the number of holes states respectively. Without distinguishing particles and holes we will refer to this as a N^4 process.

² The one-body contribution at second-order contains one particle and one hole summation resulting in a subleading contribution with computational cost $\sim n_p \cdot n_h$ or roughly a N^2 process. We see that even though the use of a HF determinant lowers the numbers of contributing diagrams the computational costs are dominated by the two-body contribution. Therefore, using a HF reference will prevent the proliferation of diagrams but will not improve upon the scaling properties of the theory.

When proceeding to third-order HF-MBPT we see that every diagram contains six single-particle summations thus making MBPT(3) a N^6 process or more precisely

$$\text{HF-MBPT}(3) \sim \max\{n_p^4 \cdot n_h^2, n_p^2 \cdot n_h^4\}, \quad (6.12)$$

where again for large model spaces the first term dominates.

One can see from the resolvent expansion that the n -th order energy correction contains n operator products of two-body operators. For n -th order HF-MBPT one gets naively

²In actual calculation one often has $n_p \gg n_h$. However, for a rough estimate of the computational complexity it is sufficient to know the overall power of the many-body theory under consideration.

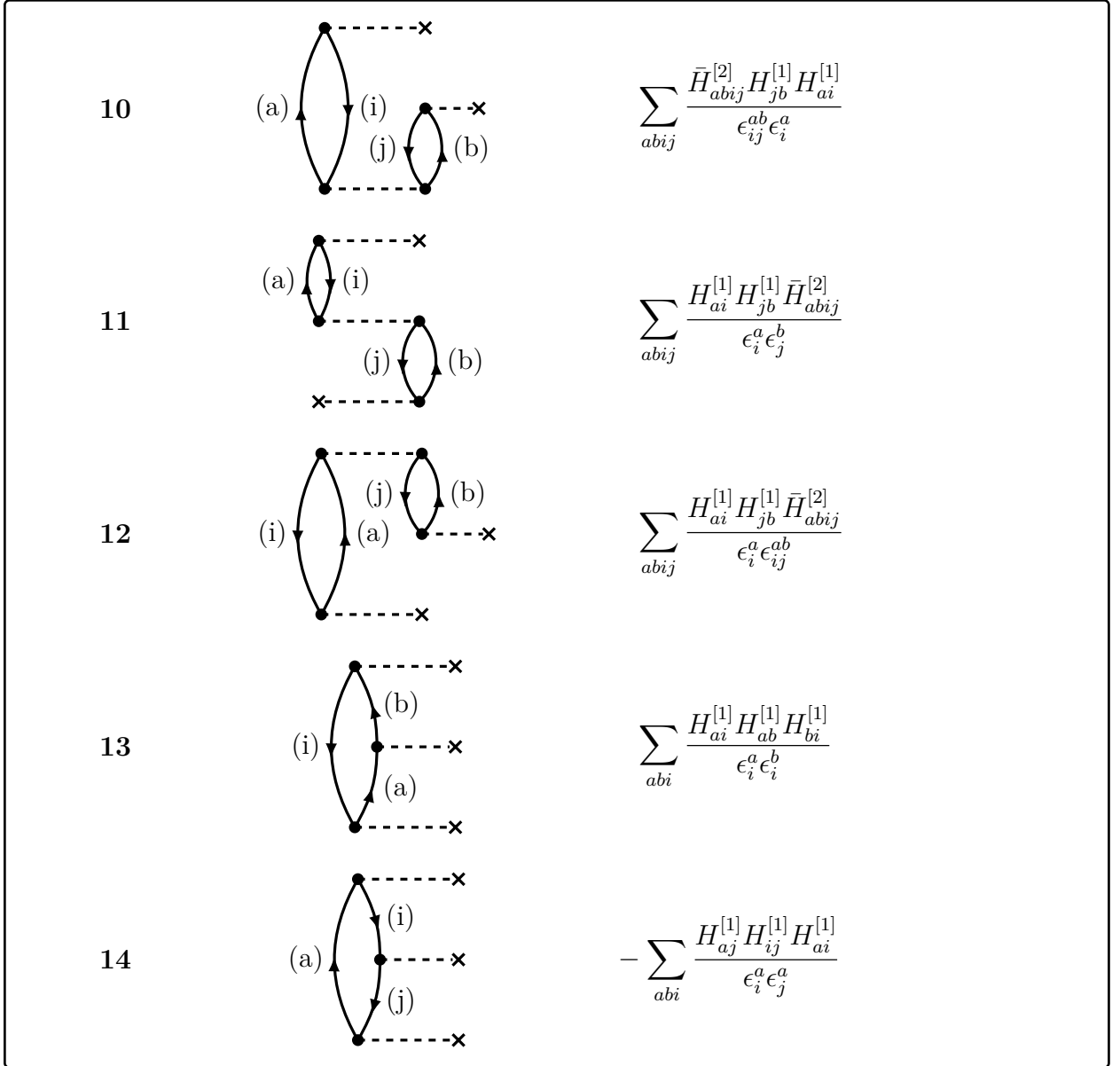


Figure 6.3: Anti-symmetrized Goldstone diagrams appearing at third-order MBPT when using a non-canonical HF reference state (continued).

$$\text{HF-MBPT}(n) \sim N^{2n}, \quad (6.13)$$

thus, yielding a polynomial scaling at every finite truncation order.³ Equation (6.13) is a worst-case estimation and one can already show that MBPT(4) is not a N^8 process but rather a N^7 process due to the factorisation of certain contributions [SB09].

In order to estimate the gain in performance when using a angular-momentum coupled formulation, we compare the size of the single-particle basis in m -scheme with the spherical

³When dealing with operators of higher particle-rank the above statement must be modified. If, e.g., three-body operators are included in the calculation the the n -th order energy correction contains up to N^{3n} single-particle summations.

single-particle basis. In our calculations we typically include 13 major oscillator shells, corresponding to single-particle bases that contain ~ 2000 single-particle states, whereas the spherical single-particle basis contains roughly ~ 100 basis states. Therefore, this yields a speedup of a factor of 20 for every single-particle summation that appears in the formulas for the energy corrections. At second-order this gives approximately a speedup of $\sim 10^5$. It is clear that the use of angular-momentum coupling techniques is a highly efficient tool to increase code performance.⁴

From the formula of the second-order correction in J -scheme we see that the angular-momentum coupling yields a decoupling of matrix elements with different total angular momenta (this is just the result of the use of the orthogonality relation). In the following we will show how to cast (6.8) into a form that is amenable for the use of matrix multiplication. To do so we define the following auxiliary quantities

$${}^J A_{\tilde{a}\tilde{b}\tilde{i}\tilde{j}} \equiv {}^J H_{\tilde{a}\tilde{b}\tilde{i}\tilde{j}}^{[2]}. \quad (6.14)$$

$${}^J B_{\tilde{a}\tilde{b}\tilde{i}\tilde{j}} \equiv \frac{1}{\epsilon_{\tilde{i}\tilde{j}}^{\tilde{a}\tilde{b}}} {}^J H_{\tilde{a}\tilde{b}\tilde{i}\tilde{j}}^{[2]}. \quad (6.15)$$

Furthermore, we define collective multi-indices M, N via

$$M = (\tilde{a}\tilde{b}) \quad \text{and} \quad N = (\tilde{i}\tilde{j}), \quad (6.16)$$

such that

$${}^J B_{MN} = {}^J B_{\tilde{a}\tilde{b}\tilde{i}\tilde{j}}. \quad (6.17)$$

With this (6.8) can be written as

$$E^{(2)} = \sum_J \hat{j}^2 \sum_{MN} {}^J B_{MN} {}^J A_{NM}, \quad (6.18)$$

where the double sum over the multi-indices M, N constitutes a trace of a matrix product

$$E^{(2)} = \sum_J \hat{j}^2 \left(\text{Tr}({}^J \underline{A} \cdot {}^J \underline{B}) \right). \quad (6.19)$$

The advantage of the last expression is that matrix multiplication can be effectively performed by means of cache-optimised linear algebra libraries, e.g., BLAS. This allows for a tremendous speedup. The direct use of BLAS-techniques for m -scheme implementations is much more difficult since the lower symmetry of the single-particle basis does not allow for

⁴Be reminded that this is still a very rough estimate since we do not distinguish between particle and hole dimensions. However, the above argument gives at least a glimpse of the importance of angular-momentum algebra in many-body physics.

a block-diagonal structure of the Hamiltonian. In particular, the size of the m-scheme matrix representation of the Hamilton matrix is too large to fit into the cache of even modern computers.

Analogously, the third-order energy correction can be cast into a form containing a trace over a double matrix product. However, additional matrices must be stored, since the particle-particle channel and hole-hole channel contain matrices that consist of four particle indices or four hole indices, respectively.

6.4 LIMITATIONS OF SINGLE-REFERENCE THEORIES

This final section is dedicated to a qualitative discussion of single-configurational many-body techniques and in particular to HF-MBPT and will motivate the extension of MBPT to multi-configurational reference states.⁵

For systems with a (sub)-shell closure, investigations using softened potentials show that MBPT with respect to a HF determinant yields accurate results at low orders that are in reasonable agreement with more sophisticated many-body techniques like CC, SCGF, or IM-SRG [Tic⁺16]. The reason for this is that closed-shell nuclei are typically dominated by a single Slater determinant. This is for example reflected by the fact that the Hartree-Fock energy constitutes up to 80% of the overall binding energy and only 20% percent are genuine correlation effects when using a sufficiently softened interaction obtained from an initial SRG transformation.⁶ Moreover, due to the shell structure, usually one has a pronounced shell gap for the single-particle energies i.e., there is a significant difference in the single-particle energies of the particle and hole states, respectively. On a more fundamental level, a single Slater determinant does even not possess good quantum numbers, e.g., total angular momentum. Using a single-determinantal reference state fails to reproduce basis symmetries of the underlying Hamiltonian in open-shell systems.

Let us now assume that we investigate a truly open-shell system, where some of the orbitals are only partially occupied. This leads to a *degeneracy* of the spherical Hartree-Fock solution since several determinants have the same zero-order energy, i.e., sum of single-particle energies. Since we want to perform MBPT on top of a single Slater determinant, we randomly choose one of the degenerate determinants as reference for the correlation expansion, thus defining the one-dimensional reference space. The calculation of perturbative corrections requires summations over many-body states that are not contained in the model

⁵The use of single-configurational reference states is also of concern in other many-body approaches like CC or IM-SRG, but due to the non-finite correlation expansion in MBPT it is more pronounced in our framework.

⁶These estimate hold for systems in nuclear physics. In quantum chemistry the Hartree-Fock approximation typically accounts for 99% of the overall binding energy of closed-shell states. However, quantum chemists aim for much higher accuracy since the Coulomb interaction is known analytically and electrons are pointlike particles.

space. These summations in particular include the many-body states that are degenerate with the reference determinant. Formulae of RS-MBPT contain denominators that consist of differences of zero-order energies. In the case of degeneracies these denominators vanish and the perturbation expansion becomes singular. Even if the zero-order energy differences are not exactly zero but very small, this can prevent the perturbation expansion from converging or yield a slow rate of convergence. This case is referred to as *quasi-degeneracy* and can occur if the shell gap between occupied and unoccupied single-particle states is too small. We note that sometimes the problem of small denominators can be overcome by altering the choice of \hat{H}_0 and going from a Møller-Plesset to an Epstein-Nesbet partitioning, since the shifted denominators lift the zero-order degeneracy.

Besides handling vanishing denominators, a single-configurational MBPT is inappropriate when a certain correlated state is dominated by more than one determinant. For example assume that two degenerate SDs $|\Phi\rangle, |\Phi'\rangle$ contribute significantly to the exact solution. Further, assume that $|\Phi'\rangle = |\Phi_{ijkl}^{abcd}\rangle$ is a quadruply-excited SD with respect to $|\Phi\rangle$. Let us take $|\Phi\rangle$ as reference for the correlation expansion. Since we know that $|\Phi'\rangle$ contributes significantly to the exact wavefunction we expect contributions from this quadruply-excited intermediate to be quite large. However, due to its high excitation rank the first contribution of the determinant appears at fourth-order HF-MBPT, which is beyond the level of current medium-mass calculations. Therefore, the third-order energy correction lacks important corrections from the other determinant. This is a generic problem of single-configurational theories and can be solved by using more complex reference states, which are themselves proper superposition of several SDs. This is the starting point of the multi-configurational MBPT.

7

Coupled-Cluster Theory

This chapter serves as a short introduction to Coupled-Cluster (CC) theory. CC calculations have become the gold standard for the determination of ground-state energies for medium-mass closed-shell nuclei [DH04; BM07; Hag⁺10; Kow⁺04; PGW09; Bin⁺14; Bin14]. An exhaustive introduction to CC theory and many of its different flavors can be found in [SB09]. For applications in nuclear physics and in particular a discussion of spherical CC theory the interested reader is referred to [Bin14].

Historically, the CC method was introduced by Kümmel and Cizék in the late 1950s [Čiž66; ČP69; CK60].

7.1 THE EXPONENTIAL ANSATZ

As MBPT, the CC approach in its basic formulation aims at the solution of the stationary Schrödinger equation

$$\hat{H}|\psi\rangle = E_0|\psi\rangle \quad (7.1)$$

for the ground-state energy E_0 . Similar to MBPT we write the exact eigenstate $|\psi\rangle$ in terms of the action of the wave operator $\hat{\Omega}$ on some reference state $|\Phi\rangle$ ¹

$$\hat{\Omega}|\Phi\rangle = |\psi\rangle. \quad (7.2)$$

In CC theory we take as ansatz for Ω an exponential form

$$\hat{\Omega}^{(\text{CC})} = e^{\hat{T}}, \quad (7.3)$$

¹Most commonly $|\Phi\rangle$ is a single determinant of Hartree-Fock type.

where \hat{T} is an excitation operator. The above choice for the wave operator ensures size extensivity of the results.

The CC wave function has the form

$$|\psi\rangle = e^{\hat{T}}|\Phi\rangle \quad (7.4)$$

where

$$\hat{T} = \hat{T}_1 + \hat{T}_2 + \hat{T}_3 + \dots \quad (7.5)$$

are the so-called *cluster operators*

$$\hat{T}_1 = \sum_{ai} t_i^a \{\hat{c}_a^\dagger \hat{c}_i\}, \quad (7.6)$$

$$\hat{T}_2 = \frac{1}{4} \sum_{abij} t_{ij}^{ab} \{\hat{c}_a^\dagger \hat{c}_b^\dagger \hat{c}_j \hat{c}_i\}, \quad (7.7)$$

$$\hat{T}_3 = \frac{1}{36} \sum_{abcijk} t_{ijk}^{abc} \{\hat{c}_a^\dagger \hat{c}_b^\dagger \hat{c}_c^\dagger \hat{c}_k \hat{c}_j \hat{c}_i\}, \quad (7.8)$$

which are in normal order with respect to the reference determinant $|\Phi\rangle$. The general cluster operator is given by

$$\hat{T}_n = \frac{1}{(n!)^2} \sum_{\substack{a_1 \dots a_n \\ i_1 \dots i_n}} t_{i_1 \dots i_n}^{a_1 \dots a_n} \{\hat{c}_{a_1}^\dagger \dots \hat{c}_{a_n}^\dagger \hat{c}_{i_n} \dots \hat{c}_{i_1}\}, \quad (7.9)$$

where the quantities $t_{i_1 \dots i_n}^{a_1 \dots a_n}$ are called *cluster amplitudes*.

7.2 SIMILARITY-TRANSFORMED HAMILTONIAN

Analogously to MBPT we are interested in correlation effects, i.e., corrections beyond the reference-state description. The normal-product Schrödinger equation for the CC wave function can be written as

$$(\hat{H}_N - \Delta E)e^{\hat{T}}|\Phi\rangle = 0. \quad (7.10)$$

Multiplication from the left by $e^{-\hat{T}}$ yields

$$(e^{-\hat{T}}\hat{H}_N e^{\hat{T}} - \Delta E)|\Phi\rangle = 0. \quad (7.11)$$

Equation (7.11) constitutes a right eigenvalue equation for the correlation energy ΔE of the non-Hermitian *similarity-transformed Hamiltonian*

$$\mathcal{H} = e^{-\hat{T}} \hat{H}_N e^{\hat{T}}. \quad (7.12)$$

An explicit form of \mathcal{H} can be obtained by making use of the Baker-Campbell-Hausdorff (BCH) expansion

$$e^{-\hat{B}} \hat{A} e^{\hat{B}} = \hat{A} + [\hat{A}, \hat{B}] + \frac{1}{2} [[\hat{A}, \hat{B}], \hat{B}] + \frac{1}{3!} [[[\hat{A}, \hat{B}], \hat{B}], \hat{B}] + \dots \quad (7.13)$$

Application to \mathcal{H} yields

$$\begin{aligned} \mathcal{H} = & \hat{H}_N + [\hat{H}_N, \hat{T}] + \frac{1}{2} [[\hat{H}_N, \hat{T}], \hat{T}] + \frac{1}{3!} [[[\hat{H}_N, \hat{T}], \hat{T}], \hat{T}] \\ & + \frac{1}{4!} [[[[\hat{H}_N, \hat{T}], \hat{T}], \hat{T}], \hat{T}], \end{aligned} \quad (7.14)$$

where the BCH series naturally truncates after fourfold nested commutators.²

By virtue of Wick's theorem it can be shown that

$$\mathcal{H} = e^{-\hat{T}} \hat{H}_N e^{\hat{T}} \quad (7.15)$$

$$= (\hat{H}_N e^{\hat{T}})_C, \quad (7.16)$$

where the subscript indicates that only connected diagrams have to be taken into account such that the normal-product Schrödinger equation takes the form

$$(\hat{H}_N e^{\hat{T}})_C |\Phi\rangle = \Delta E |\Phi\rangle. \quad (7.17)$$

By left-projecting the reference state and particle-hole excitations onto equation (7.17) we obtain the coupled cluster working equations. The first one is the so-called *energy equation*

$$\langle \Phi | (\hat{H}_N e^{\hat{T}})_C | \Phi \rangle = \Delta E. \quad (7.18)$$

Projection of excited determinants yields the (non-linear) *amplitude equations*

$$\langle \Phi_{i_1}^{a_1} | (\hat{H}_N e^{\hat{T}})_C | \Phi \rangle = 0 \quad (7.19a)$$

$$\langle \Phi_{i_1 i_2}^{a_1 a_2} | (\hat{H}_N e^{\hat{T}})_C | \Phi \rangle = 0 \quad (7.19b)$$

$$\vdots \qquad \qquad \qquad \vdots$$

which need to be solved iteratively.

²The above statement holds for a Hamiltonian that contains up to two-body operators. When going to higher particle rank, the series still terminates after a finite number of commutators, e.g., sixfold commutators for a three-body interaction.

7.3 TRUNCATION OF THE CLUSTER OPERATOR

The above discussion is completely general and the calculated correlation energy will give the exact ground-state energy. However, in actual computations the form of the cluster operator \hat{T} has to be truncated. The most common form is to take

$$\hat{T} = \hat{T}_1 + \hat{T}_2 \quad (7.20)$$

which defines the *Coupled Cluster with Singles and Doubles* (CCSD) wave operator. The CCSD wave function is then given by

$$|\psi^{(\text{CCSD})}\rangle = e^{\hat{T}_1 + \hat{T}_2} |\Phi\rangle. \quad (7.21)$$

For the energy and amplitude equations one gets

$$\langle \Phi | \hat{H}_N (\hat{T}_2 + \hat{T}_1 + \frac{1}{2} \hat{T}_2^2)_C | \Phi \rangle = \Delta E, \quad (7.22)$$

$$\langle \Phi_i^a | \hat{H}_N (1 + \hat{T}_2 + \hat{T}_1 + \hat{T}_1 \hat{T}_2 + \frac{1}{2} \hat{T}_2^2 + \frac{1}{3!} \hat{T}_1^3)_C | \Phi \rangle = 0, \quad (7.23)$$

$$\langle \Phi_{ij}^{ab} | \hat{H}_N (1 + \hat{T}_2 + \frac{1}{2} \hat{T}_2^2 + \hat{T}_1 + \hat{T}_1 \hat{T}_2 + \frac{1}{2} \hat{T}_2^2 + \frac{1}{2} \hat{T}_1^2 \hat{T}_2 + \frac{1}{3!} \hat{T}_1^3 + \frac{1}{4!} \hat{T}_1^4)_C | \Phi \rangle = 0, \quad (7.24)$$

Equations (7.22)-(7.24) are then evaluated by means of Wick's theorem.

The inclusion of higher-order cluster operators requires significantly more computational resources. Since the CC equations are a system of coupled non-linear algebraic equations they have to be solved iteratively. This requires the storage of all cluster amplitudes in every iteration. In particular the storage of \hat{T}_3 amplitudes scales with N^6 where N is the size of the single-particle basis which becomes unfeasible for larger model spaces. Therefore, one uses an approximate non-iterative treatment of the \hat{T}_3 cluster operator. This leads, for example, to the definition of $\Lambda\text{CCSD(T)}$ or CR-CC(2,3) which partially account for triply-excited clusters. Currently, the full implementation of CCSDT , i.e., a consistent iterative treatment of the \hat{T}_3 cluster operator is out of reach for medium-mass systems.

7.4 CONNECTIONS TO PERTURBATION THEORY

The exponential form of the CC wave operator yields an all-order resummation of MBPT diagrams. The following discussion is restricted to the single-configurational case, since, to our knowledge, there is no implementation of genuine multi-configurational CC in nuclear physics. The CCSD approach contains all diagrams with singly- and doubly-excited intermediate states up to infinite order, thus making it exact up to third-order HF-MBPT while including many additional diagrams of higher order. The non-iterative triple corrections

derived from CR-CC(2,3) yield a correlation energy that is exact up to fourth-order MBPT. We note, that even though there are quadruply-excited intermediates in HF-MBPT(4), these contributions can be factorized into products of doubly-excited intermediates that can be described without the use of \hat{T}_4 amplitudes.

The infinite-order resummation of certain types of MBPT diagrams is a general property shared by other non-perturbative many-body methods. A computational feature of CC is the non-linear nature of the CC amplitude equations, which requires the storage of the cluster amplitudes. Therefore, one heavily relies on using a spherical scheme for storing the cluster amplitudes. However, this prevents a direct extension to arbitrary open-shell systems since the solution of the m-scheme amplitude equations becomes intractable even for the lightest nuclei. Therefore, open-shell approaches have up to now been restricted to equation-of-motion techniques [PGW09] or the construction of valence-space Hamiltonians that make use of a frozen inert core [Jan⁺14]. Very recently, CC theory has been formulated and implemented in the context of symmetry-broken many-body theory [Dug15; Sig⁺15; DS16]. We will discuss MBPT in the context of symmetry breaking in much more detail in Part IV of this thesis.

We note that, in quantum chemistry, there exist proper multi-configurational CC theories which use generalized normal-ordering techniques to obtain energy and amplitude equations [KM97; Mah⁺98]. To our knowledge they have, however, never been transferred to the nuclear structure case.

8

Ground-state energies of closed-shell systems

In this section we apply single-configurational perturbation theory for the calculation of ground-state energies of closed-shell nuclei using state-of-the-art chiral interactions. We start with a systematic investigation of the convergence behavior using the recursive treatment introduced in chapter 5. In the second step we use low-order MBPT to proceed to medium-mass nuclei.

In the following we make use of a chiral two-body interaction at N3LO with a cut-off parameter of 500 MeV combined with an additional chiral three-body interaction at N2LO with $\Lambda_{3N} = 400$ MeV as introduced in chapter 2. The three-body part of the Hamiltonian is incorporated via the NO2B approximation. Furthermore, the nuclear Hamiltonian is SRG evolved for different values of the flow parameter.

8.1 IMPACT OF PARTITIONING

As a first step we investigate the dependence of the convergence behavior on the choice of zero-order Hamiltonian and unperturbed energies. Prior investigations in nuclear physics used the spherical harmonic oscillator (HO) Hamiltonian

$$\hat{h}^{\text{HO}} = \frac{\hat{p}^2}{2m} + \frac{1}{2}m\Omega^2\hat{r}^2 \quad (8.1)$$

to construct the zero-order Hamiltonian in first quantisation

$$\hat{H}_0^{\text{HO}} = \sum_{i=1}^A \hat{h}_i^{\text{HO}}, \quad (8.2)$$

where \hat{h}_i^{HO} denotes the HO single-particle Hamiltonian of the i -th particle. The eigenvalue equation

$$\hat{h}^{\text{HO}}|\varphi_k\rangle = \epsilon_k|\varphi_k\rangle \quad (8.3)$$

for a single-particle state $|\varphi_k\rangle = |n_k l_k j_k t_k m_k\rangle$ yields

$$\epsilon_k^{\text{HO}} = \hbar\Omega(2n_k + l_k + \frac{3}{2}), \quad (8.4)$$

and the eigenvalues obviously only depend on the radial-quantum number n_k and the orbital angular-momentum quantum number l_k . In particular the HO single-particle energies are isospin-independent. We will refer to the above choice as *HO partitioning*, which is given in second-quantized form by

$$\hat{H}_0^{\text{HO}} = \sum_p \epsilon_p^{\text{HO}} \hat{p}^\dagger \hat{p}. \quad (8.5)$$

Contrary, one can chose the unperturbed Hamiltonian as the mean-field HF Hamiltonian

$$\hat{H}_0^{\text{HF}} = \sum_p f_{pp} \hat{p}^\dagger \hat{p} \quad (8.6)$$

with matrix elements ¹

$$f_{pp} = t_{pp} + \sum_i \bar{H}_{pipi}^{[2]}, \quad (8.7)$$

where the sum over i runs over all single-particle states occupied in the HF determinant. Since the HF Hamiltonian is diagonal one-body operator the eigenvalues are given by the diagonal elements $\epsilon_p = f_{pp}$. This defines the *HF partitioning*.

Again, we note that in our analysis we make use of the Møller-Plesset scheme, where zero-order energies of the many-body states are defined as sum over single-particle energies.

In Fig 8.1 we display the impact of the choice of partitioning on the convergence characteristics of the perturbation series. In the left-hand panels we show the value of p -th order partial sum

$$E_{\text{sum}}^{(p)} = \sum_{i=1}^p E^{(i)}, \quad (8.8)$$

for perturbation order up to $p = 30$. The right-hand panels show the absolute value of the corresponding energy correction for every perturbation order. The top row we used the HO

¹For the sake of simplicity we restrict ourselves again to a two-body interaction.

partitioning and for the bottom row the HF partitioning. As benchmark system we use ^{16}O for a sequence of model spaces with $N_{\max} = 2, 4, 6$. The interaction is SRG-evolved with $\alpha = 0.08 \text{ fm}^4$ and the reference basis is taken at $\hbar\Omega = 24 \text{ MeV}$.

We see from panel (a) that the HO partitioning yields a divergent perturbation series for all model spaces, making it impossible to extract the ground-state energy directly from the sequence of partial sums. Moreover, we see from panel (c) that higher-order energy corrections are exponentially growing. Contrary, the use of HF partitioning displays a qualitatively different behavior. From panel (b) it is clear that for all model spaces the perturbation series is converging. Panel (d) shows that higher-order corrections are exponentially suppressed. Furthermore, the rate of convergence is roughly independent of the model space.

This first investigation shows the huge impact of the choice of the unperturbed Hamiltonian on the convergence characteristics of the underlying perturbation series. Even though we use a softened interaction, the HO perturbation series cannot overcome the defects that are present in the zero-order description. By construction, HF theory gives us the variational minimum of the energy functional in the test space of single Slater determinants and, thus, an optimal starting point for the perturbation series of the ground-state wave function. It is, therefore, not surprising that using the HF partitioning gives a highly robust perturbation series for closed-shell systems.

At first glance it might appear that the use of a HO partitioning is useless since we cannot directly obtain the ground-state energy from the wildly divergent series. However, it is possible to extract the ground-state energy from the divergent expansion via so-called *resummation techniques*. One uses a transformation scheme to transform the sequence of partial sum into a transformed sequence of *approximants*. It is quite often possible to find a transformation scheme such that the transformed sequence converges to the correct value, which is in our case the CI result from the same model space. The most commonly used transformation schemes are *Padé approximants*, which are closely related to continued fractions. It was shown that by applying the Padé scheme to perturbation series in HO partitioning gives a convergent sequence of approximants, thus revealing the exact CI result from the divergent perturbation expansion [RL10; LRS12]. For the construction of a particular resummation scheme one typically needs additional information about the kind of divergence, e.g., oscillatory, exponential or factorial. A major drawback is that one typically needs quite a large number of approximants and, therefore, also a large number of energy corrections, to obtain convergence in the sequence of approximants.² In medium-mass calculations, however, one is typically restricted to three terms in the perturbation series, which makes the use of, e.g., Padé approximation questionable. For light systems the use of such approximants can give additional insights and might help to further improve the convergence of the perturbation

²Typically, one needs about 10-20 approximants and correspondingly 15-20 energy corrections to reach convergence. However, this also strongly depends on the transformation scheme under consideration.

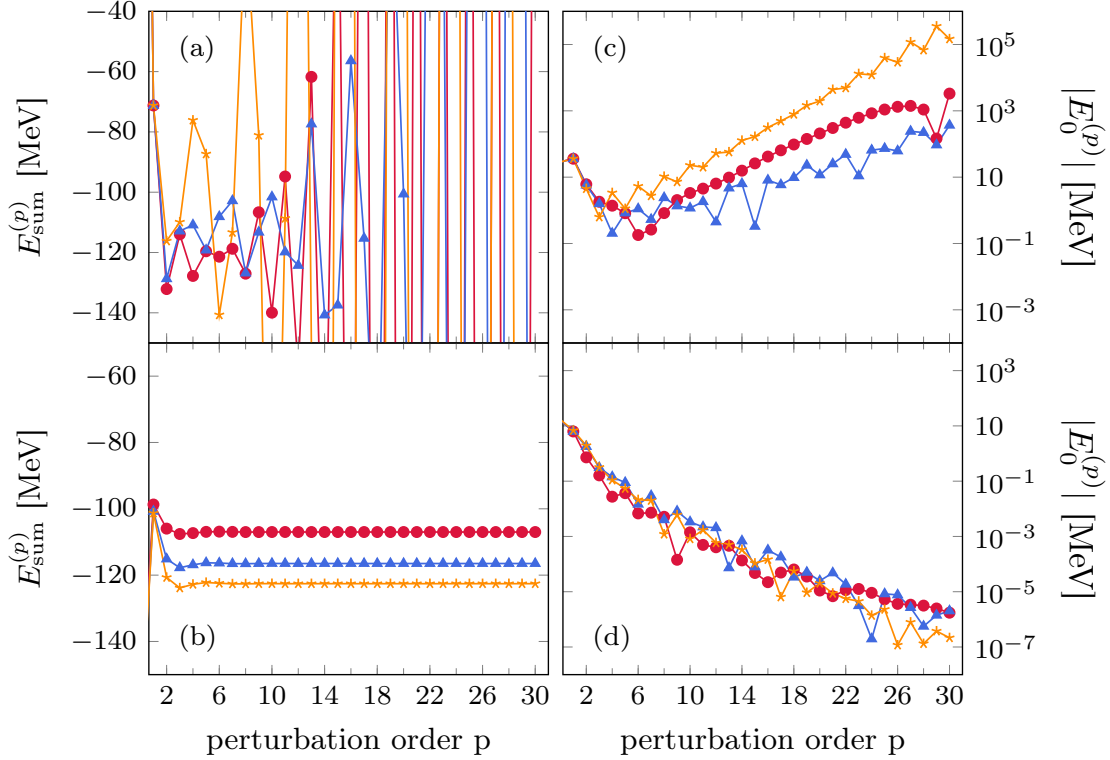


Figure 8.1: Partial sums of ^{16}O in HO basis (a) and HF basis (b) for $\alpha = 0.08\text{fm}^4$ with truncation parameters $N_{\text{max}} = 2(\bullet)$, $4(\blacktriangle)$ and $6(\star)$. The corresponding energy corrections are displayed in (c) and (d), respectively. All calculations are performed at oscillator frequency $\hbar\Omega = 24\text{ MeV}$.

series. For more details in the nuclear physics context see [Tic14].

8.2 SRG DEPENDENCE

The previous section revealed that the choice of partitioning has a major impact on the convergence behaviour of the perturbation series. In the next step the question arises, if there are other—secondary—parameters that influence the convergence pattern of the perturbation series. We will see that the "softness" of the interaction, parametrized by the value of the SRG flow parameter α , plays an important role for the correlation expansion. From now on all single-configurational MBPT calculations make use of the HF partitioning.

In Figure 8.2 we show the impact of the variation of α on the convergence behavior of the perturbation series. Again the left column shows the sequence of partial sums and the right column the absolute value of the p -th order energy corrections. All calculations are performed in $N_{\text{max}} = 6$ model spaces. The different plot markers correspond to different values of the flow parameter ranging from 'hard' interactions ($\alpha = 0.02\text{ fm}^4$) to 'soft' interactions ($\alpha = 0.08\text{ fm}^4$). As benchmark systems we use the doubly magic nuclei ^4He and ^{16}O , as well as the closed-subshell nucleus ^{24}O . A common feature for all three systems is that increasing the flow parameter and, thus, softening the interaction, increases the binding

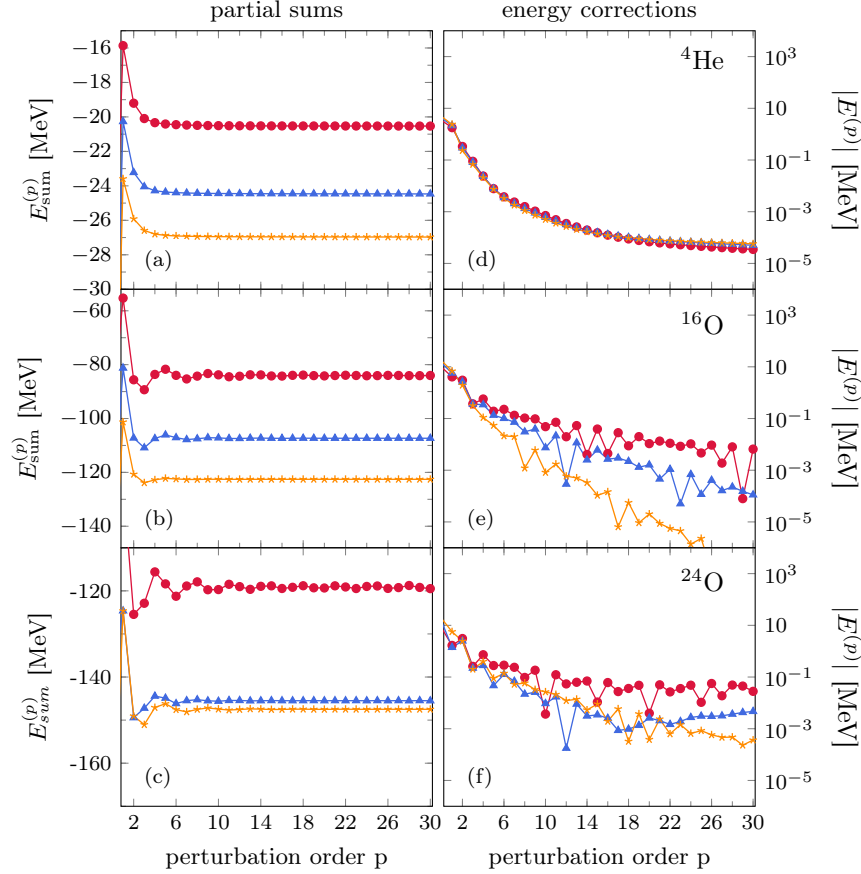


Figure 8.2: Partial sums for varying flow parameters in HF-MBPT for ${}^4\text{He}$ (a), ${}^{16}\text{O}$ (b) and ${}^{24}\text{O}$ (c). The corresponding energy corrections are given in (d), (e) and (f), respectively. The model space for the first and second panel are truncated at $N_{\text{max}} = 6$. The truncation for the third panel is given by $N_{\text{max}} = 4$. The flow parameters are given by 0.02 fm^4 (\bullet), 0.04 fm^4 (\blacktriangle) and 0.08 fm^4 (\star). All calculations use a NN+3N-full interaction with oscillator frequency $\hbar\Omega = 24 \text{ MeV}$.

energy yielding lower ground-state energies in agreement with our expectation of the SRG flow that enhances the model-space convergence. Additionally, all perturbation series are convergent, even though the convergence for $\alpha = 0.02 \text{ fm}^4$ for ${}^{24}\text{O}$ is very poor as seen from panel (c). We want to stress that all calculation are far from being converged with respect to model space size. Therefore, there appears a sizeable dependence of the results on the SRG parameter.

Obviously, HF-MBPT is very robust with respect to variations of the SRG flow parameter. However, one definitely sees a systematic dependence of the absolute value of the energy corrections on the value of α . Increasing the flow parameter yields a stronger suppression of higher-order corrections. This is most pronounced in the case of ${}^{16}\text{O}$ where the rate of convergence is systematically improved by increasing the flow parameter. ${}^{24}\text{O}$ shows also hints in this direction - however much less pronounced than in ${}^{16}\text{O}$. Finally, ${}^4\text{He}$ does not show any dependence on the flow parameter at all. For all values of α the perturbation series

		$\alpha[\text{fm}^4]$		
		0.02	0.04	0.08
${}^4\text{He}$	$E_{\text{sum}}^{(2)}$	-19.204	-20.269	-23.588
	$E_{\text{sum}}^{(3)}$	-20.334	-23.224	-26.589
	$E_{\text{sum}}^{(10)}$	-20.507	-24.444	-26.947
	$E_{\text{sum}}^{(20)}$	-20.526	-24.462	-26.964
	$E_{\text{sum}}^{(30)}$	-20.537	-24.469	-26.971
	CI	-20.539	-24.483	-26.994
	${}^{16}\text{O}$	$E_{\text{sum}}^{(2)}$	-85.620	-107.241
$E_{\text{sum}}^{(3)}$		-89.315	-110.861	-123.863
$E_{\text{sum}}^{(10)}$		-83.780	-107.199	-122.561
$E_{\text{sum}}^{(20)}$		-84.180	-107.341	-122.577
$E_{\text{sum}}^{(30)}$		-84.018	-107.331	-122.577
CI		-84.034	-107.330	-122.577
${}^{24}\text{O}$		$E_{\text{sum}}^{(2)}$	-125.460	-124.459
	$E_{\text{sum}}^{(3)}$	-122.880	-126.670	-151.059
	$E_{\text{sum}}^{(10)}$	-119.705	-121.233	-147.446
	$E_{\text{sum}}^{(20)}$	-119.335	-121.314	-147.508
	$E_{\text{sum}}^{(30)}$	-119.483	-120.948	-147.489
	CI	-119.131	-120.947	-147.488

Table 8.1: Ground-state energies in MeV for ${}^4\text{He}$, ${}^{16}\text{O}$ and ${}^{24}\text{O}$ using HF-MBPT with $p = 30$ and CI calculations for different values of α . The model spaces are truncated by $N_{\text{max}} = 6$ for ${}^4\text{He}$ and ${}^{16}\text{O}$ and $N_{\text{max}} = 4$ in the case of ${}^{24}\text{O}$. The HO frequency is $\hbar\Omega = 24$ MeV.

converges monotonically to the exact full CI limit.

Table 8.1 allows for a more quantitative analysis of Figure 8.2. Shown are the partial sums for $p = 2, 3, 10, 20, 30$, as well as the exact CI result for all three nuclei and all SRG parameters. From comparing the partial sum for $p = 30$ with the CI limit we see that the deviations are of the size of a few keV, for $\alpha = 0.04, 0.08 \text{ fm}^4$ and up to a few hundred keV, for $\alpha = 0.02 \text{ fm}^4$ in the case of ${}^{24}\text{O}$. The residual deviations between the 30th-order partial sum and the CI limit are due to the incomplete convergence of the perturbation series. In particular for very hard interactions we expect perturbative corrections beyond $p = 30$ to be necessary to agree with the CI results on a keV level. Also note that the convergence pattern for ${}^{24}\text{O}$ for $\alpha = 0.02 \text{ fm}^4$ is oscillatory such that the deviation at $p = 30$ is not surprising.

Most importantly, we find that when using softened interactions the perturbation series converges rapidly and high-order calculations reproduce the CI result with only very small deviations. On this basis we expect low-order energy corrections to be a reasonable approximation to the converged result. Note that the deviation of third-order partial sum from the CI limit is less than 3%.

From the above table we see that for ${}^{16}\text{O}$ and ${}^{24}\text{O}$ the third-order partial sum overbinds

the CI result. We want to stress that this might not be a general feature of HF-MBPT but rather a truncation effect due to the use of a N_{\max} truncation for the HF single-particle basis. The N_{\max} truncation is originally constructed for the use of HO single-particle states and simply adapting the same truncation scheme to the HF basis might lead to an unexpected behavior of the perturbation series, since HF theory naturally is formulated in e_{\max} -truncated model spaces. Unfortunately, the rapid growth of the many-body space in full CI with respect to single-particle dimension makes it hard to investigate oxygen isotopes in model spaces that are only truncated with respect to e_{\max} .

We remark that further increasing the flow parameter is not a feasible solution to further improve the rate of convergence of the perturbation series. As already noted in the discussion of the cluster decomposition, the SRG flow induces irreducible contributions of particle rank beyond two. Further increasing the SRG parameter leads to stronger induced many-body forces, which can not be accounted for in the many-body treatment. Therefore, choosing the SRG parameter of the Hamiltonian is always a trade-off between the size of the induced many-body contributions and the improved convergence with respect to model-space size and the convergence properties of the perturbation expansion.³ A value of $\alpha = 0.08 \text{ fm}^4$ seems like a good compromise that yields a rapidly converging perturbation series without inducing too strong higher-body forces.

8.3 LOW-ORDER ENERGY CORRECTIONS

In the previous sections we used a recursive high-order treatment to investigate the convergence behavior in detail. Since this uses a formulation in terms of many-body states and many-body matrix-elements, it has the same computational limitations as a full CI calculation in the same model space. Application of this scheme beyond the lower sd-shell is infeasible even for highly-parallelized numerical codes. The explicit evaluation of low-order energy corrections up to $p = 3$ allows us to investigate ground-state binding energies up to the heavy tin region. Since we are dealing with spherical systems we make use of angular-momentum coupling and evaluate the third-order partial sum. Because the investigated systems are out of reach of the IT-NCSM, we compare our results to the well-established CC approach with a sophisticated approximate treatment of triply excited clusters.

In the following we always use model spaces truncated with respect to HO quantum number $e \leq e_{\max} = 12$. We further truncate the single-particle basis by limiting the orbital angular-momentum to $l \leq l_{\max} = 10$. This saves considerable amounts of computing time while having no significant effect on the calculated result, since single-particle states with $l > 10$ correspond to very high single-particle energies, which are strongly suppressed in MBPT

³There are systems where the use of a 'bare' interaction, i.e., $\alpha = 0.00 \text{ fm}^4$ yields an unbound HF solution. It is clear that such a reference state is inappropriate to serve as a zero-order starting point for the correlation expansion.

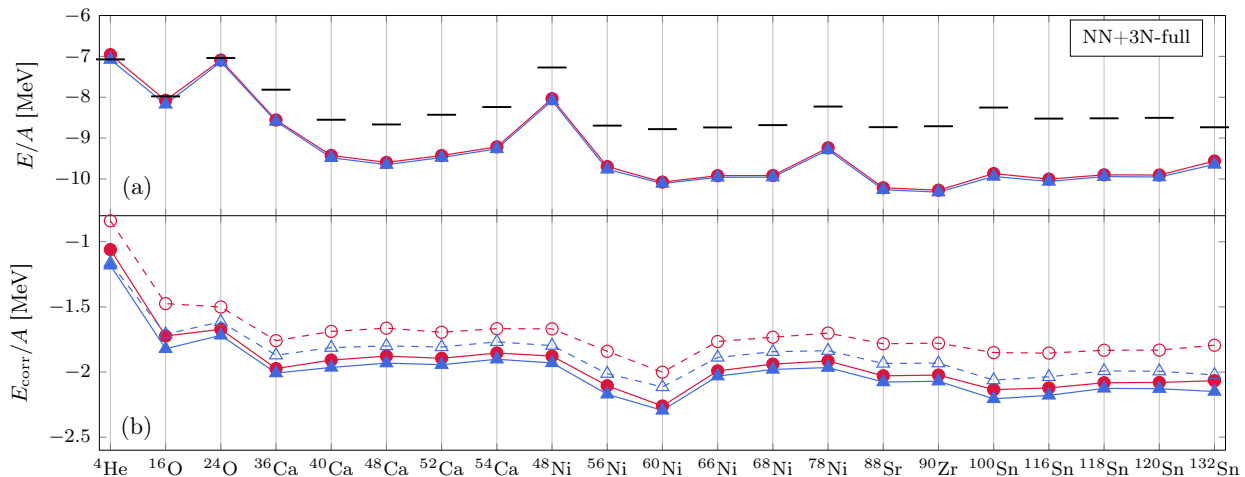


Figure 8.3: Panel (a) shows the ground-state energies per nucleon from third-order HF-MBPT (●) in comparison to CR-CC(2,3) (▲) results for selected closed-shell nuclei. Panel (b) shows the correlation energy per nucleon, $E_0^{(2)}$ (○) as well as $E_0^{(2)} + E_0^{(3)}$ (●) for HF-MBPT. Additionally, the correlation energy per nuclei for CCSD (△) and CR-CC(2,3) (▲) are shown. The SRG flow parameter is $\alpha = 0.08 \text{ fm}^4$, the HO frequency $\hbar\Omega = 24 \text{ MeV}$, for a model space truncated by $e_{\text{max}} = 12$ and $l_{\text{max}} = 10$. All calculations were performed with $NN + 3N$ -full interaction. Experimental values are indicated by black bars [Wan⁺12].

due to large denominators in the Møller-Plesset scheme. Additionally, all Hamiltonians are SRG-evolved with flow parameter $\alpha = 0.08 \text{ fm}^4$ to ensure sufficiently fast convergence of the perturbation series.

Figures 8.3 and 8.4 show the ground-state energies calculated in HF-MBPT at second and third order and in the CC framework for the $NN+3N$ -full Hamiltonian and $NN+3N$ -induced Hamiltonian for a selection of closed-subshell nuclei ranging from ${}^4\text{He}$ to ${}^{132}\text{Sn}$. The top panel shows the overall ground-state energy per nucleon at third order as well as the energy of the ground-state obtained with the CR-CC(2,3) method. Additionally, black bars indicate the experimental ground-state energies. The lower panel shows the correlation energy E_{corr} per nucleon

$$E_{\text{corr}} = E_{\text{approx}} - E_{\text{HF}}, \quad (8.9)$$

where E_{approx} stands for either approximation to the exact eigenvalue, e.g., $E_{\text{approx}} = E^{(2)}$ or $E_{\text{approx}} = E^{(\text{CCSD})}$. Investigating the correlation energy allows us to understand the subtle differences between MBPT and CC, since we get rid of the bulk of the binding energy in form of the mean-field approximation first.

The most important observation is that HF-MBPT(3) and CR-CC(2,3) are in almost perfect agreement with each other. The differences in the overall binding energy are less than 0.5% and MBPT reproduces the highly sophisticated CC approach for all nuclei and

both interaction types. Both interactions reproduce a constant energy per nucleon—a feature that is not present when dealing with a two-body interaction only. In particular the use of the NN+3N-full Hamiltonian reproduces fairly good experimental binding energies up to ^{24}O , whereas the NN+3N-induced interaction predicts too loosely-bound nuclei in this mass region. However, when going to the medium-mass regime and beyond, the calculations using the NN+3N-full exhibit a strong overbinding of up to 2 MeV per nucleon in the tin region. In contrast, the NN+3N-induced Hamiltonian reproduces the experimental trend fairly well even for heavier systems. Be reminded that the nuclear Hamiltonians in use are fitted to few-body data. Therefore, it is quite surprising how accurately heavy systems can be described given the mass-regime the parameters of the interaction were fitted to. We note that even though we only show results up to ^{132}Sn it is possible to use MBPT and CC to compute for the correlation energy of heavy closed-shell elements like, e.g., ^{208}Pb . However, when proceeding to such large mass-numbers one runs into convergence issues with respect to the truncation of the three-body matrix elements necessary for the HF calculation and the normal-ordering. Currently the upper limit for the three-body model space is $E_{3\text{max}} = 14$, which is insufficient for such heavy nuclei. Therefore, the neglected contributions associated to the cutoff in the three-body matrix elements induce an additional systematic error of up to 5% which makes a quantitative analysis challenging.

Focusing on the bottom panel of Figs. 8.3 and 8.4 we can compare the truncation effects of MBPT and CC for different degrees of sophistication. The second-order energy correction (\circ) already accounts for a large part of dynamical correlation effects and contributes typically about 1.5 MeV per nucleon to the correlation energy. Additional 0.3 MeV per nucleon come from the inclusion of the third-order energy correction. The value of the correlation energy from CCSD lies in between the second-order and third-order partial sums of the correlation energy. This is an interesting result since CCSD is exact through third-order HF-MBPT. Therefore, the additional contributions from singly- and doubly-excited intermediates at higher-order must have a repulsive effect that lowers the binding energy. The inclusion of triply-excited clusters via CR-CC(2,3) yields a method that is exact through fourth-order HF-MBPT. These contributions have an attractive effect since the CR-CC(2,3) results are always below the HF-MBPT(3) results. Effects of triply-excited intermediates are not accounted for at HF-MBPT(3), which serves as explanation for the systematic differences between HF-MBPT(3) and CR-CC(2,3). However, these differences in the correlation energy are less than 0.1 MeV per nucleon which is rather surprising.

Additionally, we note that the evaluation of the perturbative formulas at third-order requires only 1 – 3% of the computing time required for the CR-CC(2,3) calculation thus serving as cheap, high-quality alternative to state-of-the-art medium-mass methods.

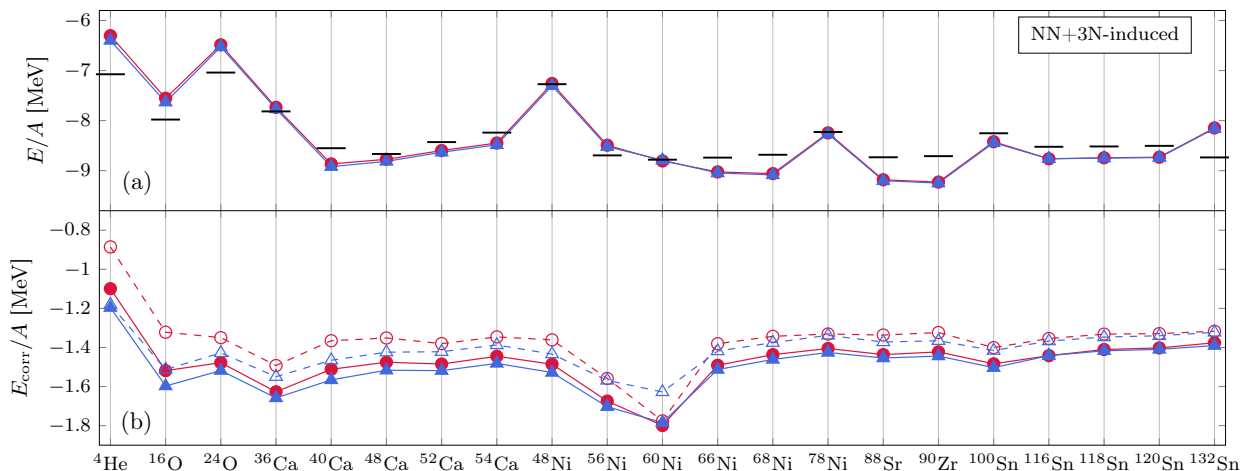


Figure 8.4: Panel (a) shows the ground-state energies per nucleon from third-order HF-MBPT (\bullet) in comparison to CR-CC(2,3) (\blacktriangle) results for selected closed-shell nuclei. Panel (b) shows the correlation energy per nucleon, $E_0^{(2)}$ (\circ) as well as $E_0^{(2)} + E_0^{(3)}$ (\bullet) for HF-MBPT. Additionally, the correlation energy per nuclei for CCSD (\triangle) and CR-CC(2,3) (\blacktriangle) are shown. The SRG flow parameter is $\alpha = 0.08 \text{ fm}^4$, the HO frequency $\hbar\Omega = 24 \text{ MeV}$, for a model space truncated by $e_{\text{max}} = 12$ and $l_{\text{max}} = 10$. All calculations were performed with $NN + 3N$ -induced interaction. Experimental values are indicated by black bars [Wan⁺12].

8.4 ANATOMY OF THE THIRD-ORDER ENERGY CORRECTION

In this section we will investigate the diagrammatic content at third-order HF-MBPT more deeply. In many-body theory one encounters the situation that a given method becomes computationally very challenging at a certain truncation order. However, for physics reasons it might be favorable to include at least some of the contributions of a given theory at a certain truncation order. One such example is CC theory: it is expected that the inclusion of triply-excited cluster into the many-body framework is necessary to improve upon the quality of the CCSD approximation. In nuclear structure the full inclusion of triples in the form of CCSDT is out of reach for computational reasons since this requires the storage of the \hat{T}_3 amplitudes. To circumvent this problem, non-iterative schemes with an approximate treatment of the triples were derived to partially account for the effect of triples beyond the CCSD model. Analogously, one can analyze the diagrammatic content at a given perturbation order and search for diagrams with critical scaling behavior that do not contribute significantly. In the following we give a detailed analysis of the third-order HF-MBPT diagrams and discuss approximation schemes beyond the perturbation order.

Recall from section 6.1 the individual contributions to the third-order energy correction

$$E_{pp}^{(3)} = \frac{1}{8} \sum_{abcdij} \frac{\bar{H}_{ijab}^{[2]} \bar{H}_{abcd}^{[2]} \bar{H}_{cdij}^{[2]}}{\epsilon_{ij}^{ab} \epsilon_{ij}^{cd}}$$

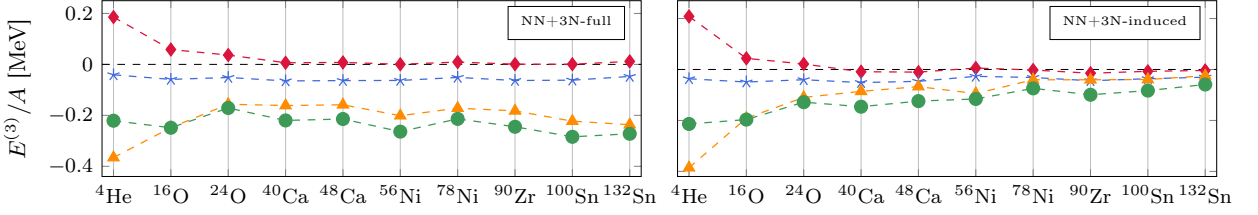


Figure 8.5: Individual contributions of the diagrams appearing at third-order perturbation theory. Show are the contributions per nucleon from the pp-diagram (◆), the hh-diagram (★) and the ph-diagram (▲). The overall contribution of the third-order correction is depicted in (●). The left panel corresponds to a $3N$ -full interaction and the right panel to a $3N$ -induced interaction. The SRG flow parameter is $\alpha = 0.08 \text{ fm}^4$, the HO frequency $\hbar\Omega = 24 \text{ MeV}$, in an $e_{\text{max}} = 12$ and $l_{\text{max}} = 10$ truncated model space.

$$E_{hh}^{(3)} = \frac{1}{8} \sum_{abijkl} \frac{\bar{H}_{ijab}^{[2]} \bar{H}_{abkl}^{[2]} \bar{H}_{klji}^{[2]}}{\epsilon_{ij}^{ab} \epsilon_{kl}^{ab}},$$

$$E_{ph}^{(3)} = - \sum_{abcijk} \frac{\bar{H}_{ijab}^{[2]} \bar{H}_{kbic}^{[2]} \bar{H}_{ackj}^{[2]}}{\epsilon_{ij}^{ab} \epsilon_{kj}^{ac}},$$

where the lower indices refer to the particle-particle, hole-hole and particle-hole channels, respectively. A possible way to approximate the third-order energy correction is to neglect a certain diagram and only evaluate the remaining expression. Figure 8.5 disentangles the individual contributions from the three terms for a selection of closed-shell nuclei. Again we show the third-order correction per particle. For both interactions, the particle-particle channel contributes only little to the overall third-order correction and is in most cases weakly attractive. The hole-hole channel gives a slightly negative contribution which is a little stronger in absolute value than the particle-particle channel. Most of the contribution to the third-order energy correction comes from the particle-hole channel. Furthermore, the third-order energy correction per nucleon is decreasing when going to heavy systems in the case of the $NN + 3N$ -induced interaction, but stays roughly constant for the $NN + 3N$ -full interaction.

Prior investigations—particularly in neutron matter—often neglected the particle-hole channel and used the sum of the particle-particle and hole-hole channel as approximations for the third-order energy correction [Heb⁺10; Krü⁺13; DHS16]. We assume the reason for this to be the much simpler handling of the particle-particle and hole-hole channel by means of a BLAS implementation, since only the particle-hole channel requires the additional use of Pandya transformations to be cast into a matrix-product form. However, simply neglecting the particle-hole channel for computational reason might induce severe systematic errors as the largest part of the third-order correction comes from this term. It is also clear that such effects may strongly depend on the Hamiltonian under consideration, i.e., a general

Hamiltonian-independent conclusion about the size of a certain contribution is difficult. We strongly recommend, however, to respect the intrinsic hierarchy of the many-body method in use. Thus, at a given order, all diagrams must be included. In particular, a selection of diagrams for computational reason must be avoided since the computational complexity is not connected to the physical content of a given channel.⁴

We note that even though an arbitrary selection of diagrams may lead to wrong estimates and is not recommended, there exist ways to partially include diagrams of a given perturbation order in a meaningful way. One possibility for example is the use *ring summations* or *ladder summations* where certain topologies are included up to infinite order. Some first test calculations can be found in Ref. [Dör15].

⁴Note that since $n_p \gg n_h$ the particle-particle channel is from the point of computational scaling the most challenging one.

PART III

PERTURBATIVELY-ENHANCED NO-CORE SHELL MODEL

Introduction to Part III

When advancing to genuine open-shell systems the use of single-determinantal reference states is, in general, not a suitable starting point for the correlation expansion. We have seen in 6 that occurring (quasi-)degeneracies can lead to singular perturbation expansions. Furthermore, the fully correlated wave function may not be dominated by single Slater determinant and requires an inclusion of high-order correlation effects. Moreover, the extension of HF-MBPT to excited states is not straightforward.

A possible solution is the use of more general states that already account for static correlation effects at zero order. In particular, proper multi-configurational reference states, i.e., a superposition of several Slater determinants, have proven to provide accurate results in quantum chemistry [RSS03; SSK04], and also in the application of the multi-reference IMSRG in nuclear structure [Her⁺16; Geb⁺16]. In general the origin of these reference states remains arbitrary. However, using eigenvectors from a prior no-core shell model calculation leads to systematically improvable zero-order states and, thus, defines a *hybrid ab-initio approach* combining configuration interaction and perturbation theory. Additionally, such an ansatz treats ground and excited states on an equal footing and, therefore, provides direct access to medium-mass spectroscopy.

We start with introducing configuration interaction as a general *ab initio* method and discuss the no-core shell model and its importance-truncated extension as particular variants thereof. Next, we present many-body perturbation theory with respect to arbitrary multi-configurational reference states. After defining the basic concept (and zero-order Hamiltonian) we introduce the diagrammatic formalism, which is used for the derivation of low-order energy corrections. Later on, we discuss no-core shell model eigenvectors as a particular choice of reference state.

Since the derivation of low-order formulas becomes very cumbersome and error-prone with increasing perturbation order, we present a systematic way for computer-aided code generation of low-order multi-configurational perturbation theory.

In the last chapter we discuss recent results for excitation spectra and ground-state energies of medium-mass nuclei using state-of-the-art chiral interactions for selected isotopic chains. Particular emphasis is put on a deeper understanding of neutron-rich isotopes and the theoretical reproduction of experimentally observed neutron driplines.

9

Configuration Interaction

One of the conceptually simplest approaches for the solution of the quantum many-body problem is the *configuration interaction* (CI) approach. The basic idea is to diagonalize the nuclear Hamiltonian in A -body space in a basis of Slater determinants for a selected single-particle basis. In principle the CI method provides an exact solution of the Schrödinger equation. In actual calculations one is restricted to a finite set of basis functions and, therefore, CI only provides upper bounds to the exact solution. A special variant of CI is the no-core shell model (NCSM) which has a long tradition in nuclear structure theory [NVB00; Bog+08; Bin10; BNV13; RN07]. Because of the high computational costs, CI approaches are limited to light nuclei. In order to advance to heavier systems extensions have been developed, which reduce the size of the Hamilton matrix and allow tackling nuclei up into the lower sd-shell. Such approaches will be described at the end of the chapter in the context of the importance-truncated NCSM (IT-NCSM).

9.1 FULL CONFIGURATION INTERACTION

The full CI wave function has the form

$$|\psi_{\text{FCI}}\rangle = |\Phi\rangle + \sum_{a,i} C_i^a |\Phi_i^a\rangle + \sum_{a<b,i<j} C_{ij}^{ab} |\Phi_{ij}^{ab}\rangle + \sum_{a<b<c,i<j<k} C_{ijk}^{abc} |\Phi_{ijk}^{abc}\rangle + \dots, \quad (9.1)$$

where $|\Phi\rangle$ is the reference determinant and all other components are build via particle-hole excitations on top of $|\Phi\rangle$. The restrictions of the summations in (9.1) ensure that every configuration is accounted for only once. When using the full configuration interaction (FCI) ansatz all components up to A p- A h-excitations are taken into account. This means, for example, that the FCI expansion in a ${}^4\text{He}$ calculation contains up to fourfold-excited

determinants, whereas for ^{208}Pb one needs to include up to 208-fold excited determinants in the many-body space.

In FCI calculations there is no other truncation than the dimension of the single-particle basis \mathcal{D}_{SP} . The many-body basis is constructed as

$$V^{\text{FCI}} \equiv \left\{ |\Phi_k\rangle = \hat{c}_{k_1}^\dagger \cdots \hat{c}_{k_A}^\dagger |0\rangle : k_1 < \dots < k_A = 1, \dots, \mathcal{D}_{SP} \right\}. \quad (9.2)$$

It can be shown that the dimension of the FCI space is given by

$$\dim(V^{\text{FCI}}) = \frac{(\mathcal{D}_{SP})!}{A!(\mathcal{D}_{SP} - A)!}. \quad (9.3)$$

The factorial growth of the FCI space with respect to, both, particle number A and single-particle dimension \mathcal{D}_{SP} , provides the main limitation of applying FCI beyond the lightest nuclei.

Sometimes it is more convenient to have a shorthand notation for the FCI expansion available. We, therefore, define so-called np - nh excitation operators

$$\hat{C}_n = \frac{1}{(n!)^2} \sum_{\substack{i_1, \dots, i_n \\ a_1, \dots, a_n}} C_{i_1, \dots, i_n}^{a_1, \dots, a_n} \hat{c}_{a_1}^\dagger \cdots \hat{c}_{a_n}^\dagger \hat{c}_{i_1} \cdots \hat{c}_{i_n}, \quad (9.4)$$

with *CI amplitudes* $C_{i_1, \dots, i_n}^{a_1, \dots, a_n}$ such that, when acting on $|\psi_0\rangle$, \hat{C}_n generates all np - nh excitations. Therefore, the *linear* FCI expansion can be written as

$$|\psi_{\text{FCI}}\rangle = (1 + \hat{C}_1 + \hat{C}_2 + \hat{C}_3 + \dots)|\Phi\rangle. \quad (9.5)$$

We can, thus, define the *FCI wave operator* by

$$|\psi_{\text{FCI}}\rangle = (\hat{1} + \hat{\Omega}^{(\text{FCI})})|\Phi\rangle, \quad \hat{\Omega}^{(\text{FCI})} \equiv \sum_{n=1}^A \hat{C}_n, \quad (9.6)$$

which reproduces the exact wave function when acting on the reference determinant.

9.2 TRUNCATED CONFIGURATION INTERACTION

Due to the large size of the many-body basis in FCI calculations such an approach becomes impractical with increasing mass number. Therefore, one introduces a truncation of the FCI wave operator in the particle rank of the excitation operators \hat{C}_n . The wave operator in *truncated configuration interaction of rank m* reads,

$$\hat{\Omega}^{\text{CI}(m)} = \sum_{n=1}^m \hat{C}_n. \quad (9.7)$$

For the lowest truncated CI variants there exists an explicit nomenclature. In the simplest case the truncated CI wave operator contains only double excitations, which is called *CI with doubles* (CID). More advanced methods include all excitation operators up to, e.g., particle rank $m = 3$ leading to *CI with singles, doubles and triples* (CISDT). Contrary to what one might expect, *CI with singles* (CIS) is not the simplest non-trivial finite CI method. Using only singles in the CI expansion correspond to performing an orbital rotation of the single-particle states which does not affect the binding energy.

The above truncation is justified since one expects a hierarchy in the importance of particle-hole excitations in the description of ground-state energies. In particular, one expects that higher-order contributions will become less significant than lower ones. However, this is a rather generic statement. In particular in quantum chemistry we know systems where, e.g., quadruples in the CI expansion are equally important as triples. The particular importance of certain types of contributions heavily depends on the system under investigation and the Hamiltonian used in the calculation.

The truncated CI expansion leads to a much milder scaling of the many-body basis size when enlarging the single-particle basis. However, in any truncated CI method there exists the so-called *size-consistency problem*. A truncation scheme is defined to be size-consistent if the energy of the two systems A and B and the energy of the combined system AB satisfy

$$E(AB) = E(A) + E(B), \quad (9.8)$$

where it is assumed that the two systems A and B are infinitely far apart such that they do not influence each other. Furthermore, the energy has to be computed in equivalent ways, e.g., in the CID approximation. Relation (9.8) is always fulfilled in the FCI ansatz. However, when truncating the FCI expansion one always introduces a source of size-inconsistency. Practical calculations in quantum chemistry showed that CISDTQ, i.e., CI with singles, doubles, triples and quadruples, is effectively size-consistent when describing systems of modest size. Additionally, it is possible to derive *a-posteriori* corrections to account for the induced size-consistency error in finite CI calculations [LD74; DD94; Rot08].

Ultimately, one is interested in formulating a many-body approach that is rigorously size-consistent at any truncation order. Coupled-cluster theory was one of the first approaches that solved the size-consistency problem by using an exponential ansatz for the wave operator instead of the linear CI form [Coe58; CK60; Číž66; ČP69]. For a more detailed discussion of the connection of coupled-cluster theory and CI theory in the context of size consistency we refer the reader to [SB09].

9.3 NO-CORE SHELL MODEL

Another possibility to truncate the FCI expansion is a restriction in the maximal excitation energy with respect to $|\Phi\rangle$ in (9.1). In the following we will always assume a HO single-particle basis. We define a shorthand notation for the *excitation energy* of a Slater determinant $|\Phi_{i_1, \dots, i_n}^{a_1, \dots, a_n}\rangle$ with respect to $|\Phi\rangle$ by ¹

$$e_{i_1, \dots, i_n}^{a_1, \dots, a_n} \equiv \sum_{k=1}^n (e_{a_k} - e_{i_k}), \quad (9.9)$$

where $e_k = (2n_k + l_k)$ denotes the HO quantum number. With this we define *No-Core Shell-Model* (NCSM) wave operator via

$$\hat{C}^{(\text{NCSM})} \equiv \sum_{n=1}^A \hat{C}_n^{(\text{NCSM})}, \quad (9.10)$$

where

$$\hat{C}_n^{(\text{NCSM})} \equiv \sum_{\substack{a_1, \dots, a_n \\ i_1, \dots, i_n}} C_{i_1, \dots, i_n}^{a_1, \dots, a_n} \hat{c}_{a_1}^\dagger \cdots \hat{c}_{a_n}^\dagger \hat{c}_{i_1} \cdots \hat{c}_{i_n} \quad (9.11)$$

is the NCSM excitation operator. The sum in (9.11) is constrained such that

$$e_{i_1, \dots, i_n}^{a_1, \dots, a_n} \leq N_{\max}, \quad (9.12)$$

where N_{\max} is the maximal value of excitation quanta of the Slater determinants that are included in the model space.

One important property of this truncation scheme is a factorization of the NCSM wave function into a center-of-mass part and a relative part when using harmonic oscillator single-particle states,

$$|\psi^{(\text{NCSM})}\rangle = |\psi_{\text{int}}\rangle \otimes |\psi_{\text{cm}}\rangle, \quad (9.13)$$

where $|\psi_{\text{int}}\rangle$ denotes the intrinsic wave function and $|\psi_{\text{cm}}\rangle$ the center-of-mass wave function. When using a total nuclear Hamiltonian

$$\hat{H}_{\text{tot}} = \hat{H}_{\text{nucl}} + \beta \hat{H}_{\text{cm}}, \quad (9.14)$$

where \hat{H}_{cm} denotes a HO Hamiltonian with respect to the center-of-mass coordinates, the NCSM scheme avoids spurious center-of-mass contaminations, which are present when deal-

¹We note that the term 'energy' is misleading since $e_{i_1, \dots, i_n}^{a_1, \dots, a_n}$ is a dimensionless quantity.

ing with CI wave functions constructed from another single-particle basis, e.g., the self-consistent field orbitals arising from Hartree-Fock calculations.

For a discussion of recent applications of the NCSM see, e.g., Ref. [BNV13].

9.4 IMPORTANCE-TRUNCATED NO-CORE SHELL MODEL

As already mentioned, the tremendous growth of basis size restricts the range of applicability of the NCSM to very light nuclei. Many applications of the NCSM with very large N_{\max} -truncated model spaces do not reach model-space convergence even with the use of massive parallelization techniques. In order to extend the reach of CI methods, several importance-truncated extensions have been formulated and applied [ALP03; RN07; Rot08; Rot09].

The main observation is that a large part of the many-body states in the NCSM basis do not significantly contribute to the expansion of a particular eigenstate. Therefore, one constructs an *a-priori* measure for the importance of a certain basis state. With this the most relevant basis states are preselected before the diagonalization is performed. We emphasize that we do not evaluate all matrix elements of the Hamiltonian and discard corresponding column vectors according to the *a-priori* measure of the corresponding basis state, but only build the many-body Hamiltonian with respect to basis states, where the measure exceeds a given threshold.

For the construction of the importance measure one uses a perturbative ansatz and investigates the amplitude of the first-order state correction. To this end, one defines a small *reference space* \mathcal{M}_{ref} in which the nuclear Hamiltonian is subsequently diagonalized,²

$$\hat{H}|\psi_{\text{ref}}\rangle = \epsilon_{\text{ref}}|\psi_{\text{ref}}\rangle. \quad (9.15)$$

Let now $|\phi_{\mu}\rangle \notin \mathcal{M}_{\text{ref}}$ be a Slater-determinantal basis function. We define the *importance measure* κ_{μ} by

$$\kappa_{\mu} \equiv -\frac{\langle \phi_{\mu} | \hat{H} | \psi_{\text{ref}} \rangle}{\epsilon_{\mu} - \epsilon_{\text{ref}}}. \quad (9.16)$$

The IT-NCSM model space is defined as

$$V^{(\text{IT-NCSM})} \equiv \text{span}\{|\phi_{\mu}\rangle \in V^{(\text{NCSM})} : |\kappa_{\mu}| \geq \kappa_{\min}\}, \quad (9.17)$$

where κ_{\min} is some fixed value, where now

$$V^{(\text{IT-NCSM})} \subset V^{(\text{NCSM})}. \quad (9.18)$$

²Typically such a reference space is defined by a full NCSM space for a small value of N_{\max} .

The NCSM wave function is obtained in the limit of $\kappa_{\min} \rightarrow 0$,

$$|\psi^{(\text{NCSM})}\rangle = \lim_{\kappa_{\min} \rightarrow 0} |\psi^{(\text{IT-NCSM})}\rangle. \quad (9.19)$$

In practice, IT-NCSM calculations are typically performed for several values of κ_{\min} . The limit $\kappa_{\min} = 0$ is then obtained by extrapolating a κ_{\min} -sequence. The extrapolation error is, in most cases, of the order of 100 keV for an absolute energy and reliable results for ground-state energies and spectra can be obtained up to heavy oxygen isotopes [Rot08; Rot09].

10

Multi-Configurational Perturbation Theory

At the end of the discussion of HF-MBPT we have discussed possible limitations of single-configurational many-body methods and single-configurational MBPT in particular. A solution to this problem is the use of more general reference states that include static correlation effects and lift the zero-order degeneracy. In this section we derive a general version of perturbation theory that is build on top of a (normalized) multi-configurational reference state consisting of several determinants. Similar techniques have already been used successfully in quantum chemistry [RSS03; SSK04]. With this we can generalize the partitioning from HF-MBPT to such multi-configurational reference states while sticking to a Møller-Plesset philosophy, where unperturbed energies are defined in terms of sums of suitably chosen single-particle energies. We derive low-order energy corrections and introduce a new normal-ordering formalism, which makes use of several (single-determinantal) Fermi vacua allowing for the derivation of perturbative energy corrections in terms of one- and two-body quantities. After presenting an exhaustive list of all second-order diagrams we discuss computational aspects of the implementation.

Finally, by using particular reference states obtained from prior NCSM calculations we define a novel *hybrid ab initio* approach which merges NCSM and MBPT technology, thus, allowing to improve the zero-order reference states in a controlled way.

10.1 DEFINITION OF PARTITIONING

We start with a discussion of the partitioning and the reference space in depth and derive a low-order many-body perturbation theory from it.

We use a reference state obtained from a prior diagonalization in a model space \mathcal{M}_{ref} ,

$$|\psi_{\text{ref}}\rangle = \sum_{|\Phi_\nu\rangle \in \mathcal{M}_{\text{ref}}} C_\nu |\Phi_\nu\rangle, \quad (10.1)$$

where c_ν denote the expansion coefficients of the eigenvector with respect to the Slater-determinantal basis functions $\{|\Phi_\nu\rangle\}$ spanning \mathcal{M}_{ref} .

We formally define the zero-order Hamiltonian \hat{H}_0 by

$$\hat{H}_0 = \sum_I E_I |\psi_I\rangle \langle \psi_I| + \sum_{|\Phi_\mu\rangle \notin \mathcal{M}_{\text{ref}}} E_\mu^{(0)} |\Phi_\mu\rangle \langle \Phi_\mu|, \quad (10.2)$$

where $\{|\Phi_\mu\rangle\}$ denote the Slater determinants spanning $\mathcal{M}_{\text{ref}}^\perp$. The first term corresponds to the solution of the eigenvalue problem in \mathcal{M}_{ref} with corresponding eigenstates $|\psi_I\rangle$. In particular $|\psi_{\text{ref}}\rangle$ corresponds to one of the eigenvectors $|\psi_I\rangle$.

With this it holds that

$$\hat{H}_0 |\psi_{\text{ref}}\rangle = E_{\text{ref}} |\psi_{\text{ref}}\rangle, \quad (10.3)$$

where E_{ref} is yet to be specified. In the spirit of the Møller-Plesset partitioning in HF-MBPT we define the reference energy by

$$E_{\text{ref}} = \sum_p \epsilon_p \gamma_{pp}, \quad (10.4)$$

where ϵ_p denote suitably chosen single-particle energies and γ the (correlated) one-body density matrix with respect to the multi-configurational reference state

$$\gamma_{pq} = \langle \psi_{\text{ref}} | \hat{c}_p^\dagger \hat{c}_q | \psi_{\text{ref}} \rangle. \quad (10.5)$$

The diagonal elements $\gamma_{pp} \in [0, 1]$ can be seen as generalizations of the occupation numbers from HF theory.

The unperturbed energies of the states $|\Phi_\mu\rangle \in \mathcal{M}_{\text{ref}}^\perp$ are defined by

$$E_\mu^{(0)} = \sum_{i \text{ occupied in } |\Phi_\mu\rangle} \epsilon_i. \quad (10.6)$$

For the definition of single-particle energies we use the Baranger Hamiltonian with matrix elements

$$f_{pq} = H_{pq}^{[1]} + \sum_{rs} \bar{H}_{pqrs}^{[2]} \gamma_{rs}, \quad (10.7)$$

and define

$$\epsilon_p = f_{pp}. \quad (10.8)$$

Again structural information about the reference state enters the definition of the single-particle energies. With the above partitioning the zero- and first-order energy corrections read

$$E^{(0)} = \langle \psi_{\text{ref}} | \hat{H}_0 | \psi_{\text{ref}} \rangle = E_{\text{ref}}, \quad (10.9)$$

$$E^{(1)} = \langle \psi_{\text{ref}} | \hat{W} | \psi_{\text{ref}} \rangle = \langle \psi_{\text{ref}} | \hat{H} | \psi_{\text{ref}} \rangle - E_{\text{ref}}, \quad (10.10)$$

such that

$$E^{(0)} + E^{(1)} = \langle \psi_{\text{ref}} | \hat{H} | \psi_{\text{ref}} \rangle, \quad (10.11)$$

thus, corresponding to the eigenvalue of \hat{H} restricted to \mathcal{M}_{ref} .

According to the resolvent expansion the first non-trivial energy correction appears at second order and can be written as

$$E^{(2)} = \sum_{|\Phi_\nu\rangle \notin \mathcal{M}_{\text{ref}}} \frac{|\langle \psi_{\text{ref}} | \hat{W} | \Phi_\nu \rangle|^2}{E_{\text{ref}} - E_\nu^{(0)}}, \quad (10.12)$$

where the sum runs over all determinants $\{|\Phi_\nu\rangle\} \notin \mathcal{M}_{\text{ref}}$.

The restriction of the above sum to states from $\mathcal{M}_{\text{ref}}^\perp$ is a particular feature of using an eigenvector of \hat{H} in the reference space. In general there appears the additional term

$$\sum_{\substack{|\psi_I\rangle \in \mathcal{M}_{\text{ref}} \\ |\psi_{\text{ref}}\rangle \neq |\psi_I\rangle}} \frac{|\langle \psi_{\text{ref}} | \hat{W} | \psi_I \rangle|^2}{E_{\text{ref}} - E_I^{(0)}}, \quad (10.13)$$

which runs over the other eigenvectors $|\psi_I\rangle$. However, by orthogonality of the eigenvectors follows

$$\begin{aligned} \langle \psi_{\text{ref}} | \hat{W} | \psi_I \rangle &= \langle \psi_{\text{ref}} | \hat{H} | \psi_I \rangle - \langle \psi_{\text{ref}} | \hat{H}_0 | \psi_I \rangle \\ &= \langle \psi_{\text{ref}} | E_{\text{ref}}^{\text{NCSM}} | \psi_I \rangle - \langle \psi_{\text{ref}} | E_I | \psi_I \rangle = 0, \end{aligned} \quad (10.14)$$

where E_I^{NCSM} denotes the NCSM eigenvalue of the state $|\psi_I\rangle$. Therefore, other many-body states than $|\psi_{\text{ref}}\rangle$ in \mathcal{M}_{ref} do not contribute to the evaluation of the second-order correction. This is of particular importance since the many-body dimension of the reference states can contain up to several millions of states. ¹

We note that this holds no longer true for MCPT beyond third-order, where other P -

¹Note that we require here a solution of the *complete* eigensystem and not just the lowest one. Therefore, Lanczos methods for the solution of extremal eigenvalue are inapplicable.

space states may contribute indirectly through intermediate states.

THE LIMIT OF A ONE-DIMENSIONAL REFERENCE SPACE

After discussing the generalities of the above choice of \hat{H}_0 we investigate the limit of a one-dimensional reference space, i.e., where $|\psi_{\text{ref}}\rangle$ is (again) a single Slater determinant. In this case the one-body density matrix becomes diagonal. Moreover, γ_{pq} vanishes if p and q are not both hole states.²

The formal definition of E_{ref} becomes

$$E_{\text{ref}} = \sum_p \epsilon_p \gamma_{pp} = \sum_i \epsilon_i, \quad (10.15)$$

where the sum over i in the last expression runs over all occupied single-particle states in the reference state $|\psi_{\text{ref}}\rangle$.

With this, the one-body operator used for the definition of single-particle energies reduces to

$$\begin{aligned} f_{pq} &= H_{pq}^{[1]} + \sum_{rs} \bar{H}_{psqs}^{[2]} \gamma_{rs} \\ &= H_{pq}^{[1]} + \sum_i \bar{H}_{piqi}^{[2]}, \end{aligned} \quad (10.16)$$

which is just the definition of the mean-field Fock operator from HF theory. Thus, the above choice of \hat{H}_0 leads to ordinary single-configurational MBPT, which we have already discussed in chapter 6.

10.2 DERIVATION OF LOW-ORDER CORRECTIONS

The second-order energy correction to an arbitrary multi-determinantal reference state can be calculated using (10.12). However, this expression is formulated entirely in terms of many-body quantities. Therefore, for the evaluation of the second-order correction one must, in principle, construct all many-body configurations $\{|\Phi_\nu\rangle\}$ for a given Hilbert space \mathcal{H} and calculate the corresponding many-body matrix elements $\langle\psi_{\text{ref}}|\hat{W}|\Phi_\nu\rangle$.³ Such a strategy becomes impractical when proceeding to heavier systems since the size of the many-body space is too large. Therefore, we will reformulate energy corrections using normal-ordering techniques and cast them into a form that only depends on one- and two-body quantities. The sums over many-body configurations will then be replaced by sums over single-particle

²Note that in the case of a single-determinantal reference state we have again a well-defined particle-hole picture which is not the case when using a multi-determinantal reference state.

³In quantum chemistry such approaches are entitled 'sum over configuration'.

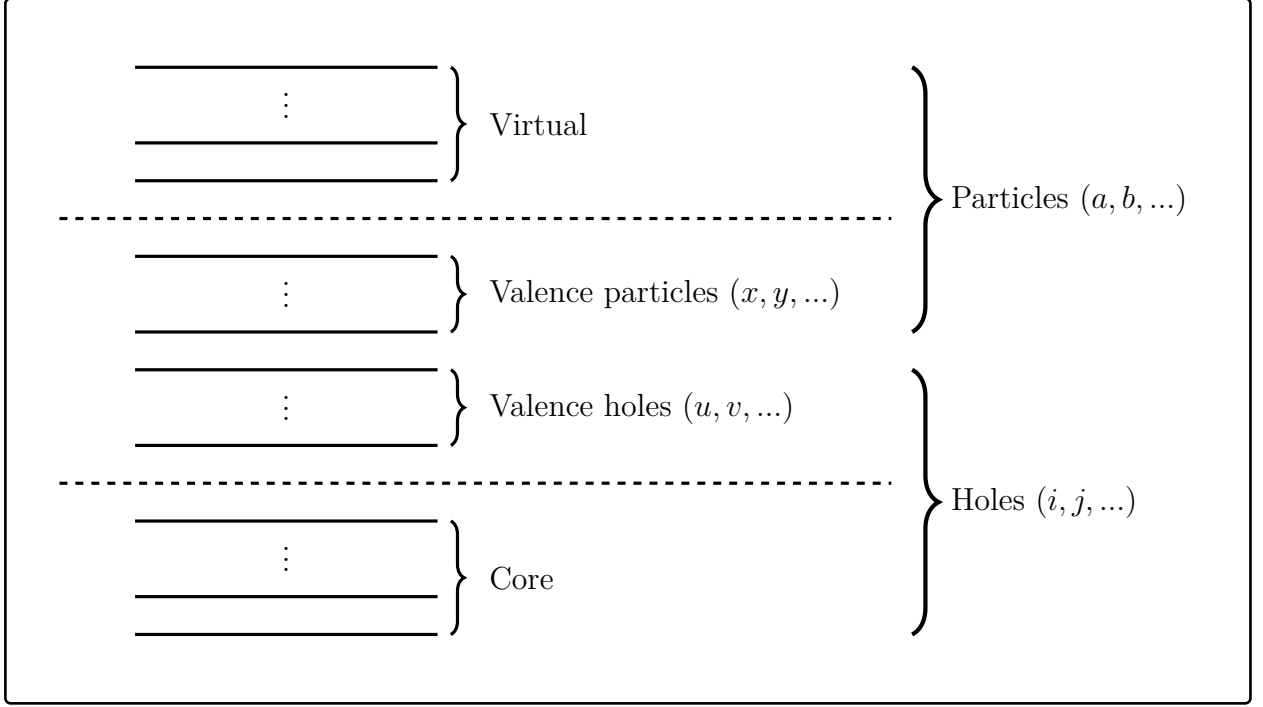


Figure 10.1: Classification of single-particle states in MCPT.

states.⁴ We start with expanding the reference state in (10.12) with respect to its Slater determinant components

$$E^{(2)} = \sum_{|\Phi_\mu\rangle, |\Phi'_\mu\rangle \in \mathcal{M}_{\text{ref}}} c_{\mu'} c_\mu^* \sum_{|\Phi_\nu\rangle \notin \mathcal{M}_{\text{ref}}} \frac{\langle \Phi_{\mu'} | \hat{W} | \Phi_\nu \rangle \langle \Phi_\nu | \hat{W} | \Phi_\mu \rangle}{E_{\text{ref}} - E_\nu^{(0)}}. \quad (10.17)$$

Fixing the determinants in the outer summation ($\mu \neq \mu'$) leads to the evaluation of expressions like

$$\sum_{|\Phi_\nu\rangle \notin \mathcal{M}_{\text{ref}}} \frac{\langle \Phi_{\mu'} | \hat{W} | \Phi_\nu \rangle \langle \Phi_\nu | \hat{W} | \Phi_\mu \rangle}{E_{\text{ref}} - E_\nu^{(0)}}. \quad (10.18)$$

The above expression only contains matrix elements with respect to single Slater determinants. To make use of Wick's theorem we must write all operators in normal-order with respect to a fixed reference state. We conveniently chose the rightmost determinant $|\Phi_\mu\rangle$ as Fermi vacuum. All other determinants appearing in the above expressions are expressed as particle-hole excitations with respect to $|\Phi_\mu\rangle$, e.g.,

$$\langle \Phi_{\mu'} | = \langle \Phi_\mu | \{i_1^\dagger \cdots i_p^\dagger a_p \cdots a_1\} | \Phi_\mu \rangle. \quad (10.19)$$

⁴Contrary to 'sum over configuration' approaches these methods are called 'sum over orbital' approaches.

As we will see, diagrams appearing in the formulas for the energy correction in MCPT contain open legs, which are not present in the energy corrections in single-configurational MBPT. Accordingly, some of the single-particle indices are occupied in all reference determinants corresponding to *core* indices while others are only occupied in some reference determinants corresponding to *valence* indices. Further, states that are unoccupied in all reference determinants are called *virtual* states. When specifying a particular determinant in the (multi-determinantal) reference state there is again a well-defined particle-hole picture and we can unambiguously refer to particle and hole indices, respectively. However, the particular set of particle and hole states depends on the determinant under consideration.

Figure 10.1 gives an overview of the naming convention for the different classes of single-particle states. However, we note that the ordering of the single-particle states does not reflect the energetic ordering and the classification of valence states relies on the particular reference state $|\psi_{\text{ref}}\rangle$. In particular in the most general case the core space is empty.

DIAGRAMMATIC RULES IN MCPT

The diagrammatic rules of single-configurational MBPT need to be extended to the multi-configurational setting. First we rewrite the perturbation operator \hat{W} in normal-product form with respect to the Slater determinant $|\Phi_\mu\rangle$,

$$W^{(\mu)} = \hat{h}_0^{(\mu)} + \hat{h}_1^{(\mu)} + \hat{h}_2^{(\mu)} \quad (10.20)$$

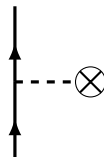
$$= \hat{h}_0^{(\mu)} + \sum_{pq} \langle p | \hat{h}_1^{(\mu)} | q \rangle \{ \hat{c}_p^\dagger \hat{c}_q \}_{|\Phi_\mu\rangle} + \sum_{pqrs} \langle pq | \hat{h}_2^{(\mu)} | rs \rangle \{ \hat{c}_p^\dagger \hat{c}_q^\dagger \hat{c}_s \hat{c}_r \}_{|\Phi_\mu\rangle}, \quad (10.21)$$

with matrix elements

$$\langle p | \hat{h}_1^{(\mu)} | q \rangle = (H_{pq}^{[1]} - \epsilon_p) \delta_{pq} + \frac{1}{2} \sum_{i \in |\Phi_\mu\rangle} \bar{H}_{piqi}^{[2]} \quad (10.22)$$

$$\langle pq | \hat{h}_2^{(\mu)} | rs \rangle = \bar{H}_{pqrs}^{[2]}. \quad (10.23)$$

In the following when we derive the energy corrections from the diagrams it is implied that we always use the normal-ordered part of the operators with respect to a fixed Fermi vacuum $|\Phi_\mu\rangle$. Note that the matrix elements of the one-body part implicitly depend on $|\Phi_\mu\rangle$. While we use the same diagrammatic representation for the two-body part of the perturbation operator as in chapter 6, we introduce a new vertex style to distinguish the determinant-dependent one-body vertices in MCPT from the ordinary HF-MBPT one-body vertices



Furthermore, the energy denominators are not given by differences of single-particle energies since $E_{\text{ref}}^{(0)}$ contains a non-trivial dependence on the one-body density. We rewrite the denominator as

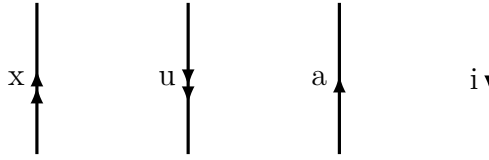
$$E_{\text{ref}}^{(0)} - E_{\nu}^{(0)} = E_{\text{ref}}^{(0)} - E_{\mu}^{(0)} + E_{\mu}^{(0)} - E_{\nu}^{(0)} \quad (10.24)$$

and define the quantity

$$\Delta_{\mu} \equiv E_{\text{ref}}^{(0)} - E_{\mu}^{(0)}. \quad (10.25)$$

Since both $|\Phi_{\mu}\rangle$ and $|\Phi_{\nu}\rangle$ are SDs, the difference of zero-order energies in MP partitioning is given by the difference of single-particle energies plus the contribution from (10.25) depending on the reference determinant. The difference of the single-particle energies can be read off from the *resolvent-line crossings* in the MCPT diagrams. The resolvent line is an imaginary horizontal line between adjacent vertices of the perturbation operators. Typically, it is *not* included in drawings of MBPT diagrams. We include the resolvent line in (10.29) for pedagogical reasons. Note that for open diagrams there is no additional resolvent line between the external legs and the top perturbation-operator vertex. In general a diagram of order p contains $p - 1$ resolvent lines.

Since the number of different index types increases, we introduce the following convention for the labelling of single-particle lines



which corresponds (from left to right) to valence particles and valence holes as well as general particles and general holes, respectively. External lines, i.e., lines corresponding to valence indices, are indicated with double arrows.

In the following we extensively use different kinds of permutation operators. Let $\mathcal{P}(pq)$ denote the transposition of single-particle indices p and q . We further define

$$\mathcal{P}(p/qr) \equiv 1 - \mathcal{P}(pq) - \mathcal{P}(pr), \quad (10.26)$$

as well as

$$\mathcal{P}_{(i/jk)}^{(a/bc)} \equiv \mathcal{P}(a/bc)\mathcal{P}(i/jk). \quad (10.27)$$

Diagrammatic Rules for MCPT

1. Every vertex corresponds to a one- or two-body matrix element. Reading the diagram from left to right lines are identified as follows

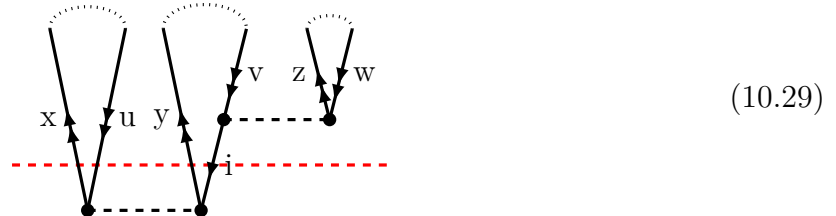
$$\langle \text{1st ingoing line, 2nd ingoing line} | \dots | \text{1st outgoing line, 2nd outgoing line} \rangle$$

2. Every internal line corresponds to a single-particle summation.
3. Downgoing lines correspond to hole indices and upgoing lines correspond to particle indices.
4. Each equivalent pair of lines gives a prefactor $\frac{1}{2}$.
5. The sign of the expression is given by $(-1)^{h+l}$ where h denotes the number of holes and l the number of loops.
6. For open diagrams one has to take into account all permutations of single-particle indices corresponding to open lines with their proper sign.
7. To every resolvent line corresponds an energy denominator

$$\epsilon_{i_1 \dots i_k}^{a_1 \dots a_k} + \Delta_\mu = \sum_{n=1}^k (\epsilon_{a_n} - \epsilon_{i_n}) + E_{\text{ref}}^{(0)} - E_\mu^{(0)} \quad (10.28)$$

depending on the number of single-particle lines crossing the resolvent line and current Fermi vacuum $|\Phi_\mu\rangle$.

The diagrammatic rules are best understood when applied to an example. In the following diagram we investigate a second-order contribution coming from two two-body operators and a triply-excited determinant $|\Phi_\mu\rangle = |\Phi_{uvw}\rangle$. In the following the red dashed line denotes the resolvent line used for the construction of energy denominators.



First we identify the two two-body matrix elements $\bar{H}_{xyui}^{[2]}$ and $\bar{H}_{vwiz}^{[2]}$. The resolvent operator yields an energy denominator $\epsilon_{ui}^{xy} + \Delta_\mu$. For the determination of the prefactor we need to count equivalent lines. The two pairs x and y as well as v and w are equivalent thus yielding

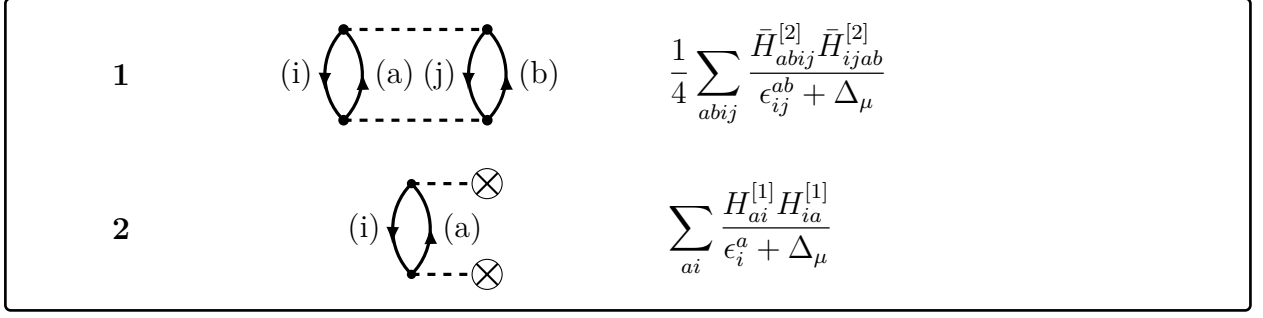


Figure 10.2: Closed ASG diagrams appearing at second-order MCPT.

a prefactor of $\frac{1}{4}$. The number of hole lines is $h = 4$ since u, v, w, i point downwards. For the calculation of the number of closed loops we added the dotted lines on top of the diagram. Obviously, the paths (x, u) , (y, v, i) and (z, w) are all closed. Within these loops every vertex is reached exactly once and the overall loop number is $l = 3$.

Additionally, making use of the permutation operators and summing over internal lines the overall expression reads

$$-\mathcal{P}_{(u/vw)}^{(z/xy)} (-1)^\sigma \frac{1}{4} \sum_i \frac{\bar{H}_{xyui}^{[2]} \bar{H}_{vwiz}^{[2]}}{\epsilon_{ui}^{xy} + \Delta_\mu}, \quad (10.30)$$

where σ denotes the sign of the permutation of external indices.

SECOND-ORDER ENERGY CORRECTION

The diagrammatic derivation of the second-order correction contains many more diagrams than the simpler single-configurational MBPT case. In general the diagrams can be classified according to the number of pairs of open legs, i.e., non-internal lines. In the case where the leftmost and rightmost determinant in (10.17) coincide ($\mu = \mu'$) the diagrams are closed and are the same as in single-configurational MBPT. However, note that since we are working with a multi-configurational reference state, the energy denominator is different and contains the additional contribution Δ_μ as eluded before. Additionally, since the 1B part does also contain a normal-ordered contribution depending on the current Fermi vacuum $|\Phi_\mu\rangle$, there is no analogue to Brillouin's theorem and, hence, the one-body part does not vanish. Therefore, we are always left with two closed diagrams. Figure 10.2 displays both topologies and their individual contribution.

New diagrammatic content appears when the leftmost determinant is different from the current Fermi vacuum, i.e., $\mu \neq \mu'$. At second-order MCPT when using two-body operators the leftmost determinant can be an up to 4p-4h excitation with respect to the Fermi vacuum. In general the highest possible excitation rank at a given order p is given by

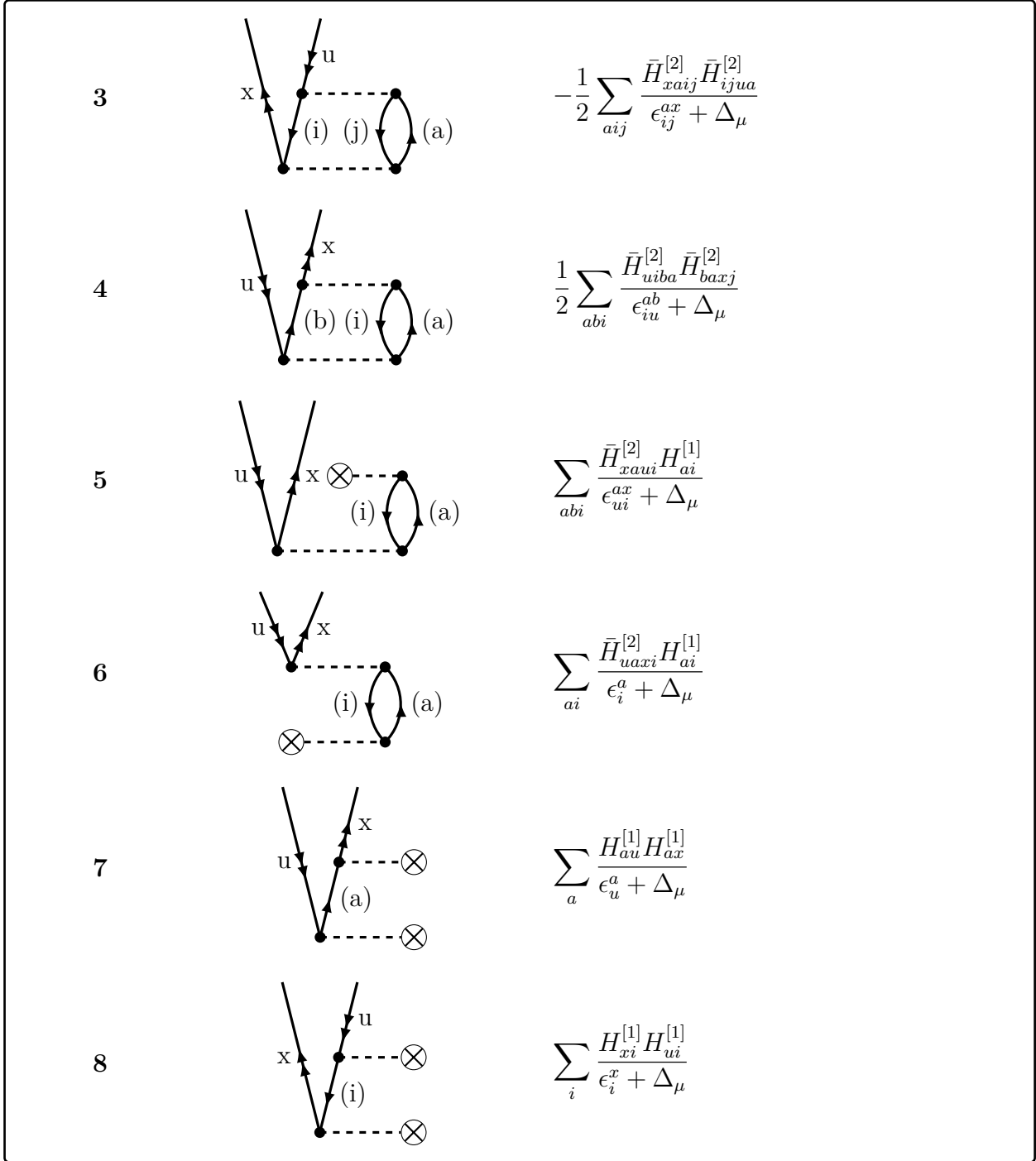


Figure 10.3: ASG diagrams with single-replacement at second-order MCPT.

$$p \cdot \text{rank}(\hat{H}), \quad (10.31)$$

where $\text{rank}(\hat{H})$ denotes the highest particle-rank in the Hamiltonian.

In the simplest case the leftmost determinant is a single excitation with respect to $|\Phi_\mu\rangle$. The corresponding six topologies (3 – 8) are shown in 10.3. Recall that there is no summation over external lines and the single-particle indices x, u correspond to the particle-hole

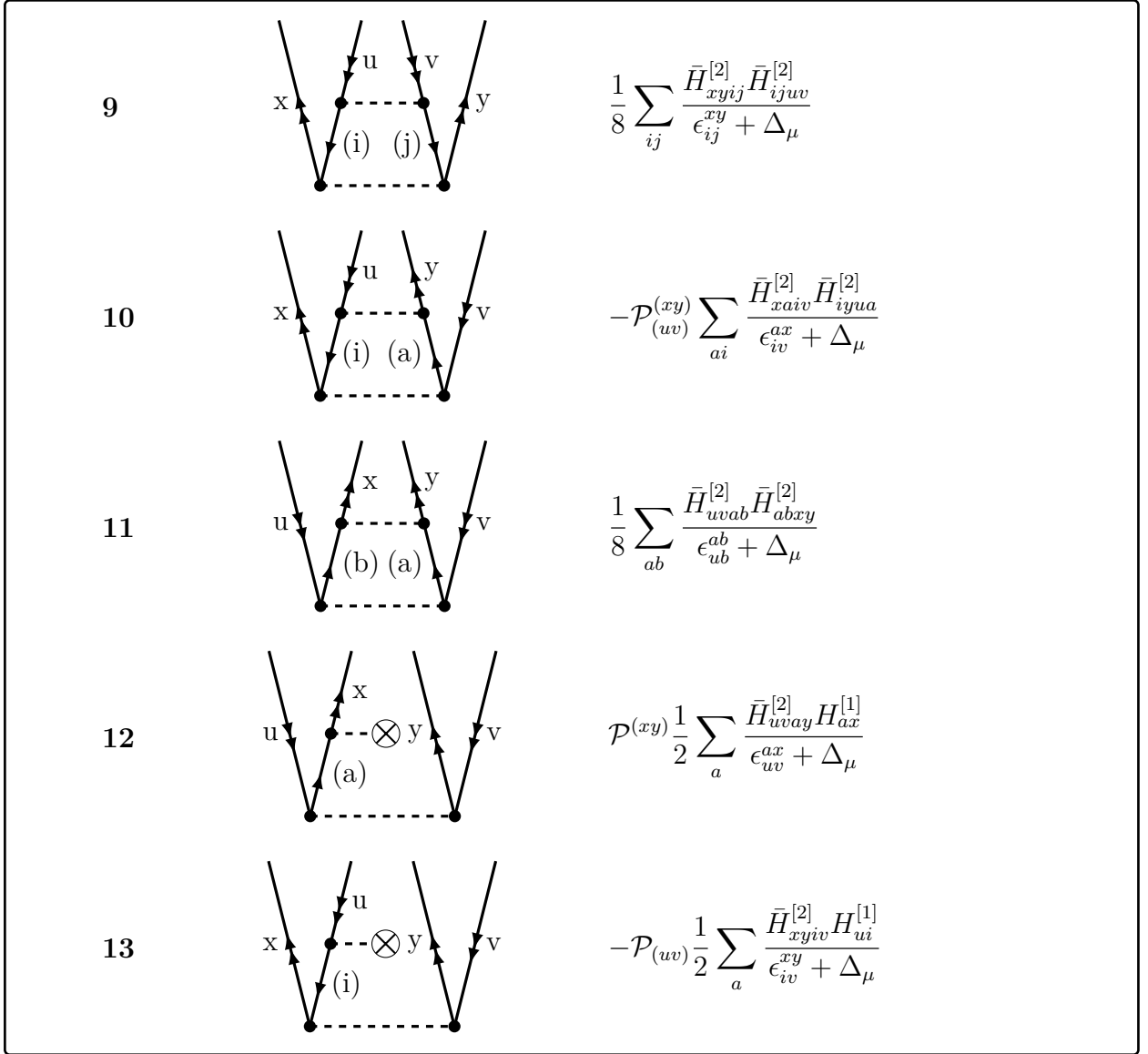


Figure 10.4: ASG diagrams with double-replacements at second-order MCPT.

representation of $|\Phi_{\mu'}\rangle$ with respect to $|\Phi_\mu\rangle$.

In the next case the leftmost determinant is a double excitation with respect to $|\Phi_\mu\rangle$ and there are eight ASG diagrams (9–16) contributing according to Wick's theorem. Figure 10.4 and 10.5 disentangle the individual contributions. Note that in the case of double excitations the permutation operator $\mathcal{P}_{(uv)}^{(xy)}$ enters for the first time thus giving up to four contributions for each individual diagram. Figure 10.6 displays all topologies for triple (17–20) and quadruple excitations (21) which yield additional five diagrams. Here, of course, higher permutation operators $\mathcal{P}_{(uvw)}^{(xyz)}$ and $\mathcal{P}_{(u_1u_2u_3u_4)}^{(x_1x_2x_3x_4)}$ enter. Overall there are 21 diagrams at second-order MCPT for two-body operators making the implementation much more cumbersome than in single-configurational MBPT.

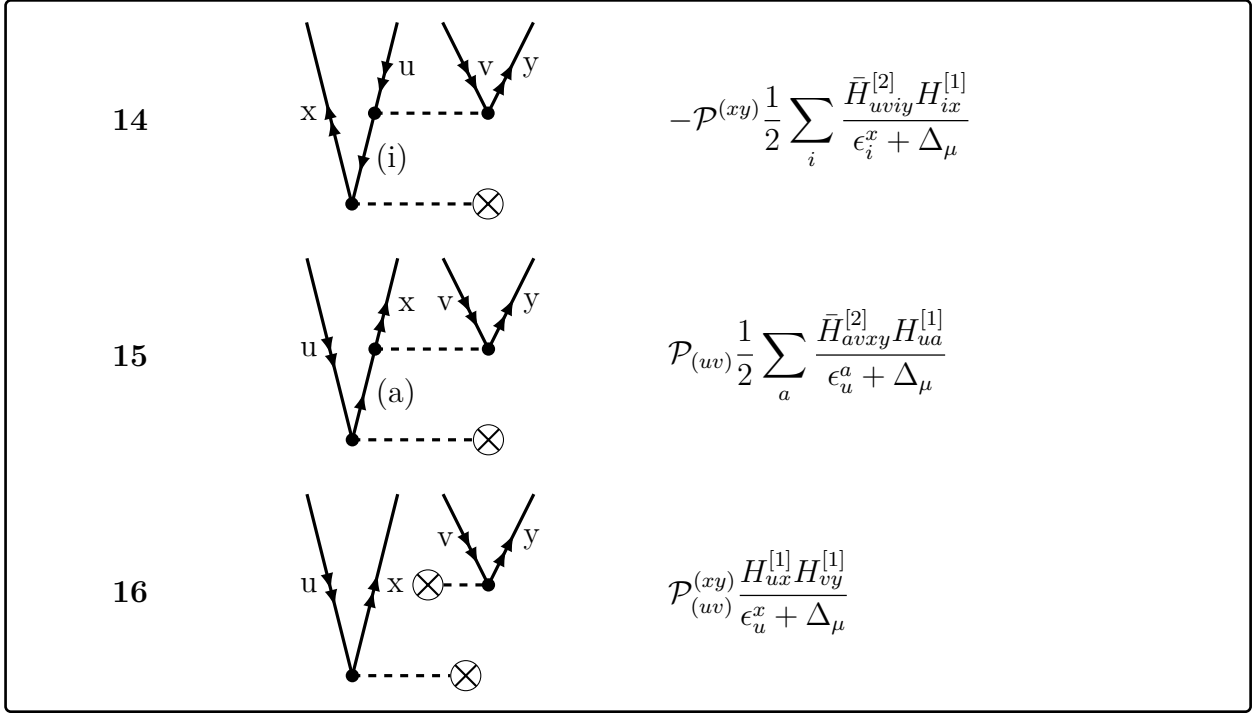


Figure 10.5: ASG diagrams with double-replacements at second-order MCPT, continued.

COMPUTATIONAL CONSIDERATIONS

Our implementation of MCPT uses a formulation in m -scheme. In this way we are not restricted to even-even nuclei and 0^+ states. However, the m -scheme basis dimension is much larger compared to using a spherical single-particle basis as we did in the case of single-configurational MBPT. Again single-particle summations can be classified into particle and hole summations. When changing the Fermi vacuum the particular hole states change, their number n_h , however, stays the same. The same holds for the particle states and their number n_p . Taking for example the first closed diagram in Figure 10.2 with two two-body vertices we have two particle and two hole summations, giving a scaling

$$\sim n_p^2 \cdot n_h^2. \quad (10.32)$$

Note, however, that this diagram has to be evaluated for every determinant. Let in the following

$$\mathcal{D}_{\text{ref}} \equiv \dim(\mathcal{M}_{\text{ref}}) \quad (10.33)$$

denote the size of the reference space, i.e., the number of SDs which $|\psi_{\text{ref}}\rangle$ is composed of. Therefore, diagram **1** yields an overall scaling of

$$\mathbf{1} \sim \mathcal{D}_{\text{ref}} \cdot n_p^2 \cdot n_h^2. \quad (10.34)$$

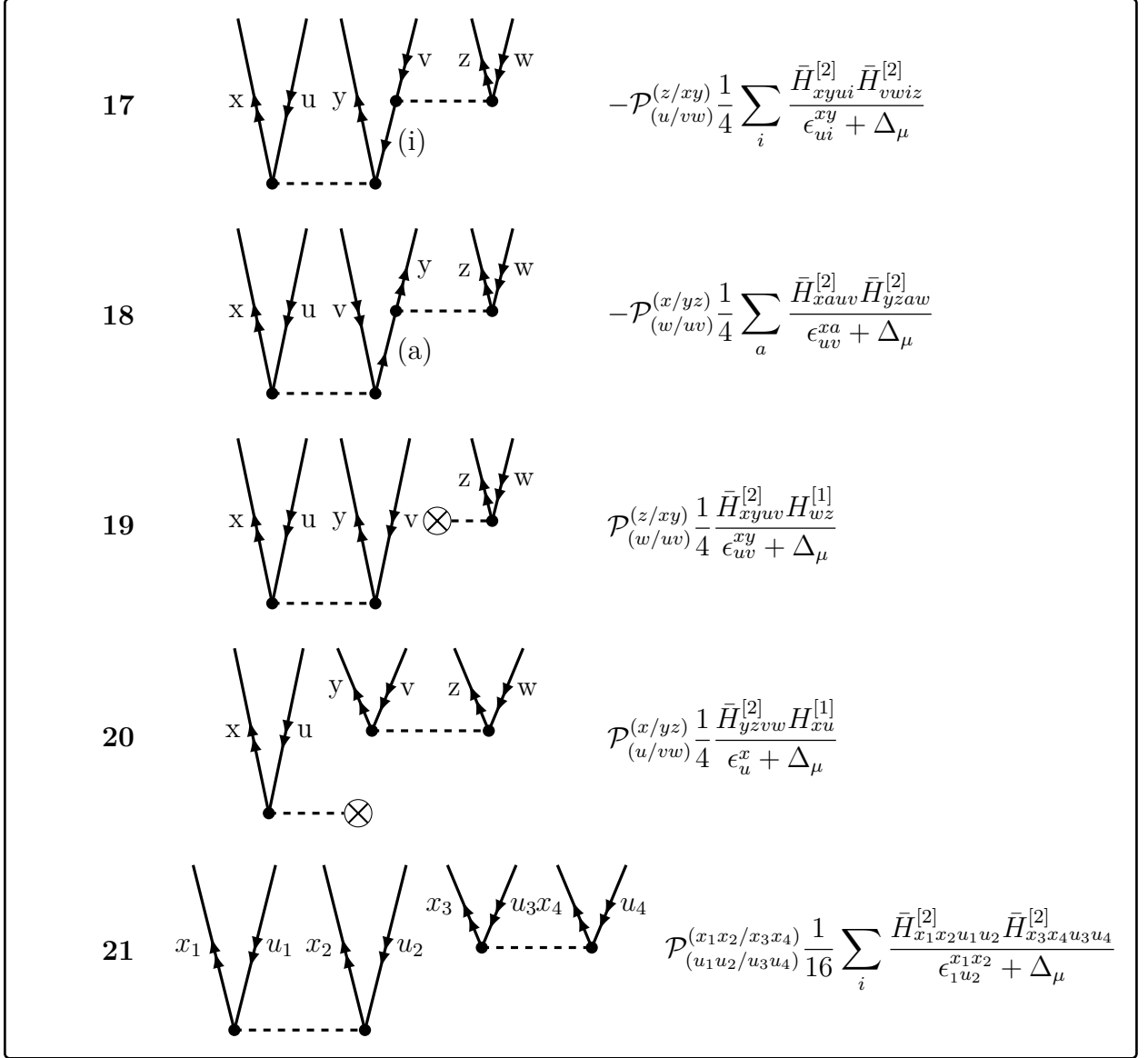


Figure 10.6: ASG diagrams with triple- and quadruple-replacements at second-order MCPT.

The second closed diagram containing two one-body vertices has two internal summations, making it naively a $\mathcal{D}_{\text{ref}} \cdot n_p \cdot n_h$ process. The one-body vertices are, however, not single matrix elements but contain, due to the normal-ordering with respect to the Fermi vacuum, each an additional hole summation. Therefore, diagram **2** exhibits a scaling

$$\mathbf{2} \sim \mathcal{D}_{\text{ref}} \cdot n_p \cdot n_h^3. \quad (10.35)$$

Since typically $n_p \gg n_h$ the two-body diagram **1** dominates the second-order MCPT corrections. We note that, due to the additional hole summations, the one-body diagram **2** is computationally more demanding than the closed one-body diagram in single-configurational

MBPT.⁵ The scaling of the closed diagrams at MCPT(2) is comparable to performing \mathcal{D}_{ref} copies of HF-MBPT(2). In particular calculations using very large reference spaces, where several millions of SDs are incorporated in the zero-order state, are numerically challenging. Additionally, we must evaluate the open-diagrams. For every tuple (μ, μ') of indices one class of diagrams has to be computed. In the worst case these contain up to three particle summations, i.e., diagrams **3** and **4**. This is the case for the first two diagrams for single replacements, see Figure 10.3. Since the number of tuples (μ, μ') is given by $\mathcal{D}_{\text{ref}}^2$, an upper bound for the scaling of the open diagrams is given by

$$\sim \mathcal{D}_{\text{ref}}^2 \cdot n_p^2 \cdot n_h. \quad (10.36)$$

We note that this is a very crude estimate since not every pair (μ, μ') corresponds to the case where $|\Phi_{\mu'}\rangle$ is a single excitation with respect to $|\Phi_{\mu}\rangle$. If $|\Phi_{\mu'}\rangle$ is, e.g., a double excitation then the diagrams involve at most two single-particle summations and the scaling is milder. However, (10.36) indicates how the scaling depends on the size of the reference space.

In summary we conveniently write⁶

$$\text{MCPT}(2) \sim \max\{\mathcal{D}_{\text{ref}} \cdot n_p^2 \cdot n_h^2, \mathcal{D}_{\text{ref}}^2 \cdot n_p^2 \cdot n_h\}, \quad (10.37)$$

to indicate the scaling behavior of second-order MCPT, where the first element corresponds to the scaling of the closed diagrams and the second one to the scaling of the open diagrams. Most importantly we see the different powers of \mathcal{D}_{ref} that enter the description.

EXTENSION TO THIRD ORDER AND THREE-BODY OPERATORS

We already discussed that the second-order energy correction required the derivation of a lot of diagrams. When proceeding to the third-order energy correction the proliferation of diagrams makes the error-prone derivation of the diagrams and the implementation of the code very tedious. There appear 377 diagrams at third order which contain up to hextuple, i.e., sixfold replacements. Therefore, one relies on the use of symbolic manipulation tools to support the implementation of MCPT(3). However, even modern packages that are used to evaluate Wick contractions automatically, might run into problems due to the high particle-rank of the leftmost excited determinants. An alternative to this approach is provided by the use of *combinatorial graph theory*, where the structure of the diagrams are encoded in terms of matrices. In a second step both the desired formulas and the source code can be generated from these matrices leading to an automated code generator. We will show how to deal with this problem in a systematic way in chapter 11.

⁵In this analysis we assume that we evaluate the one-body matrix elements on the fly. This is a reasonable assumption since the storage of $\mathcal{D}_{\text{ref}} \cdot n_p \cdot n_h$ matrix elements is impractical for large reference states.

⁶Here we assume again $n_p \gg n_h$ which is the regime we are interested in.

Another possible extension involves the inclusion of full three-body operators. This greatly increases the number of diagrams even at second order. Moreover, more complicated topologies arise containing up to hextuple replacements. Furthermore, not only the one-body part of the normal-ordered perturbation operator depends on the current Fermi vacuum but also the two-body part due to the contracted three-body part. Overall this tremendously increases the computational scaling already at second-order. It does, however, offer the possibility to account for three-body effects beyond the NO2B approximation, which is currently impossible for medium-mass open-shell nuclei.

10.3 MERGING MCPT AND NCSM

The above discussion is valid for arbitrary multi-configurational reference states $|\psi_{\text{ref}}\rangle$ with the sole restriction that the reference state is normalized. The use of eigenvectors from a NCSM calculation has a lot of advantages. As already introduced in chapter 9 the NCSM and its importance-truncated extension are very powerful *ab initio* techniques for the investigation of up to medium-light nuclei. While the NCSM renders a fully variational approach, the strong computational scaling prohibits its use beyond the oxygen chain. MCPT on the other hand is a non-variational many-body approach, which can access very large model spaces and effectively describe correlation effects perturbatively, provided the perturbation series is convergent. By using multi-configurational reference states static correlation effects are already included in the zero-order description and perturbative corrections take into account the residual dynamic correlations. In this way the *perturbatively-improved no-core shell model* (NCSM-PT) combines the advantages of both NCSM and MBPT and defines a novel *hybrid ab initio* approach, which is capable of describing complex nuclei in a controlled way from first principles.

In the NCSM-PT framework there exist two independent limits, where the exact wave function is reproduced. First lets assume we have a fixed model space \mathcal{M}_{ref} characterized by the value of $N_{\text{max}}^{(\text{ref})}$. If one calculates perturbative corrections up to infinite order the exact wave function and binding energy is reproduced, provided the perturbation series is convergent. On the other hand, if we alternatively enlarge the reference space we get in the limit where $N_{\text{max}}^{(\text{ref})} \rightarrow \infty$

$$E^{(p)} = 0, \quad \text{for } p \geq 2. \quad (10.38)$$

All correlation effects are included in the reference state and all perturbative corrections vanish. Therefore, there are two independent limits of the theory, which reproduce the exact solution of the Schrödinger equation.

In the simplest non-trivial case one uses the truncation

$$(N_{\max}^{(\text{ref})} = 0, p = 2). \tag{10.39}$$

If this does not provide an accurate approximation to the exact result one either increases the reference space size or includes higher-order effects depending on the particular problem under consideration. In many cases the use of $N_{\max} = 0$ in NCSM calculations does not reproduce the correct level ordering. Therefore, enlarging the reference to $N_{\max}^{(\text{ref})} = 2$ might help improving spectra in NCSM-PT. On the other hand, there are many known states where very particular correlation effects play a dominant role. For example excited states in ^{12}C are known to show notoriously slow convergence in the NCSM with respect to model space. Due to the α -clustering structure one expects the correlation expansion to be driven by quadruply-excited and eightfold-excited intermediate states and the inclusion of higher-order corrections beyond a simple second-order treatment might improve upon this. Thus our hybrid framework enables us to adapt the truncation to the specific state we are interested in.

However, we do note that increasing the perturbation order heavily increases computational demands and in applications even a third-order treatment is very challenging.

11

Automated Code Generation

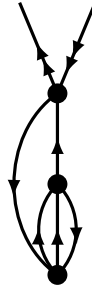
Automated generation and computer-aided derivation of formulas becomes increasingly important in modern nuclear theory. The tremendous increase in computing power enables for the implementation of more sophisticated truncation schemes of many-body techniques, e.g., MBPT, CC or IM-SRG. While the relaxation of the truncation schemes enables for a more accurate description of nuclear systems, the complexity of the formalism typically increases tremendously. This makes a more systematic treatment desirable. We particularly aim for an application to the derivation of low-order MCPT formulas. However, by introducing additional constraints for diagrams the same formalism may also be extended to other frameworks.

Historically, string-based algorithms for the derivation of perturbative corrections were introduced by Paldus and Wong for the computation of vacuum-to-vacuum amplitudes of Feynman diagrams [PW73; WP73] and later applied to fourth- and fifth-order order perturbation theory [Kal76].

11.1 ENCODING DIAGRAMS AS GRAPHS

In the first step we investigate a convenient representation of a diagram in terms of a graph. A *graph* G is an ordered triple (V, E, I) of a set of *vertices* V , a set of *edges* E , and an *incidence relation* I , which indicates which vertices are joined by which edges. We further call a graph *simple* if no edge starts and ends at the same vertex.

In the following we make use of a representation in terms of *Hugenholtz diagrams* where all two-body vertices are collapsed into a dot. A typical example of a diagram appearing at third-order MCPT is



Closed diagrams at order p contain p vertices whereas open diagrams contain additional pairs of external legs. In the following we will encode such diagrams by means of so-called *adjacency matrices*.¹ An adjacency matrix A_G of a graph G is the $|V| \times |V|$ matrix with entries

$$(A_G)_{ij} = \text{number of edges going from vertex } i \text{ to vertex } j. \quad (11.1)$$

This notation requires, of course an ordering of the vertices. We, therefore, label the vertices in the diagrams from bottom to top starting with $i = 1$ for the lowest vertex. For open diagrams we will identify the external lines with an additional *exceptional vertex* - denoted by a square - corresponding to the particle-hole excitations of the left-most determinant. The above diagram will subsequently be presented by



where the dots correspond to one-body and two-body matrix elements and the square vertex displays the excited determinant in the perturbation theory formulas. Here we also included the numbering of the vertices for pedagogical reasons. However, we suppress the numbering in the following.

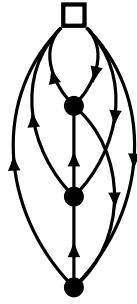
By the definition (11.1) the adjacency matrix of the above diagram is given by

$$\begin{pmatrix} 0 & 2 & 0 & 0 \\ 1 & 0 & 1 & 0 \\ 1 & 0 & 0 & 1 \\ 0 & 0 & 1 & 0 \end{pmatrix}. \quad (11.3)$$

¹In the literature some authors use the generalized adjacency matrices whereas the term adjacency matrix is reserved for unordered graphs. However, we will always work with ordered graphs and, therefore, will not distinguish the two terms. Note that in general this yields non-symmetric adjacency matrices.

PROPERTIES OF ADJACENCY MATRICES

Before proceeding let us note some important observations. First all diagonal entries are vanishing, i.e., $(A_G)_{ii} = 0$ which is a general feature of MBPT diagrams. This is related to the fact that we are working with normal-ordered operators and, therefore, self-contractions vanish. Further, the sum of all entries of a row or column determines the particle-rank of the corresponding vertex.² Matrix-element vertices which are presented by a dot always have particle rank one or two. The exceptional vertices corresponding to the excited determinants (vertex number 4 in the above picture) can have excitation rank $\deg(v) = 1, \dots, 6$, where we define the *degree* $\deg(v)$ of a vertex v to be the number of incoming (or outgoing lines). The following diagram—corresponding to a triple-replacement—displays this property³



(11.4)

As a first step of the automatized generation of formulas we need to generate all possible adjacency matrices at a given perturbation order. In the following we make use of the notion of a k -partitioning⁴ of a natural number n defined to be the set of distinct ordered tuples (a_1, \dots, a_k) with $a_i \in \mathbb{N}$ such that

$$\sum_{i=1}^k a_i = n. \quad (11.5)$$

As an example the following set \mathcal{S} lists all 4-partitionings of the number two:

$$\begin{aligned} \mathcal{S} = \{ & (2, 0, 0, 0), (0, 2, 0, 0), (0, 0, 2, 0), (0, 0, 0, 2), (1, 1, 0, 0), (1, 0, 1, 0), \\ & (1, 0, 0, 1), (0, 1, 0, 1), (0, 0, 1, 1), (0, 1, 1, 0) \}. \end{aligned} \quad (11.6)$$

²Note that there is no difference between summing over the row or column entries since we are working with particle-number conserving operators and, therefore, the number of ingoing and outgoing lines always coincide.

³The maximal particle rank depends on the particle rank of the perturbation operator $\text{rank}(\hat{W})$ and the perturbation order p . In general the particle rank of external legs is $\text{rank}(\hat{W}) \cdot p$, which is six for $p = 3$ and $\text{rank}(\hat{W}) = 2$.

⁴The notion of a k -partitioning is not to be confused with the partitioning of the Hamiltonian from MBPT. The terms are completely unrelated.

SYSTEMATIC GENERATION OF ADJACENCY MATRICES

In order to generate all open diagrams at p -th order MCPT one must generate all $p + 1$ -partitionings of the degree of the corresponding vertices. The degree of the vertices is $\deg(v_i) = 1, 2$ for $i = 1, \dots, p$ for all vertices except for the highest vertex v_p , which can have degree of up to $\deg(v_p) = 1, \dots, 2p$. The degree of the p lowest vertices is fixed by the one- and two-body nature of the interaction vertices, whereas the degree of the highest vertex is bound from above by the maximal excitation rank of the leftmost determinant, which is $2p$ for a two-body interaction. The adjacency matrices of p -th order open diagrams are $(p + 1) \times (p + 1)$ matrices. ⁵

We define an auxiliary *rank vector*

$$R^{(p)} = (\deg(v_1), \dots, \deg(v_p), \deg(v_{p+1})), \quad (11.7)$$

containing the particle ranks of all interaction vertices in the diagrams including the exceptional vertex v_{p+1} that corresponds to the excitation rank of the leftmost determinant. As a first step we classify a diagram \mathcal{D} according to the vector of the operator rank $R_{\mathcal{D}}$. For example, diagram (11.4) corresponds to

$$R_{\mathcal{D}}^{(3)} = (2, 2, 2, 3). \quad (11.8)$$

From the above rank vector we can already deduce if it is possible to create a valid diagram. Take for example the vector

$$R^{(3)} = (1, 2, 1, 6) \quad (11.9)$$

corresponding to a hextuple-replacement as can be seen from its fourth component $\tilde{R}_4^{(3)} = 6$. It is impossible to connect all twelve lines from the exceptional vertex with the other three vertices since two one-body operators and one two-body operator only have eight edges. A necessary condition for the validity of a given combination of particle ranks is thus given by

$$\sum_{i=1}^p \deg(v_i) \geq \deg(v_{p+1}). \quad (11.10)$$

Note that the sum of the ranks of the first p vertices can be greater than $\deg(v_{p+1})$ like diagram (11.2), corresponding to the vector $(2, 2, 2, 1)$, shows.

In the first step we generate, at a given order in perturbation theory, all valid rank vectors under the minimal requirement that the constraint (11.10) is fulfilled. It is important to note that rank vectors are not in one-to-one correspondence to ASG diagrams. Usually, several

⁵Closed diagrams are considered as the special case of $\deg(v_{p+1}) = 0$.

diagrams have the same rank vector. For example, all rank vectors for single replacements at third-order MCPT are given by

$$\left\{ \begin{pmatrix} 2 \\ 2 \\ 2 \\ 1 \end{pmatrix}^T, \begin{pmatrix} 1 \\ 2 \\ 2 \\ 1 \end{pmatrix}^T, \begin{pmatrix} 2 \\ 1 \\ 2 \\ 1 \end{pmatrix}^T, \begin{pmatrix} 2 \\ 2 \\ 1 \\ 1 \end{pmatrix}^T, \begin{pmatrix} 1 \\ 1 \\ 2 \\ 1 \end{pmatrix}^T, \begin{pmatrix} 1 \\ 2 \\ 1 \\ 1 \end{pmatrix}^T, \begin{pmatrix} 2 \\ 1 \\ 1 \\ 1 \end{pmatrix}^T, \begin{pmatrix} 1 \\ 1 \\ 1 \\ 1 \end{pmatrix}^T \right\}. \quad (11.11)$$

Now assume we are given a particular rank vector $R^{(p)}$ at perturbation order p . In the next step we generate to every entry $R_i^{(p)}$ all p -partitionings in a set \mathcal{P}_i . We further define the collection of all p -partitionings

$$\mathcal{P} = \{\mathcal{P}_1, \dots, \mathcal{P}_{p+1}\}. \quad (11.12)$$

The i -th row of the adjacency matrix is given by an element of \mathcal{P}_i . In order to generate all distinct diagrams we loop over all elements in the p -partitionings \mathcal{P}_i for $i = 1, \dots, p + 1$. For example consider the rank vector $(1, 2, 1, 1)$. Then the set of p -partitionings is given by

$$\begin{aligned} \mathcal{P}_1 &= \{(1, 0, 0, 0), (0, 1, 0, 0), (0, 0, 1, 0), (0, 0, 0, 1)\}, \\ \mathcal{P}_2 &= \{(2, 0, 0, 0), (0, 2, 0, 0), (0, 0, 2, 0), (0, 0, 0, 2), (1, 1, 0, 0), (1, 0, 1, 0), \\ &\quad (1, 0, 0, 1), (0, 1, 0, 1), (0, 0, 1, 1), (0, 1, 1, 0)\}, \\ \mathcal{P}_3 &= \{(1, 0, 0, 0), (0, 1, 0, 0), (0, 0, 1, 0), (0, 0, 0, 1)\}, \\ \mathcal{P}_4 &= \{(1, 0, 0, 0), (0, 1, 0, 0), (0, 0, 1, 0), (0, 0, 0, 1)\}. \end{aligned} \quad (11.13)$$

Every entry of \mathcal{P}_i defines the i -th row of a generalized adjacency matrix, e.g.,

$$\begin{pmatrix} 1 & 0 & 0 & 0 \\ 2 & 0 & 0 & 0 \\ 0 & 0 & 0 & 1 \\ 0 & 0 & 1 & 0 \end{pmatrix}. \quad (11.14)$$

From the above rank vector we can derive

$$|\mathcal{P}_1| \cdot |\mathcal{P}_2| \cdot |\mathcal{P}_3| \cdot |\mathcal{P}_4| = 640 \quad (11.15)$$

different adjacency matrices. We will see in the following that most of them can be excluded since they do not correspond to a proper Hugenholtz diagram.

We call an adjacency matrix A_G *valid* if the following constraints are satisfied

1. $(A_G)_{ii} = 0$ for all $i = 1, \dots, p + 1$

2. For all $i = 1, \dots, p + 1$:

$$\sum_j (A_G)_{ij} = \deg(v_i) \quad (11.16)$$

3. For all $j = 1, \dots, p + 1$:

$$\sum_i (A_G)_{ij} = \deg(v_j) \quad (11.17)$$

The first property ensures that the graph is simple, i.e., there are no loops which—since corresponding to self contractions—are forbidden by Wick’s theorem. The second and third properties relate to the fact that we are working with particle-number conserving operators and, therefore, the number of ingoing and outgoing lines is the same.

11.2 DERIVATION OF PERTURBATIVE FORMULAS

The second step consists in the derivation of the working formulas from the matrix representation of the diagrams. We start with introducing a new representation of graphs. Instead of using a *vertex-based* description of the diagrams in terms of adjacency matrices we can equally well use an *edge-based* description where matrix elements encode the incidence information in terms of the start and end vertices of the edges.

Assume a graph G with a finite number of edges and vertices, i.e., $|E| < \infty$ and $|V| < \infty$, where $|\cdot|$ denotes the cardinality of the set. We define the $|E| \times |V|$ *incidence matrix* B_G via

$$(B_G)_{ij} = \begin{cases} 1, & \text{if edge } e_{ij} \text{ enters vertex } v_i \\ -1, & \text{if edge } e_{ij} \text{ leaves vertex } v_i \\ 0, & \text{otherwise} \end{cases} \quad (11.18)$$

Again considering the single-replacement diagram (11.2) the incidence matrix is given by

$$B_G = \begin{pmatrix} -1 & -1 & 1 & 1 & 0 & 0 & 0 \\ 1 & 1 & -1 & 0 & -1 & 0 & 0 \\ 0 & 0 & 0 & -1 & 1 & -1 & 1 \\ 0 & 0 & 0 & 0 & 0 & 1 & -1 \end{pmatrix}. \quad (11.19)$$

We note that there is no difference in using adjacency matrices or incidence matrices for the encoding of diagrams. For the actual implementation, it is more convenient to start from vertex-based description in terms of adjacency matrices since the physical constraints, e.g., from Wick’s theorem, manifest themselves quite obviously in the above mentioned rules.

However, it is much simpler to derive the perturbative formulas from the incidence matrix representation. Therefore, we transfer the adjacency matrices into incidence matrices.⁶

We deduce from the above example some basic properties:

1. The sum over all entries of a row is zero.
2. The sum over all entries of a column is zero.
3. The number of entries that are equal 1 (-1) in each row corresponds to the degree of the associated vertex.
4. Every column contains non-vanishing matrix elements.

The above properties are directly related to properties of the adjacency matrices. Since we restrict ourselves to particle-number conserving operators the number of ingoing and outgoing lines is equal. Therefore, the number of entries 1 (-1) is equal. Further, since self-contractions are forbidden, every edge must start and end at different vertices thus yielding non-trivial column vectors.

DECODING INCIDENCE MATRICES

Incidence matrices are very convenient when extracting MCPT formulas. The following set of rules synthesize how to extract the expression from the incidence matrix:

Extraction of MCPT formulas from incidence matrices

1. Every column j corresponds to one single-particle index s_j . More precisely it corresponds to a hole index if the column vector \vec{c} contains the element -1 before the element 1 when reading it from top to bottom and a particle otherwise. If further $c_{p+1} \neq 0$ the corresponding single-particle index is of valence type.
2. Every row $i = 1, \dots, p$ corresponds to one matrix element. The bra indices correspond to indices where $B_{ij} = -1$. The ket indices correspond to row indices where $B_{ij} = 1$.
3. If n columns, corresponding to internal lines, are identical the diagram is multiplied by $\frac{1}{n!}$.
4. Denominators D_i for $i = 1, \dots, p-1$ correspond to pairs of subsequent row vectors (r_i, r_{i+1}) for $i = 1, \dots, p-1$. A single-particle index s_j contributes to D_i if

⁶Typically, modern software packages have built-in functions that convert adjacency matrices into incidence matrices and vice versa. In our case we made use of the 'Combinatorica' package of MATHEMATICA.

$$\sum_{k=1}^i B_{kj} \neq 0. \quad (11.20)$$

Denominators are given by

$$D_i = \sum_j \text{sgn}(s_j) \epsilon_{s_j} + \Delta, \quad (11.21)$$

where the $\text{sgn}(s_j)$ is positive (negative) for holes (particles) and Δ is the determinant-dependent zero-order shift encountered in chapter 10.

5. Add a permutation operator $\mathcal{P}_{(u_1 \dots u_p)}^{(x_1 \dots x_p)}$ for every tuple of external single-particle states.

Reconsidering again the above example we add the single-particle indices to columns of the incidence matrix

$$B_G = \begin{pmatrix} & a & b & i & j & c & x & u \\ -1 & -1 & 1 & 1 & 0 & 0 & 0 & 0 \\ 1 & 1 & -1 & 0 & -1 & 0 & 0 & 0 \\ 0 & 0 & 0 & -1 & 1 & -1 & 1 & 1 \\ 0 & 0 & 0 & 0 & 0 & 1 & -1 & 1 \end{pmatrix} \quad (11.22)$$

The first three column correspond to two-body matrix elements which are given by

$$M_1 = \bar{H}_{abij}^{[2]} \quad (11.23a)$$

$$M_2 = \bar{H}_{abjc}^{[2]} \quad (11.23b)$$

$$M_3 = \bar{H}_{jxcu}^{[2]}. \quad (11.23c)$$

The first and second row, corresponding to single-particle indices a and b , are identical yielding a prefactor $\frac{1}{2}$. Further the above diagram contains two denominators D_1, D_2 . The first denominator is given by

$$D_1 = \epsilon_{ij}^{ab} + \Delta_\mu, \quad (11.24)$$

since

$$B_{1j} \neq 0 \quad \text{for } j = 1, \dots, 4. \quad (11.25)$$

Analogously we get for the second denominator

$$D_2 = \epsilon_j^c + \Delta_\mu. \quad (11.26)$$

Overall this gives the contribution

$$\frac{1}{2} \sum_{abcij} \frac{\bar{H}_{abij}^{[2]} \bar{H}_{abic}^{[2]} \bar{H}_{jxcu}^{[2]}}{(\epsilon_{ij}^{ab} + \Delta_\mu)(\epsilon_j^c + \Delta_\mu)}. \quad (11.27)$$

Note that up to now we have completely neglected the phase factor which is given by $(-1)^{h+l}$, where h corresponds to the number of hole indices and l counts the number of closed loops. The number of hole lines can easily be determined once all single-particle states are classified. In the above example $h = 3$ since i, j, u are hole indices.

The determination of the loop number is a little more involved and can be performed by means of backtracking algorithms which explicitly construct a closed path in the graph. However, here the representation in terms of adjacency matrices renders quite convenient since one can show that

$$l = \det(A_G), \quad (11.28)$$

which can straightforwardly be computed because the corresponding adjacency matrices are small for low orders in MCPT.

11.3 FURTHER EXTENSIONS

The above discussion explicitly aimed for the derivation of the Hugenholtz diagrams appearing at third-order MCPT. However, the concepts we introduced are rather generic and can be straightforwardly extended in many directions. An immediate application is the generalization to three-body operators. Remember that all calculations in this thesis are restricted to two-body operators. The inclusion of explicit three-body operators and beyond requires a relaxation of some of the constraints in the above framework.

Assume that we want to include many-body operators up to particle rank A . As a first consequence the rank vectors are more general,

$$R_i \in \{1, \dots, A\} \text{ for } i = 1, \dots, p \quad (11.29)$$

and furthermore it holds that

$$R_{p+1} \in \{1, \dots, p \cdot A\} \quad (11.30)$$

where p is the perturbation order under consideration. Equation (11.30) is due to the highest particle rank of replacements in open-diagrams in MCPT(p).

Other than in MBPT, diagrammatic approaches are used in almost every many-body method at play. In particular CC theory strongly benefits from the use of diagrams to make the working equations more transparent. Even though we did not discuss CC theory in detail, chapter 7 provided a first insight in the general structure of the CC amplitude equations. A particularly important role is played by the cluster operators \hat{T}_n , which correspond to the lowest vertex in CC diagrams. We expect the same graph-theoretical approach to apply also for the derivation of amplitude equations at high-level coupled cluster truncation schemes, e.g., CCSDT. In quantum chemistry automated code generation was successfully applied to various CC models [LIA05; JS91; Hir03].

12

Open-shell ground states and spectra

In the following we apply NCSM-PT to the calculation of binding energies of open-shell systems. In analogy to HF-MBPT we start with a discussion of the convergence properties of the perturbation series and proceed with a detailed investigation of low-order partial sums in the remainder. We focus on the calculation of both ground-state energies and spectra of open-shell systems in second-order NCSM-PT and compare to large-scale diagonalizations in bare NCSM.

12.1 CONVERGENCE BEHAVIOR IN NCSM-PT

For the demonstration that the NCSM-PT perturbation series is well behaved we evaluate high-order energy corrections by making use of the recursive scheme already applied to high-order HF-MBPT. For the following analysis we use the already introduced chiral NN+3N-full Hamiltonian with $\Lambda_{3N} = 400$ MeV.

As benchmark systems we use ${}^6\text{Li}$ and ${}^7\text{Li}$. Reference states are obtained from a prior NCSM diagonalization within a $N_{\text{max}}^{\text{ref}} = 0$ model space. Subsequently, perturbative corrections are calculated in a small model space with $N_{\text{max}} = 4$. Figure 12.1 shows the p -th partial sums (left panels) and absolute value of the size of the p -th order energy correction (right panel) for both lithium isotopes. The different plotmarkers correspond to different eigenstates from the NCSM diagonalization characterized by their value of J^{II} . For all states the obtained sequence of partial sums converges very quickly and agrees within a range of a few keV with the exact NCSM result in the same model space. Moreover, the semi-logarithmic plot reveals an exponential suppression of higher-order energy corrections. In particular for the case of ${}^7\text{Li}$ the rate of convergence seems to be independent of the targeted reference eigenvector. Even though all of the states exhibit rapid convergence, they display differences

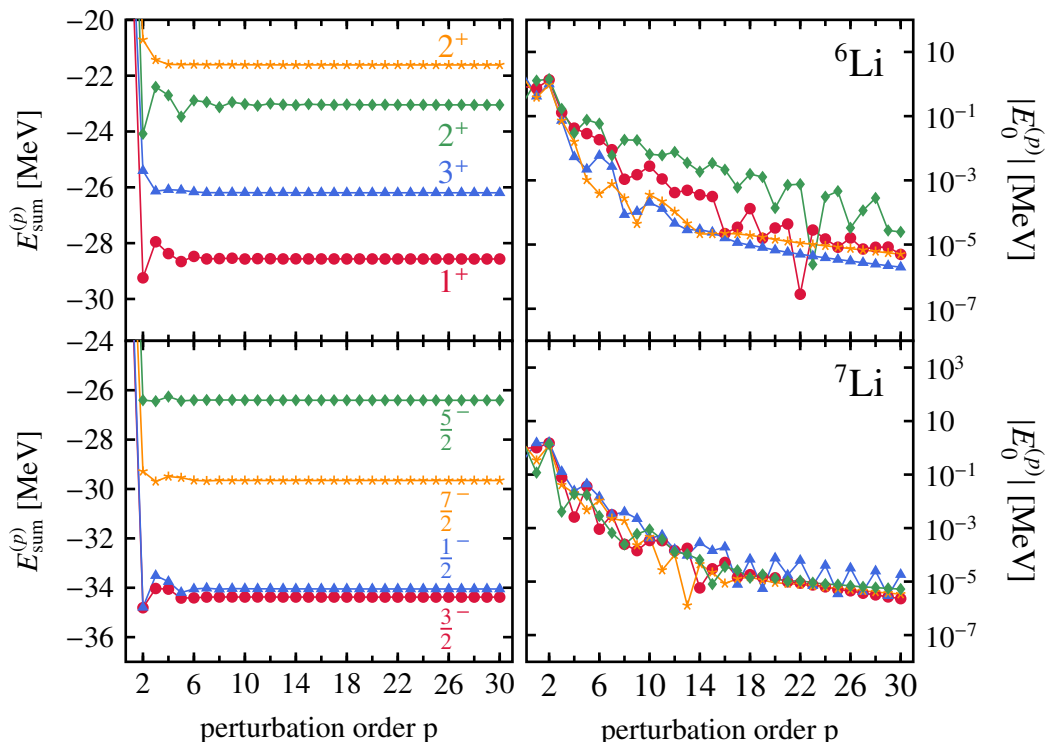


Figure 12.1: Partial sums (left panel) of ${}^6\text{Li}$ and ${}^7\text{Li}$ for the chiral NN+3N interaction with $\alpha = 0.08 \text{ fm}^4$ and truncation parameters $N_{\text{max}} = 4$. The corresponding energy corrections for each order are displayed in the right panel, respectively. All calculations are performed at $\hbar\Omega = 20 \text{ MeV}$.

in the convergence behavior. For example, the convergence pattern of the 1^+ ground state and the first excited 2^+ state in ${}^6\text{Li}$ share the same damped oscillatory behavior at low order. This similarity is even more pronounced when looking at the size of the corresponding energy corrections. For both states there appears a significant chip at perturbation order 22 and 23, respectively. Even though this may serve as a hint for structural similarities of the both states, one needs additional characteristic data to confirm relation of intrinsic properties.

Most importantly the above high-order results motivate the use of low-order partial sums to be a reasonable approximation to the exact binding energy.

12.2 SECOND-ORDER NCSM-PT FOR GROUND-STATE ENERGIES OF ISOTOPIC CHAINS

In the next step we apply NCSM-PT at second-order for the calculation of ground-state energies of heavier systems in larger model spaces, where the recursive scheme cannot be applied due to the rapidly growing size of the many-body basis. We explore binding properties throughout the carbon and oxygen isotopes, including systems of even and odd mass number. For such medium-light systems the IT-NCSM is still applicable and yields an exact benchmark for second-order NCSM-PT.

In the following calculation we use reference states from $N_{\text{max}}^{(\text{ref})} = 0$ and 2 model spaces and compute their corresponding second-order energy corrections.

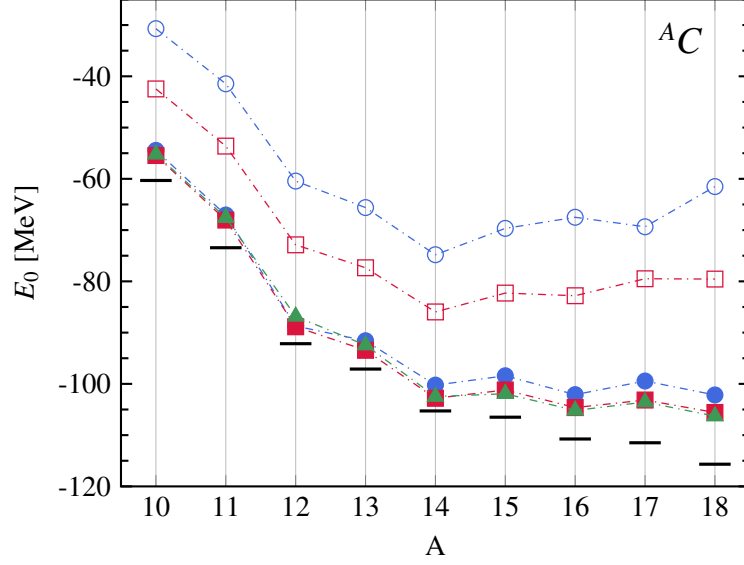


Figure 12.2: Reference energy (○/□) and second-order partial sums (●/■) for $N_{\max}^{(\text{ref})} = (0/2)$ for the ground-state energy of carbon $^{11-18}\text{C}$ for the NN+3N-full interaction with $\alpha = 0.08 \text{ fm}^4$ and truncation parameters $e_{\max} = 12$. All calculations are performed at $\hbar\Omega = 20 \text{ MeV}$. Importance-truncated NCSM calculations (▲) are shown for comparison. Experimental values are indicated by black bars [Wan⁺12].

CARBON CHAIN

We start with an investigation of the carbon isotopic chain. Figure 12.2 shows ground-state energies of even and odd carbon isotopes ranging from carbon ^{10}C to ^{18}C . The reference energy

$$E_{\text{NCSM}} = E^{(0)} + E^{(1)} \quad (12.1)$$

corresponds to the first-order partial sum. The NCSM reference energy is shown as open symbols for $N_{\max} = 0$ (○) and $N_{\max} = 2$ (□). The corresponding second-order partial sums

$$E_{\text{sum}}^{(2)} = E_{\text{NCSM}} + E^{(2)} \quad (12.2)$$

are indicated by filled plot markers. Although there is a significant difference in the reference energy when going from $N_{\max}^{(\text{ref})} = 0$ to $N_{\max}^{(\text{ref})} = 2$ the associated second-order partial sums are very similar within a narrow band of 3%. Most remarkably the second-order partial sums show excellent agreement with large-scale IT-NCSM calculations (▲) with deviations of about 1% for heavy carbon isotopes. The typical size of the reference states ranges from a couple of hundred configurations for ^{10}C in $N_{\max}^{(\text{ref})} = 0$ up to several tens of thousand for ^{18}C in a $N_{\max}^{(\text{ref})} = 2$ model space. We particularly note that NCSM-PT yields consistent results over a huge mass range of a factor of two in binding energy when going from ^{10}C to ^{18}C .

Further, note that both large-scale IT-NCSM and NCSM-PT underbind the experimental

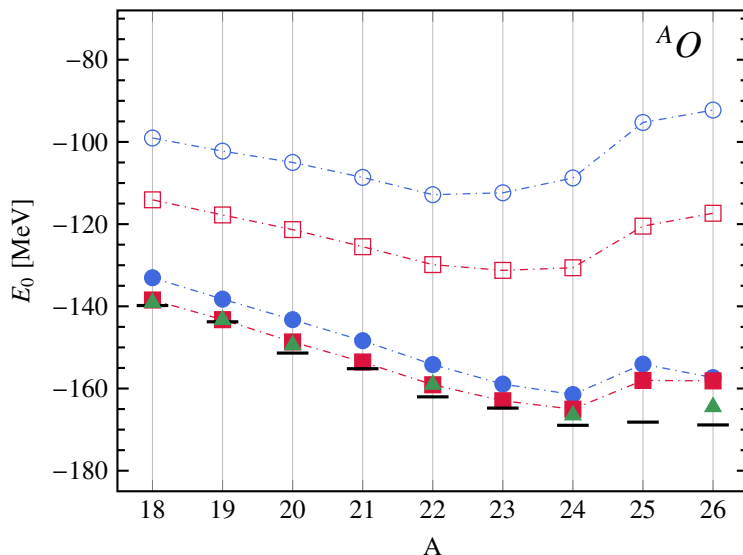


Figure 12.3: Reference energy (\circ/\square) and second-order partial sums (\bullet/\blacksquare) for the ground-state energy of oxygen $^{18-24}\text{O}$. All parameters are the same as in Figure 12.2.

values indicated by black bars. However, this is due to defects of the chiral Hamiltonian. Deviations from experimental values become worse for neutron rich isotopes due to the coupling to the continuum. Such effects are not adequately described in a HO single-particle basis and require the extension to a consistent inclusion of resonances in a Gamow or Bergren scheme.

OXYGEN CHAIN

Analogously, we performed NCSM-PT studies for the oxygen isotopic chain starting from ^{18}O up to very neutron-rich ^{26}O . Figure 12.3 summarizes the second-order NCSM-PT results using the same chiral Hamiltonian and model-space parameters as for the carbon chain. Again there is a big gain in reference energy when going from a $N_{\text{max}}^{(\text{ref})} = 0$ to $N_{\text{max}}^{(\text{ref})} = 2$ reference space, but the second-order partial sums agree within 3%. A closer investigation shows that second-order partial sums for reference spaces from a $N_{\text{max}}^{(\text{ref})} = 2$ model space are systematically stronger bound than the ones obtained from $N_{\text{max}}^{(\text{ref})} = 0$ reference states with the sole exception of the very neutron rich ^{26}O isotope. The second-order partial sums for $N_{\text{max}}^{(\text{ref})} = 2$ are in excellent agreement with large-scale IT-NCSM results. We particularly exclude ^{26}O from this statement due to the importance of continuum effects, which are neither incorporated in NCSM nor in NCSM-PT [Hag⁺12]. Most interestingly, NCSM-PT confirms the experimental observed neutron dripline at ^{24}O . In particular, the inclusion of three-body effects—in this case on the normal-ordered two-body level—is key for obtaining the correct dripline physics [GCR16; Her⁺13; Hag⁺09; Ots⁺10; CBN13].

Theoretical deviations from experiment are of the order of less than 3% for oxygen isotopes up to ^{24}O . As already noted, the growing deviations for more neutron rich are due

to missing coupling to continuum physics are not expected to be improved by including higher-order correlations.

Again the size of reference states ranges from a few tens of SDs for ^{18}O in $N_{\text{max}}^{(\text{ref})} = 0$ up to several hundreds of thousands SDs for ^{26}O in $N_{\text{max}}^{(\text{ref})} = 2$.

In conclusion, for both carbon and oxygen isotopic chains, NCSM-PT with $N_{\text{max}}^{(\text{ref})} = 2$ reference states provides accurate ground-state energies and a good compromise between accuracy and computational efficiency. In particular, a single NCSM-PT calculations typically requires two or three orders of magnitude less computing time than the corresponding IT-NCSM calculation thus enabling us to go beyond the oxygen chain, which is the current limit of IT-NCSM implementations.

12.3 EXCITATION SPECTRA

In the discussion of MCPT we have seen that the framework is completely agnostic about the reference states, i.e., the reference states in NCSM-PT does not need to correspond to the ground-state wave function. Therefore, excitation energies in NCSM-PT can be straightforwardly calculated as energy differences of the correlated second-order partial sums. In practice one targets several different eigenvectors from the prior NCSM calculation

$$|\psi_1\rangle, \dots, |\psi_M\rangle, \quad (12.3)$$

and correspondingly obtains M different second-order partial sum

$$E_{\text{sum},1}^{(2)}, \dots, E_{\text{sum},M}^{(2)}. \quad (12.4)$$

We then take the minimal value

$$E_{\text{min}} = \min_M \{E_{\text{sum},1}^{(2)}, \dots, E_{\text{sum},M}^{(2)}\} \quad (12.5)$$

and define the set of excitation energies

$$E^* \equiv \{E_{\text{sum},1}^{(2)} - E_{\text{min}}, \dots, E_{\text{sum},M}^{(2)} - E_{\text{min}}\}, \quad (12.6)$$

where obviously one of the elements of E^* is zero, thus corresponding to the (second-order) ground state. We note that the lowest eigenvector for a small reference space does not necessarily correspond to the exact ground state and NCSM-PT may induce level crossings.

We apply the above procedure to selected carbon and oxygen isotopes. In Figure 12.4 we compare the NCSM-PT spectra to direct NCSM excitation energies. The ground-state energies are shown numerically below the ground-state level. Additionally, to $N_{\text{max}}^{(\text{ref})} = 0$ and $N_{\text{max}}^{(\text{ref})} = 2$ we investigate reference states from $N_{\text{max}}^{(\text{ref})} = 4$ model spaces. For the sake

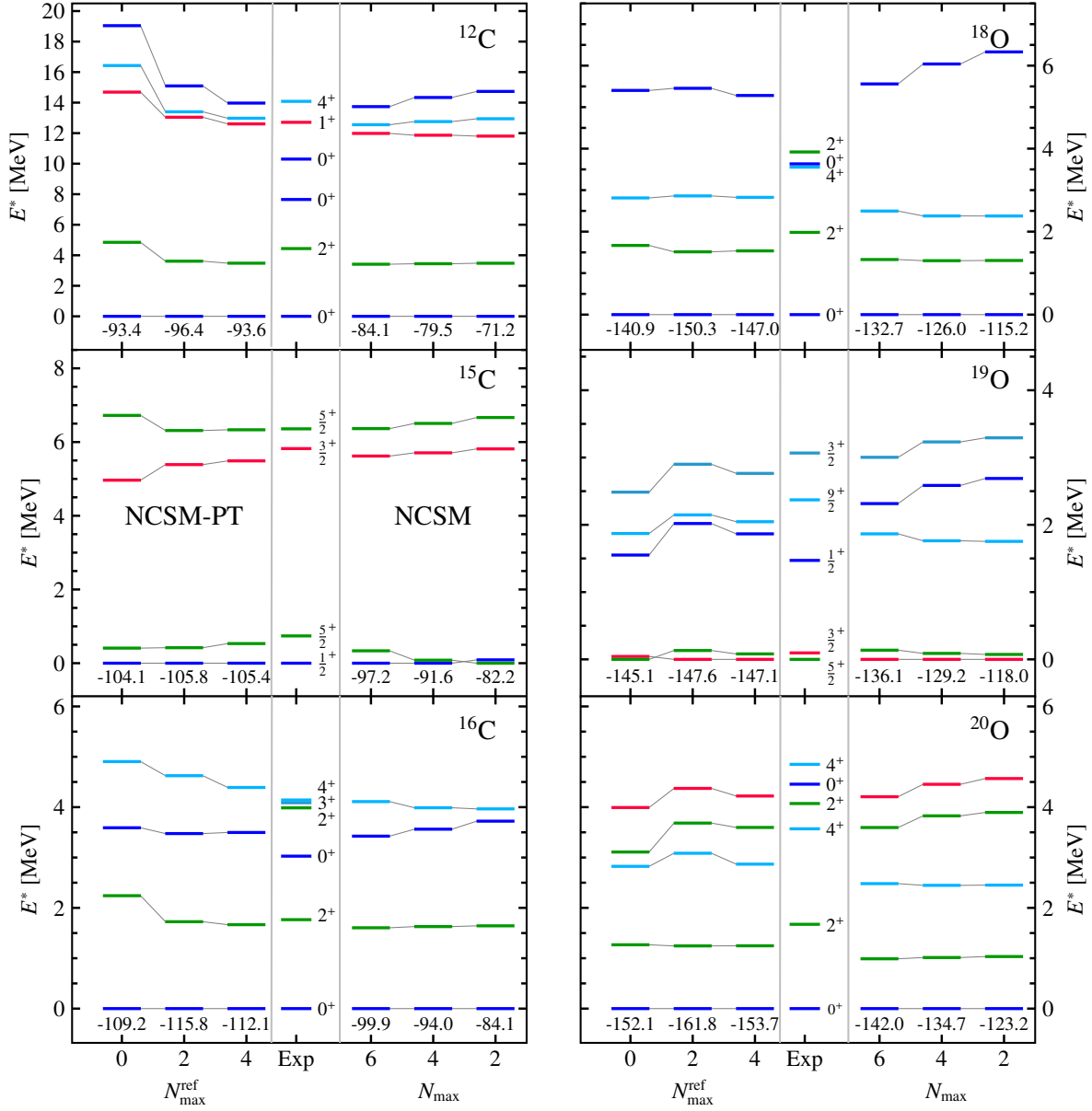


Figure 12.4: Spectra obtained via second-order NCSM-PT for selected carbon and oxygen isotopes for the NN+3N-full interaction with $\alpha = 0.08 \text{ fm}^4$ and truncation parameter $e_{\max} = 12$. All calculations are performed at $\hbar\Omega = 16 \text{ MeV}$. Importance-truncated NCSM calculations for a sequence of model-spaces are displayed in the right panel. For $^{19,20}\text{O}$ and $N_{\max}^{(\text{ref})} = 4$ we introduced an additional truncation $c_{\mu}c_{\mu'} \geq 10^{-6}$ ($\mu \neq \mu'$) for the calculation of the second-order energy corrections in NCSM-PT in order to reduce computing time.

of computing power we introduce an additional truncation for $N_{\text{max}}^{(\text{ref})} = 4$ reference states, which will be discussed in the next section. In the majority of cases, further enlarging the reference space beyond $N_{\text{max}}^{(\text{ref})} = 2$ does not improve the quality of the excitation energies and most excitation energies seem to be stable under variation of $N_{\text{max}}^{(\text{ref})}$. An exception is the first excited 0^+ state in ^{12}C , which exhibits notoriously slow convergence with respect to both N_{max} and $N_{\text{max}}^{(\text{ref})}$. In the experimental spectrum there appears an excited 0^+ state at about 8 MeV which is expected to exhibit strong α clustering. This so-called *Hoyle state* is expected to be dominated by particle-hole excitations of high excitation rank, e.g., 4p4h and 8p8h excitations. These are, however, neither incorporated in a second-order NCSM-PT calculation, nor is a direct $N_{\text{max}} = 6$ NSCM calculation sufficient to capture these effects. Apart from this, the level ordering in ^{12}C is reproduced correctly, even though the energy gap is widened compared to experimental excitation energies.

Even though excitation spectra of NCSM and NCSM-PT are in good agreement the absolute binding energies in NCSM are far from being converged, whereas the ground-state energies in NCSM-PT are already quite stable. This again shows that second-order NCSM-PT effectively incorporates the bulk of residual correlation effects from the large model space.

We want to put particular emphasize on the reversed level ordering in the odd system ^{15}C . Note that in the NCSM for $N_{\text{max}} = 2$ the ground-state level ordering is reversed and the $\frac{5}{2}^+$ state is the ground state. However, when performing NCSM-PT this ordering is reversed and the $\frac{1}{2}^+$ state is predicted to be the ground state. Therefore, the correct level ordering is reproduced with a reasonable excitation energy of the first $\frac{5}{2}^+$ state. From the NCSM-PT ground-state energy in $N_{\text{max}}^{(\text{ref})} = 0$ for ^{19}O we see that in such a small model space the correct level ordering is not reproduced. However, when enlarging the reference space this deficiency can be corrected. Typically, $N_{\text{max}}^{(\text{ref})} = 0$ reference states contain too few physically important states to be a reasonable approximation to the true ground state.

12.4 C_{MIN}^2 TRUNCATION

The number of determinants in the reference space grows very rapidly when relaxing the $N_{\text{max}}^{(\text{ref})}$ truncation and calculations beyond $N_{\text{max}}^{(\text{ref})} = 4$ are computationally expensive. In order to handle very large reference states an additional truncation scheme can be adopted to approximately evaluate the second-order NCSM-PT correction. Reconsidering the second-order energy correction expanded with respect to the Slater determinantal components of the reference state yields

$$E^{(2)} = \sum_{|\Phi_\mu\rangle, |\Phi_{\mu'}\rangle \in \mathcal{M}_{\text{ref}}} C_\mu C_{\mu'}^* \sum_{|\Phi_\nu\rangle \notin \mathcal{M}_{\text{ref}}} \frac{\langle \Phi_{\mu'} | \hat{W} | \Phi_\nu \rangle \langle \Phi_\nu | \hat{W} | \Phi_\mu \rangle}{E_{\text{ref}} - E_\nu^{(0)}}. \quad (12.7)$$

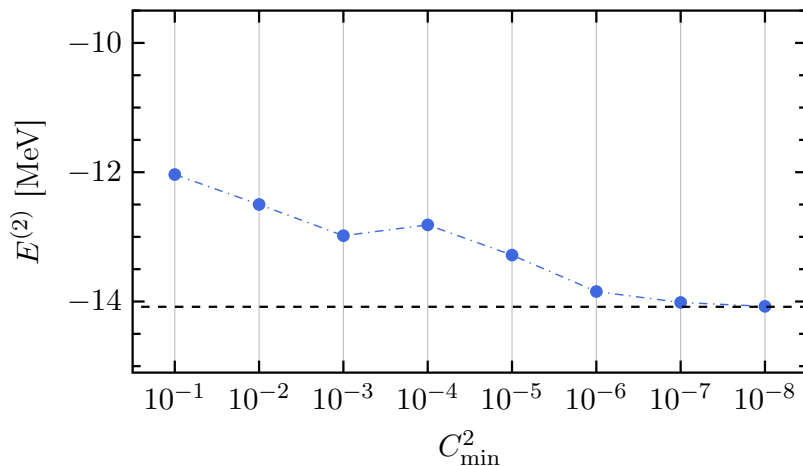


Figure 12.5: Second-order MCPT correction over C_{\min}^2 truncation for ^{12}C in $N_{\max}^{(\text{ref})} = 4$ reference space using a chiral NN+3N-full interaction. The oscillator frequency is given by $\hbar\Omega = 16$ MeV. The dashed line corresponds to the exact result, i.e., $C_{\min}^2 = 0$.

Fixing a particular tuple (μ, μ') , the contribution is small if either $C_{\mu}C_{\mu}'^*$ or

$$\sum_{|\Phi_{\nu}\rangle \notin \mathcal{M}_{\text{ref}}} \frac{\langle \Phi_{\mu'} | \hat{W} | \Phi_{\nu} \rangle \langle \Phi_{\nu} | \hat{W} | \Phi_{\mu} \rangle}{E_{\text{ref}} - E_{\nu}^{(0)}} \quad (12.8)$$

becomes small. Therefore, the absolute of the value $C_{\mu}C_{\mu}'^*$ serves as an *a-priori* measure for the importance of the expression (12.8). We define a C_{\min}^2 *threshold* such that all tuples (μ, μ') in the evaluation of (12.7) are included with

$$|C_{\mu}C_{\mu}'^*| \geq C_{\min}^2. \quad (12.9)$$

In this way, we may discard a lot of pairs determinants determinants from the perturbative treatment just by evaluating their respective expansion coefficient in the NCSM reference state.

Figure 12.5 displays the effect of the C_{\min}^2 truncation on the magnitude of the second-order NCSM-PT energy correction. For the case of ^{12}C we can still perform a full $N_{\max}^{(\text{ref})} = 4$ calculation even though the reference state already contains several million configurations. Obviously, for truncation parameter $C_{\min}^2 = 10^{-6}$ the approximate second-order energy correction is already in very good agreement with the exact second-order energy correction and deviations are on a level of a few ten keV. However, even though agreeing on a sub percent level, the approximate evaluation requires up to one order of magnitude less computational resources. We note that there is no reason for a monotone decreasing behavior of the second-order energy correction when decreasing the value of C_{\min}^2 . Even though the overall second-order correction is given by a squared matrix elements, the expansion into Slater determinant components does not conserve this, as can be seen from the peak in Figure 12.5

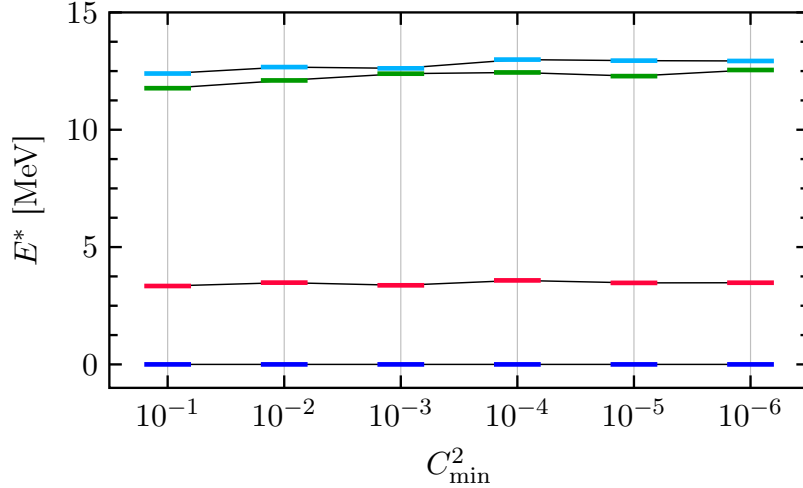


Figure 12.6: Second-order NCSM-PT excitation energies over C_{\min}^2 truncation for ^{12}C in $N_{\max}^{(\text{ref})} = 4$ reference space using a chiral NN+3N-full interaction. The oscillator frequency is given by $\hbar\Omega = 16$ MeV.

at $C_{\min}^2 = 10^{-4}$.

We further investigate the dependence of excitation spectra on the C_{\min}^2 truncation. In Figure 12.6 we show low-lying spectroscopy of ^{12}C for a sequence of values of C_{\min}^2 . We recognize only a small impact of the change of C_{\min}^2 on excitation spectra. The excitation energies are almost independent of the value of C_{\min}^2 such that we conclude that the C_{\min}^2 truncation acts on different reference states in a similar way.

12.5 DEPENDENCE ON THE OSCILLATOR FREQUENCY

We have seen that second-order NCSM-PT yields very good agreement with large-scale NCSM calculations. An important parameter in NCSM calculations is the oscillator frequency fixing the width of the HO potential used for the definition of the reference single-particle basis. In the limit $N_{\max} \rightarrow \infty$, the NCSM results must agree for all values of the oscillator frequency. In actual applications, when restricted to finite basis size, the NCSM results do carry residual dependence on the oscillator frequency. In the following we will investigate how this dependence transfers to the second-order NCSM-PT corrections.

As benchmark system we choose the fluorine isotopic chain using the same NN+3N-full Hamiltonian as for carbon and oxygen isotopic chains. Figure 12.7 displays the dependence of the reference energy and second-order partials sum on variations of the oscillator frequency. The reference energy, i.e., NCSM eigenvalue, is roughly independent of the oscillator frequency up to mass number $A \approx 23$. For larger mass numbers there appear large deviations between the reference energies obtained for different values of the oscillator frequency. In particular lower frequencies yield more tightly bound systems. Even more pronounced is the impact of variations with respect to the oscillator frequencies on the NCSM-PT energies.

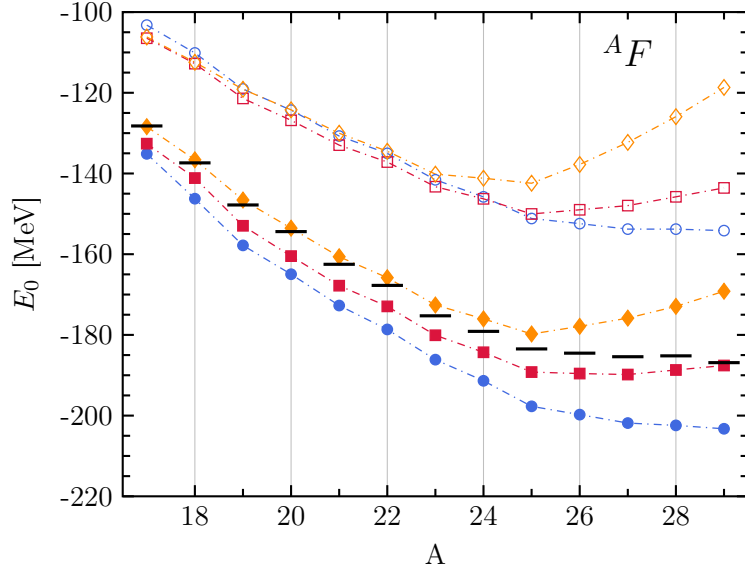


Figure 12.7: Ground-state energies obtained from NCSM (open symbols) and second-order NCSM-PT (solid symbols) for $^{17-29}\text{F}$ using $N_{\text{max}}^{(\text{ref})} = 2$ reference states with a chiral NN+3N-full Hamiltonian. The oscillator frequency is given by $\hbar\Omega = 14$ (\bullet), 16 (\blacksquare), 20 (\blacklozenge) MeV.

Even for the lightest fluorine isotope considered here, ^{17}F , there is considerable dependence on the oscillator frequency. The second-order NCSM-PT varies by roughly 7 MeV from $\hbar\Omega = 14$ MeV to 20 MeV, which is already a deviation of the order of 5% of the overall binding energy. The dependence of the oscillator frequency grows considerably with increasing mass number. For neutron-rich fluorine isotopes the difference of binding energies can be up to 35 MeV. It is clear that the particular choice of the basis strongly affects the binding properties of heavy fluorine isotopes. Moreover, the prediction of the neutron dripline is extremely sensitive to the choice of $\hbar\Omega$.

In order to overcome the deficiency inherent when using HO single-particle states we extend NCSM-PT to other single-particle basis. From the discussion of HF-MBPT we already know that HF orbitals may strongly affect the quality of the perturbation expansion. Therefore, applying NCSM-PT to a HF single-particle basis provides a reasonable solution to implement the correct asymptotic behavior of the single-particle wave functions.

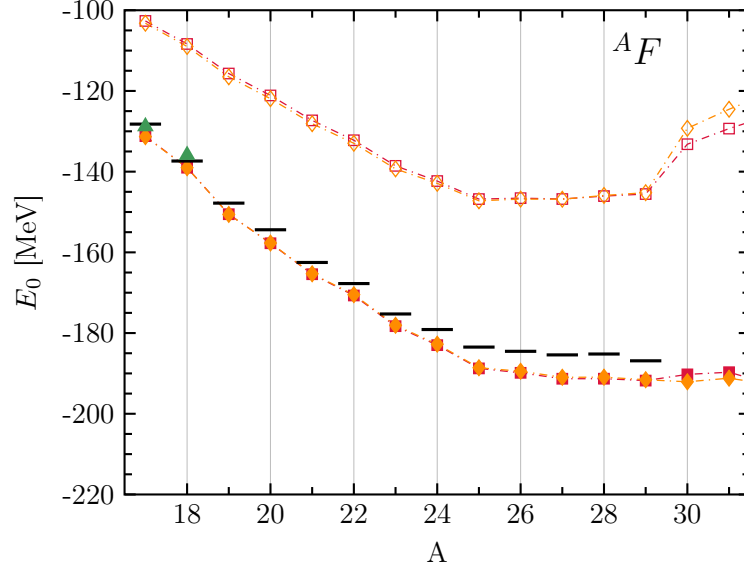


Figure 12.8: Ground-state energies obtained from NCSM (open symbols) and second-order NCSM-PT (solid symbols) for $^{17-31}\text{F}$ using $N_{\text{max}}^{(\text{ref})} = 2$ reference states with a chiral NN+3N-full Hamiltonian using HF single-particle states. The oscillator frequency is given by $\hbar\Omega = 16$ (■), 20 (◆) MeV.

12.6 NCSM-PT WITH HARTREE-FOCK BASIS

In the following we will work with HF single-particle states obtained from a prior HF calculation. Nuclear one-, two- and three-body matrix elements are transformed from HO to HF basis and subsequently normal-ordered with respect to the multi-configurational reference state. The initial CI calculation is performed in HF basis with full three-body forces.

We note that we introduced NCSM as a particular CI variant with N_{max} -truncation scheme. However, we still keep the terminology NCSM-PT for the many-body method at play, even though we replace the HO basis with HF single-particle states.

FLUORINE CHAIN

The use of the HF single-particle basis is expected to improve the stability of NCSM-PT with respect to variations of the oscillator frequency. Figure 12.8 displays the impact of variations of the oscillator frequency on reference energies and second-order NCSM-PT results when using a HF single-particle basis with $N_{\text{max}}^{(\text{ref})} = 2$ reference states. Clearly, we see that both NCSM reference energies and second-order NCSM-PT results are independent of the value of $\hbar\Omega$ over the entire mass range of the fluorine isotopes. Deviations are much less than 1 MeV. Note that for deviations between these oscillator frequencies were of the order of 20 MeV for the HO basis in ^{29}F as depicted in Figure 12.7. We note that we can extend the calculations to heavier isotopes. However, proceeding to ^{30}F opens up the new neutron pf-shell which yields a significant increase in reference energy, while at the same time the

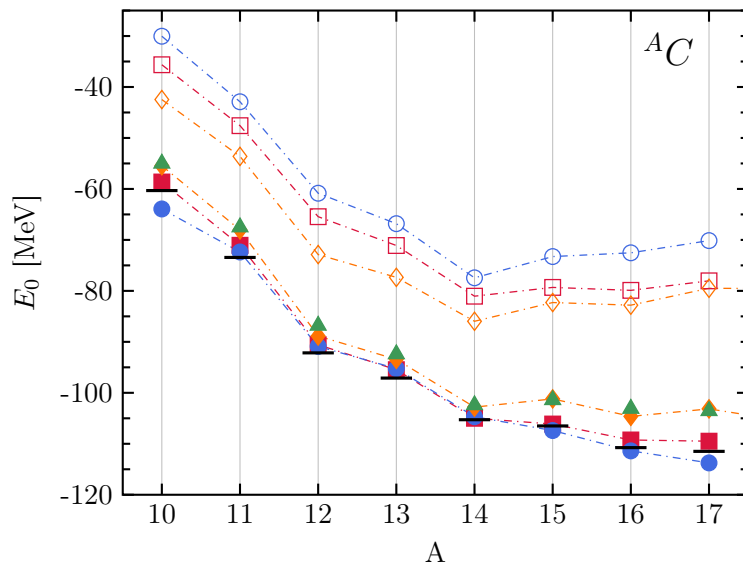


Figure 12.9: Ground-state energies obtained from NCSM (open symbols) and second-order NCSM-PT (solid symbols) for $^{18-26}\text{O}$ with a chiral NN+3N-full Hamiltonian. The oscillator frequency is given by $\hbar\Omega = 20\text{ MeV}$. Blue (\bullet) and red (\blacksquare) plotmarkers correspond to HF single-particle states in $N_{\text{max}}^{(\text{ref})} = 0, 2$ and yellow plotmarkers to HO single-particle states with $N_{\text{max}}^{(\text{ref})} = 2$ (\blacklozenge). IT-NCSM calculations are shown for comparison (\blacktriangle). Experimental values are indicated by black bars.

NCSM-PT energies remain constant.

We emphasize that this is the first *ab initio* calculation of even and odd fluorine isotopes in a no-core approach in large model spaces reaching beyond $A = 20$. Due to having both open neutron and proton shells, fluorine provides a complex test case for many-body methods. The generality if the NCSM-PT enables to proceed along the fluorine isotopic chains which is presently impossible in standard NCSM calculations due to computational requirements.

CARBON CHAIN

Figure 12.9 provides a comparison between NCSM-PT with HF and HO orbitals. First of all we notice that the reference energies from $N_{\text{max}}^{(\text{ref})} = 2$ are always lower when using HO orbitals. However, for the second-order partial sum we encounter the opposite behavior, where NCSM-PT with HF orbitals is bound tighter than with HO orbitals. The NCSM-PT results using HF single-particle states are in good agreement with large-scale NCSM calculation up to $A = 14$ and start to deviate more strongly for heavier carbon isotopes. However, we have already seen in the case of fluorine isotopes that the dependence on the oscillator frequency is more pronounced for neutron-rich systems. Therefore, a possible explanation for the larger deviations might be the use of too high values for $\hbar\Omega$ in the HO-based calculations. Going to smaller values of $\hbar\Omega$ would yield stronger binding.

For all cases second-order NCSM-PT with HF orbitals tends to overbind the exact IT-NCSM result. This effect is more pronounced when using $N_{\text{max}}^{(\text{ref})} = 0$ reference states—we

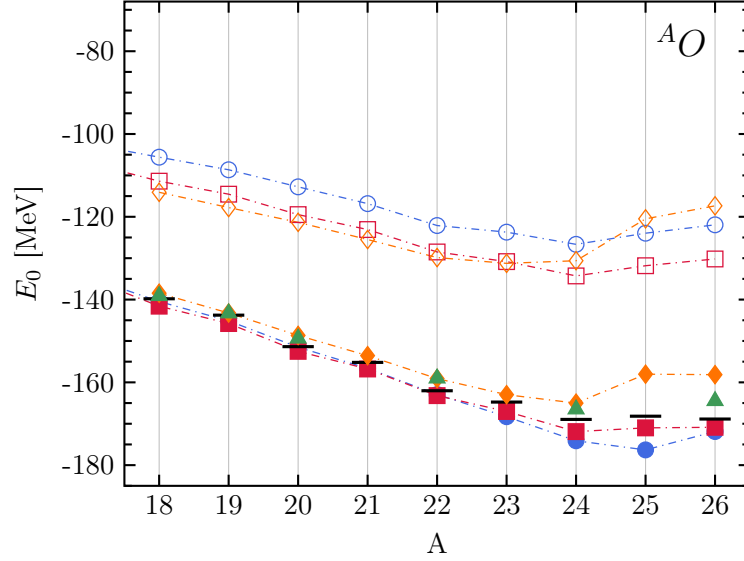


Figure 12.10: Ground-state energies obtained from NCSM (open symbols) and second-order NCSM-PT (solid symbols) for $^{18-26}\text{O}$ with a chiral NN+3N-full Hamiltonian. The oscillator frequency is given by $\hbar\Omega = 20$ MeV. Blue (\bullet) and red (\blacksquare) plotmarkers correspond to HF single-particle states in $N_{\text{max}}^{(\text{ref})} = 0, 2$ and yellow plotmarkers to HO single-particle states with $N_{\text{max}}^{(\text{ref})} = 2$ (\blacklozenge). IT-NCSM calculations are shown for comparison (\blacktriangle). Experimental values are indicated by black bars.

have already seen in the investigation of excitation energies that such small reference spaces contain too few physical significant states to yield reliable results.

OXYGEN CHAIN

We reassess our results for the oxygen chain in the context of NCSM-PT with HF orbitals. In Figure 12.10 we compare NCSM-PT results obtained using different single-particle bases. Up to mass number $A \approx 22$ the second-order NCSM-PT results for HO and HF single-particle bases are approximately the same. Deviations are of the order of 3 MeV. We also note that the reference energies are very similar for the case of $N_{\text{max}}^{(\text{ref})} = 2$ up to $A = 24$. Larger deviations in reference energies are obtained for $^{25,26}\text{O}$. Correspondingly, the second-order NCSM-PT results reveal larger deviations as well. Remember, however, the strong dependence on oscillator frequency when using HO single-particle states. In particular for heavy, neutron-rich isotopes the corresponding value of $\hbar\Omega$ might be too large and lowering the oscillator frequency might yield stronger binding in, both, NCSM and NCSM-PT. Furthermore, we note the deviations of NCSM-PT with HF orbitals from large-scale IT-NCSM calculations for $^{25,26}\text{O}$. Again this is due to stronger coupling to continuum states, which was already present in NCSM-PT with HO single-particle states. Even though HF orbitals are able to cure the strong dependence on the oscillator frequency, continuum effects are not accounted for. However, experimental binding energies are well reproduced in the range $^{18-24}\text{O}$.

PART IV

SYMMETRY-BROKEN MANY-BODY PERTURBATION THEORY

Introduction to Part IV

For closed-shell systems the Hartree-Fock mean-field approach provides a proper starting point for the construction of systematic correlation expansion methods. In particular, single-configurational perturbation theory and coupled-cluster theory have shown to give excellent results.

Hartree-Fock-Bogoliubov (HFB) theory is the simplest way to include pairing correlation effects in a mean-field model. By solving a set of constrained mean-field equations using a particle-number non-conserving vacuum one enters the realm of *symmetry-breaking many-body theory*, where a symmetry of the Hamiltonian is broken by the reference state.

Similar to HF theory, the HFB framework does not only allow to perform calculations of medium-mass open-shell systems, but also is used as a convenient tool for the construction of open-shell reference states, which enter a perturbative treatment at the next stage. Of course, the subsequent many-body method must be grounded on the same foundations, namely symmetry breaking. In this part we will introduce a novel flavour of many-body perturbation theory that uses a particle-number broken HFB reference state. The is approach is called *Bogoliubov many-body perturbation theory* (BMBPT).

Even though symmetry-breaking many-body methods have existed for a long time, they have only scarcely been applied in nuclear physics and quantum chemistry. Only very recently many-body theories on top of a particle-number broken vacuum were formulated and implemented, e.g., the Gorkov extension of self-consistent Green's function theory (GGF) [SDB11; Som⁺14] or Bogoliubov coupled cluster (BCC) [Sig⁺15; DS16]. The use of BMBPT provides a simple yet efficient alternative to the above methods. In particular we know from the investigations in HF-MBPT that when using sufficiently softened interactions, a perturbative treatment yields excellent results at low computational cost. However, when dealing with finite quantum systems the eventual restoration of the broken symmetry becomes mandatory. Up to now a consistent restoration of $U(1)$ symmetry still poses a future problem in the GGF framework even at a formal level. Furthermore, the restoration of particle-number in BCC becomes numerically much more demanding due to the symmetry restoration protocol outlined in [DS16]. Current BCC codes make use of an axially-deformed single-particle basis, which significantly increases both runtime and required storage space for the cluster amplitudes [Sig⁺15]. Therefore, the simplest way to

implement a symmetry-broken and restored many-body theory with full open-shell capabilities is to perform low-order BMBPT using a spherical formulation. In particular, this requires the derivation and implementation of an angular-momentum coupled framework for the treatment of quasiparticle operators.

We note that the consistent restoration of particle-number symmetry is implemented on a HFB level in several ways. Furthermore, there have been studies of approximate restoration protocols of quasiparticle perturbation theory for the pairing Hamiltonian [Hen⁺14]. However, there are no studies of symmetry-restored beyond-HFB calculations using chiral interactions.

We start this part of the thesis with an introduction to HFB theory and properties of the HFB solution. The main part is dedicated to the introduction of BMBPT as well as the derivation of the low-order corrections. We consider the formal treatment of BMBPT in an m -scheme single-particle basis; the technicalities due to angular-momentum coupling can be found in appendix E. We proceed with a brief introduction to the nuclear energy density functional approach and its links to symmetry-broken many-body theory. Finally, we present first results of second-order BMBPT using state-of-the-art chiral interactions with additional emphasis on pairing properties of the nuclear Hamiltonian.

13

Hartree-Fock-Bogoliubov Theory

The Hartree-Fock approximation is the simplest form of a mean-field approach and serves as starting point for more elaborate approaches to treat correlation effects. Hartree-Fock-Bogoliubov (HFB) theory is the simplest approach to consistently include pairing correlation effects on a mean-field level. In HFB theory nucleons are described as independent *quasi-particles* which are themselves superpositions of proper particles and holes.

The breaking of particle-number conservation is an intrinsic feature of HFB theory. Therefore, observables obtained in the HFB framework are contaminated due to symmetry-breaking. Different strategies can be employed to resolve the pathology. Either one can solve a set of particle-number projected HFB equations or perform a particle-number projection of the variational solution. For a comparison of both approaches see, e.g., [Her08; HR09a]. Furthermore, approximate ways of restoring particle-number symmetry can be obtained via using cumulant expansions in the Lipkin-Nogami approach.

In the following we give a brief introduction to the fundamentals of HFB theory and fix the notation for future reference. This chapter roughly follows [RS80].

13.1 BOGOLIUBOV ALGEBRA

We make a transition from a independent-particle to an independent-quasiparticle picture which is mediated by the so-called canonical *Bogoliubov transformation*,

$$\beta_k^\dagger = \sum_l (U_{lk} \hat{c}_l^\dagger + V_{lk} \hat{c}_l), \quad (13.1a)$$

$$\beta_k = \sum_l (U_{lk}^* \hat{c}_l + V_{lk}^* \hat{c}_l^\dagger), \quad (13.1b)$$

where the creators (annihilators) c^\dagger (c) are taken with respect to the reference basis. ¹

The transformed quasiparticle operators obey the usual canonical anti-commutation relations

$$\{\hat{\beta}_k, \hat{\beta}_l^\dagger\} = \delta_{kl}, \quad (13.2)$$

$$\{\hat{\beta}_k, \hat{\beta}_l\} = 0, \quad (13.3)$$

$$\{\hat{\beta}_k^\dagger, \hat{\beta}_l^\dagger\} = 0. \quad (13.4)$$

The transformation (13.1b) can be written in matrix representation by

$$\mathcal{W} = \begin{pmatrix} U & V^* \\ V & U^* \end{pmatrix}. \quad (13.5)$$

The unitarity relation $\mathcal{W}\mathcal{W}^\dagger = \mathcal{W}^\dagger\mathcal{W} = 1$ translates into

$$UU^\dagger + V^*V^T = 1, \quad UV^\dagger + V^*U^T = 0, \quad (13.6a)$$

$$VU^\dagger + U^*V^T = 0, \quad VV^\dagger + U^*U^T = 1, \quad (13.6b)$$

$$U^\dagger U + V^\dagger V = 1, \quad U^\dagger V^* + V^\dagger U^* = 0, \quad (13.6c)$$

$$V^T U + U^T V = 0, \quad V^T V^* + U^T U^* = 1. \quad (13.6d)$$

The nuclear ground state $|\psi\rangle$ is then given by the *quasiparticle vacuum*

$$\hat{\beta}_k|\psi\rangle = 0. \quad (13.7)$$

Further we associate a *generalized density matrix* \mathcal{R} with the quasiparticle vacuum $|\psi\rangle$,

$$\mathcal{R} = \begin{pmatrix} \rho & \kappa \\ -\kappa^* & 1 - \rho^* \end{pmatrix}, \quad (13.8)$$

where

$$\rho_{kl} = \langle\psi|\hat{c}_l^\dagger\hat{c}_k|\psi\rangle, \quad (13.9)$$

$$\kappa_{kl} = \langle\psi|\hat{c}_l\hat{c}_k|\psi\rangle, \quad (13.10)$$

define the (*normal*) *density matrix* and *anomalous density*, respectively. ² The generalized density matrix is also Hermitian and idempotent, i.e., $\mathcal{R} = \mathcal{R}^2 = \mathcal{R}^\dagger$. We further note the Hermiticity and anti-Hermiticity of ρ and κ , respectively,

¹In the following we use greek letters to denote creators/annihilators in quasiparticle space and roman letters to denote creators/annihilators in single-particle space.

²The anomalous density is also often called *pairing tensor*.

$$\rho_{k_1 k_2} = \rho_{k_2 k_1}^* \quad (13.11)$$

$$\kappa_{k_1 k_2} = -\kappa_{k_2 k_1}^* \quad (13.12)$$

Transformation of the generalized density matrix \mathcal{R} to the quasiparticle basis yields

$$\mathbf{R} \equiv \mathcal{W}^\dagger \mathcal{R} \mathcal{W}, \quad (13.13)$$

with

$$\mathbf{R} = \begin{pmatrix} \frac{\langle \Phi | \beta_p^\dagger \beta_q | \Phi \rangle}{\langle \Phi | \Phi \rangle} & \frac{\langle \Phi | \beta_p \beta_q | \Phi \rangle}{\langle \Phi | \Phi \rangle} \\ \frac{\langle \Phi | \beta_p^\dagger \beta_q^\dagger | \Phi \rangle}{\langle \Phi | \Phi \rangle} & \frac{\langle \Phi | \beta_p \beta_q^\dagger | \Phi \rangle}{\langle \Phi | \Phi \rangle} \end{pmatrix} \equiv \begin{pmatrix} R_{pq}^{+-} & R_{pq}^{--} \\ R_{pq}^{++} & R_{pq}^{-+} \end{pmatrix} = \begin{pmatrix} 0 & 0 \\ 0 & 1 \end{pmatrix}, \quad (13.14)$$

which can be obtained from the action of quasiparticle operators on the symmetry-broken vacuum. Equation 13.14 will be key in the derivation of the unperturbed propagators in symmetry-broken MBPT.

13.2 THE HARTREE-FOCK-BOGOLIUBOV EQUATIONS

In the following we invoke the Ritz variational principle to derive working equations similar to the ones derived in the HF scheme. Again we restrict ourselves to the discussion of a two-body interaction even though the extension to three-body forces is straightforward but cumbersome. The energy functional in terms of normal and anomalous densities reads

$$E[\rho, \kappa, \kappa^*] = \frac{\langle \psi | \hat{H} | \psi \rangle}{\langle \psi | \psi \rangle} \quad (13.15)$$

$$= \sum_{k_1 k_2} H_{k_1 k_2}^{[1]} \rho_{k_1 k_2} + \frac{1}{2} \sum_{k_1 k_2 q_1 q_2} \bar{H}_{k_1 q_2 k_2 q_1}^{[2]} \rho_{k_2 k_1} \rho_{q_1 q_2} - \frac{1}{4} \sum_{k_1 k_2 q_1 q_2} \bar{H}_{k_1 k_2 q_1 q_2}^{[2]} \kappa_{k_2 k_1} \kappa_{q_1 q_2}^*. \quad (13.16)$$

Since the quasiparticle vacuum $|\psi\rangle$ explicitly breaks the conservation of particle number, i.e., $|\psi\rangle$ is not an eigenstate on the number operator \hat{A} , we need to perform the variation under the constraint

$$\text{Tr} \rho = A, \quad (13.17)$$

such that the *mean particle number* is equal to the actual number of particle of the system under consideration. The above constraint is implemented in terms of a Lagrange multiplier leading to

$$\delta(E - \lambda \text{Tr} \rho) = \sum_{k_1 k_2} \left(\frac{\partial E}{\partial \rho_{k_1 k_2}} - \lambda \delta_{k_1 k_2} \right) + \frac{1}{2} \sum_{k_1 k_2} \left(\frac{\partial E}{\partial \kappa_{k_1 k_2}^*} \delta \kappa_{k_1 k_2}^* + \frac{\partial E}{\partial \kappa_{k_1 k_2}} \delta \kappa_{k_1 k_2} \right). \quad (13.18)$$

It is convenient to define the so-called *Hartree-Fock* and *pairing fields*, h and Δ , respectively,

$$h_{k_1 k_2} = \frac{\partial E}{\partial \rho_{k_1 k_2}} = t_{k_1 k_2} + \sum_{q_1 q_2} \bar{v}_{k_1 q_1 k_2 q_2} \rho_{k_1 k_2}, \quad (13.19)$$

$$\Delta_{k_1 k_2} = \frac{\partial E}{\partial \kappa_{k_1 k_2}} = \frac{1}{2} \sum_{q_1 q_2} \bar{v}_{k_1 q_1 k_2 q_2} \kappa_{k_1 k_2}. \quad (13.20)$$

With this we define the *Hartree-Fock-Bogoliubov Hamiltonian* \mathcal{H} and obtain the Hartree-Fock-Bogoliubov equations

$$\mathcal{H} \begin{pmatrix} U \\ V \end{pmatrix} = \begin{pmatrix} h - \lambda & \Delta \\ -\Delta^* & -h^* + \lambda \end{pmatrix} \begin{pmatrix} U \\ V \end{pmatrix} = E \begin{pmatrix} U \\ V \end{pmatrix}, \quad (13.21)$$

or equivalently [RS80]

$$[\mathcal{H}, \mathcal{R}] = 0, \quad (13.22)$$

which ensures the existence a common eigenbasis of the HFB Hamiltonian and the generalized density matrix in complete analogy to the HF case.

One obtains a set of conjugate HFB equations

$$\begin{pmatrix} h - \lambda & \Delta \\ -\Delta^* & -h^* + \lambda \end{pmatrix} \begin{pmatrix} V^* \\ U^* \end{pmatrix} = -E \begin{pmatrix} V^* \\ U^* \end{pmatrix}. \quad (13.23)$$

Obviously, to every eigenvector $(U, V)^T$ of \mathcal{H} with eigenvalue E there exist an eigenvector $(V^*, U^*)^T$ with eigenvalue $-E$.³ This follows from the use of a quasiparticle formulation, where quasiparticle creators and annihilators are taken to be independent. A physical solution is obtained by taking N out of the $2N$ eigenstates. It is common to take the eigenstates $(U, V)^T$ that correspond to the N positive energy eigenvalues.⁴

13.3 THE CANONICAL BASIS

From the definition of the quasiparticle vacuum according to (13.7), the quasiparticle annihilators are fixed only up to a unitary transformation among themselves. Apart from the quasiparticle basis $\{\hat{\beta}_k^\dagger\}$ there is another convenient basis for the discussion of HFB wave function. The connection to this so-called *canonical basis* is due to *Bloch-Messiah-Zumino theorem* (BMZ), which yields a decomposition of \mathcal{W} via

³Such an eigenvector is called *adjoint eigenvector*.

⁴We will stick to this convention when using HFB reference states for perturbative calculations.

$$\mathcal{W} = \begin{pmatrix} D & 0 \\ 0 & D^* \end{pmatrix} \begin{pmatrix} \bar{U} & \bar{V} \\ \bar{V} & \bar{U} \end{pmatrix} \begin{pmatrix} C & 0 \\ 0 & C^* \end{pmatrix} \quad (13.24)$$

or equivalently

$$U = D\bar{U}C, \quad (13.25)$$

$$V = D^*\bar{V}C, \quad (13.26)$$

where D and C are unitary transformations among the particle and quasiparticle operators, respectively

$$\hat{a}_k^\dagger = \sum_l D_{lk} \hat{c}_l^\dagger \quad (13.27)$$

$$\hat{\alpha}_k^\dagger = \sum_l C_{lk} \hat{\beta}_l^\dagger. \quad (13.28)$$

The matrices \bar{U} and \bar{V} define the *special Bogoliubov transformation*

$$\hat{\alpha}_p^\dagger = u_p \hat{a}_p^\dagger - v \hat{a}_{\bar{p}} \quad (13.29)$$

$$\hat{\alpha}_{\bar{p}}^\dagger = u_p \hat{a}_{\bar{p}}^\dagger + v \hat{a}_p, \quad (13.30)$$

which resembles formal equivalence with the transformation in standard BCS theory. The *canonical conjugate states* (p, \bar{p}) are connected via time-reversal symmetry. From the unitarity of \mathcal{W} we get for the occupation probabilities

$$u_k^2 + v_k^2 = 1. \quad (13.31)$$

Furthermore, the BMZ theorem implies the following block structure for paired levels with $(u_k > 0, v_k > 0)$:

$$\bar{U}_{kl} = +u_{\bar{k}} \delta_{kl}, \quad u_{\bar{k}} = +u_k, \quad (13.32)$$

$$\bar{V}_{kl} = -v_{\bar{k}} \delta_{\bar{k}l}, \quad v_{\bar{k}} = -v_k. \quad (13.33)$$

The quasiparticle vacuum can be rewritten in the canonical basis

$$|\Phi\rangle = \prod_p \hat{\alpha}_p^\dagger |0\rangle = \prod_{p>0} \left(u_p + v_p \hat{a}_p^\dagger \hat{a}_{\bar{p}}^\dagger \right) |0\rangle, \quad (13.34)$$

where we restricted the product to count every pair only once. A particular feature of this state is that it can only contain an even number of particles. This symmetry is referred to *number parity* and plays a crucial role in many-body techniques using a HFB vacuum.

13.4 THE INTRINSIC HAMILTONIAN

For self-bound systems, such as nuclei, the proper starting point for a many-body calculation is defined by a translationally invariant intrinsic Hamiltonian

$$\hat{H}_{\text{int}} = \hat{T} - \hat{T}_{\text{cm}} + \hat{V} = \hat{T}_{\text{int}} + \hat{V}. \quad (13.35)$$

Considering operators in Fock space, the intrinsic kinetic energy $\hat{T} - \hat{T}_{\text{cm}}$ can be written either composed as a sum of a one- and two-body operator

$$\hat{T}_{\text{int}}^{(a)} = \left(1 - \frac{1}{\hat{A}}\right) \sum_i \frac{\hat{p}_i^2}{2m} - \frac{1}{\hat{A}m} \sum_{i<j} \hat{p}_i \cdot \hat{p}_j, \quad (13.36)$$

or as a sum of two-body operators only, which corresponds to relative kinetic energies of nucleonic pairs

$$\hat{T}_{\text{int}}^{(b)} = \frac{2}{\hat{A}} \sum_{i<j} \frac{\hat{q}_{ij}^2}{2m} = \frac{1}{2\hat{A}} \sum_{i<j} \frac{(\hat{p}_i - \hat{p}_j)^2}{m}. \quad (13.37)$$

While both of the above choices coincide in the case of a particle-number conserving theory, they are not equivalent in the case the reference state breaks $U(1)$ symmetry. In particular the naive replacement of particle-number operator \hat{A} by its expectation value leads to wrong estimates.

By using a Taylor expansion of the particle-number operator it was shown that the one- plus two-body-form of the intrinsic kinetic energy is superior in particle-number non-conserving theories [HR09b].

14

Bogoliubov Many-Body Perturbation Theory

In Part II and III we introduced several flavors of MBPT with respect to different reference states. While the simplest version of MBPT is formulated with respect to a single-determinantal reference state, the MCPT extension provides one possible way of generalizing MBPT to open-shell systems, while having a reference state that still possesses the symmetries of the underlying Hamiltonian. Another strategy for including correlation effects is to allow the reference state to explicitly break some of the symmetries. Such an approach is called *symmetry-broken many-body perturbation theory* and has already been applied in the context of other many-body techniques like CC or SCGF [Dug15; DS16; SDB11; Som⁺14].

In the most common form one uses reference states that break conservation of particle number or total angular momentum. The corresponding reference states are then given as superpositions of several irreducible representations (IRREPS) of the corresponding symmetry group, e.g., for particle number conservation the symmetry group is $U(1)$ while for rotational symmetry it is $SU(2)$. In this work we focus entirely on the case of $U(1)$ symmetry-breaking, which corresponds to using a reference state of HFB type yielding *Bogoliubov many-body perturbation theory* (BMBPT).

Even though many-body theories using symmetry-broken reference states have been known for a long time, there have been no systematic studies and in particular no implementations using modern interactions. There are, however, studies in the context of the attractive pairing Hamiltonian, e.g., using quasiparticle CC [Hen⁺14] or projected quasiparticle MBPT [LG12].

The discussion of the many-body formalism below is based on an extensive collaboration with Thomas Duguet and Pierre Arthuis from CEA in Saclay, France. At the time of writing of this thesis, the corresponding work was unpublished. Therefore, we present a condensed version and refer to the literature when particular derivations are needed.

14.1 THE SYMMETRY GROUP $U(1)$

The breaking of particle-number conservation in HFB calculations is based on breaking global $U(1)$ symmetry. Therefore, we start with a brief discussion of some formal aspects of the underlying symmetry group.

The abelian Lie group

$$U(1) \equiv \{\hat{S}(\phi), \phi \in [0, 2\pi]\} \quad (14.1)$$

is a symmetry group of the Hamiltonian \hat{H} , the particle-number operator \hat{A} and some operator \hat{O} ,

$$[\hat{H}, \hat{S}(\phi)] = 0, \quad (14.2)$$

$$[\hat{A}, \hat{S}(\phi)] = 0, \quad (14.3)$$

$$[\hat{O}, \hat{S}(\phi)] = 0, \quad (14.4)$$

where we assumed that \hat{O} commutes with both \hat{A} and \hat{H} , as well as \hat{H} is a particle-number-conserving operator

$$[\hat{H}, \hat{A}] = 0. \quad (14.5)$$

The *unitary representation* of $U(1)$ on the Fock space \mathcal{F} is defined by

$$\hat{S}(\varphi) = e^{i\hat{A}\varphi}. \quad (14.6)$$

Consider now the stationary Schrödinger equation

$$\hat{H}|\psi_\mu^A\rangle = E_\mu^A|\psi_\mu^A\rangle, \quad (14.7)$$

where E_μ^A denotes the eigenvalue for a fixed value of A with increasing value for $\mu = 0, 1, 2, \dots$. Note that by (14.3) $|\psi_\mu^A\rangle$ is also an eigenstate of \hat{A}

$$\hat{A}|\psi_\mu^A\rangle = A|\psi_\mu^A\rangle. \quad (14.8)$$

With this, matrix elements of the *irreducible representations* (IRREPs) are given by

$$\langle\psi_\mu^A|\hat{S}(\varphi)|\psi_{\mu'}^{A'}\rangle = e^{iA\varphi}\delta_{AA'}\delta_{\mu\mu'}. \quad (14.9)$$

One defines the *volume* of the group by

$$\text{Vol}(U(1)) \equiv \int_0^{2\pi} d\varphi = 2\pi. \quad (14.10)$$

We further quote the orthogonality relation of the IRREPs,

$$\frac{1}{\text{Vol}(U(1))} \int_0^{2\pi} d\varphi e^{-iA\varphi} e^{+iA'\varphi} = \delta_{AA'}, \quad (14.11)$$

where the volume of the group enters for the sake of normalization.

14.2 TIME-DEPENDENT FORMALISM

In a particle-number broken approach we introduce a Lagrange parameter to constrain the Hamiltonian to the correct particle-number on average. This yields the definition of the *grand potential*

$$\hat{\Omega} \equiv \hat{H} - \lambda \hat{A}, \quad (14.12)$$

which takes the role of the Hamiltonian \hat{H} .¹ Making use of the eigenvalue relations of \hat{H} and \hat{A} we get

$$\hat{\Omega}|\psi_\mu^A\rangle = \Omega_\mu^A|\psi_\mu^A\rangle, \quad (14.14)$$

where the eigenvalue is given by

$$\Omega_\mu^A = E_\mu^A - \lambda A. \quad (14.15)$$

The Lagrange parameter λ is conveniently called *chemical potential*. In general, the Lagrange parameter for proton and neutron number do not coincide and, therefore, the chemical potential is isospin dependent.

TIME-DEPENDENT STATES

For the following we introduce the *imaginary-time evolution operator* by

$$\hat{\mathcal{U}}(\tau) \equiv e^{-\tau\hat{\Omega}}, \quad (14.16)$$

for some real τ . With this we define the time-evolved many-body state via

$$|\psi(\tau)\rangle = \hat{\mathcal{U}}(\tau)|\Phi\rangle \quad (14.17)$$

¹More precisely the above constraint reads

$$\hat{\Omega} - \lambda_N \hat{N} - \lambda_Z \hat{Z}, \quad (14.13)$$

where \hat{N} , \hat{Z} are neutron- and proton-number operators. For the sake of simplicity we refer to \hat{A} to be either one of them.

for some particle-number-broken vacuum $|\Phi\rangle$. By making use of the completeness relation

$$\mathbb{1} = \sum_{A \in \mathbb{N}} \sum_{\mu} |\psi_{\mu}^A\rangle \langle \psi_{\mu}^A| \quad (14.18)$$

in Fock space the time evolved-state can be written as

$$|\psi(\tau)\rangle = \sum_{A \in \mathbb{N}} \sum_{\mu} e^{-\tau \Omega_{\mu}^A} |\psi_{\mu}^A\rangle \langle \psi_{\mu}^A | \Phi\rangle. \quad (14.19)$$

In the following we will be interested in investigating the *large τ limit* and eventually taking the limit of *infinite τ* . The large time limit is defined by

$$\tau \gg \Delta E^{-1}, \quad (14.20)$$

where ΔE is the difference between the ground and first excited state of the grand potential Ω . We use the notation

$$\lim_{\tau \rightarrow \infty} \quad (14.21)$$

to indicate the large time limit of some quantity. Note, however, that there remains residual τ dependence and the large time limit is not a a limit in an mathematical sense but rather a regime.

In the large time limit the time-evolved state corresponds to the ground-state in the formulas

$$|\psi_0^{A_0}\rangle \equiv \lim_{\tau \rightarrow \infty} |\psi(\tau)\rangle \quad (14.22)$$

$$= e^{-\tau \Omega_0^{A_0}} |\psi_0^{A_0}\rangle \langle \psi_0^{A_0}|, \quad (14.23)$$

where the chemical λ is fixed such that for the targeted particle number A_0 , $\Omega_0^{A_0}$ is the lowest eigenvalue,

$$\hat{\Omega} |\psi_{\mu}^{A_0}\rangle = \Omega_0^{A_0} |\psi_{\mu}^{A_0}\rangle. \quad (14.24)$$

We note that, in principle, the above condition only ensures a stationary point of the functional. In applications, the chemical potential is fixed to a particle number A_0 such that $\Omega_0^{A_0}$ corresponds to the lowest energy eigenvalue. In general this can only be achieved if the convexity of the energy functional in a neighborhood of A_0 is guaranteed.

TIME-DEPENDENT OPERATOR KERNELS

In the following we assume an arbitrary operator \hat{O} that commutes with \hat{H} and \hat{A} . We define the *time-dependent kernel* of the operator \hat{O} by

$$O(\tau) \equiv \langle \psi(\tau) | \hat{O} | \Phi \rangle. \quad (14.25)$$

Application to the identity operator, Hamiltonian, particle-number operator and grand potential gives

$$N(\tau) \equiv \langle \psi(\tau) | \mathbb{1} | \Phi \rangle, \quad (14.26)$$

$$H(\tau) \equiv \langle \psi(\tau) | \hat{H} | \Phi \rangle, \quad (14.27)$$

$$A(\tau) \equiv \langle \psi(\tau) | \hat{A} | \Phi \rangle, \quad (14.28)$$

$$\Omega(\tau) \equiv \langle \psi(\tau) | \hat{\Omega} | \Phi \rangle, \quad (14.29)$$

where the time-dependent kernel of the grand potential corresponds to

$$\Omega(\tau) = H(\tau) - \lambda A(\tau). \quad (14.30)$$

Furthermore, we define the *reduced kernel* of an operator \hat{O} by

$$\mathcal{O}(\tau) \equiv \frac{O(\tau)}{N(\tau)}, \quad (14.31)$$

which leads to the case of *intermediate normalization*, i.e., $\mathcal{N}(\tau) = 1$ for the reduced norm kernel.

Making use of the expansion of the time-evolved many-body state we get

$$N(\tau) = \sum_{A \in \mathbb{N}} \sum_{\mu} e^{-\tau \Omega_{\mu}^A} |\langle \Phi | \psi_{\mu}^A \rangle|^2, \quad (14.32)$$

$$H(\tau) = \sum_{A \in \mathbb{N}} \sum_{\mu} E_{\mu}^A e^{-\tau \Omega_{\mu}^A} |\langle \Phi | \psi_{\mu}^A \rangle|^2, \quad (14.33)$$

$$A(\tau) = \sum_{A \in \mathbb{N}} \sum_{\mu} A e^{-\tau \Omega_{\mu}^A} |\langle \Phi | \psi_{\mu}^A \rangle|^2, \quad (14.34)$$

$$\Omega(\tau) = \sum_{A \in \mathbb{N}} \sum_{\mu} \Omega_{\mu}^A e^{-\tau \Omega_{\mu}^A} |\langle \Phi | \psi_{\mu}^A \rangle|^2. \quad (14.35)$$

We define the large τ limit of an operator kernel by

$$O(\infty) \equiv \lim_{\tau \rightarrow \infty} O(\tau) \quad (14.36)$$

thus obtaining

$$N(\infty) = e^{-\tau\Omega_0^{A_0}} |\langle \Phi | \psi_0^{A_0} \rangle|^2, \quad (14.37a)$$

$$H(\infty) = E_0^{A_0} e^{-\tau\Omega_0^{A_0}} |\langle \Phi | \psi_0^{A_0} \rangle|^2, \quad (14.37b)$$

$$A(\infty) = A_0 e^{-\tau\Omega_0^{A_0}} |\langle \Phi | \psi_0^{A_0} \rangle|^2, \quad (14.37c)$$

$$\Omega(\infty) = \Omega_0^{A_0} e^{-\tau\Omega_0^{A_0}} |\langle \Phi | \psi_0^{A_0} \rangle|^2. \quad (14.37d)$$

Obviously, the following eigenvalue-like relations hold in the large time limit

$$H(\infty) = E_0^{A_0} N(\infty), \quad (14.38a)$$

$$A(\infty) = A_0 N(\infty), \quad (14.38b)$$

$$\Omega(\infty) = \Omega_0^{A_0} N(\infty), \quad (14.38c)$$

which by employing reduced kernels lead to

$$\mathcal{H}(\infty) = E_0^{A_0}, \quad (14.39a)$$

$$\mathcal{A}(\infty) = A_0, \quad (14.39b)$$

$$\mathcal{\Omega}(\infty) = \Omega_0^{A_0}. \quad (14.39c)$$

The quantities in (14.39) refer to the exact, i.e., untruncated reduced operator kernels which are in one-to-one correspondence to a physical IRREP in the large-time limit. However, in actual applications the expressions of the kernels are approximated leading to a breaking of $U(1)$ symmetry. This typically leads to approximations for the reduced kernels that have the form

$$\mathcal{N}_{\text{app}} \equiv \sum_{A \in \mathbb{Z}} N_{\text{app}}^A, \quad (14.40a)$$

$$\mathcal{A}_{\text{app}} \equiv \sum_{A \in \mathbb{Z}} A_{\text{app}}^A N_{\text{app}}^A, \quad (14.40b)$$

$$\mathcal{H}_{\text{app}} \equiv \sum_{A \in \mathbb{Z}} H_{\text{app}}^A N_{\text{app}}^A. \quad (14.40c)$$

The remaining summation over several values of A displays the contamination from breaking particle-number conservation in a given truncation scheme.

14.3 NORMAL-ORDERING WITH RESPECT TO THE HFB VACUUM

In the end we are using reference states from a HFB calculation. Therefore, it is convenient to formulate the formalism that follows with respect to a quasiparticle basis and use a normal ordered representation of the operators with respect to $|\Phi\rangle$. The version of Wick theorem used in symmetry-conserving many-body approaches makes use of the particle-hole

formalism. However, in the quasiparticle basis there is no distinction between particle and hole single-particle states. Therefore, an extension to particle-number breaking reference states is required [BB69].

Given an arbitrary two-body operator \hat{O} its normal-ordered form is given by

$$O \equiv O^{[0]} + O^{[2]} + O^{[4]} \quad (14.41a)$$

$$\equiv O^{00} + \left[O^{11} + \{O^{20} + O^{02}\} \right] + \left[O^{22} + \{O^{31} + O^{13}\} + \{O^{40} + O^{04}\} \right] \quad (14.41b)$$

$$= O^{00} \quad (14.41c)$$

$$+ \frac{1}{1!} \sum_{k_1 k_2} O_{k_1 k_2}^{11} \beta_{k_1}^\dagger \beta_{k_2} \quad (14.41d)$$

$$+ \frac{1}{2!} \sum_{k_1 k_2} \left\{ O_{k_1 k_2}^{20} \beta_{k_1}^\dagger \beta_{k_2}^\dagger + O_{k_1 k_2}^{02} \beta_{k_2} \beta_{k_1} \right\} \quad (14.41e)$$

$$+ \frac{1}{(2!)^2} \sum_{k_1 k_2 k_3 k_4} O_{k_1 k_2 k_3 k_4}^{22} \beta_{k_1}^\dagger \beta_{k_2}^\dagger \beta_{k_4} \beta_{k_3} \quad (14.41f)$$

$$+ \frac{1}{3!} \sum_{k_1 k_2 k_3 k_4} \left\{ O_{k_1 k_2 k_3 k_4}^{31} \beta_{k_1}^\dagger \beta_{k_2}^\dagger \beta_{k_3}^\dagger \beta_{k_4} + O_{k_1 k_2 k_3 k_4}^{13} \beta_{k_1} \beta_{k_4} \beta_{k_3} \beta_{k_2} \right\} \quad (14.41g)$$

$$+ \frac{1}{4!} \sum_{k_1 k_2 k_3 k_4} \left\{ O_{k_1 k_2 k_3 k_4}^{40} \beta_{k_1}^\dagger \beta_{k_2}^\dagger \beta_{k_3}^\dagger \beta_{k_4}^\dagger + O_{k_1 k_2 k_3 k_4}^{04} \beta_{k_4} \beta_{k_3} \beta_{k_2} \beta_{k_1} \right\}, \quad (14.41h)$$

where each term \hat{O}^{ij} is characterized by its number i (j) of quasiparticle creation (annihilation) operators. The classes $\hat{O}^{[k]}$ collect all terms \hat{O}^{ij} with $i + j = k$.

In analogy to the standard Wick theorem the contribution

$$\hat{O}^{[0]} \equiv \hat{O}^{00} = \frac{\langle \Phi | \hat{O} | \Phi \rangle}{\langle \Phi | \Phi \rangle} \quad (14.42)$$

denotes the zero-body part of the normal-ordered operator in quasiparticle space.

We further note that all matrix elements are anti-symmetric,

$$O_{k_1, \dots, k_i, k_{i+1}, \dots, k_{i+j}}^{ij} = (-1)^{\sigma(\Pi)} O_{\Pi(k_1, \dots, k_i, k_{i+1}, \dots, k_{i+j})}^{ij}, \quad (14.43)$$

where $\sigma(\Pi)$ denotes the signature of the permutation Π . We only consider permutations among quasiparticle creation or annihilation operators, respectively. A compilation of fully anti-symmetrized normal-ordered matrix elements of various operators of particular importance for the implementation are presented in appendix C.

14.4 UNPERTURBED SYSTEM

In analogy to the symmetry-conserving approaches, we introduce a partitioning of the grand-canonical potential via

$$\hat{\Omega} = \hat{\Omega}_0 + \hat{\Omega}_1, \quad (14.44)$$

such that

$$\hat{\Omega}_0 \equiv \hat{\Omega}^{00} + \hat{\hat{\Omega}}^{11}, \quad (14.45)$$

$$\begin{aligned} \hat{\Omega}_1 \equiv & \hat{\Omega}^{20} + \hat{\hat{\Omega}}^{11} + \hat{\Omega}^{02} \\ & + \hat{\Omega}^{40} + \hat{\Omega}^{31} + \hat{\Omega}^{22} + \hat{\Omega}^{13} + \hat{\Omega}^{04}, \end{aligned} \quad (14.46)$$

where $\hat{\hat{\Omega}}^{11} \equiv \hat{\Omega}^{11} - \hat{\hat{\Omega}}^{11}$. The term $\hat{\hat{\Omega}}^{11}$ has the same formal structure as $\hat{\Omega}^{11}$. The specific choice of $\hat{\hat{\Omega}}^{11}$ remains open and will later be chosen conveniently. Note that we assume that the unperturbed system is defined in terms of a one-quasiparticle operator. The use of HFB reference states leads to choosing an operator $\hat{\Omega}_0$ that breaks particle-number conservation, i.e.,

$$[\hat{\Omega}_0, \hat{S}(\varphi)] \neq 0, \quad (14.47)$$

for general $\varphi \in [0, 2\pi]$. From this we also get

$$[\hat{\Omega}_1, \hat{S}(\varphi)] \neq 0. \quad (14.48)$$

From a set of quasiparticle energies $\{E_k\}$ we construct the unperturbed grand potential

$$\hat{\Omega}_0 \equiv \hat{\Omega}^{00} + \sum_k E_k \hat{\beta}_k^\dagger \hat{\beta}_k, \quad (14.49)$$

where we chose $E_k > 0$ for each k . Quasiparticle excitations with respect to the HFB vacuum are defined by

$$|\Phi^{k_1 \dots k_p}\rangle \equiv \hat{\beta}_{k_1}^\dagger \dots \hat{\beta}_{k_p}^\dagger |\Phi\rangle, \quad (14.50)$$

where we assume p to be an even number since we are working with states of even number parity.

The action of $\hat{\Omega}_0$ on the HFB vacuum is given by

$$\hat{\Omega}_0 |\Phi\rangle = \Omega^{00} |\Phi\rangle + \sum_k E_k \hat{\beta}_k^\dagger \hat{\beta}_k |\Phi\rangle \quad (14.51)$$

$$= \Omega^{00} |\Phi\rangle, \quad (14.52)$$

since by construction $\{\hat{\beta}_k\}$ annihilate the HFB vacuum. Analogously, the eigenvalues of $\hat{\Omega}_0$ for quasiparticle excitations are given by

$$\hat{\Omega}_0|\Phi^{k_1\cdots k_p}\rangle = \Omega^{00}|\Phi^{k_1\cdots k_p}\rangle + \sum_k E_k \hat{\beta}_k^\dagger \hat{\beta}_k |\Phi^{k_1\cdots k_p}\rangle, \quad (14.53)$$

$$= \Omega^{00}|\Phi^{k_1\cdots k_p}\rangle + \sum_k E_k \hat{\beta}_k^\dagger \hat{\beta}_k \hat{\beta}_{k_1}^\dagger \hat{\beta}_{k_1} \cdots \hat{\beta}_{k_p}^\dagger \hat{\beta}_{k_p} |\Phi\rangle, \quad (14.54)$$

$$= \Omega^{00}|\Phi^{k_1\cdots k_p}\rangle + \sum_k E_k \left(\sum_{k_i} \delta_{kk_i} \right) |\Phi^{k_1\cdots k_p}\rangle, \quad (14.55)$$

$$= \left(\Omega^{00} + E_{k_1} + \cdots + E_{k_p} \right) |\Phi^{k_1\cdots k_p}\rangle. \quad (14.56)$$

14.5 PERTURBATIVE EXPANSION OF OPERATOR KERNELS

In the following we will derive the perturbative expansion of norm and operator kernels. In a first step this requires the discussion of the unperturbed propagators.

UNPERTURBED PROPAGATOR

The transformation of the quasiparticle creation and annihilation operators to the interaction presentation reads

$$\hat{\beta}_k(\tau) \equiv e^{+\tau\Omega_0} \hat{\beta}_k e^{-\tau\Omega_0} = e^{-\tau E_0} \hat{\beta}_k, \quad (14.57)$$

$$\hat{\beta}_k^\dagger(\tau) \equiv e^{+\tau\Omega_0} \hat{\beta}_k^\dagger e^{-\tau\Omega_0} = e^{+\tau E_0} \hat{\beta}_k^\dagger. \quad (14.58)$$

In quasiparticle space the unperturbed propagator is defined as a 2×2 matrix

$$\mathbf{G}^0 = \begin{pmatrix} G^{+-}(0) & G^{--}(0) \\ G^{++}(0) & G^{-+}(0) \end{pmatrix}, \quad (14.59)$$

whose components are defined as

$$G_{k_1 k_2}^{+-}(0)(\tau_1, \tau_2) \equiv \frac{\langle \Phi | T[\hat{\beta}_{k_1}^\dagger(\tau_1) \hat{\beta}_{k_2}(\tau_2)] | \Phi \rangle}{\langle \Phi | \Phi \rangle}, \quad (14.60a)$$

$$G_{k_1 k_2}^{--}(0)(\tau_1, \tau_2) \equiv \frac{\langle \Phi | T[\hat{\beta}_{k_1}(\tau_1) \hat{\beta}_{k_2}(\tau_2)] | \Phi \rangle}{\langle \Phi | \Phi \rangle}, \quad (14.60b)$$

$$G_{k_1 k_2}^{++}(0)(\tau_1, \tau_2) \equiv \frac{\langle \Phi | T[\hat{\beta}_{k_1}^\dagger(\tau_1) \hat{\beta}_{k_2}^\dagger(\tau_2)] | \Phi \rangle}{\langle \Phi | \Phi \rangle}, \quad (14.60c)$$

$$G_{k_1 k_2}^{-+}(0)(\tau_1, \tau_2) \equiv \frac{\langle \Phi | T[\hat{\beta}_{k_1}(\tau_1) \hat{\beta}_{k_2}^\dagger(\tau_2)] | \Phi \rangle}{\langle \Phi | \Phi \rangle}. \quad (14.60d)$$

The quantity T denotes the *time-ordering operator* which orders a product of operators in a decreasing fashion with respect to their associated time labels. One can show that

$$G_{k_1 k_2}^{+- (0)}(\tau_1, \tau_2) = -e^{-(\tau_2 - \tau_1)E_{k_1}} \theta(\tau_2 - \tau_1) \delta_{k_1 k_2}, \quad (14.61a)$$

$$G_{k_1 k_2}^{-- (0)}(\tau_1, \tau_2) = 0, \quad (14.61b)$$

$$G_{k_1 k_2}^{++ (0)}(\tau_1, \tau_2) = 0, \quad (14.61c)$$

$$G_{k_1 k_2}^{-+ (0)}(\tau_1, \tau_2) = +e^{-(\tau_1 - \tau_2)E_{k_1}} \theta(\tau_1 - \tau_2) \delta_{k_1 k_2}, \quad (14.61d)$$

where

$$\theta(\tau) = \begin{cases} 1, & \tau > 0 \\ 0, & \text{else} \end{cases} \quad (14.62)$$

is the *Heaviside θ -function*. Derivations of (14.61) can be found in appendix D.

A particular feature of this approach is that it does not involve *anomalous propagators*, i.e., propagators containing two quasiparticle creation or annihilation operators.² Furthermore, it holds that the *equal-time propagators* vanish, i.e.,

$$G_{k_1 k_2}^{-+ (0)}(\tau, \tau) = 0, \quad (14.63)$$

$$G_{k_1 k_2}^{+- (0)}(\tau, \tau) = 0, \quad (14.64)$$

since they involve contractions arising from the vanishing R^{+-} matrix.

OPERATOR EXPANSION OF THE EVOLUTION OPERATOR

An expansion of $\mathcal{U}(\tau)$ in powers of Ω_1 can be obtained by starting from

$$\mathcal{U}(\tau) \equiv e^{-\tau\Omega_0} \mathcal{U}_1(\tau) \quad (14.65)$$

which gives

$$\mathcal{U}_1(\tau) = e^{\tau\Omega_0} e^{-\tau(\Omega_0 + \Omega_1)}. \quad (14.66)$$

From this we get a first-order differential equation

$$\partial_\tau \mathcal{U}_1(\tau) = -e^{\tau\Omega_0} \Omega_1 e^{-\tau\Omega_0} \mathcal{U}_1(\tau) \quad (14.67)$$

with solution

²The situation in the symmetry-restoration step is different. There one encounters matrix elements between different bra and ket state which differ by a gauge rotation. In such cases anomalous contractions do occur and the framework becomes more involved. This will, however, not be investigated in this thesis.

$$\mathcal{U}_1(\tau) = \text{T}e^{-\int_0^\tau dt \Omega_1(t)}. \quad (14.68)$$

In this case

$$\Omega_1(\tau) \equiv e^{\tau \Omega_0} \Omega_1 e^{-\tau \Omega_0} \quad (14.69)$$

defines the perturbation in the *interaction representation* and shall not be confused with a time-dependent operator kernel introduced before. Finally, the time evolution operator is given by

$$\mathcal{U}(\tau) = e^{-\tau \Omega_0} \text{T}e^{-\int_0^\tau dt \Omega_1(t)}. \quad (14.70)$$

EXPANSION OF THE OPERATOR KERNEL

We now come back to the derivation of the perturbation expansion of an arbitrary operator kernel $O(\tau)$. By the definition of the operator kernel we get

$$O(\tau) = \langle \psi(\tau) | O | \Phi \rangle, \quad (14.71)$$

$$= \langle \Phi | \mathcal{U}(\tau) O | \Phi \rangle, \quad (14.72)$$

$$= \langle \Phi | e^{-\tau \Omega_0} \text{T}e^{-\int_0^\tau dt \Omega_1(t)} O | \Phi \rangle. \quad (14.73)$$

Expanding the exponential gives

$$\begin{aligned} O(\tau) &= e^{-\Omega^{00}} \langle \Phi | \left(O(0) - \int_0^\tau d\tau_1 T[\Omega_1(\tau_1) O(0)] + \frac{1}{2!} \int_0^\tau d\tau_1 d\tau_2 T[\Omega_1(\tau_1) \Omega(\tau_2) O(0)] + \dots \right) | \Phi \rangle \\ &= e^{-\Omega^{00}} \left(\sum_{p=0}^{\infty} \frac{(-1)^p}{p!} \sum_{i_1+j_1=2,4} \int_0^\tau d\tau_1 \dots d\tau_p \right. \\ &\quad \times \sum_{\substack{k_1, \dots, k_{i_1} \\ k_{i_1+1}, \dots, k_{i_1+j_1} \\ \vdots \\ l_1, \dots, l_{i_p} \\ l_{i_p+1}, \dots, l_{i_p+j_p}}} \frac{\Omega_{k_1 \dots k_{i_1}, k_{i_1+1} \dots k_{i_1+j_1}}^{i_1 j_1}}{(i_1)! (j_1)!} \dots \frac{\Omega_{l_1 \dots l_{i_1}, l_{i_1+1} \dots l_{i_1+j_1}}^{i_p j_p}}{(i_p)! (j_p)!} \\ &\quad \times \langle \Phi | T[\hat{\beta}_{k_1}^\dagger(\tau_1) \dots \hat{\beta}_{k_{i_1}}^\dagger(\tau_1) \hat{\beta}_{k_{i_1+1}}(\tau_1) \dots \hat{\beta}_{k_{i_1+1}}(\tau_1) \dots \\ &\quad \dots \hat{\beta}_{l_1}^\dagger(\tau_p) \dots \hat{\beta}_{l_{i_p}}^\dagger(\tau_p) \hat{\beta}_{l_{i_p+1}}(\tau_p) \dots \hat{\beta}_{l_{i_p+1}}(\tau_p)] | \Phi \rangle \Big). \end{aligned} \quad (14.74)$$

By means of the generalized Wick theorem the expectation values of products of time-dependent field operators can be evaluated explicitly.

14.6 EXTRACTION OF DIAGRAMMATIC RULES

In the following we will investigate the first- and second-order norm kernel to derive a set of diagrammatic rules which will be applied subsequently for the derivation of low-order formulas.

FIRST-ORDER EXPANSION OF THE NORM KERNEL

In the following we suppress the additional prefactor $e^{-\Omega^{00}}$ in the expansion of the norm kernel. Starting with the first-order norm kernel we get for $p = 1$

$$\begin{aligned}
 N^{(1)}(\tau) &= - \int_0^\tau d\tau_1 \langle \Phi | \Omega_1(\tau_1) | \Phi \rangle \\
 &= - \int_0^\tau d\tau_1 \left(\sum_{k_1 k_2} \frac{\check{\Omega}_{k_1 k_2}^{11}}{1! 1!} \langle \Phi | T \left[\beta_{k_1}^\dagger(\tau_1) \beta_{k_2}(\tau_1) \right] | \Phi \rangle \right. \\
 &\quad + \sum_{k_1 k_2} \frac{\Omega_{k_1 k_2}^{20}}{2! 0!} \langle \Phi | T \left[\beta_{k_1}^\dagger(\tau_1) \beta_{k_2}^\dagger(\tau_1) \right] | \Phi \rangle \\
 &\quad + \sum_{k_1 k_2} \frac{\Omega_{k_1 k_2}^{02}}{0! 2!} \langle \Phi | T \left[\beta_{k_2}(\tau_1) \beta_{k_1}(\tau_1) \right] | \Phi \rangle \\
 &\quad + \sum_{k_1 k_2 k_3 k_4} \frac{\Omega_{k_1 k_2 k_3 k_4}^{22}}{2! 2!} \langle \Phi | T \left[\beta_{k_1}^\dagger(\tau_1) \beta_{k_2}^\dagger(\tau_1) \beta_{k_3}(\tau_1) \beta_{k_4}(\tau_1) \right] | \Phi \rangle \\
 &\quad + \sum_{k_1 k_2 k_3 k_4} \frac{\Omega_{k_1 k_2 k_3 k_4}^{31}}{3! 1!} \langle \Phi | T \left[\beta_{k_1}^\dagger(\tau_1) \beta_{k_2}^\dagger(\tau_1) \beta_{k_3}^\dagger(\tau_1) \beta_{k_4}(\tau_1) \right] | \Phi \rangle \\
 &\quad + \sum_{k_1 k_2 k_3 k_4} \frac{\Omega_{k_1 k_2 k_3 k_4}^{13}}{1! 3!} \langle \Phi | T \left[\beta_{k_1}^\dagger(\tau_1) \beta_{k_4}(\tau_1) \beta_{k_3}(\tau_1) \beta_{k_2}(\tau_1) \right] | \Phi \rangle \\
 &\quad + \sum_{k_1 k_2 k_3 k_4} \frac{\Omega_{k_1 k_2 k_3 k_4}^{40}}{4! 0!} \langle \Phi | T \left[\beta_{k_1}^\dagger(\tau_1) \beta_{k_2}^\dagger(\tau_1) \beta_{k_3}^\dagger(\tau_1) \beta_{k_4}^\dagger(\tau_1) \right] | \Phi \rangle \\
 &\quad \left. + \sum_{k_1 k_2 k_3 k_4} \frac{\Omega_{k_1 k_2 k_3 k_4}^{04}}{0! 4!} \langle \Phi | T \left[\beta_{k_4}(\tau_1) \beta_{k_3}(\tau_1) \beta_{k_2}(\tau_1) \beta_{k_1}(\tau_1) \right] | \Phi \rangle \right) \quad (14.75)
 \end{aligned}$$

Evaluating the corresponding normal-ordered strings we get sums of products of unperturbed propagators

$$\begin{aligned}
 N^{(1)}(\tau) &= - \int_0^\tau d\tau_1 \left\{ \sum_{k_1 k_2} \check{\Omega}_{k_1 k_2}^{11} G_{k_1 k_2}^{+- (0)}(\tau_1, \tau_1) + \frac{1}{2} \sum_{k_1 k_2} \Omega_{k_1 k_2}^{20} G_{k_1 k_2}^{++ (0)}(\tau_1, \tau_1) \right. \\
 &\quad + \frac{1}{2} \sum_{k_1 k_2} \Omega_{k_1 k_2}^{02} G_{k_2 k_1}^{-- (0)}(\tau_1, \tau_1) \\
 &\quad \left. + \frac{1}{4} \sum_{k_1 k_2 k_3 k_4} \Omega_{k_1 k_2 k_3 k_4}^{22} \left(G_{k_1 k_2}^{++ (0)}(\tau_1, \tau_1) G_{k_4 k_3}^{-- (0)}(\tau_1, \tau_1) - G_{k_1 k_4}^{+- (0)}(\tau_1, \tau_1) G_{k_2 k_3}^{+- (0)}(\tau_1, \tau_1) \right) \right.
 \end{aligned}$$

$$\begin{aligned}
 & + G_{k_1 k_3}^{+- (0)}(\tau_1, \tau_1) G_{k_2 k_4}^{+- (0)}(\tau_1, \tau_1) \\
 & + \frac{1}{3!} \sum_{k_1 k_2 k_3 k_4} \Omega_{k_1 k_2 k_3 k_4}^{31} \left(G_{k_1 k_2}^{++ (0)}(\tau_1, \tau_1) G_{k_3 k_4}^{+- (0)}(\tau_1, \tau_1) - G_{k_1 k_3}^{++ (0)}(\tau_1, \tau_1) G_{k_2 k_4}^{+- (0)}(\tau_1, \tau_1) \right. \\
 & + G_{k_1 k_4}^{+- (0)}(\tau_1, \tau_1) G_{k_2 k_3}^{++ (0)}(\tau_1, \tau_1) \\
 & + \frac{1}{3!} \sum_{k_1 k_2 k_3 k_4} \Omega_{k_1 k_2 k_3 k_4}^{13} \left(G_{k_1 k_4}^{+- (0)}(\tau_1, \tau_1) G_{k_3 k_2}^{-- (0)}(\tau_1, \tau_1) - G_{k_1 k_3}^{+- (0)}(\tau_1, \tau_1) G_{k_4 k_2}^{-- (0)}(\tau_1, \tau_1) \right. \\
 & + G_{k_1 k_2}^{+- (0)}(\tau_1, \tau_1) G_{k_4 k_3}^{-- (0)}(\tau_1, \tau_1) \\
 & + \frac{1}{4!} \sum_{k_1 k_2 k_3 k_4} \Omega_{k_1 k_2 k_3 k_4}^{40} \left(G_{k_1 k_2}^{++ (0)}(\tau_1, \tau_1) G_{k_3 k_4}^{++ (0)}(\tau_1, \tau_1) - G_{k_1 k_3}^{++ (0)}(\tau_1, \tau_1) G_{k_2 k_4}^{++ (0)}(\tau_1, \tau_1) \right. \\
 & + G_{k_1 k_4}^{++ (0)}(\tau_1, \tau_1) G_{k_2 k_3}^{++ (0)}(\tau_1, \tau_1) \\
 & + \frac{1}{4!} \sum_{k_1 k_2 k_3 k_4} \Omega_{k_1 k_2 k_3 k_4}^{04} \left(G_{k_4 k_3}^{++ (0)}(\tau_1, \tau_1) G_{k_2 k_1}^{++ (0)}(\tau_1, \tau_1) - G_{k_4 k_2}^{++ (0)}(\tau_1, \tau_1) G_{k_3 k_1}^{++ (0)}(\tau_1, \tau_1) \right. \\
 & \left. \left. + G_{k_4 k_1}^{++ (0)}(\tau_1, \tau_1) G_{k_3 k_2}^{++ (0)}(\tau_1, \tau_1) \right) \right\} \\
 & = 0, \tag{14.76}
 \end{aligned}$$

since all contractions involve equal-time propagators which vanish identically.

SECOND-ORDER NORM KERNEL

Application of the Taylor expansion at second-order yields the following contributions at second-order for the norm kernel

$$\begin{aligned}
 N^{(2)}(\tau) & = N^{(1)}(\tau) + \frac{1}{2!} \int_0^\tau d\tau_1 d\tau_2 \langle \Phi | T [\Omega_1(\tau_1) \Omega_1(\tau_2)] | \Phi \rangle \\
 & = N^{(1)}(\tau) \\
 & + \frac{1}{2!} \int_0^\tau d\tau_1 d\tau_2 \left\{ \sum_{k_1 k_2 l_1 l_2} \frac{\check{\Omega}_{k_1 k_2}^{11}}{1! 1!} \frac{\check{\Omega}_{l_1 l_2}^{11}}{1! 1!} \langle \Phi | T [\beta_{k_1}^\dagger(\tau_1) \beta_{k_2}(\tau_1) \beta_{l_1}^\dagger(\tau_2) \beta_{l_2}(\tau_2)] | \Phi \rangle \right. \\
 & + \sum_{k_1 k_2 l_1 l_2} \frac{\Omega_{k_1 k_2}^{02}}{0! 2!} \frac{\Omega_{l_1 l_2}^{20}}{2! 0!} \langle \Phi | T [\beta_{k_2}(\tau_1) \beta_{k_1}(\tau_1) \beta_{l_1}^\dagger(\tau_2) \beta_{l_2}^\dagger(\tau_2)] | \Phi \rangle \\
 & + \sum_{k_1 k_2 l_1 l_2} \frac{\Omega_{k_1 k_2}^{20}}{2! 0!} \frac{\Omega_{l_1 l_2}^{02}}{0! 2!} \langle \Phi | T [\beta_{k_1}^\dagger(\tau_1) \beta_{k_2}^\dagger(\tau_1) \beta_{l_2}(\tau_2) \beta_{l_1}(\tau_2)] | \Phi \rangle \\
 & + \sum_{k_1 k_2 l_1 l_2} \frac{\check{\Omega}_{k_1 k_2}^{11}}{1! 1!} \frac{\Omega_{l_1 l_2}^{02}}{0! 2!} \langle \Phi | T [\beta_{k_1}^\dagger(\tau_1) \beta_{k_2}(\tau_1) \beta_{l_2}(\tau_2) \beta_{l_1}(\tau_2)] | \Phi \rangle \\
 & \left. + \sum_{k_1 k_2 l_1 l_2} \frac{\check{\Omega}_{k_1 k_2}^{11}}{1! 1!} \frac{\Omega_{l_1 l_2}^{20}}{2! 0!} \langle \Phi | T [\beta_{k_1}^\dagger(\tau_1) \beta_{k_2}(\tau_1) \beta_{l_1}^\dagger(\tau_2) \beta_{l_2}^\dagger(\tau_2)] | \Phi \rangle \right\}
 \end{aligned}$$

$$\begin{aligned}
 & + \sum_{k_1 k_2 l_1 l_2} \frac{\Omega_{k_1 k_2}^{20}}{2! 0!} \frac{\check{\Omega}_{l_1 l_2}^{11}}{1! 1!} \langle \Phi | T \left[\beta_{k_1}^\dagger(\tau_1) \beta_{k_2}^\dagger(\tau_1) \beta_{l_1}^\dagger(\tau_2) \beta_{l_2}(\tau_2) \right] | \Phi \rangle \\
 & + \sum_{k_1 k_2 l_1 l_2} \frac{\Omega_{k_1 k_2}^{02}}{0! 2!} \frac{\check{\Omega}_{l_1 l_2}^{11}}{1! 1!} \langle \Phi | T \left[\beta_{k_2}(\tau_1) \beta_{k_1}(\tau_1) \beta_{l_1}^\dagger(\tau_2) \beta_{l_2}(\tau_2) \right] | \Phi \rangle \\
 & + \sum_{k_1 k_2 l_1 l_2} \frac{\Omega_{k_1 k_2}^{02}}{0! 2!} \frac{\Omega_{l_1 l_2}^{02}}{0! 2!} \langle \Phi | T \left[\beta_{k_2}(\tau_1) \beta_{k_1}(\tau_1) \beta_{l_2}(\tau_2) \beta_{l_1}(\tau_2) \right] | \Phi \rangle \\
 & + \sum_{k_1 k_2 l_1 l_2} \frac{\Omega_{k_1 k_2}^{20}}{2! 0!} \frac{\Omega_{l_1 l_2}^{20}}{2! 0!} \langle \Phi | T \left[\beta_{k_1}^\dagger(\tau_1) \beta_{k_2}^\dagger(\tau_1) \beta_{l_1}^\dagger(\tau_2) \beta_{l_2}^\dagger(\tau_2) \right] | \Phi \rangle \\
 & + \dots \left. \vphantom{\sum_{k_1 k_2 l_1 l_2}} \right\}, \tag{14.77}
 \end{aligned}$$

where the listed number of second-order terms is incomplete. We aim at calculating a few terms in the series and deduce the diagrammatic rules from them. As an example we take the term containing $\hat{\Omega}^{02} \hat{\Omega}^{20}$. Applying all possible Wick contractions yields

$$\begin{aligned}
 N_{02.20}^{(2)}(\tau) & \equiv \frac{1}{2!} \int_0^\tau d\tau_1 d\tau_2 \sum_{k_1 k_2 l_1 l_2} \frac{\Omega_{k_1 k_2}^{02}}{0! 2!} \frac{\Omega_{l_1 l_2}^{20}}{2! 0!} \langle \Phi | T \left[\beta_{k_2}(\tau_1) \beta_{k_1}(\tau_1) \beta_{l_1}^\dagger(\tau_2) \beta_{l_2}^\dagger(\tau_2) \right] | \Phi \rangle \\
 & = \frac{1}{8} \int_0^\tau d\tau_1 d\tau_2 \sum_{k_1 k_2 l_1 l_2} \Omega_{k_1 k_2}^{02} \Omega_{l_1 l_2}^{20} \left\{ G_{k_2 k_1}^{--(0)}(\tau_1, \tau_1) G_{l_1 l_2}^{++(0)}(\tau_2, \tau_2) \right. \\
 & \quad \left. - G_{k_2 l_1}^{-+(0)}(\tau_1, \tau_2) G_{k_1 l_2}^{-+(0)}(\tau_1, \tau_2) + G_{k_2 l_2}^{-+(0)}(\tau_1, \tau_2) G_{k_1 l_1}^{-+(0)}(\tau_1, \tau_2) \right\} \\
 & = \frac{1}{8} \int_0^\tau d\tau_1 d\tau_2 \sum_{k_1 k_2 l_1 l_2} \Omega_{k_1 k_2}^{02} \Omega_{l_1 l_2}^{20} \left\{ -G_{k_2 l_1}^{-+(0)}(\tau_1, \tau_2) G_{k_1 l_2}^{-+(0)}(\tau_1, \tau_2) \right. \\
 & \quad \left. + G_{k_2 l_2}^{-+(0)}(\tau_1, \tau_2) G_{k_1 l_1}^{-+(0)}(\tau_1, \tau_2) \right\} \\
 & = \frac{1}{8} \sum_{k_1 k_2 l_1 l_2} \Omega_{k_1 k_2}^{02} \Omega_{l_1 l_2}^{20} \int_0^\tau d\tau_1 d\tau_2 \left\{ -\theta(\tau_1 - \tau_2) \delta_{k_2 l_1} \delta_{k_1 l_2} e^{-(\tau_1 - \tau_2)(E_{k_1} + E_{k_2})} \right. \\
 & \quad \left. + \theta(\tau_1 - \tau_2) \delta_{k_2 l_2} \delta_{k_1 l_1} e^{-(\tau_1 - \tau_2)(E_{k_1} + E_{k_2})} \right\} \\
 & = \frac{1}{8} \sum_{k_1 k_2 l_1 l_2} \Omega_{k_1 k_2}^{02} \Omega_{l_1 l_2}^{20} (-\delta_{k_2 l_1} \delta_{k_1 l_2} + \delta_{k_2 l_2} \delta_{k_1 l_1}) \int_0^\tau d\tau_1 d\tau_2 \theta(\tau_1 - \tau_2) e^{-(\tau_1 - \tau_2)(E_{k_1} + E_{k_2})} \\
 & = \frac{1}{8} \sum_{k_1 k_2} (-\Omega_{k_1 k_2}^{02} \Omega_{k_2 k_1}^{20} + \Omega_{k_1 k_2}^{02} \Omega_{k_1 k_2}^{20}) \left[\frac{\tau}{E_{k_1} + E_{k_2}} + \frac{e^{-\tau(E_{k_1} + E_{k_2})} - 1}{(E_{k_1} + E_{k_2})^2} \right] \\
 & = \frac{1}{4} \sum_{k_1 k_2} \frac{\Omega_{k_1 k_2}^{02} \Omega_{k_1 k_2}^{20}}{E_{k_1} + E_{k_2}} \left[\tau - \frac{1 - e^{-\tau(E_{k_1} + E_{k_2})}}{E_{k_1} + E_{k_2}} \right], \tag{14.78}
 \end{aligned}$$

In a similar way we obtain for the $\hat{\Omega}^{20} \hat{\Omega}^{02}$ term

$$N_{20.02}^{(2)}(\tau) \equiv \frac{1}{2!} \int_0^\tau d\tau_1 d\tau_2 \sum_{k_1 k_2 l_1 l_2} \frac{\Omega_{k_1 k_2}^{20}}{2! 0!} \frac{\Omega_{l_1 l_2}^{02}}{0! 2!} \langle \Phi | T \left[\beta_{k_1}^\dagger(\tau_1) \beta_{k_2}^\dagger(\tau_1) \beta_{l_2}(\tau_2) \beta_{l_1}(\tau_2) \right] | \Phi \rangle$$

$$\begin{aligned}
 &= \frac{1}{8} \int_0^\tau d\tau_1 d\tau_2 \sum_{k_1 k_2 l_1 l_2} \Omega_{k_1 k_2}^{20} \Omega_{l_1 l_2}^{02} \left\{ G_{k_1 k_2}^{++(0)}(\tau_1, \tau_1) G_{l_2 l_1}^{--(0)}(\tau_2, \tau_2) \right. \\
 &\quad \left. - G_{k_1 l_2}^{+- (0)}(\tau_1, \tau_2) G_{k_2 l_1}^{+- (0)}(\tau_1, \tau_2) + G_{k_1 l_1}^{+- (0)}(\tau_1, \tau_2) G_{k_2 l_2}^{+- (0)}(\tau_1, \tau_2) \right\} \\
 &= \frac{1}{8} \sum_{k_1 k_2 l_1 l_2} \Omega_{k_1 k_2}^{20} \Omega_{l_1 l_2}^{02} (-\delta_{k_2 l_1} \delta_{k_1 l_2} + \delta_{k_2 l_2} \delta_{k_1 l_1}) \int_0^\tau d\tau_1 d\tau_2 \theta(\tau_2 - \tau_1) e^{-(\tau_2 - \tau_1)(E_{k_1} + E_{k_2})} \\
 &= \frac{1}{4} \sum_{k_1 k_2} \frac{\Omega_{k_1 k_2}^{20} \Omega_{k_1 k_2}^{02}}{E_{k_1} + E_{k_2}} \left[\tau - \frac{1 - e^{-\tau(E_{k_1} + E_{k_2})}}{E_{k_1} + E_{k_2}} \right]. \tag{14.79}
 \end{aligned}$$

Obviously both contributions coincide and finding two individual diagrammatic representation of the above terms would yield topologically equivalent diagrams. Therefore, both contributions will be represented by one diagram.

As an additional example consider the term containing $\check{\Omega}^{11} \Omega^{02}$,

$$\begin{aligned}
 N_{11.02}^{(2)}(\tau) &\equiv \frac{1}{2!} \int_0^\tau d\tau_1 d\tau_2 \sum_{k_1 k_2 l_1 l_2} \frac{\check{\Omega}_{k_1 k_2}^{11} \Omega_{l_1 l_2}^{02}}{1! 1! 0! 2!} \langle \Phi | \text{T} \left[\beta_{k_1}^\dagger(\tau_1) \beta_{k_2}(\tau_1) \beta_{l_2}(\tau_2) \beta_{l_1}(\tau_2) \right] | \Phi \rangle \\
 &= \frac{1}{4} \int_0^\tau d\tau_1 d\tau_2 \sum_{k_1 k_2 l_1 l_2} \check{\Omega}_{k_1 k_2}^{11} \Omega_{l_1 l_2}^{02} \left\{ G_{k_1 k_2}^{+- (0)}(\tau_1, \tau_1) G_{l_1 l_2}^{-- (0)}(\tau_2, \tau_2) \right. \\
 &\quad \left. - G_{k_1 l_2}^{+- (0)}(\tau_1, \tau_2) G_{k_2 l_1}^{-- (0)}(\tau_1, \tau_2) + G_{k_1 l_1}^{+- (0)}(\tau_1, \tau_2) G_{k_2 l_2}^{-- (0)}(\tau_1, \tau_2) \right\} \\
 &= 0, \tag{14.80}
 \end{aligned}$$

which vanishes identically due to anomalous unperturbed propagators. Anomalous propagators originate from contractions from either two creation or two annihilation operators. Therefore, from the very start we can exclude contributions with a different number of creation and annihilation operators.

Last consider the term $\check{\Omega}^{11} \check{\Omega}^{11}$,

$$\begin{aligned}
 N_{11.11}^{(2)}(\tau) &\equiv \frac{1}{2!} \int_0^\tau d\tau_1 d\tau_2 \sum_{k_1 k_2 l_1 l_2} \frac{\check{\Omega}_{k_1 k_2}^{11} \check{\Omega}_{l_1 l_2}^{11}}{1! 1! 1! 1!} \langle \Phi | \text{T} \left[\beta_{k_1}^\dagger(\tau_1) \beta_{k_2}(\tau_1) \beta_{l_1}^\dagger(\tau_2) \beta_{l_2}(\tau_2) \right] | \Phi \rangle \\
 &= \frac{1}{2!} \int_0^\tau d\tau_1 d\tau_2 \sum_{k_1 k_2 l_1 l_2} \check{\Omega}_{k_1 k_2}^{11} \check{\Omega}_{l_1 l_2}^{11} \left\{ G_{k_1 k_2}^{+- (0)}(\tau_1, \tau_1) G_{l_1 l_2}^{+- (0)}(\tau_2, \tau_2) \right. \\
 &\quad \left. - G_{k_1 l_1}^{++ (0)}(\tau_1, \tau_2) G_{k_2 l_2}^{-- (0)}(\tau_1, \tau_2) + G_{k_1 l_2}^{+- (0)}(\tau_1, \tau_2) G_{k_2 l_1}^{-+ (0)}(\tau_1, \tau_2) \right\} \\
 &= -\frac{1}{2!} \sum_{k_1 k_2 l_1 l_2} \check{\Omega}_{k_1 k_2}^{11} \check{\Omega}_{l_1 l_2}^{11} \delta_{k_1 l_2} \delta_{k_2 l_1} \int_0^\tau d\tau_1 d\tau_2 \theta(\tau_2 - \tau_1) \theta(\tau_1 - \tau_2) e^{-(\tau_2 - \tau_1)(E_{k_1} - E_{k_2})} \\
 &= 0, \tag{14.81}
 \end{aligned}$$

which vanished as well since we have

$$\theta(\tau_2 - \tau_1)\theta(\tau_1 - \tau_2) = 0. \quad (14.82)$$

Therefore, normal propagators linking two vertices with different time labels are forced to propagate in the same direction.

The manual evaluation of the above contribution allows us to infer the diagrammatic rules in BMBPT which are subsequently used for a more efficient evaluation of low-order corrections.

14.7 DIAGRAMMATIC TREATMENT

The following provides an overview of the relevant diagrammatic rules in low-order BMBPT.

Diagrammatic Rules of BMBPT

1. Closed vacuum-to-vacuum Feynman diagrams of order p consist of p vertices corresponding to $\Omega^{ij}(\tau_k)$.
2. Edges represent fermionic quasiparticle lines corresponding to unperturbed propagators $G^{gg'(0)}$ which form a set of closed loops.
3. Each vertex is labeled by a time label whereas each line is labeled by two quasiparticle indices and two time labels at its end. Vertices contribute a factor

$$\Omega_{k_1 \dots k_i k_{i+1} \dots k_{i+j}}^{ij}$$

and edges contribute a factor $G_{k_1 k_2}^{gg'(0)}(\tau_k, \tau_{k'})$ where $g, g' = \pm$ determines the type of unperturbed propagator which needs to be considered.

4. The contributions to $N(\tau)$ arising at order p are given by drawing all possible *topologically distinct* vacuum-to-vacuum diagrams involving p perturbation operators $\hat{\Omega}_1(\tau_k)$. Two diagrams are called topologically equivalent if they can be obtained from each other by relabelling vertex and edge labels.
5. One must sum over all internal quasiparticle indices and integrate over all time labels from 0 to ∞ .
6. One must assign a phase factor $(-1)^{p+n_c}$ where p denotes the perturbation order and n_c denotes the number of crossing lines.
7. Add a prefactor $\frac{1}{(n_e)!}$ for each group of n_e *equivalent lines*. Two lines are considered equivalent, if they connect the same vertices and the corresponding unperturbed propagators are characterized by the same superscripts g and g' .

8. A *symmetry prefactor* $\frac{1}{n_s}$ needs to be considered corresponding to the of number of ways one produces a topologically distinct diagram when exchanging time labels.

The normal-ordering in quasiparticle space yields many different contributions even if restricting oneself to two-body operators in the first place. Therefore, the large number of diagrams is a severe problem. Fortunately, there are some properties which tremendously reduce the number of allowed diagrams.

Selection Rules

1. Anomalous propagators vanish identically and do not need to be considered.
2. Each string of operators needs to have the same amount of creation and annihilation operators

$$n_a \equiv \sum_{k=1}^p (j_k - i_k) \neq 0 \quad \Rightarrow \quad \langle \Phi | \Omega^{i_1 j_1}(\tau_1) \Omega^{i_2 j_2}(\tau_2) \cdots \Omega^{i_p j_p}(\tau_p) | \Phi \rangle = 0. \quad (14.83)$$

3. All equal-time propagators vanish since there are no self contractions.

14.8 EXPONENTIATION OF CONNECTED DIAGRAMMS

In the following we will argue why the disconnected diagrams do not contribute, which is important for the correct scaling behavior with respect to the size of the system, i.e., mass number for finite nuclei.

Consider a disconnected diagram which consists of several connected components denoted by $\Gamma_i^c(\tau)$ where none of the connected components are joined by edges. Furthermore, the same connected part may appear several times in the overall diagram. The overall value of a diagram $\Gamma(\tau)$ is proportional to

$$\Gamma(\tau) \propto \Gamma_1^c(\tau)^{n_1} \Gamma_2^c(\tau)^{n_2} \cdots \quad (14.84)$$

Taking further into account permutations of the time labels of identical disconnected parts we get

$$\Gamma(\tau) = \frac{1}{n_1!} \Gamma_1^c(\tau)^{n_1} \frac{1}{n_2!} \Gamma_2^c(\tau)^{n_2} \cdots \quad (14.85)$$

such that we can finally write by means of the power series representation of the exponential function

$$\langle \Phi | \mathcal{U}_1 | \Phi \rangle = \sum_{\Gamma} \Gamma(\tau)$$

$$\begin{aligned}
 &= \sum_{\Gamma} \frac{1}{n_1!} \Gamma_1^c(\tau)^{n_1} \frac{1}{n_2!} \Gamma_2^c(\tau)^{n_2} \dots \\
 &= e^{\Gamma_1^c(\tau) + \Gamma_2^c(\tau) + \dots}
 \end{aligned} \tag{14.86}$$

which shows that the time-evolution operator can be expanded in a exponential of the sum of connected diagrams only. The norm can, *prior* to any truncation be written as

$$N(\tau) = e^{-\tau\Omega^{00} + n(\tau)} \langle \Phi | \Phi \rangle, \tag{14.87}$$

where $n(\tau) \equiv \sum_{n=1}^{\infty} n^{(n)}(\tau)$, with $n^{(n)}(\tau)$ being the sum of all *connected* Feynman vacuum-amplitude diagrams of order n .

14.9 SECOND-ORDER CORRECTION TO THE NORM KERNEL

In the following we derive the second-order contributions to the norm kernel using the diagrammatic rules outlined before. The relevant diagrams are displayed in Figure 14.1. The two-body contribution gives

$$\begin{aligned}
 \text{PN2.2} &= + \frac{1}{4!} \sum_{\substack{k_1 k_2 k_3 k_4 \\ k_5 k_6 k_7 k_8}} \Omega_{k_1 k_2 k_3 k_4}^{40} \Omega_{k_5 k_6 k_7 k_8}^{04} \\
 &\quad \times \int_0^{\tau} d\tau_1 d\tau_2 G_{k_1 k_5}^{+- (0)}(\tau_1, \tau_2) G_{k_2 k_6}^{+- (0)}(\tau_1, \tau_2) G_{k_3 k_7}^{+- (0)}(\tau_1, \tau_2) G_{k_4 k_8}^{+- (0)}(\tau_1, \tau_2) \\
 &= + \frac{1}{4!} \sum_{\substack{k_1 k_2 k_3 k_4 \\ k_5 k_6 k_7 k_8}} \Omega_{k_1 k_2 k_3 k_4}^{40} \Omega_{k_5 k_6 k_7 k_8}^{04} \delta_{k_1 k_5} \delta_{k_2 k_6} \delta_{k_3 k_7} \delta_{k_4 k_8} \\
 &\quad \times \int_0^{\tau} d\tau_1 d\tau_2 \theta(\tau_2 - \tau_1) e^{-(\tau_2 - \tau_1)(E_{k_1} + E_{k_2} + E_{k_3} + E_{k_4})} \\
 &= + \frac{1}{4!} \sum_{k_1 k_2 k_3 k_4} \frac{\Omega_{k_1 k_2 k_3 k_4}^{40} \Omega_{k_1 k_2 k_3 k_4}^{04}}{E_{k_1} + E_{k_2} + E_{k_3} + E_{k_4}} \left[\tau - \frac{1 - e^{-\tau(E_{k_1} + E_{k_2} + E_{k_3} + E_{k_4})}}{E_{k_1} + E_{k_2} + E_{k_3} + E_{k_4}} \right].
 \end{aligned} \tag{14.88}$$

Adopting the large time limit the above expression gives

$$\text{PN2.2} = + \frac{1}{4!} \sum_{k_1 k_2 k_3 k_4} \frac{\Omega_{k_1 k_2 k_3 k_4}^{40} \Omega_{k_1 k_2 k_3 k_4}^{04}}{E_{k_1} + E_{k_2} + E_{k_3} + E_{k_4}} \left[\tau - \frac{1}{E_{k_1} + E_{k_2} + E_{k_3} + E_{k_4}} \right]. \tag{14.89}$$

14.10 NORM KERNEL AND CORRELATION ENERGY

Starting from

$$N(\infty) = e^{-\tau\Omega_0^{A_0}} |\langle \Phi | \Psi_0^{A_0} \rangle|^2 \tag{14.90}$$

and matching (14.87) we get

$$\lim_{n \rightarrow \infty} n(\tau) \equiv -\tau \Delta \Omega_0^{A_0} + \ln |\langle \Phi | \psi_0^{A_0} \rangle|^2, \quad (14.91)$$

where

$$\begin{aligned} \Delta \Omega_0^{A_0} &\equiv \hat{\Omega}_0^{A_0} - \hat{\Omega}_0^{00} \\ &= \langle \Phi | \hat{\Omega}_1 \sum_{k=1}^{\infty} \left(\frac{1}{\hat{\Omega}_0^{00} - \hat{\Omega}_0} \right)^{k-1} | \Phi \rangle_c \end{aligned} \quad (14.92)$$

is the analogue of the correlation expansion for the superfluid HFB reference state.

14.11 PERTURBATIVE EXPANSION OF GENERIC OPERATOR KERNELS

After deriving the perturbative expansion of the norm kernel we can apply similar arguments for a generic operator \hat{O} where one assumes that \hat{O} commutes with \hat{H} and \hat{A} . For the time-dependent operator kernel we get

$$O(\tau) = \langle \Phi | e^{-\tau \Omega_0} \mathbb{T} e^{-\int_0^\tau dt \Omega_1(t)} O | \Phi \rangle \quad (14.93)$$

$$\begin{aligned} &= e^{-\tau \Omega_0} \langle \Phi | \left\{ O(0) - \int_0^\tau d\tau_1 \mathbb{T} [\Omega_1(\tau_1) O(0)] \right. \\ &\quad \left. + \frac{1}{2!} \int_0^\tau d\tau_1 d\tau_2 \mathbb{T} [\Omega_1(\tau_1) \Omega_1(\tau_2) O(0)] + \dots \right\} | \Phi \rangle, \end{aligned} \quad (14.94)$$

where the key difference to the expansion of the norm kernel is given by the extra appearance of the operator kernel $O(0)$ at fixed time $t = 0$.

Analogously, to the expansion of the norm kernel we write

$$O(\tau) \equiv e^{-\tau \Omega_0} \sum_{i+j=0,2,4} \sum_{n=0}^{\infty} O^{ij(n)}(\tau) \langle \Phi | \Phi \rangle, \quad (14.95)$$

where again the first sum displays the restriction to quasiparticle operators of rank four. Here $O^{ij(n)}(\tau)$ denotes the sum of connected vacuum diagrams of order n .

FACTORIZATION OF CONNECTED DIAGRAMS

As already indicated the operator kernel diagrams correspond to insertions at time $\tau = 0$ of \hat{O} into the perturbative expansion of the norm kernel. In particular any diagram $O^{ij(n)}(\tau)$ consists of a part, which is linked to the vertex $O^{ij}(0)$, and a part that is disconnected. Therefore, the expression of operator kernel factorizes into

$$O^{ij}(\tau) \equiv o^{ij}(\tau) N(\tau). \quad (14.96)$$

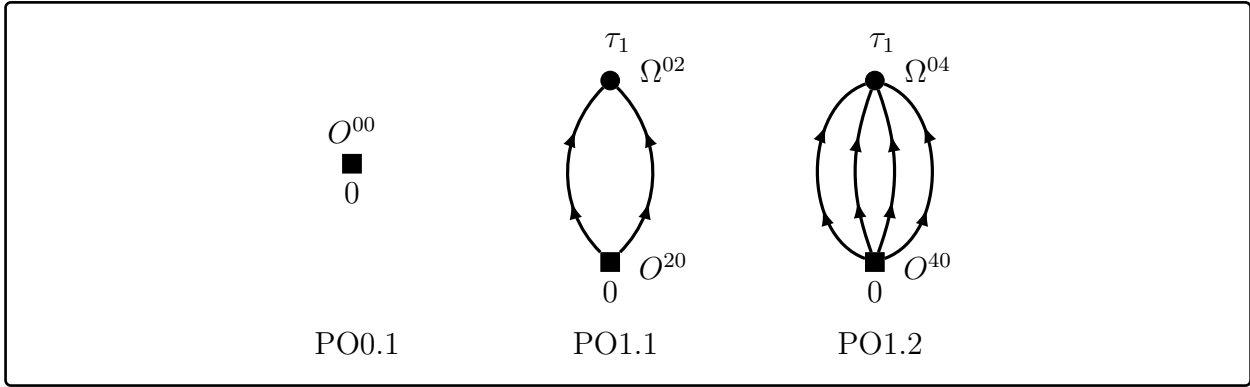


Figure 14.1: First- and second-order vacuum diagrams contributing to $o(\tau)$ in BMBPT.

By virtue of reduced operator kernels this yields

$$\mathcal{O}^{ij}(\tau) = o^{ij}(\tau) , \tag{14.97}$$

where we define

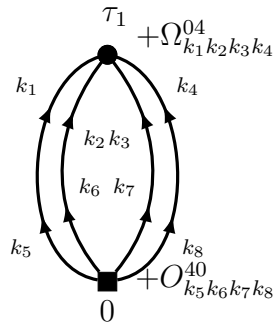
$$o^{ij}(\tau) \equiv \sum_{n=0}^{\infty} o^{ij(n)}(\tau) \tag{14.98}$$

sums up all vacuum diagrams which are *linked* to the bottom vertex corresponding to the operator of interest.

SECOND-ORDER DIAGRAMS

At second-order BMBPT there appear two non-vanishing linked diagrams which contribute to $o(\tau)$. Both involve the perturbation operator $\Omega_1(\tau_1)$ at time $\tau_1 > 0$ as well as the operator kernel $O(0)$ at fixed time $t = 0$.

Figure 14.1 displays the corresponding diagrams at first- and second-order BMBPT. In the following we will derive the contribution arising from the last diagram explicitly to show how to work with the diagrammatic formalism. The fully labeled diagram is given by



which contain eight single-particle summations. Since there are no crossing lines and the

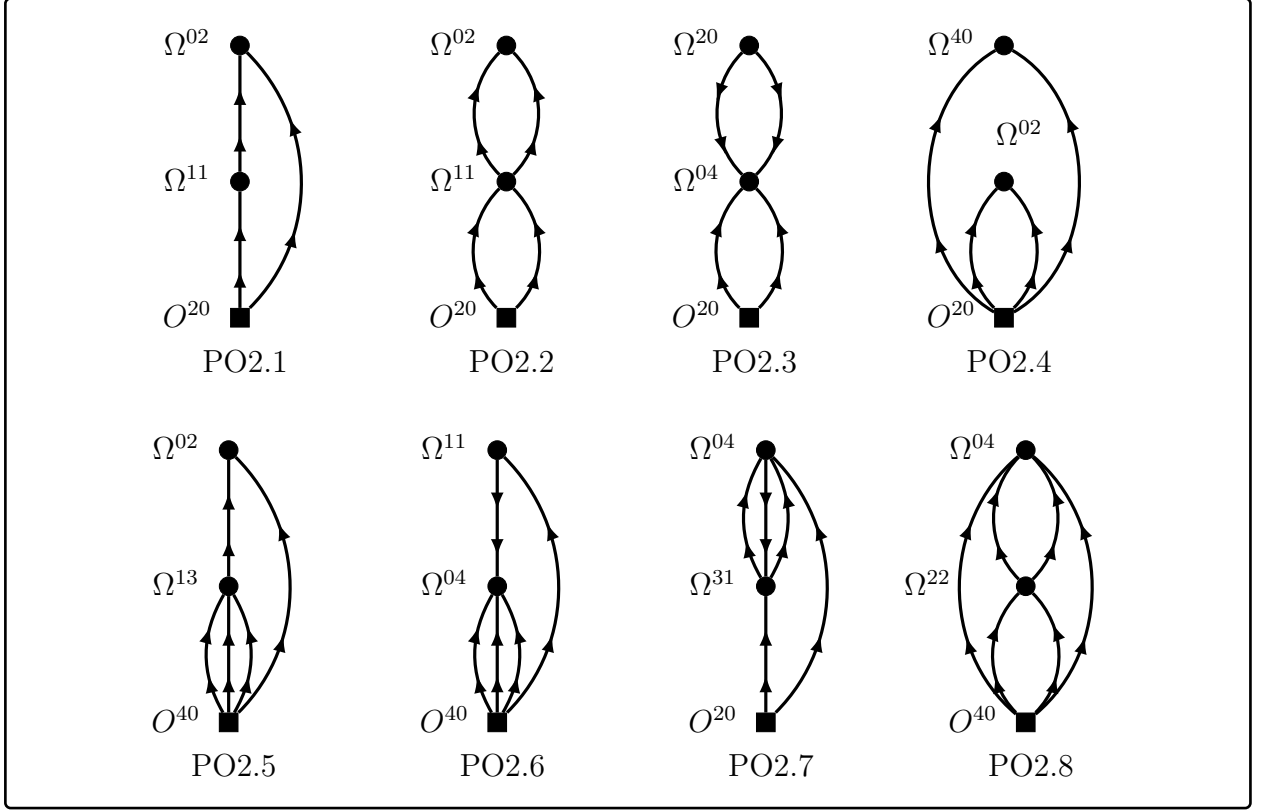


Figure 14.2: Third-order vacuum BMBPT diagrams of a generic operator \hat{O} . Single-particle and time labels are suppressed.

diagram contains exactly one vertex the phase is given by $(-1)^{p+n_c} = -1$. Further, there are four equivalent lines starting and ending at the same vertex. In particular since only one vertex carries a non-trivial time label the symmetry factor $n_s = 1$. The algebraic value is thus given by

$$\begin{aligned}
 \text{PO1.2} &= (-1)^1 \frac{1}{4!} \sum_{\substack{k_1 k_2 k_3 k_4 \\ k_5 k_6 k_7 k_8}} O_{k_1 k_2 k_3 k_4}^{40} \Omega_{k_5 k_6 k_7 k_8}^{04} \\
 &\quad \times \int_0^\tau d\tau_1 G_{k_5 k_1}^{-+(0)}(\tau_1, 0) G_{k_6 k_2}^{-+(0)}(\tau_1, 0) G_{k_7 k_3}^{-+(0)}(\tau_1, 0) G_{k_8 k_4}^{-+(0)}(\tau_1, 0) \\
 &= -\frac{1}{4!} \sum_{\substack{k_1 k_2 k_3 k_4 \\ k_5 k_6 k_7 k_8}} O_{k_1 k_2 k_3 k_4}^{40} \Omega_{k_5 k_6 k_7 k_8}^{04} \delta_{k_5 k_1} \delta_{k_6 k_2} \delta_{k_7 k_3} \delta_{k_8 k_4} \int_0^\tau d\tau_1 \theta(\tau_1) e^{-\tau_1 (E_{k_1} + E_{k_2} + E_{k_3} + E_{k_4})} \\
 &= -\frac{1}{4!} \sum_{k_1 k_2 k_3 k_4} \frac{O_{k_1 k_2 k_3 k_4}^{40} \Omega_{k_1 k_2 k_3 k_4}^{04}}{E_{k_1} + E_{k_2} + E_{k_3} + E_{k_4}} [1 - e^{-\tau (E_{k_1} + E_{k_2} + E_{k_3} + E_{k_4})}] , \tag{14.99}
 \end{aligned}$$

where we made use of the integral identities provided in appendix B. In the infinite-time limit the above expression is given by

$$\text{PO1.2} = -\frac{1}{4!} \sum_{k_1 k_2 k_3 k_4} \frac{O_{k_1 k_2 k_3 k_4}^{40} \Omega_{k_1 k_2 k_3 k_4}^{04}}{E_{k_1} + E_{k_2} + E_{k_3} + E_{k_4}}. \quad (14.100)$$

PROCEEDING TO HIGHER ORDERS

When proceeding to higher order in BMBPT the proliferation of diagrams makes a more systematic treatment of the diagrammatic approach desirable. The following algorithm safely generates all distinct BMBPT diagrams at order p :

Generation of BMBPT diagrams

1. All propagators starting from the lowest vertex corresponding to O must travel upwards, therefore only O^{20} and O^{40} need to be considered.
2. At perturbation order p restrict to the collection

$$\{O^{i_0 j_0}, \Omega^{i_1 j_1}, \dots, \Omega^{i_{p-1} j_{p-1}}\} \quad (14.101)$$

such that

$$\sum_{k=0}^{p-1} (i_k - j_k) = 0. \quad (14.102)$$

3. Draw all sets of propagators, starting from the bottom vertex corresponding to the operator O since propagators connecting the same vertices must propagate in the same direction.
4. Eliminate all topologically identical diagrams.

By applying the above set of rules at third order one gets the following set of eight topologically distinct third-order BMBPT diagrams, cf. Figure 14.2.

14.12 MONITORING SYMMETRY BREAKING

14.12.1 PARTICLE-NUMBER

Of particular importance in BMBPT or any other particle-number non-conserving approach is the monitoring of the expectation value of the particle number operator as well as its variance. In particular the BMBPT equation must be solved such that

$$\begin{aligned} \mathcal{A}(\infty) &= \lim_{\tau \rightarrow \infty} \frac{\langle \Psi(\tau) | \hat{A} | \Phi \rangle}{\langle \Psi(\tau) | \Phi \rangle} \\ &= a(\infty) \end{aligned}$$

$$= A_0, \quad (14.103)$$

with A_0 being the particle number of the target system and

$$a(\infty) \equiv \sum_{i+j=0,2} \sum_{n=0}^{\infty} a^{ij(n)}(\infty), \quad (14.104)$$

where $a^{ij(n)}(\infty)$ denotes the set of all vacuum BMBPT diagrams of order n which are linked to A^{ij} at fixed time $t = 0$.

We note that in an actual implementation this has to be done separately for both neutron number N and proton number Z . In the above discussion A serves as a placeholder for either of them. Typically, reference states are constructed from a prior solution of a mean field equation, e.g., a HFB solution. Even though the HFB reference has the correct particle number on average, this is no longer true for the correlated BMBPT state. In particular, the evaluation of perturbative corrections will have an impact on the average particle number of the perturbed state and the particle number expectation value of this state will in general not coincide with the particle number of the target nucleus. Therefore, the calculation of perturbative corrections to the particle number in BMBPT is an intrinsic feature and it is necessary to ensure correct particle number on average of the perturbed state.

PARTICLE-NUMBER VARIANCE

Beyond the average value of the particle number operator the particle number variance

$$\Delta A^2 \equiv a^2(\infty) - a(\infty)^2 \quad (14.105)$$

is of particular interest since it measures the dispersion of both protons and neutrons. In the above relation $a^2(\infty)$ is the infinite-time limit of the square of the particle-number operator, while $a(\infty)^2 \equiv (a(\infty))^2$ denotes the square of the infinite-time limit of the particle-number operator. Making use of second quantization the square of the particle-number operator is given by

$$\begin{aligned} A^2 &= \left(\sum_{pq} \delta_{pq} \hat{c}_p^\dagger \hat{c}_q \right) \left(\sum_{rs} \delta_{rs} \hat{c}_r^\dagger \hat{c}_s \right) \\ &= \sum_{pq} a_{pq}^{(1)} \hat{c}_p^\dagger \hat{c}_q + \frac{1}{2} \sum_{pqrs} a_{pqrs}^{(2)} \hat{c}_p^\dagger \hat{c}_q^\dagger \hat{c}_s \hat{c}_r. \end{aligned} \quad (14.106)$$

In second-quantized form A^2 consists of a one-body and a two-body part. Introducing fully anti-symmetrized matrix elements the two-body part of A^2 reads

$$\begin{aligned}
 \bar{a}_{pqrs}^{(2)} &\equiv a_{pqrs}^{(2)} - a_{pqsr}^{(2)} \\
 &= 2\delta_{pr}\delta_{qs} - 2\delta_{ps}\delta_{qr} \\
 &= 2(\delta_{pr}\delta_{qs} - \delta_{ps}\delta_{qr}) ,
 \end{aligned} \tag{14.107}$$

and concludingly

$$A^2 = \sum_{pq} a_{pq}^{(1)} \hat{c}_p^\dagger \hat{c}_q + \frac{1}{4} \sum_{pqrs} \bar{a}_{pqrs}^{(2)} \hat{c}_p^\dagger \hat{c}_q^\dagger \hat{c}_s \hat{c}_r . \tag{14.108}$$

The introduction of anti-symmetrized matrix elements enables for the use of formulas of transformations of quasiparticle matrix elements in Fock space in appendix C.

14.13 IMPLEMENTATION

In the following we will summarize the formalism outlined before and describe the algorithm that is necessary for its implementation. We assume that the reference state arises from a HFB calculation. However, the procedure outlined below can easily be generalized to arbitrary particle-number broken reference states.

Algorithm

1. Solve the HFB equations in a given single-particle basis

$$\begin{pmatrix} h & \Delta \\ -\Delta^* & -h^* \end{pmatrix} \begin{pmatrix} U_k \\ V_k \end{pmatrix} = E_k \begin{pmatrix} U_k \\ V_k \end{pmatrix}, \tag{14.109}$$

with quantities according to chapter 13. This yields a HFB vacuum $|\Phi\rangle$, the unperturbed grand potential $\hat{\Omega}_0$ and a set

$$\{U_k, V_k, E_k \geq 0\}. \tag{14.110}$$

A first guess of the Lagrange multiplier is given by

$$\langle \Phi | \hat{A} | \Phi \rangle = A^{00} \equiv A_{\text{aux}} \tag{14.111}$$

2. Calculate the matrix elements in quasiparticle space

$$\Omega_{k_1, \dots, k_{i+j}}^{ij}, A_{k_1, \dots, k_{i+j}}^{ij}, H_{k_1, \dots, k_{i+j}}^{ij}, A_{k_1, \dots, k_{i+j}}^{2ij} \tag{14.112}$$

3. Compute the observable of interest in the infinite-time limit by

$$\mathcal{O}(\infty) = o(\infty) \tag{14.113}$$

at order p according to

$$o^{(n)}(\infty) = \sum_{i,j=0,2,4} \sum_{l=0}^p o^{ij(l)}(\infty). \quad (14.114)$$

4. Compute the expectation value of the particle-number operator $a(\infty)$ such that

$$a(\infty) = A_0. \quad (14.115)$$

In the case $a(\infty) \neq A_0$ adjust the chemical potential λ and repeat from step 1.

5. When convergence is reached, compute the observables $\omega(\infty), a(\infty), a^2(\infty), h(\infty)$ as well as the particle-number variance

$$\Delta A^2 = a^2(\infty) - a(\infty)^2. \quad (14.116)$$

Application of the above algorithm gives correlated observables in BMBPT for genuine open-shell systems with the constraint that the average value of the particle number operator with respect to the perturbed wave function is equal to the particle number of the targeted nucleus.

A peculiarity arises when applying BMBPT at second order with respect to a HFB reference state. In this case—due to the one-body nature of the particle-number operator—the second-order correction to $a(\infty)$ vanishes and the expectation value of the particle-number operator is equal to A if the HFB equations were solved under this constraint. Therefore, the adjustment of particle number is not necessary. This is, however, a particular feature of the HFB reference state and does not hold for arbitrary symmetry-breaking vacua. Furthermore, at third-order, corrections to $a(\infty)$ arise also in the HFB scheme and the above outlined particle-number adaptation step becomes mandatory.

14.14 SPHERICAL SYMMETRY

The formalism presented above makes use of m -scheme quantities only. In actual applications for computational reasons we exploit spherical symmetry to reach model space convergence.

The reference state used in BMBPT arises from a HFB calculation using a spherical reference basis and in particular has good total angular momentum. In particular the Bogoliubov matrices $U_{k_1 k_2}$ and $V_{k_1 k_2}$ are diagonal with respect to isospin projection t , orbital-angular momentum l and total angular momentum j . Thus, there appear only non-vanishing matrix elements between states with different n quantum numbers within the same $(l j t)$ block. Additionally, all matrix elements are independent of m . Equally, the HFB quasiparticle energies E_k do not depend on m either.

For the formulation of spherical BMBPT it is, therefore, required to derive angular-momentum coupled quasiparticle matrix element for the different $\hat{\Omega}^{ij}$ operators. These expressions are derived in detail in appendix E.

15

Towards Correlated Energy Density Functional Kernels

The formulation of symmetry-broken MBPT introduces a novel framework to the pool of medium-mass *ab initio* methods. Even though the development of novel many-body approaches is interesting in its own right, many-body approaches rooted in symmetry-breaking and restoration offer additional potential beyond sole *ab initio* applications. The aim of this chapter is to give a brief introduction to nuclear energy density functional (EDF) theory and show a way how symmetry-broken (and restored) many-body methods can be used to constrain modern EDFs in a systematically improvable way. For a recent account of nuclear EDF theory see [Dug14].

The forthcoming discussion serves as motivation of why one further needs to investigate symmetry-broken MBPT. In particular, it serves as a guideline for the merging of *ab initio* nuclear structure with state-of-the-art EDF theory. For a detailed discussion with particular emphasis on the symmetry group $SU(2)$ see [Dug⁺15] and references therein.

15.1 BASIC ELEMENTS OF GROUP THEORY

In the discussion of the EDF formalism basic elements of group theory are required, which will be introduced in this section. For the interested reader we refer to Ref. [Geo99] for a discussion of symmetry groups in physics. A mathematically thorough introduction of Lie algebras can for example be found in the classic textbooks by Kac [Kac08] or Humphreys [Hum72].

Let G be an arbitrary symmetry group of the nuclear Hamiltonian \hat{H} , which is assumed to be parametrized by a set of r parameters α , i.e., $G = \{R(\alpha)\}$, where $\alpha \equiv \{\alpha_i \in D_i : i = 1, \dots, r\}$ is defined over a domain of definition

$$D_G \equiv \{D_i : i = 1, \dots, r\}. \quad (15.1)$$

This yields

$$[R(\alpha), H] = 0 \quad \text{for all } R(\alpha) \in G. \quad (15.2)$$

We further define the *invariant measure on G* as $dm(\alpha)$,

$$\text{Vol}(G) = \int_{D_G} dm(\alpha). \quad (15.3)$$

and introduce the set of *infinitesimal generators* $C \equiv \{C_i : i = 1, \dots, r\}$ which build the *Lie algebra associated to G* obtained by lifting the transformations $R(\alpha)$ via the *exponential map*.

The key elements are the IRREPS $S_{ab}^\lambda(\alpha)$ of the group, where the upper label corresponds to the eigenvalue of the *Casimir operator* $\hat{\Lambda}$. It can be shown that the following holds

$$\sum_c S_{ca}^{\lambda*}(\alpha') S_{cb}^\lambda(\alpha) = \sum_c S_{ac}^{\lambda*}(-\alpha') S_{cb}^\lambda(\alpha) = S_{ab}^\lambda(a - \alpha'). \quad (15.4)$$

Further, orthogonality of the IRREPS reads

$$\int_G dm(\alpha) S_{ab}^{\lambda*}(\alpha) S_{a'b'}^{\lambda'}(\alpha) = \frac{\text{Vol}(G)}{d_\lambda} \delta_{\lambda\lambda'} \delta_{aa'} \delta_{bb'}. \quad (15.5)$$

where d_λ denotes the dimension of the IRREP. A key property in the following analysis is that any function $f(\alpha)$ defined on the domain of the group D_G can be decomposed over the IRREPS,

$$f(\alpha) \equiv \sum_{\lambda ab} f_{ab}^\lambda S_{ab}^\lambda(\alpha), \quad (15.6)$$

where $\{f_{ab}^\lambda\}$ is the corresponding set of expansion coefficients.

Since the discussion of group properties is rather abstract, Tab. 15.1 gathers properties of the most prominent symmetry groups relevant in EDF theory, i.e., $U(1)$ for the case of breaking particle-number conservation, and $SU(2)$ for breaking angular-momentum conservation.

15.2 OFF-DIAGONAL KERNELS

The key ingredients of the nuclear EDF method are the *off-diagonal* norm $N(g'; g)$ and energy $H(g'; g)$ kernels,

G	α	$dm(\alpha)$	$\text{Vol}(G)$	$\hat{\Lambda}$	$S_{ab}^\lambda(\alpha)$	d_λ
$U(1)$	φ	$d\varphi$	2π	\hat{A}^2	$e^{im\varphi}$	1
$SU(2)$	α, β, γ	$\sin \beta d\alpha d\beta d\gamma$	$16\pi^2$	\hat{J}^2	$\mathcal{D}_{MK}^J(\Omega)$	$2J + 1$

Table 15.1: Overview of group properties of $U(1)$ and $SU(2)$. IRREPs of $SU(2)$ are given by the so-called Wigner functions $\mathcal{D}_{MK}^J(\Omega)$, where $\Omega \equiv (\alpha, \beta, \gamma) \in [0, 4\pi] \times [0, \pi] \times [0, 2\pi]$ parametrises the set of Euler angles.

G	$ g $	$\arg(g)$
$U(1)$	$ \kappa $	φ
$SU(2)$	$\rho_{\lambda\mu}$	α, β, γ

Table 15.2: Parameters appearing in symmetry breaking of $U(1)$ and $SU(2)$. Here $\rho_{\lambda\mu}$ corresponds to the multipole moments of the matter distribution.

$$N(g'; g) \equiv \langle \Phi(g') | \Phi(g) \rangle \quad (15.7)$$

where

$$|\Phi(g)\rangle = C \prod_{\mu} \beta_{\mu}^{(g)} |0\rangle \quad (15.8)$$

denotes a many-body state of Bogoliubov type, obtained from the single-particle basis via a unitary Bogoliubov transformation

$$\beta_{\mu}^{(g)} = \sum_k U_{k\mu}^{(g)*} \hat{c}_k + V_{k\mu}^{(g)*} \hat{c}_k^{\dagger}, \quad (15.9)$$

$$\beta_{\mu}^{(g)\dagger} = \sum_k V_{k\mu}^{(g)*} \hat{c}_k + U_{k\mu}^{(g)*} \hat{c}_k^{\dagger}, \quad (15.10)$$

with corresponding Bogoliubov matrices $U^{(g)}$ and $V^{(g)}$. The quantity $g \equiv |g|e^{i\alpha}$ labels a set of order parameters which characterizes the breaking of the underlying symmetry. Explicit correspondence for the case of $U(1)$ and $SU(2)$ is given in Tab. 15.2.

In general, the off-diagonal energy kernel

$$H(g'; g) \equiv h(g'; g)N(g'; g), \quad (15.11)$$

invokes a functional

$$h(g'; g) \equiv h(\rho^{g'g}, \kappa^{g'g}, \kappa^{g'g^*}), \quad (15.12)$$

of the off-diagonal normal and anomalous one-body densities defined by

$$\rho_{k_1 k_2}^{g'g} \equiv \frac{\langle \Phi(g') | \hat{c}_{k_2} \hat{c}_{k_1}^\dagger | \Phi(g) \rangle}{\langle \Phi(g') | \Phi(g) \rangle}, \quad (15.13)$$

$$\kappa_{k_1 k_2}^{g'g} \equiv \frac{\langle \Phi(g') | \hat{c}_{k_2} \hat{c}_{k_1} | \Phi(g) \rangle}{\langle \Phi(g') | \Phi(g) \rangle}, \quad (15.14)$$

$$\kappa_{k_1 k_2}^{g'g^*} \equiv \frac{\langle \Phi(g') | \hat{c}_{k_1}^\dagger \hat{c}_{k_2}^\dagger | \Phi(g) \rangle}{\langle \Phi(g') | \Phi(g) \rangle}. \quad (15.15)$$

15.3 EFFECTIVE-HAMILTONIAN KERNELS

Historically, one of the first routes for the definition of energy kernels made use of an *effective Hamiltonian*,

$$\hat{H}_{\text{eff}} \equiv \hat{T} + \hat{V}_{\text{eff}}^{[2]} + \hat{V}_{\text{eff}}^{[3]} \quad (15.16)$$

$$= \sum_{pq} t_{pq} \hat{c}_q^\dagger \hat{c}_q + \frac{1}{4} \sum_{pqrs} \bar{v}_{pqrs}^{\text{eff}} \hat{c}_p^\dagger \hat{c}_q^\dagger \hat{c}_s \hat{c}_r + \frac{1}{36} \sum_{pqrstu} \bar{v}_{pqrstu}^{\text{eff}} \hat{c}_p^\dagger \hat{c}_q^\dagger \hat{c}_r^\dagger \hat{c}_u \hat{c}_t \hat{c}_s \quad (15.17)$$

where t_{pq} denotes the one-body part of the kinetic energy and $\bar{v}_{pqrs}^{\text{eff}}$ and $\bar{v}_{pqrstu}^{\text{eff}}$ denote (anti-symmetric) two- and three-body matrix elements of suitably chosen effective potentials, respectively.

The off-diagonal operator kernel of \hat{H}_{eff} is then given by

$$h_{\text{eff}}(\Omega) \equiv \frac{\langle \Phi(0) | \hat{H}_{\text{eff}} | \Phi(\Omega) \rangle}{\langle \Phi(0) | \Phi(\Omega) \rangle}, \quad (15.18)$$

$$= \sum_{pq} t_{pq} \rho_{qp}^{0\Omega} + \frac{1}{2} \sum_{pqrs} \bar{v}_{pqrs}^{\text{eff}} \rho_{rp}^{0\Omega} \rho_{sq}^{0\Omega} + \frac{1}{6} \sum_{pqrstu} \bar{v}_{pqrstu}^{\text{eff}} \rho_{sp}^{0\Omega} \rho_{tq}^{0\Omega} \rho_{ur}^{0\Omega}, \quad (15.19)$$

which is obtained by evaluating contractions according to the generalized Wick theorem. Equation (15.19) constitutes nothing but the mean-field approximation of \hat{H}_{eff} . When using a energy kernel which is strictly based on an effective Hamiltonian, the Pauli principle is automatically implemented. However, over the last past decades it appeared that a strict effective-Hamiltonian-based description of energy kernels was too limiting in applications.

15.4 SINGLE-REFERENCE EDF

EDF calculations are implemented in two successive stages. In the first step, one makes use of the diagonal energy kernel only,

$$H(g; g) = h(g; g), \quad (15.20)$$

which involves only one symmetry-breaking state, leading to the name *single-reference EDF method*. For a targeted value of $|g|$ the SR energy $E_{\text{SR}}^{|g|}$ is obtained through the minimization

$$E_{\text{SR}}^{|g|} \equiv \min_{\{|\Phi^{(g)}\rangle\}} \mathcal{E}_{|g|} \quad (15.21)$$

with

$$\mathcal{E}_{|g|} \equiv h(g; g) - \lambda(A - \langle \Phi^{(g)} | \hat{A} | \Phi^{(g)} \rangle) - \lambda_{|g|}(|g| - \langle \Phi^{(g)} | \hat{G} | \Phi^{(g)} \rangle) \quad (15.22)$$

where the operator \hat{G} characterizes the order parameter. The SR energy landscape is then generated via repeated solution of (15.21) for several target values of $|g|$.

Equation (15.21) leads to solving a constrained Bogoliubov eigenvalue problem,

$$\begin{pmatrix} h - \lambda 1 & \Delta \\ -\Delta^* & -h^* + \lambda 1 \end{pmatrix}^{(g)} \begin{pmatrix} U \\ V \end{pmatrix}_{\mu}^{(g)} = E_{\mu}^{(g)} \begin{pmatrix} U \\ V \end{pmatrix}_{\mu}^{(g)}, \quad (15.23)$$

where the one-body fields are given by functional derivatives with respect to the normal and anomalous one-body densities, respectively,

$$h^{(g)} - \lambda 1 \equiv \frac{\delta \mathcal{E}_{|g|}}{\delta \rho^{gg^*}} \quad (15.24)$$

$$\Delta^{(g)} \equiv \frac{\delta \mathcal{E}_{|g|}}{\delta \kappa^{gg^*}} \quad (15.25)$$

It is important to note that the above SR energy does not depend on the angle α of g which indicates the existence of a pseudo-Goldstone mode. In particular the value of the norm and energy kernels are independent under simultaneous rotation of bra and ket states about the same angle and direction. Therefore, off-diagonal kernels may only depend on the difference of the angles of bra and ket states,

$$N(|g'|, \alpha'; |g|, \alpha) = N(|g'|, 0; |g|, \alpha' - \alpha) \quad (15.26)$$

and analogously

$$h(|g'|, \alpha'; |g|, \alpha) = h(|g'|, 0; |g|, \alpha' - \alpha). \quad (15.27)$$

15.5 MULTI-REFERENCE EDF

In any finite quantum system, good symmetries must be restored and the symmetry breaking becomes fictitious. The symmetry-broken state, corresponding to the diagonal energy kernel, is a mixture of several IRREPs of the broken symmetry group and consequently E_{SR} is contaminated as well. A symmetry-restoration step is ultimately needed to obtain a binding energy that is in one-to-one-correspondence to a single IRREP of the symmetry group.

First we rewrite the kernels with respect to their Fourier expansion,

$$N(|g'|, 0; |g|, \alpha) \equiv \sum_{ab\lambda} \mathcal{N}_{ab}^\lambda(|g'|, |g|) S_{ab}^\lambda(\alpha) \quad (15.28)$$

as well as

$$E(|g'|, 0; |g|, \alpha) N(|g'|, 0; |g|, \alpha) \equiv \sum_{\lambda ab} \mathcal{E}_{ab}^\lambda(|g'|, |g|) \mathcal{N}_{ab}^\lambda(|g'|, |g|) S_{ab}^\lambda(\alpha). \quad (15.29)$$

The particle-number restored kernels are then extracted via

$$\mathcal{N}_{ab}^\lambda(|g'|; |g|) = \frac{d_\lambda}{\text{Vol}(G)} \int_{D_G} dm(\alpha) S_{ab}^{\lambda*}(\alpha) N(|g'|, 0; |g|, \alpha) \quad (15.30)$$

and

$$\mathcal{E}_{ab}^\lambda(|g'|; |g|) \mathcal{N}_{ab}^\lambda(|g'|, |g|) = \frac{d_\lambda}{\text{Vol}(G)} \int_{D_G} dm(\alpha) S_{ab}^{\lambda*}(\alpha) E(|g'|, 0; |g|, \alpha) N(|g'|, 0; |g|, \alpha), \quad (15.31)$$

thus relating the particle-number restored kernels with the particle-number broken ones. For the particular case of $\alpha = 0$ we obtain with $S_{ab}^\lambda(0) = \delta_{ab}$

$$N(|g'|, 0; |g|, 0) = \sum_{\lambda a} \mathcal{N}_{aa}^\lambda(|g'|; |g|), \quad (15.32)$$

$$E(|g'|, 0; |g|, 0) N(|g'|, 0; |g|, 0) = \sum_{\lambda a} \mathcal{E}_{aa}^\lambda(|g'|; |g|) \mathcal{N}_{aa}^\lambda(|g'|; |g|), \quad (15.33)$$

and further specifying $|g'| = |g|$ yields the sum rules

$$1 = \sum_{\lambda} d_\lambda \mathcal{N}^\lambda(|g|; |g|), \quad (15.34)$$

$$E_{\text{SR}}^{|g|} = \sum_{\lambda} d_\lambda \mathcal{E}^\lambda(|g|; |g|) \mathcal{N}^\lambda(|g|; |g|). \quad (15.35)$$

which relates the SR energy to the entire set of symmetry-number restored energies \mathcal{E}_{ab}^λ .

Starting from the symmetry-restored kernel one then obtains the *multi-reference EDF*

energy by performing a minimization according to

$$E_{\lambda k}^{\text{MR}} = \min_{f_{|g|a}^{\lambda k}} \frac{\sum_{|g'|,|g|} \sum_{ab} f_{|g'|a}^{\lambda k*} f_{|g|b}^{\lambda k} \mathcal{E}_{ab}^{\lambda}(|g'|, |g|) \mathcal{N}_{ab}^{\lambda}(|g'|, |g|)}{\sum_{|g'|,|g|} \sum_{ab} f_{|g'|a}^{\lambda k*} f_{|g|b}^{\lambda k} \mathcal{N}_{ab}^{\lambda}(|g'|, |g|)}. \quad (15.36)$$

In actual applications the set of mixing coefficients $\{f_{|g|b}^{\lambda k}\}$ is determined by solving the *Hill-Wheeler equation of motion* [HW53],

$$\sum_{|g|b} \mathcal{E}_{ab}^{\lambda}(|g'|, |g|) \mathcal{N}_{ab}^{\lambda}(|g'|, |g|) f_{|g|b}^{\lambda k} = E_{\lambda k}^{\text{MR}} \sum_{|g|b} \mathcal{N}_{ab}^{\lambda}(|g'|, |g|) f_{|g|b}^{\lambda k}, \quad (15.37)$$

which constitutes an eigenvalue problem expressed in a non-orthogonal basis.

15.6 PATHOLOGIES IN MR APPLICATIONS

In current applications, the above MR-EDF formalism is limited to even-even nuclei, where proton and neutron numbers and angular momentum of axially deformed Bogoliubov states are restored simultaneously. Furthermore, the mixing is performed over several shapes of the quadrupole deformation. Even though the capabilities of modern MR-EDF codes are remarkable in accessing nuclear observables to very high accuracy [Ben08; Rod10; Yao10], the EDF framework is not completely free from pathologies as will be discussed below.

Recent investigations identified a number of divergences in potential energy surfaces, e.g., in the context of proton-number-restored energy kernels for different Skyrme parametrizations. It was later analyzed that such pathological behavior is due to non-analyticities of the off-diagonal energy kernel [Dob+07; BDL09; LDB09]. In particular, it was shown that the violation of the Pauli principle leads to self-interaction processes causing anomalous behaviour of the shape of potential energy surfaces. These pathologies can—in principle—be avoided when working with a strict effective-Hamiltonian-based description.

Such spuriousities become even more interesting in the discussion of particle-number restoration. For the case of $U(1)$ restoration the sum rule (15.34) becomes

$$1 = \sum_{A \in \mathbb{Z}} \mathcal{N}^A(|\kappa'|, |\kappa|). \quad (15.38)$$

Contributions from $A \leq 0$ strictly vanish when working with a effective-potential energy kernel. However, for arbitrary energy kernel one gets

$$\mathcal{N}^A \mathcal{E}^A \neq 0 \quad \text{for } A \leq 0. \quad (15.39)$$

Figure 15.1 illustrates the appearance of such pathologies for the proton-number restoration of ^{18}O . Obviously, the particle-number restored energies have contributions from systems

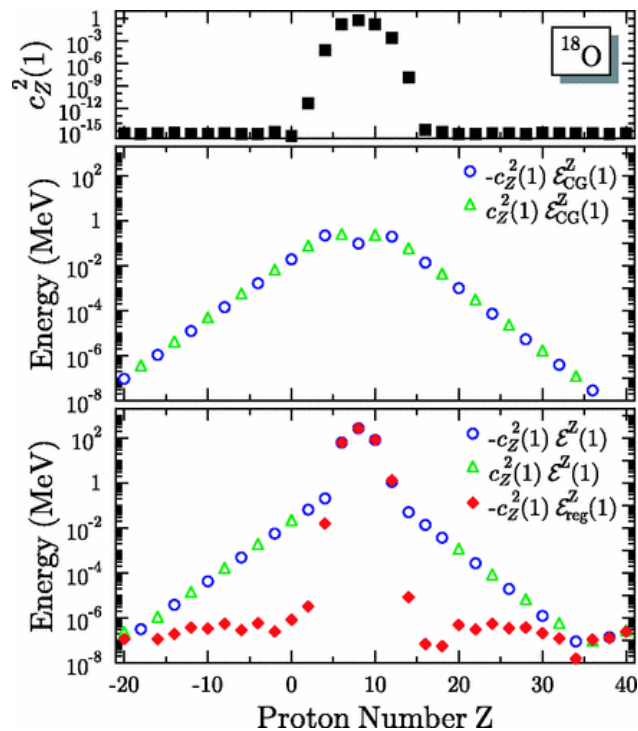


Figure 15.1: Proton-number restored kernels as a function of Z . The top panel corresponds to the norm kernel \mathcal{N}^Z and the middle panel corresponds to spurious contributions from the energy kernel. The lower panel shows $\mathcal{N}^Z \mathcal{E}^Z$ as well as regularized $\mathcal{N}^Z \mathcal{E}^Z$ proton-number-restored energy kernels. In none of the calculations neutron number was restored. The picture is taken from [BDL09].

with negative particle number which spreads up to values $Z = -20$. While the range of summations in the particle-number restored kernels runs a priori over all integers, physically allowed states must be restricted to positive proton number. However, there is no guarantee for this for an arbitrary EDF parametrization. In particular none of the currently applied Skyrme or Gogny parametrizations in modern EDF theory are *strictly* derived from an effective Hamiltonian.

The current status in the field is that a sound MR-EDF formalism requires the usage of energy kernels which derive from effective Hamiltonian thus circumventing unwanted pathologies due to self-interaction processes from the very beginning by enforcing the Pauli principle.

15.7 EDF KERNELS FROM *ab initio* THEORY

Recent applications indicate that the restriction to (uncorrelated) mean-field kernels are incapable of providing a qualitatively correct description of nuclear observables, independently of the particular form of \hat{H}_{eff} . A recently applied strategy to circumvent this problem is the inclusion of higher-order many-body terms to \hat{H}_{eff} in term of non-integer powers of the one-body densities for the description of off-diagonal operator kernels [Agr06]. While (15.19)

contains linear, bilinear and trilinear terms the inclusion of fractional powers of the off-diagonal densities offers a potential way of simulating missing correlation effects. However, it is not at all clear how to proceed with this systematically.

It is highly desirable to have an approach which is capable of *systematically* encoding missing correlations beyond the mean-field in a *controlled* way. This requires a fully consistent expansion technique of off-diagonal operator kernels.

Even though modern nuclear MR-EDF calculations provide highly accurate observables, they still lack predictive power when proceeding to the experimentally unknown region. Therefore, one aims to complement the design of modern EDF parametrizations by so-called non-empirical kernels which possess a direct link to the underlying nuclear Hamiltonian. There are two separate ways to achieve this:

1. Use *ab-initio* tools to generate pseudo data for experimentally unknown nuclei to validate EDF extrapolations and constrain parameters entering the functional form of nuclear EDF kernels.
2. Use expansion methods for the Schrödinger equation to serve as guidance for parametrizations of EDF kernels.

The first approach does not (yet) pose a viable alternative since the maturity of state-of-the-art many-body methods is not high enough to put strong restrictions on the parametrizations of EDF kernels. Furthermore, no restriction on the functional form of the EDF kernel at play is gained through the use of such pseudo data.

The second approach on the other hand yields the possibility of guessing the *functional form* from the nuclear interaction and not just the value of the coupling parameters. It was argued, that the mean-field form of (15.19) is too restrictive to grasp complex correlation effects. Performing a systematic expansion of off-diagonal operator kernels is expected to resolve the pathologies of modern MR-EDF calculations [Dug⁺15]. However, a key feature is the fact that the expansion method at play must rely on the same underlying concepts, i.e. the spontaneous breaking and restoration of symmetries.

While we extensively discussed the formulation symmetry-broken MBPT, i.e., MBPT for diagonal operator kernels, the next step requires the development and implementation of the symmetry-restoration step which corresponds to MBPT for off-diagonal operator kernels. This is not only mandatory to yield a full-fledged symmetry-restored many-body approach but also is highly beneficial in constraining state-of-the-art EDF kernels. Instead of performing symmetry-restored MBPT with a chiral *ab initio* Hamiltonian, we take an effective Hamiltonian \hat{H}_{eff} as input for the calculation. In a first step the calculation of second-order off-diagonal energy kernels yields new insights into correlations in modern EDF effective potentials and enriches the correlation content of off-diagonal operator kernels in a systematic way.

We note that in principle other many-body approaches can be considered as well. However, it is required that the many-body formalism under consideration is based on the *same principles* as EDF, namely the breaking and restoration of symmetries. Due to the mild scaling behaviour low-order MBPT is highly favorable. In particular since ultimately one wants to break several symmetries at a time. Going beyond second-order MBPT in a non-spherical scheme for heavy nuclei is expected to require intractable computational resources, in particular with a full inclusion of three-body forces.

16

Medium-Mass Semi-Magic Isotopic Chains

In the following we will apply second-order BMBPT to the calculation of ground-state energies of even-even nuclei of medium-mass isotopic chains. We use three different chiral interactions, NN_{500}^4 , $\text{NN}_{500}^4 + 3\text{N}_{400}^3$ and N2LO_{sat} as introduced in chapter 2. Three-body interactions are included via using the Hamiltonian in NO2B approximation. Furthermore, in all calculations the kinetic-energy operator is incorporated in its one- plus two-body form as introduced in chapter 13. For validating our results, we compare to recent MR-IM-SRG calculation using the same chiral interaction [Her14]. We particularly include a NN-only interactions, to benchmark the effect of the NO2B approximation, since in particle-number-broken approaches there are no systematic studies on the effect of neglecting the residual three-body part of the Hamiltonian. However, it is clear from the beginning that a NN-only interaction will suffer from systematic overbinding.

We focus on two-neutron separation energies defined via

$$S_{2n}(A) \equiv E_{\text{gs}}(A-1) - E_{\text{gs}}(A), \quad (16.1)$$

where $E_{\text{gs}}(A)$ denotes the ground-state energy of the A -body system. This allows for a investigation of shell-closure effects.

All of the following calculations are performed for semi-magic nuclei, i.e., we investigate isotopic chains which possess a proton shell closure. Therefore, the particle-number variance actually coincides with the neutron-number variance.

16.1 OXYGEN ISOTOPES

We start with the discussion of oxygen isotopes starting from the doubly-magic ^{16}O up to ^{26}O . Figure 16.1 shows the binding energy per nucleon, the particle-number variance and

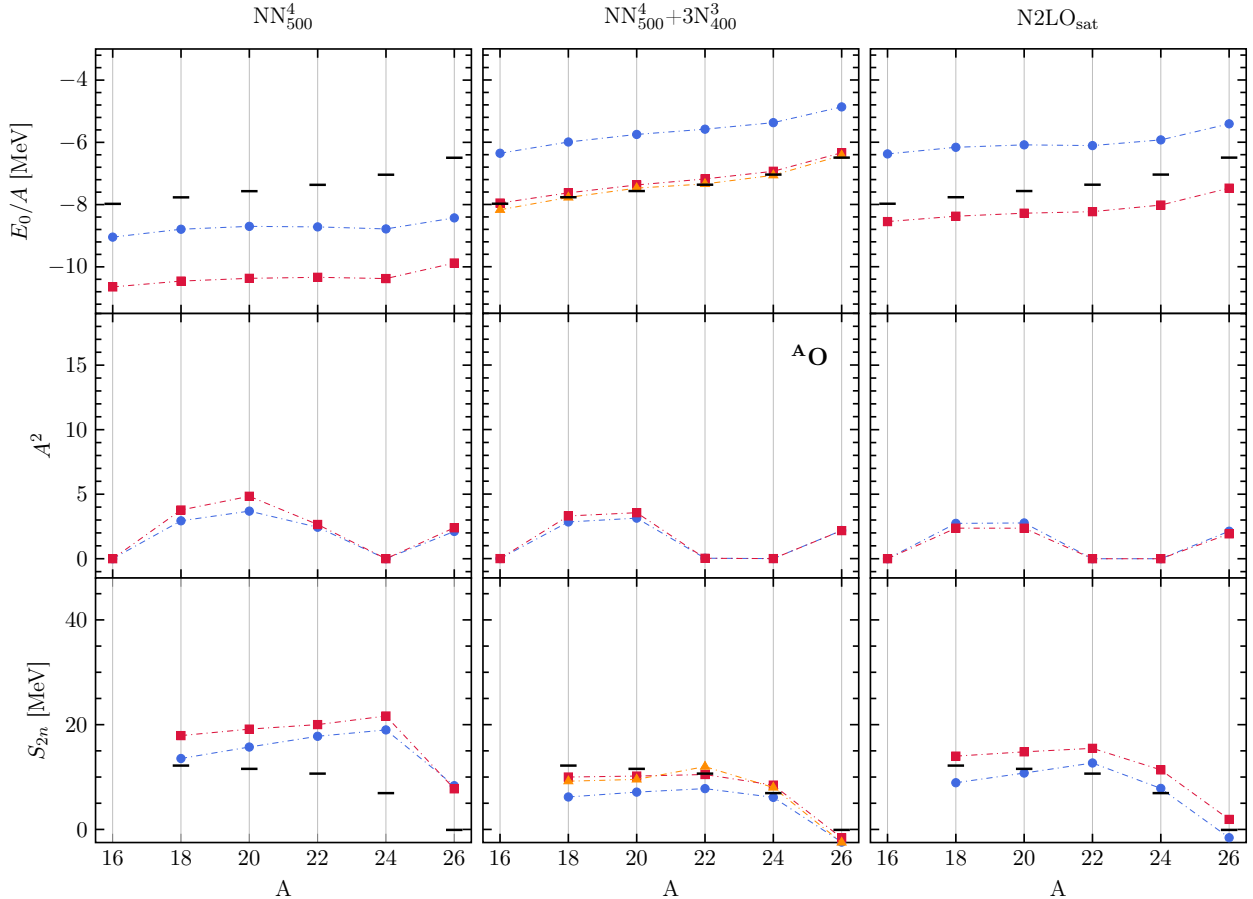


Figure 16.1: Ground-state energy per particle, particle-number variance and two-neutron separation energies for HFB (●) and second-order BMBPT (■) for oxygen isotopic chain using different chiral interactions. Binding energies obtained from MR-IMSRG (▲) are included for the $\text{NN}_{500}^4+3\text{N}_{400}^3$ interaction. Calculations were performed for $e_{\text{max}} = 12$, $\hbar\Omega = 20$ MeV and $\alpha = 0.08$ fm⁴. Experimental values are indicated by black bars [Wan⁺12].

two-neutron separation energies for three different interactions. The different plotmarkers correspond to the mean-field HFB results (●) and BMBPT(2) partial sums (■).

From the top panel we recognize strong overbinding when restricting to two-body interactions only. When including three-body interactions the binding energy becomes reduced to a value of 7 – 8 MeV per nucleon in the oxygen chain. Interestingly, the correlation energy per nucleon, i.e., the size of the second-order correction per nucleon is roughly the same for all interactions namely 1.5 – 2 MeV per nucleon. For oxygen isotopes the N2LO_{sat} interaction yields larger absolute values for the second-order correction compared to the $\text{NN}_{500}^4+3\text{N}_{400}^3$ interaction. As already indicated the monitoring of the breaking of symmetry is key in BMBPT, therefore, the evaluation of the second-order particle-number variance becomes mandatory. We see that the HFB particle-number variance is very close to the second-order partial sum. For the case of NN-only and $\text{NN}_{500}^4+3\text{N}_{400}^3$ interactions the correction to the particle-number variance is positive such that the second-order partial sum is larger than the mean-field value. Therefore, the correlated second-order states have a

particle-number distribution, which is more smeared out than the one from HFB, while still possessing the same mean-value. This behavior changes when using the $N2LO_{\text{sat}}$ interaction, where the particle-number-variance corrections become negative thus yielding a more narrow particle-number distribution. However, this effect is quite small and the dispersion is still of the order of three units. Further, note that the particle-number variance vanishes for closed-shell systems, since BMBPT reduces to (symmetry-conserving) HF-MBPT for these systems.

By means of the ground-state binding energies we obtain two-neutron separation energies for both HFB and second-order BMBPT. One can see a clear gap when going from ^{24}O to ^{26}O indicating the shell closure for the doubly-magic nucleus ^{24}O . Furthermore, the two-neutron separation energy is negative for ^{26}O indicating the neutron dripline.

For these medium-light isotopic chains BMBPT ground-state energies are in good agreement with experimental value when including a three-body interaction.

Furthermore, we note the very good agreement of second-order BMBPT ground-state energies with results obtained from MR-IM-SRG.

16.2 CALCIUM ISOTOPES

The calcium chain is an ideal candidate for proceeding to the heavy-mass regime. Again the use of a NN-only interaction displays the strong overbinding with ground-state energies of up to 16 MeV per nucleon. Contrarily, $NN_{500}^4 + 3N_{400}^3$ and $N2LO_{\text{sat}}$ interaction produce saturated binding energies of approximately 9 MeV per nucleon at second-order BMBPT. As in the case of oxygen isotopes, the second-order correction is larger for the $N2LO_{\text{sat}}$ interaction. However, the second-order partial sum for both three-body interactions is approximately the same, but the HFB energy is lower for the $NN_{500}^4 + 3N_{400}^3$ interaction. For both interactions the minimal value for the second-order corrections is taken at ^{48}Ca , i.e., for a closed-shell systems. For the $NN_{500}^4 + 3N_{400}^3$ interaction comparison to recent MR-IMSRG calculations reveals very good agreement of the ground-state energy with deviations of less than one percent.

The particle-number variance tends to show pathological behavior for all three interactions. While for closed-shell systems the particle-number-variance correction trivially vanishes, it exhibits quite large contributions for $^{42-46}\text{Ca}$, in particular for a NN-only interaction, such that in BMBPT the correlated states are extremely smeared out. Similar tendencies also occur when including three-body effects.

From looking at the bottom row of Figure 16.2 two-neutron separation energies clearly indicate shell closures at both HFB level and for correlated BMBPT and MR-IMSRG binding energies. In particular shell closures for ^{40}Ca and ^{48}Ca are well reproduced. Additionally, a larger step appears from the transition from ^{50}Ca to ^{52}Ca .

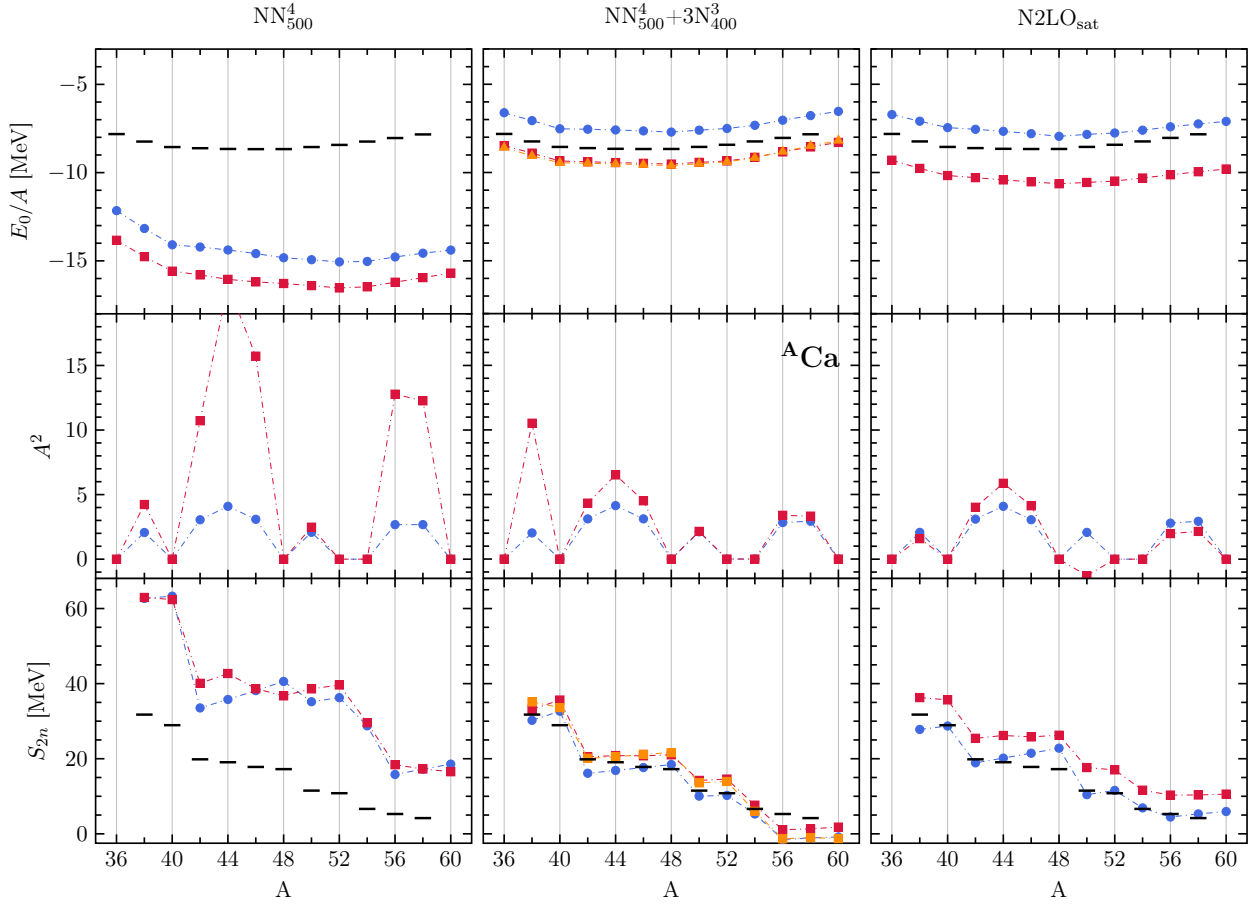


Figure 16.2: Ground-state energy per particle, particle-number variance and two-neutron separation energies for HFB (●) and second-order BMBPT (■) for calcium isotopic chain using different chiral interactions. Binding energies obtained from MR-IMSRG (▲) are included for the $\text{NN}_{500}^4 + 3\text{N}_{400}^3$ interaction. Calculations were performed for $e_{\text{max}} = 12$, $\hbar\Omega = 20$ MeV and $\alpha = 0.08$ fm⁴. Experimental values are indicated by black bars [Wan⁺12].

16.3 NICKEL ISOTOPES

Figure 16.3 reveals the same systematic overbinding of the NN-only interaction which is cured by including induced three-body forces. Again, for the $\text{NN}_{500}^4 + 3\text{N}_{400}^3$ interaction comparison with MR-IMSRG shows excellent agreement of ground-state energies. From looking at second-order energies for the N2LO_{sat} interaction we see slight dips for ⁵⁰Ni and ⁷⁴Ni, where the second-order corrections are larger compared to neighboring systems. This effect is not present at the HFB level.

The particle-number variance corrections reveal similar behavior as in calcium isotopes, i.e., while the HFB wave function admits moderate particle-number dispersion, the correlated BMBPT ground-state has much larger particle-number variance—⁷⁴Ni being the most extreme case for all three interactions.

Two-neutron separation energies indicate shell closure effects for the $\text{NN}_{500}^4 + 3\text{N}_{400}^3$ interaction at ^{56,68,78}Ni and an additional step from ^{60–64}Ni. In the case of NN-only and N2LO_{sat}

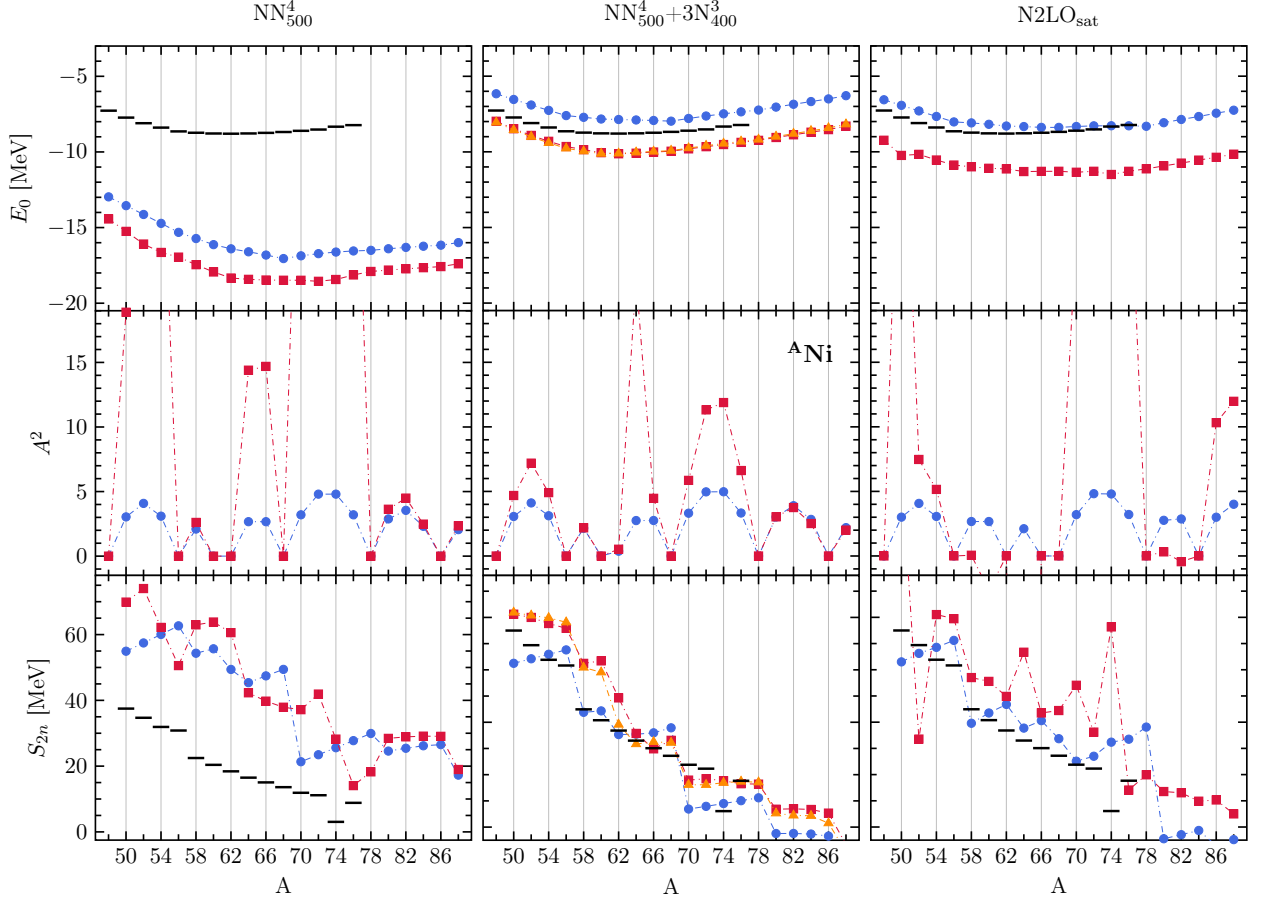


Figure 16.3: Ground-state energy per particle, particle-number variance and two-neutron separation energies for HFB (●) and second-order BMBPT (■) for nickel isotopic chain using different chiral interactions. Binding energies obtained from MR-IMSRG (▲) are included for the $\text{NN}_{500}^4 + 3\text{N}_{400}^3$ interaction. Calculations were performed for $e_{\text{max}} = 12$, $\hbar\Omega = 20$ MeV and $\alpha = 0.08$ fm⁴. Experimental values are indicated by black bars [Wan⁺12].

interactions, no clear conclusion about shell closures can be drawn. For the N2LO_{sat} interaction HFB ground-state energies suggest shell closures at $^{56,78}\text{Ni}$. However, the BMBPT calculations do not support this statement, which might be due to the simple HFB vacuum or missing symmetry restoration step.

Again we note that, both, absolute binding energies as well as two-neutron separation energies are in very good agreement to MR-IM-SRG calculations.

16.4 TIN ISOTOPES

Tin isotopes are typically beyond the range of applicability of an accurate *ab initio* description because the interaction—fitted to the two- and three-body sector—is not accurate enough. *A priori* one might expect that this can be overcome by going to higher order in the chiral perturbation expansion. Additionally, in heavy systems it is more challenging reaching model-space convergence with respect to the $E_{3\text{max}}$ truncation of the three-body

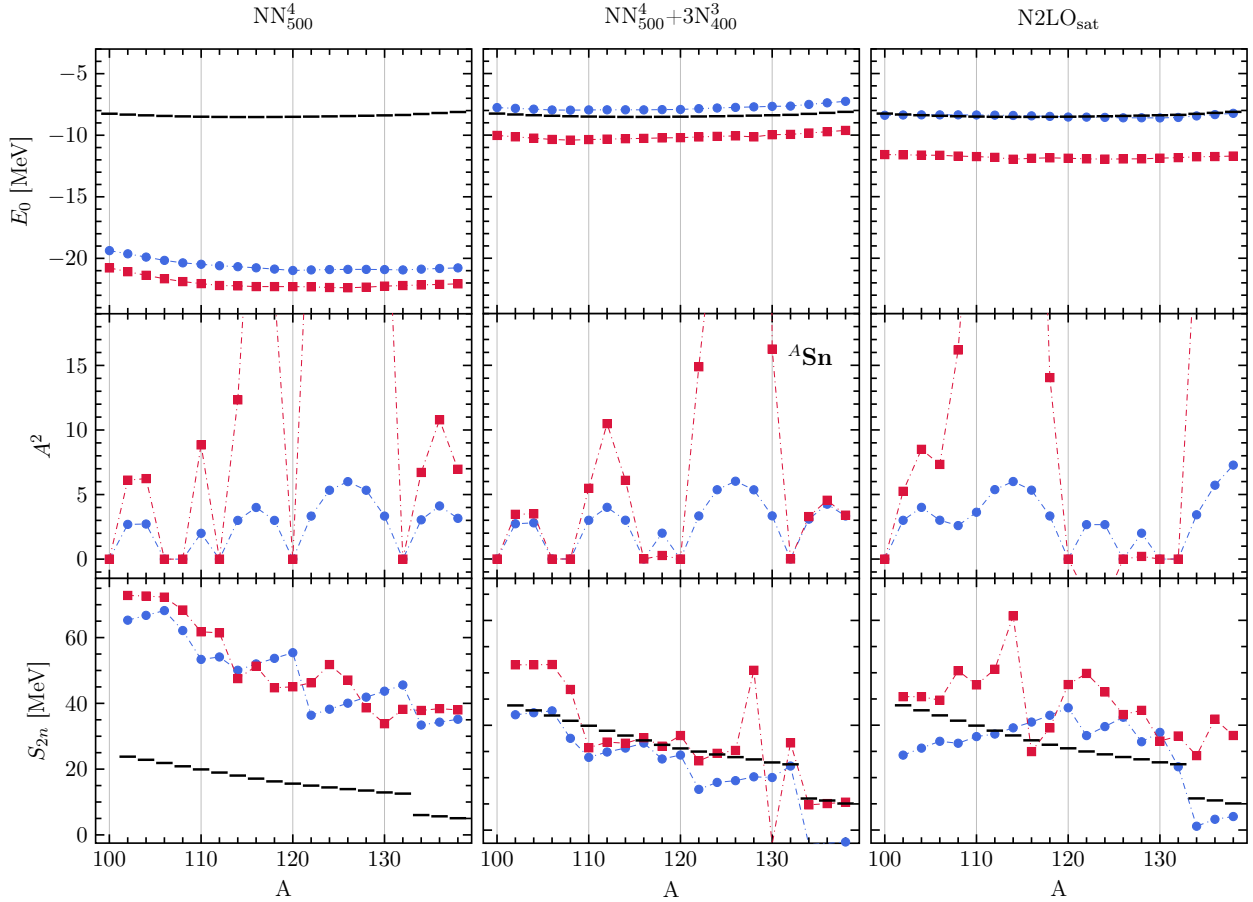


Figure 16.4: Ground-state energy per particle, particle-number variance and two-neutron separation energies for HFB (●) and second-order BMBPT (■) for tin isotopic chain using different chiral interactions. Calculations were performed for $e_{\max} = 12$, $\hbar\Omega = 20$ MeV and $\alpha = 0.08$ fm⁴. Experimental values are indicated by black bars [Wan⁺12].

matrix elements.

From the upper left plot of Figure 16.4 we see the strong overbinding of the NN forces, which contradicts the experimentally observed ground-state energies. This overbinding can be resolved when including three-body effects, either with the $NN_{500}^4 + 3N_{400}^3$ or $N2LO_{\text{sat}}$ Hamiltonian.

Investigation of particle-number variance reveals similar conclusions as in the other isotopic chains. While the particle-number dispersion is comparably small at the mean-field level the second-order corrections can be quite large. Particular examples are ^{118,124,126}Sn. However, for the NN-only and $NN_{500}^4 + 3N_{400}^3$ interaction, the second-order correction for the particle-number variance vanishes in agreement with the collapse of the HFB theory to HF theory, without any symmetry breaking. This behavior is not reproduced for the $N2LO_{\text{sat}}$ Hamiltonian. Many shell closures are not reproduced on the HFB level, e.g., ^{106,108}Sn. Such deficiencies of an interaction can have several reasons. First, note that the $N2LO_{\text{sat}}$ interaction was fitted to A -body observables to give a better reproduction of binding properties of

medium-mass systems, which can have negative effects on the performance of this interaction in a regime far away from the one it is initially fitted to. We further note that deformation effects play a more important role than in lighter systems. Those are not accounted for in using a spherical BMBPT framework but require using, e.g., an axially deformed single-particle basis with additional angular-momentum projection.

Two-neutron separation energies leave no clear sign for shell closures, even though for mass numbers $A = 108$ a significant drop appears for the NN-only interaction and the $NN_{500}^4 + 3N_{400}^3$ interaction at both HFB and BMBPT level. While the HFB calculations also support shell closures for $^{120,132}\text{Sn}$, this is not clear from the BMBPT energies. In particular, this might be due to large particle-number-variance corrections for neighboring systems that smear out the drop in the two-neutron separation energies.

In general the results obtained for tin isotopes using the $N2LO_{\text{sat}}$ interaction serve as a indication of severe pathologies one may encounter when using chiral interactions in the heavy-mass regime.

16.5 PAIRING PROPERTIES

There appeared several cases where particle-number-variance corrections were comparably large to other systems in the same isotopic chain. Closer investigation showed, that for these nuclei quasiparticle energies—obtained from the HFB calculation—were very small. While for most nuclei the lowest quasiparticle energies were of the order 1–2 MeV, systems exhibiting pathological large particle-number-variance corrections revealed quasiparticle energies of the order 10^{-2} MeV. Since quasiparticle energies enter BMBPT energy denominators, such small quasiparticle energies can cause singularities in the perturbation expansion. However, the second-order energy correction seems to be more stable. A possible explanation is that the denominator in the formula of the energy correction contains four quasiparticle energies, whereas the one for the particle-number-variance contains only two quasiparticle energies. Therefore, the particle-number variance might be more susceptible to small quasiparticle energies.

A general conclusion might be that the investigated chiral interactions tend to exhibit low pairing. However, this needs to be validated in a more complete benchmark with additional variations of parameter of the interaction and the reference basis. Additionally, the use of other particle-number-broken vacua might overcome this problem.

16.6 COMPUTATIONAL SCALING

Finally, we discuss computational characteristics of second-order BMBPT. The most important feature is the fact that the runtime of a second-order calculation is independent of the target nucleus. More precisely, the combined evaluation of the the second-order energy and

variance correction requires 20-30 CPU hours for all cases discussed here. Due to working in quasiparticle basis, the scaling is independent of the mass number, which is different for frameworks that make use of a particle-hole formalism. Therefore, the framework presented here can easily be extended to even higher masses. We note, however, that both uncertainties in the chiral Hamiltonian and the demands of reaching model-space convergence prohibit the application of BMBPT to heavier systems in a controlled way.

In particular the mild scaling is a desirable feature, particularly in the context of merging *ab initio* and EDF technology as outlined in chapter 15.

Summary and Outlook

Ab initio nuclear structure theory has made great progress in the description of nuclear observables in recent years. By using chiral interactions with a sound link to QCD one is able to accurately reproduce experimental quantities up to high accuracy in the medium-light systems using large-scale diagonalization techniques like NCSM with a full inclusion of chiral three-body forces. The strong computational scaling prohibits the use of such techniques in heavier systems. The goal of this thesis was to develop novel and innovative versions of many-body perturbation theory, which are applicable to genuine open-shell medium-mass nuclei.

SINGLE-CONFIGURATIONAL MANY-BODY PERTURBATION THEORY

We present three different flavours of MBPT that are applicable to different kinds of nucleonic systems. In the simplest version MBPT is performed on top of a single Slater determinant. Such techniques have been known for a long time and by now became a standard tool for the description of closed-shell nuclei. However, such a single-configurational theory is only viable if the exact ground state is expected to be dominated by a single determinant. Therefore, it does not directly extend to the description of truly open-shell systems. In applications to light closed-shell systems, we compared the sensitivity of the order-by-order convergence behavior of the perturbation series on the choice of partitioning by calculating high-order partial sums with respect to HO and HF unperturbed Hamiltonians. An appropriate choice of \hat{H}_0 strongly affects the rate of convergence of the perturbation series. Whereas the series was exponentially converging when using HF orbitals, the use of HO single-particle states yields a divergent perturbation expansion. The convergence with HF orbitals was very robust and the high-order results encourage the use of low-order partial sums as approximations in medium-mass systems.

Naturally the question arises what other parameters may affect the perturbation series. We illustrated that the proper choice of the SRG flow parameter is crucial for a perturbative treatment. The use of sufficiently 'softened' interactions is key for many-body methods. While a bare, i.e., untransformed interaction, yields unbound systems on the mean-field level, we see a systematic dependence of the convergence behavior on variations of the SRG flow parameter α . For larger values of the flow parameter (i.e. softer interactions) the perturbation series converges more rapidly. However, the HF-MBPT perturbation series is still very robust and even hard interactions give convergent perturbation series, even though

the convergence rate is in some cases quite poor.

When using SRG transformed potentials and a HF partitioning, the perturbation series always reveals rapid convergence and the explicit evaluation of second- and third-order formulae via normal-ordering techniques enables for proceeding to the medium-mass region. In particular, the use of HF orbitals in MBPT simplifies the diagrammatic treatment considerably and gives a much lower number of Hugenholtz diagrams compared to MBPT with respect to an arbitrary single-determinantal reference state at the same order. Furthermore, the use of angular-momentum coupling techniques allows us to cast the working equations in matrix-product form, which can be efficiently evaluated using modern linear algebra libraries. The algorithmic simplicity allows for the evaluation of third-order partial sums in large model spaces up to heavy tin isotopes. Comparison with state-of-the-art CC calculations shows excellent agreement on a sub-percent level for various interactions, while requiring significantly less computing time. Thus, HF-MBPT provides a light-weighted alternative to more sophisticated approaches like CC or IM-SRG.

Additionally, we investigated a subtle issue of MBPT which is, however, present in almost all many-body approaches—a detailed analysis of effects of the individual contributions at a given truncation order. At third order, there appear three Hugenholtz diagrams with different computational characteristics. Previous applications in neutron-matter calculations neglected the particle-hole channel for the sake of simplicity. Our calculations, however, show that the particle-hole channel contributes significantly and a neglect may lead to wrong estimates for the third-order energy correction. From our analysis it is clear that only a full inclusion of all contributing diagrams at a given order is reasonable and a selective omission of certain contributions breaks the hierarchy of the correlation expansion of the many-body framework under consideration.

Even though, HF-MBPT is a well-established many-body approach, there are still many possible directions for future research. The most straightforward extension is the relaxation of the truncation order and the derivation of higher-order energy corrections. This has already been performed in our group in the case of fourth-order HF-MBPT. The proliferation of diagrams makes the implementation and coupling tedious and error-prone. However, at higher order new topologies arise which for example account for the effect of quadruply-excited intermediates. Such states are expected to dominantly contribute to nuclei that exhibit alpha-cluster structure, which are typically only poorly described at lower truncation order. Furthermore, our investigations in HF-MBPT are restricted to ground-state energies. An extension to other excited states can, for example, be achieved in an EOM framework, which allows also to investigate spectra of closed-shell nuclei. Other observables, such as charge radii, can be accessed by means of correlated one- and two-body densities. With the advent of high-precision calculations, the inclusion of three-body forces beyond the normal-ordered two-body approximation will be necessary. Therefore, an extension of HF-

MBPT to three-body operators is of great interest. While this will tremendously increase the computational cost, the implementation is straightforward once three-body matrix elements are available in a suitable format. An corresponding investigation in the CC framework has already been presented [Bin⁺13; Bin14].

Another aspect, which is not related to the extension of MBPT machinery, is probing the correlation expansion. In the past five years the rigorous quantification of theoretical uncertainties has become an important tool in *ab initio* nuclear theory. Recent investigations are restricted to studying the impact of systematic errors in the chiral Hamiltonian, e.g., from truncations in the chiral power counting, in the framework of *Bayesian statistics*. Ultimately, one aims for a consistent propagation of systematic errors starting from the input Hamiltonian up to the truncation schemes of the many-body method under consideration. The simplicity of the MBPT ansatz makes it an ideal candidate for probing such effects. However, it is unclear how to apply probabilistic methods for a rigorous quantification of theoretical uncertainties in the many-body framework.

PERTURBATIVELY-IMPROVED NO-CORE SHELL MODEL

Closed-shell nuclei provide the simplest testbed for a many-body framework. However, in the case of open-shell systems, the HF determinant typically does not provide an adequate reference point for the correlation expansion and the degeneracy of several zero-order states may yield divergent single-configurational theories. An integral part of this thesis is the development of an extension of HF-MBPT capable of treating genuine open-shell nuclei. To overcome the degeneracy of the zero-order solution, we introduced reference states that are superpositions of several Slater determinant, i.e., multi-configurational reference states, and derived a formalism in which these generalized zero-order states are perturbed. While initially the choice of the reference states remained arbitrary, we later introduced a novel *hybrid ab initio* approach that uses NCSM reference states and, therefore, merges CI and MBPT technology to overcome their individual drawbacks. This allows incorporating static correlation effects in the NCSM reference states and treat residual dynamic correlation effects perturbatively in the MCPT framework.

First benchmark calculations explore the convergence behavior of the MCPT perturbation and use an extension of the machinery already applied in high-order HF-MBPT. NCSM-PT reveals a very robust convergence behavior for light nuclei and several target states with different values for J^Π . The rate of convergence was again exponential such that low-order partial sums are expected to be excellent approximations to the converged result. MCPT is formulated in m -scheme and, therefore, equally applies to even and odd nuclei and arbitrary values of J . However, the use of an uncoupled formulation significantly increases computing time and, therefore, the current implementation is restricted to the calculation

of second-order energy corrections. The NCSM-PT code was applied for the calculation of ground-state energies for both carbon and oxygen isotopic chains. All results were in remarkable agreement compared to large-scale IT-NCSM calculation at significantly lower cost. Furthermore, we varied the size of the reference space from the prior diagonalization. Typically, the use of $N_{\max}^{(\text{ref})} = 2$ yields better agreement than the use of $N_{\max}^{(\text{ref})} = 0$, which is the smallest possible model space. When applying NCSM-PT using HO single-particle states to ground states in the fluorine isotopic chain, we encounter a large dependence of NCSM-PT results on the oscillator frequency. When switching to HF orbitals, second-order NCSM-PT results are very robust to variations in the oscillator frequency up to very neutron-rich fluorine isotopes. This allows, for the first time, for an *ab initio* treatment of even and odd fluorine isotopes in a no-core approach beyond $A = 20$.

Further improvement in NCSM-PT can be gained through the use of other single-particle bases. An alternative to HO and HF single-particle states, which has attracted attention in recent years, are natural orbitals, i.e., eigenstates obtained via the diagonalization of the one-body density matrix. Applications in the NCSM have revealed improved model space convergence which is expected to transfer to NCSM-PT as well. The construction of correlated one-body density matrices can be obtained, e.g., in a perturbative framework.

In order to overcome deficiencies of second-order NCSM-PT, higher-order correlations can be incorporated via the calculation of the third-order energy correction. Even though the derivation of the formulas is straightforward and can be automated as discussed in chapter 11, the third-order corrections exhibits a stronger scaling and, therefore, are computationally more demanding. However, it is unclear if the extension to higher perturbation order can overcome the problem of accounting for multi-particle-multi-hole excitations, e.g., the Hoyle state in ^{12}C . It might be more convenient to derive another flavour of MBPT based on using generalized multi-particle multi-hole excitations and the extended Wick theorem as in the MR-IM-SRG, which are able to account for these collective excitations. However, up to now the formal derivation of such a perturbation theory still poses a future challenge.

Other variants of MCPT can be obtained by using different zero-order Hamiltonians. Either following a Epstein-Nesbet philosophy, i.e., diagonal matrix elements in a given many-body basis or sticking to the Møller-Plesset partitioning but use another definition of single-particle energies.

A very important extension of NCSM-PT for future applications is the inclusion of three-body operators without making use of the NO2B approximation. Due to significantly growing computational demands of modern medium-mass methods when using three-body operators, one is typically restricted to two-body operators. A second-order treatment provides the simplest way of including three-body operators. Due to the increasing particle rank the number of second-order diagrams grows significantly. In particular the contributing topologies can be more complex, i.e., there appear up to hexuple replacements. Furthermore, the

normal-ordered two-body part in the MCPT formalism also depends on the current Fermi vacuum.

When proceeding to higher mass numbers, the generation of reference states, i.e., performing full CI calculations can be computationally very demanding. For the calculation of calcium isotopes the many-body basis in $N_{\max} = 2$ model space already contains several millions configurations. A possible ansatz for the reduction of the vast amount of basis states is the use of restricted CI instead of full CI, e.g., in the form of CISD. The lack of size extensivity can be approximately accounted for in terms of *a-posteriori* corrections. This significantly lower computational scaling of second-order NCSM-PT and allows to proceed to heavier systems.

BOGOLIUBOV MANY-BODY PERTURBATION THEORY

In the final part of this thesis, we introduced symmetry-broken MBPT as an alternative way to NCSM-PT to extend a perturbative approach to genuine open-shell systems. Instead of a proper multi-configurational reference state, we use a particle-number broken HFB vacuum as starting point for the correlation expansion. Pairing correlation are already included via the self-consistent HFB iteration. Conveniently, particle-number broken methods are formulated in quasiparticle space. A large part of this work was spent on the derivation of angular-momentum-coupled quasiparticle matrix elements and the implementation of spherical BMBPT at second-order.

In first benchmark calculations, we investigated second-order energy corrections along even-even nuclei in the oxygen, calcium, nickel and tin isotopic chains using state-of-the-art chiral interactions. The results are in very good agreement with other medium-mass many-body methods. However, second-order BMBPT requires significantly less computational resources and provides a simple alternative to more advanced many-body approaches such as MR-IM-SRG or the Gorkov extension of SCGF.

From the ground-state binding energies we derived two-neutron separation energies at the HFB and BMBPT level along the isotopic chains. These served as an indicator for effects of shell closures. However, since BMBPT is a particle-number broken approach, the correlated many-body states do only possess good particle-number on average. Therefore, the wave function contains components with different particle-numbers. This can lead to smeared-out edges in two-neutron separation energies when looking at the systematics throughout the chain and shell closures appear less pronounced.

In addition to binding properties, the monitoring of the symmetry breaking is mandatory in a symmetry-broken approach. In particular, this includes the investigation of corrections to the particle-number variance at second-order BMBPT. In most cases this correction appeared to be positive and the correlated state was smeared out even further, i.e., has a large

particle-number dispersion. This behavior was surprising and one expected the correlated wave function to have a sharper peak about the mean-particle number.

Additional investigations of the pairing properties of the chiral Hamiltonians exhibit quite small pairing gaps and quasiparticle energies for some selected isotopes, which lead to pathological corrections to the particle-number variance. In particular, small quasiparticle energies can cause severe problems since these quantities enter denominators of perturbative formulas and can cause an (almost) singular perturbation expansion.

Symmetry-broken MBPT provides a plethora of different directions for future research. In order to include additional correlation effects, BMBPT can be extended to third order. The contributing diagrams for the ground-state energy were already introduced in this work. However, at third order additional features appear. Most importantly, not only corrections to the particle-number variance appear but also corrections to the particle-number itself. Therefore, the correlated state has no correct particle-number on average. To overcome this problem has to adjust the HFB constraint in such a way that the correlated particle number (and not the HFB particle number) coincide with the target value. This can be done by means of an additional iteration scheme.

The derivation of fourth-order diagrams is under investigation and will be part of future research. Of course, one needs to include particle-number corrections at fourth order consistently and solve the iteration scheme for the particle-number adjustment.

The inclusion of higher-order correlation effects beyond simply increasing the perturbation order can be achieved via applying the Bogoliubov extension to other infinite-order methods such as CC and IM-SRG. While the implementation of BCC was already performed using an axially-deformed single-particle basis, the formulation and implementation of Bogoliubov IM-SRG has not been performed yet. In a first step an implementation of BCC with doubles in spherical scheme poses a computationally feasible alternative to low-order BMBPT allowing for an all-order treatment of four-quasi-particle-excitations up to infinite order in large model spaces.

Besides investigating binding energies of ground-state wave functions BMBPT can be applied to other operators as well, e.g., charge radii. However, there appears the additional complication that typically such operators do not commute with the Hamiltonian and, therefore, the formalism needs to be generalized. In the BCC framework this is done in terms a of Λ extension [Sig⁺15; DS16]. It is, however, straightforward to derive a degraded second-order Λ framework for the evaluation of observables that do not commute with the Hamiltonian.

As already indicated, the breaking of symmetries is an auxiliary tool for the development of novel many-body approaches. In finite systems this symmetry breaking does not appear, and eventually the symmetry needs to be restored consistently. In particular all calculated quantities still carry a pathological dependence on the particle-number variance. The most important step in the validation of BMBPT is the restoration of good particle number. While

the theory has already been introduced in the CC framework for the restoration of $U(1)$ and $SU(2)$ symmetries the corresponding MBPT variant needs to be worked out. However, this can be achieved by performing a second-order reduction of the symmetry-restoration step in BCCSD and thus does not pose a major challenge on a formal level [DS16].

In the longer term the inclusion of deformation effects via the breaking of angular-momentum conservation is envisioned. Again the CC counterpart has already been introduced and, therefore, the introduction of an MBPT version is comparably simple. However, due to the non-abelian character of $SU(2)$ the formal part of the derivation is more involved than in BMBPT. The consistent breaking and restoration of both $U(1)$ and $SU(2)$ at the same time poses an additional challenge for the following years to come.

Ultimately, symmetry-broken many-body methods yield a natural link to the constraining of state-of-the-art EDF kernels. Thus, the further development of symmetry-breaking many-body theory provides a unique opportunity to close the gap between *ab initio* methods and EDF theory. In this way off-diagonal norm and energy kernels entering modern EDF parametrizations can be systematically improved.

APPENDICES



Spherical Hartree-Fock Many-Body Perturbation Theory

The aim of this section is to derive the third-order energy correction in J -coupled scheme when using canonical HF orbitals. In this way due to Brillouin's theorem the one-body part vanishes and we are left with three ASG diagrams which already have been introduced in Fig. 6.1.

We again use Baranger notation

$$k = (\tilde{k}, m_k) \quad (\text{A.1})$$

to split the single-particle states into a spherical part and a m -dependent part.

A.1 THE PARTICLE-PARTICLE CHANNEL

We start with the coupling of the particle-particle channel

$$\begin{aligned}
 E_{pp}^{(3)} &= \frac{1}{8} \sum_{abcdij} \frac{\bar{H}_{ijab}^{[2]} \bar{H}_{abcd}^{[2]} \bar{H}_{cdij}^{[2]}}{\epsilon_{ij}^{ab} \epsilon_{ij}^{cd}} \\
 &= \frac{1}{8} \sum_{\tilde{a}\tilde{b}\tilde{c}\tilde{d}\tilde{i}\tilde{j}} \sum_{m_a m_b m_c} \sum_{\substack{J J' J'' \\ M M' M''}} \frac{J H_{\tilde{i}\tilde{j}\tilde{a}\tilde{b}}^{[2]} J' H_{\tilde{a}\tilde{b}\tilde{c}\tilde{d}}^{[2]} J'' H_{\tilde{c}\tilde{d}\tilde{i}\tilde{j}}^{[2]}}{\epsilon_{ij}^{ab} \epsilon_{ij}^{cd}} \\
 &\quad \times \begin{pmatrix} j_i & j_j & J \\ m_i & m_j & M \end{pmatrix} \begin{pmatrix} j_a & j_b & J \\ m_a & m_b & M \end{pmatrix} \begin{pmatrix} j_a & j_b & J' \\ m_a & m_b & M' \end{pmatrix} \begin{pmatrix} j_c & j_d & J' \\ m_c & m_d & M' \end{pmatrix} \begin{pmatrix} j_c & j_d & J'' \\ m_c & m_d & M'' \end{pmatrix} \begin{pmatrix} j_i & j_j & J'' \\ m_i & m_j & M'' \end{pmatrix}
 \end{aligned}$$

$$\begin{aligned}
 &= \frac{1}{8} \sum_{\tilde{a}\tilde{b}\tilde{c}\tilde{d}\tilde{i}\tilde{j}} \sum_{\substack{JJ'J'' \\ MM'M''}} \frac{J H_{\tilde{i}\tilde{j}\tilde{a}\tilde{b}}^{[2]} J' H_{\tilde{a}\tilde{b}\tilde{c}\tilde{d}}^{[2]} J'' H_{\tilde{c}\tilde{d}\tilde{i}\tilde{j}}^{[2]}}{\epsilon_{\tilde{i}\tilde{j}}^{\tilde{a}\tilde{b}} \epsilon_{\tilde{i}\tilde{j}}^{\tilde{c}\tilde{d}}} \delta_{JJ'} \delta_{J'J''} \delta_{J''J} \delta_{MM'} \delta_{M'M''} \delta_{M''M} \\
 &= \frac{1}{8} \sum_{\tilde{a}\tilde{b}\tilde{c}\tilde{d}\tilde{i}\tilde{j}} \sum_J \hat{j}^2 \frac{J H_{\tilde{i}\tilde{j}\tilde{a}\tilde{b}}^{[2]} J H_{\tilde{a}\tilde{b}\tilde{c}\tilde{d}}^{[2]} J H_{\tilde{c}\tilde{d}\tilde{i}\tilde{j}}^{[2]}}{\epsilon_{\tilde{i}\tilde{j}}^{\tilde{a}\tilde{b}} \epsilon_{\tilde{i}\tilde{j}}^{\tilde{c}\tilde{d}}}
 \end{aligned} \tag{A.2}$$

We see that by using orthogonality of the CG coefficients the final expression is independent of m quantum numbers and can be written as matrix product of the Hamiltonian for each J -block. Additionally, we use that single-particle energies do not depend on the m quantum number, i.e., $\epsilon_{\tilde{i}\tilde{j}}^{\tilde{a}\tilde{b}} = \epsilon_{\tilde{i}\tilde{j}}^{ab}$.

A.2 THE HOLE-HOLE CHANNEL

In complete analogy we get for the hole-hole channel

$$\begin{aligned}
 E_{pp}^{(3)} &= \frac{1}{8} \sum_{abijkl} \frac{\bar{H}_{abij}^{[2]} \bar{H}_{ijkl}^{[2]} \bar{H}_{klab}^{[2]}}{\epsilon_{ij}^{ab} \epsilon_{kl}^{ab}} \\
 &= \frac{1}{8} \sum_{\tilde{a}\tilde{b}\tilde{i}\tilde{j}\tilde{k}\tilde{l}} \sum_{\substack{m_a m_b m_i \\ m_j m_k m_l}} \sum_{JJ'J''} \frac{J H_{\tilde{a}\tilde{b}\tilde{i}\tilde{j}}^{[2]} J' H_{\tilde{i}\tilde{j}\tilde{k}\tilde{l}}^{[2]} J'' H_{\tilde{k}\tilde{l}\tilde{a}\tilde{b}}^{[2]}}{\epsilon_{\tilde{i}\tilde{j}}^{ab} \epsilon_{\tilde{k}\tilde{l}}^{ab}} \\
 &\quad \times \begin{pmatrix} j_i & j_j & J \\ m_i & m_j & M \end{pmatrix} \begin{pmatrix} j_a & j_b & J \\ m_a & m_b & M \end{pmatrix} \begin{pmatrix} j_i & j_j & J' \\ m_i & m_j & M' \end{pmatrix} \begin{pmatrix} j_k & j_l & J' \\ m_k & m_l & M' \end{pmatrix} \begin{pmatrix} j_k & j_l & J'' \\ m_k & m_l & M'' \end{pmatrix} \begin{pmatrix} j_a & j_b & J'' \\ m_a & m_b & M'' \end{pmatrix} \\
 &= \frac{1}{8} \sum_{\tilde{a}\tilde{b}\tilde{i}\tilde{j}\tilde{k}\tilde{l}} \sum_{JJ'J''} \frac{J H_{\tilde{a}\tilde{b}\tilde{i}\tilde{j}}^{[2]} J' H_{\tilde{i}\tilde{j}\tilde{k}\tilde{l}}^{[2]} J'' H_{\tilde{k}\tilde{l}\tilde{a}\tilde{b}}^{[2]}}{\epsilon_{\tilde{i}\tilde{j}}^{\tilde{a}\tilde{b}} \epsilon_{\tilde{k}\tilde{l}}^{\tilde{a}\tilde{b}}} \delta_{JJ'} \delta_{J'J''} \delta_{J''J} \delta_{MM'} \delta_{M'M''} \delta_{M''M} \\
 &= \frac{1}{8} \sum_{\tilde{a}\tilde{b}\tilde{i}\tilde{j}\tilde{k}\tilde{l}} \sum_J \hat{j}^2 \frac{J H_{\tilde{a}\tilde{b}\tilde{i}\tilde{j}}^{[2]} J' H_{\tilde{i}\tilde{j}\tilde{k}\tilde{l}}^{[2]} J'' H_{\tilde{k}\tilde{l}\tilde{a}\tilde{b}}^{[2]}}{\epsilon_{\tilde{i}\tilde{j}}^{\tilde{a}\tilde{b}} \epsilon_{\tilde{k}\tilde{l}}^{\tilde{a}\tilde{b}}},
 \end{aligned} \tag{A.3}$$

which also display the structure of a matrix product.

A.3 THE PARTICLE-HOLE CHANNEL

For the coupling of the particle-hole channel we introduce the Pandya-transformed matrix elements

$$K H_{\tilde{c}\tilde{j}\tilde{k}\tilde{b}}^{[2]} = \sum_J \hat{j}^2 \cdot^J H_{\tilde{k}\tilde{c}\tilde{j}\tilde{b}}^{XC} \begin{Bmatrix} j_j & j_c & K \\ j_k & j_b & J \end{Bmatrix} \tag{A.4}$$

$$K H_{\tilde{j}\tilde{i}\tilde{a}\tilde{b}}^{[2]} = \sum_J \hat{j}^2 \cdot^J H_{\tilde{k}\tilde{b}\tilde{a}\tilde{j}}^{XC} \begin{Bmatrix} j_a & j_i & K \\ j_j & j_b & J \end{Bmatrix} \tag{A.5}$$

$${}^K H_{i\tilde{k}\tilde{a}\tilde{c}}^{[2]} = \sum_J \hat{j}^2 \cdot^J H_{k\tilde{c}\tilde{a}\tilde{i}}^{XC} \left\{ \begin{matrix} j_k & j_c & K \\ j_a & j_i & J \end{matrix} \right\} \quad (\text{A.6})$$

Starting with the third-order particle-hole diagram

$$E_{ph}^{(3)} = \sum_{abcijk} \frac{\bar{H}_{abij}^{[2]} \bar{H}_{cikb}^{[2]} \bar{H}_{jkac}^{[2]}}{\epsilon_{ij}^{ab} \epsilon_{jk}^{ac}} \quad (\text{A.7})$$

we define an auxiliary quantity

$$B_{abij} \equiv \frac{\bar{H}_{abij}^{[2]}}{\epsilon_{ij}^{ab}}, \quad (\text{A.8})$$

and rewrite

$$E_{ph}^{(3)} = \sum_{abcijk} B_{abij} \bar{H}_{cjk b}^{[2]} B_{ikac}. \quad (\text{A.9})$$

Transformation into J -scheme yields

$$\begin{aligned} E_{ph}^{(3)} &= \sum_{abcijk} B_{abij} \bar{H}_{cikb}^{[2]} B_{kjac} \\ &= \sum_{abcijk} \sum_{JJ'J''} \sum_{MM'M''} {}^J B_{abji} \cdot {}^{J'} H_{ickb}^{[2]} \cdot {}^{J''} B_{kjac} \\ &\quad \times \begin{pmatrix} j_a & j_b & | & J \\ m_b & m_b & | & M \end{pmatrix} \begin{pmatrix} j_j & j_i & | & J \\ m_j & m_i & | & M \end{pmatrix} \begin{pmatrix} j_i & j_c & | & J' \\ m_i & m_c & | & M' \end{pmatrix} \begin{pmatrix} j_k & j_b & | & J' \\ m_k & m_b & | & M' \end{pmatrix} \begin{pmatrix} j_k & j_j & | & J'' \\ m_k & m_j & | & M'' \end{pmatrix} \begin{pmatrix} j_a & j_c & | & J'' \\ m_a & m_c & | & M'' \end{pmatrix} \end{aligned} \quad (\text{A.10})$$

We start from

$$\begin{aligned} &\sum_{m_c m_k M' M''} \begin{pmatrix} j_i & j_c & | & J' \\ m_i & m_c & | & M' \end{pmatrix} \begin{pmatrix} j_k & j_b & | & J' \\ m_k & m_b & | & M' \end{pmatrix} \begin{pmatrix} j_k & j_j & | & J'' \\ m_k & m_j & | & M'' \end{pmatrix} \begin{pmatrix} j_a & j_c & | & J' \\ m_a & m_c & | & M' \end{pmatrix} \\ &= \sum_{m_c m_k M' M''} (-1)^{2(j_k - m_k) + 2(j_c + m_c)} \\ &\quad \times \frac{\hat{j}^2 \hat{j}''^2}{\hat{j}_a \hat{j}_b \hat{j}_i \hat{j}_j} \begin{pmatrix} J' & j_c & | & j_i \\ -M' & m_c & | & -m_i \end{pmatrix} \begin{pmatrix} j_k & J' & | & j_b \\ m_k & -M' & | & -m_b \end{pmatrix} \begin{pmatrix} j_k & J'' & | & j_j \\ m_k & -M'' & | & -m_j \end{pmatrix} \begin{pmatrix} J'' & j_c & | & j_a \\ -M'' & m_c & | & -m_a \end{pmatrix} \\ &= \sum_{m_c m_k M' M''} (-1)^{j_i - j_c - J' + j_j - j_k - J''} \\ &\quad \times \frac{\hat{j}^2 \hat{j}''^2}{\hat{j}_a \hat{j}_b \hat{j}_i \hat{j}_j} \begin{pmatrix} j_c & J' & | & j_i \\ m_c & -M' & | & -m_i \end{pmatrix} \begin{pmatrix} j_k & J' & | & j_b \\ m_k & -M' & | & -m_b \end{pmatrix} \begin{pmatrix} J'' & m_k & | & j_j \\ j_k & -M'' & | & -m_j \end{pmatrix} \begin{pmatrix} J'' & j_c & | & j_a \\ -M'' & m_c & | & -m_a \end{pmatrix} \end{aligned}$$

$$\begin{aligned}
 &= \sum_{J'''M'''} (-1)^{j_i-j_c-J'+j_j-j_k-J''} \hat{j}'^2 \hat{j}''^2 \begin{pmatrix} j_j & j_i & J''' \\ -m_j & m_i & M''' \end{pmatrix} \begin{pmatrix} j_a & j_b & J''' \\ -m_a & -m_b & M''' \end{pmatrix} \left\{ \begin{matrix} J' & j_k & j_b \\ j_c & J'' & j_a \\ j_i & j_j & J''' \end{matrix} \right\} \\
 &= \sum_{J'''M'''} (-1)^{j_i-j_c-J'+j_j-j_k-J''-j_a-j_b+2(J'''-j_i-j_k)} \hat{j}'^2 \hat{j}''^2 \begin{pmatrix} j_i & j_j & J''' \\ m_i & m_j & M''' \end{pmatrix} \begin{pmatrix} j_a & j_b & J''' \\ m_a & m_b & M''' \end{pmatrix} \left\{ \begin{matrix} J' & j_k & j_b \\ j_c & J'' & j_a \\ j_i & j_j & J''' \end{matrix} \right\}
 \end{aligned} \tag{A.11}$$

where we made use of identity (20) in section (8.7.4) of [VMK88] and further renamed summations indices and used time-reversal symmetry of the CGs. We can further write

$$\begin{aligned}
 &\sum_{m_a m_b m_i m_j} \sum_{J'''M'''} (-1)^{j_i-j_c-J'+j_j-j_k-J''-j_a-j_b+2(J'''-j_i-j_k)} \hat{j}'^2 \hat{j}''^2 \\
 &\quad \times \begin{pmatrix} j_i & j_j & J \\ m_i & m_j & M \end{pmatrix} \begin{pmatrix} j_a & j_b & J \\ m_a & m_b & M \end{pmatrix} \begin{pmatrix} j_i & j_j & J''' \\ m_i & m_j & M''' \end{pmatrix} \begin{pmatrix} j_a & j_b & J''' \\ m_a & m_b & M''' \end{pmatrix} \left\{ \begin{matrix} J' & j_k & j_b \\ j_c & J'' & j_a \\ j_i & j_j & J''' \end{matrix} \right\} \\
 &= \sum_{J'''M'''} (-1)^{j_i-j_c-J''+j_j-j_k-J'-j_a-j_b} \hat{j}'^2 \hat{j}''^2 \delta_{JJ'''} \delta_{MM'''} \left\{ \begin{matrix} J' & j_k & j_b \\ j_c & J'' & j_a \\ j_i & j_j & J''' \end{matrix} \right\} \\
 &= (-1)^{j_i-j_c-J''+j_j-j_k-J-j_a-j_b} \hat{j}'^2 \hat{j}''^2 \left\{ \begin{matrix} J' & j_k & j_b \\ j_c & J'' & j_a \\ j_i & j_j & J \end{matrix} \right\} \\
 &= (-1)^{j_i-j_c-J''+j_j-j_k-J-j_a-j_b} \hat{j}'^2 \hat{j}''^2 \left\{ \begin{matrix} j_k & j_b & J' \\ J'' & j_a & j_c \\ j_j & J & j_i \end{matrix} \right\} \\
 &= \hat{j}'^2 \hat{j}''^2 \left\{ \begin{matrix} j_k & j_b & J' \\ j_j & J & j_i \\ J'' & j_a & j_c \end{matrix} \right\}
 \end{aligned} \tag{A.12}$$

where we used permutation symmetry of the 9j symbol according to equation (5) in section (10.4) of [VMK88]. Further using that the 9j symbol can be expanded into three 6j symbol we get (cf. equation (20), section (10.2.4) in [VMK88])

$$\left\{ \begin{matrix} j_k & j_b & J' \\ j_j & J & j_i \\ J'' & j_a & j_c \end{matrix} \right\} = \sum_{J'''} (-1)^{J'''} \hat{j}''' \left\{ \begin{matrix} j_k & j_c & J''' \\ j_i & j_b & J' \end{matrix} \right\} \left\{ \begin{matrix} j_a & j_j & J''' \\ j_k & j_c & J'' \end{matrix} \right\} \left\{ \begin{matrix} j_a & j_b & J \\ j_i & j_j & J''' \end{matrix} \right\}. \tag{A.13}$$

We finally write the third-order particle-hole term as

$$\begin{aligned}
E_{ph}^{(3)} &= \sum_{\tilde{a}\tilde{b}\tilde{c}\tilde{i}\tilde{j}\tilde{k}} \sum_{JJ'J''J'''} \hat{j}^2 \hat{j}'^2 \hat{j}''^2 \hat{j}'''^2 {}^J B_{\tilde{a}\tilde{b}\tilde{i}\tilde{j}} \cdot {}^{J'} H_{\tilde{i}\tilde{c}\tilde{k}\tilde{b}}^{[2]} \cdot {}^{J''} B_{\tilde{k}\tilde{j}\tilde{a}\tilde{c}} \begin{Bmatrix} j_k & j_c & J''' \\ j_i & j_b & J' \end{Bmatrix} \begin{Bmatrix} j_a & j_j & J''' \\ j_k & j_c & J'' \end{Bmatrix} \begin{Bmatrix} j_a & j_b & J \\ j_i & j_j & J''' \end{Bmatrix} \\
&= \sum_{abcijk} \sum_J \hat{j}^{2J} B_{\tilde{a}\tilde{j}\tilde{i}\tilde{b}}^{XC} \cdot {}^{J'} H_{\tilde{k}\tilde{c}\tilde{i}\tilde{b}}^{XC} \cdot {}^{J''} B_{\tilde{a}\tilde{j}\tilde{k}\tilde{c}}^{XC} \\
&= \sum_K \hat{j}^2 \text{Tr} ({}^J B^{XC} \cdot {}^J \bar{H}^{XC} \cdot {}^J B^{XC}) . \tag{A.14}
\end{aligned}$$

B

Integral Identities

For the derivation of Feynman diagrams the following integrals have to be evaluated frequently. We, therefore, list them here for further reference

$$\int_0^\tau d\tau_1 e^{a\tau_1} = \frac{1}{a} (e^{\tau a} - 1) , \quad (\text{B.1a})$$

$$\begin{aligned} \int_0^\tau d\tau_1 d\tau_2 \theta(\tau_1 - \tau_2) e^{a(\tau_1 - \tau_2)} &= \int_0^\tau d\tau_1 e^{a\tau_1} \int_0^{\tau_1} d\tau_2 e^{-a\tau_2} \\ &= -\frac{\tau}{a} + \frac{1}{a^2} (e^{\tau a} - 1) , \end{aligned} \quad (\text{B.1b})$$

$$\begin{aligned} \int_0^\tau d\tau_1 d\tau_2 \theta(\tau_1 - \tau_2) e^{a\tau_1 + b\tau_2} &= \int_0^\tau d\tau_1 e^{a\tau_1} \int_0^{\tau_1} d\tau_2 e^{b\tau_2} \\ &= \frac{1}{b(a+b)} (e^{\tau(a+b)} - 1) - \frac{1}{ab} (e^{\tau a} - 1) . \end{aligned} \quad (\text{B.1c})$$

When applying the above identities to Feynman diagrams it holds that $a < 0$ and $a + b < 0$. Therefore, one obtains the following large time limits

$$\lim_{\tau \rightarrow \infty} \int_0^\tau d\tau e^{a\tau} = -\frac{1}{a} , \quad (\text{B.2a})$$

$$\lim_{\tau \rightarrow \infty} \int_0^\tau d\tau_1 d\tau_2 \theta(\tau_1 - \tau_2) e^{a(\tau_1 - \tau_2)} = -\frac{\tau}{a} - \frac{1}{a^2} , \quad (\text{B.2b})$$

$$\lim_{\tau \rightarrow \infty} \int_0^\tau d\tau_1 d\tau_2 \theta(\tau_1 - \tau_2) e^{a\tau_1 + b\tau_2} = \frac{1}{a(a+b)} . \quad (\text{B.2c})$$

Note that the first and third identity are positive due to a and $a + b$ being negative.



Normal-ordered matrix elements

In this section we quote the expression of the normal-ordered matrix elements in quasiparticle space which were already published in [Sig⁺15].

C.1 GENERIC OPERATOR \hat{O}

As the $\hat{O}^{[6]}$ terms are not considered for practical applications at this point, the matrix elements $O_{k_1 k_2 k_3 k_4 k_5 k_6}^{ij}$, with $i + j = 6$, are excluded for brevity. The generic operator \hat{O} of (14.41h), up to and including $\hat{O}^{[4]}$

$$\hat{O} \equiv \hat{O}^{[0]} + \hat{O}^{[2]} + \hat{O}^{[4]} \quad (\text{C.1})$$

$$\equiv \hat{O}^{00} + \left[\hat{O}^{11} + \{ \hat{O}^{20} + \hat{O}^{02} \} \right] + \left[\hat{O}^{22} + \{ \hat{O}^{31} + \hat{O}^{13} \} + \{ \hat{O}^{40} + \hat{O}^{04} \} \right], \quad (\text{C.2})$$

displays fully anti-symmetrized matrix elements, whose explicit expressions in terms of anti-symmetrized matrix elements of O^{1N} , O^{2N} and O^{3N} , as well as of U and V matrices defining the reference Bogoliubov state, are given by

$$O^{00} = \sum_{l_1 l_2} \left[\Lambda_{l_1 l_2}^{1N} \rho_{l_2 l_1} + \frac{1}{2} \Lambda_{l_1 l_2}^{2N} \rho_{l_2 l_1} + \frac{1}{3} \Lambda_{l_1 l_2}^{3N} \rho_{l_2 l_1} - \frac{1}{2} \Upsilon_{l_1 l_2}^{2N} \kappa_{l_2 l_1}^* + \frac{1}{3} \Upsilon_{l_1 l_2}^{3N} \kappa_{l_2 l_1}^* \right], \quad (\text{C.3a})$$

$$O_{k_1 k_2}^{11} = \sum_{l_1 l_2} \left[U_{k_1 l_1}^\dagger \Lambda_{l_1 l_2} U_{l_2 k_2} - V_{k_1 l_1}^\dagger \Lambda_{l_1 l_2}^T V_{l_2 k_2} + U_{k_1 l_1}^\dagger \Upsilon_{l_1 l_2} V_{l_2 k_2} - V_{k_1 l_1}^\dagger \Upsilon_{l_1 l_2}^* U_{l_2 k_2} \right], \quad (\text{C.3b})$$

$$O_{k_1 k_2}^{20} = \sum_{l_1 l_2} \left[U_{k_1 l_1}^\dagger \Lambda_{l_1 l_2} V_{l_2 k_2}^* - V_{k_1 l_1}^\dagger \Lambda_{l_1 l_2}^T U_{l_2 k_2}^* + U_{k_1 l_1}^\dagger \Upsilon_{l_1 l_2} U_{l_2 k_2}^* - V_{k_1 l_1}^\dagger \Upsilon_{l_1 l_2}^* V_{l_2 k_2}^* \right], \quad (\text{C.3c})$$

$$O_{k_1 k_2}^{02} = \sum_{l_1 l_2} \left[-V_{k_1 l_1}^T \Lambda_{l_1 l_2} U_{l_2 k_2} + U_{k_1 l_1}^T \Lambda_{l_1 l_2}^T V_{l_2 k_2} - V_{k_1 l_1}^T \Upsilon_{l_1 l_2} V_{l_2 k_2} + U_{k_1 l_1}^T \Upsilon_{l_1 l_2}^* U_{l_2 k_2} \right], \quad (\text{C.3d})$$

$$\begin{aligned}
 O_{k_1 k_2 k_3 k_4}^{22} = & \sum_{l_1 l_2 l_3 l_4} \left[\Theta_{l_1 l_2 l_3 l_4} \left(U_{l_1 k_1}^* U_{l_2 k_2}^* U_{l_3 k_3} U_{l_4 k_4} + V_{l_3 k_1}^* V_{l_4 k_2}^* V_{l_1 k_3} V_{l_2 k_4} + U_{l_1 k_1}^* V_{l_4 k_2}^* V_{l_2 k_3} U_{l_3 k_4} \right. \right. \\
 & \left. \left. - V_{l_4 k_1}^* U_{l_1 k_2}^* V_{l_2 k_3} U_{l_3 k_4} - U_{l_1 k_1}^* V_{l_4 k_2}^* U_{l_3 k_3} V_{l_2 k_4} + V_{l_4 k_1}^* U_{l_1 k_2}^* U_{l_3 k_3} V_{l_2 k_4} \right) \right. \\
 & + \Xi_{l_1 l_2 l_3 l_4} \left(U_{l_1 k_1}^* U_{l_2 k_2}^* U_{l_4 k_3} V_{l_3 k_4} + U_{l_1 k_1}^* V_{l_4 k_2}^* V_{l_3 k_3} V_{l_2 k_4} \right. \\
 & \left. - U_{l_1 k_1}^* U_{l_2 k_2}^* V_{l_3 k_3} U_{l_4 k_4} - V_{l_4 k_1}^* U_{l_1 k_2}^* V_{l_3 k_3} V_{l_2 k_4} \right) \\
 & \left. - \Xi_{l_1 l_2 l_3 l_4}^* \left(V_{l_3 k_1}^* U_{l_4 k_2}^* U_{l_1 k_3} U_{l_2 k_4} + V_{l_3 k_1}^* V_{l_2 k_2}^* V_{l_4 k_3} U_{l_1 k_4} \right. \right. \\
 & \left. \left. - U_{l_4 k_1}^* V_{l_3 k_2}^* U_{l_1 k_3} U_{l_2 k_4} - V_{l_3 k_1}^* V_{l_2 k_2}^* V_{l_4 k_4} U_{l_1 k_3} \right) \right], \quad (C.3e)
 \end{aligned}$$

$$\begin{aligned}
 O_{k_1 k_2 k_3 k_4}^{31} = & \sum_{l_1 l_2 l_3 l_4} \left[\Theta_{l_1 l_2 l_3 l_4} \left(U_{l_1 k_1}^* V_{l_4 k_2}^* V_{l_3 k_3} V_{l_2 k_4} - V_{l_4 k_1}^* U_{l_1 k_2}^* V_{l_3 k_3} V_{l_2 k_4} - V_{l_3 k_1}^* V_{l_4 k_2}^* U_{l_1 k_3} V_{l_2 k_4} \right. \right. \\
 & \left. \left. + V_{l_3 k_1}^* U_{l_2 k_2}^* U_{l_1 k_3} U_{l_4 k_4} - U_{l_2 k_1}^* V_{l_3 k_2}^* U_{l_1 k_3} U_{l_4 k_4} - U_{l_1 k_1}^* U_{l_2 k_2}^* V_{l_3 k_3} U_{l_4 k_4} \right) \right. \\
 & + \Xi_{l_1 l_2 l_3 l_4} \left(U_{l_1 k_1}^* U_{l_2 k_2}^* U_{l_3 k_3} U_{l_4 k_4} + V_{l_4 k_1}^* U_{l_2 k_2}^* U_{l_1 k_3} V_{l_3 k_4} \right. \\
 & \left. - U_{l_2 k_1}^* V_{l_4 k_2}^* U_{l_1 k_3} V_{l_3 k_4} + U_{l_2 k_1}^* U_{l_1 k_2}^* V_{l_4 k_3} V_{l_3 k_4} \right) \\
 & + \Xi_{l_1 l_2 l_3 l_4}^* \left(U_{l_4 k_1}^* V_{l_3 k_2}^* V_{l_2 k_3} U_{l_1 k_4} - V_{l_3 k_1}^* U_{l_4 k_2}^* V_{l_2 k_3} U_{l_1 k_4} \right. \\
 & \left. + V_{l_3 k_1}^* V_{l_2 k_2}^* U_{l_4 k_3} U_{l_1 k_4} - V_{l_3 k_1}^* V_{l_2 k_2}^* V_{l_1 k_3} V_{l_4 k_4} \right) \right], \quad (C.3f)
 \end{aligned}$$

$$\begin{aligned}
 O_{k_1 k_2 k_3 k_4}^{13} = & \sum_{l_1 l_2 l_3 l_4} \left[\Theta_{l_1 l_2 l_3 l_4} \left(V_{l_4 k_1}^* U_{l_3 k_2} V_{l_2 k_3} V_{l_1 k_4} - V_{l_4 k_1}^* V_{l_2 k_2} U_{l_3 k_3} V_{l_1 k_4} - V_{l_4 k_1}^* V_{l_1 k_2} V_{l_2 k_3} U_{l_3 k_4} \right. \right. \\
 & \left. \left. + U_{l_1 k_1}^* V_{l_2 k_2} U_{l_3 k_3} U_{l_4 k_4} - U_{l_1 k_1}^* U_{l_3 k_2} V_{l_2 k_3} U_{l_4 k_4} + U_{l_1 k_1}^* U_{l_3 k_2} U_{l_4 k_3} V_{l_2 k_4} \right) \right. \\
 & + \Xi_{l_1 l_2 l_3 l_4} \left(U_{l_1 k_1}^* V_{l_2 k_2} V_{l_3 k_3} U_{l_4 k_4} - V_{l_4 k_1}^* V_{l_1 k_2} V_{l_2 k_3} V_{l_3 k_4} \right. \\
 & \left. + U_{l_1 k_1}^* U_{l_4 k_2} V_{l_2 k_3} V_{l_3 k_4} - U_{l_1 k_1}^* V_{l_2 k_2} U_{l_4 k_3} V_{l_3 k_4} \right) \\
 & + \Xi_{l_1 l_2 l_3 l_4}^* \left(V_{l_3 k_1}^* V_{l_4 k_2} U_{l_1 k_3} U_{l_2 k_4} - V_{l_3 k_1}^* U_{l_1 k_2} V_{l_4 k_3} U_{l_2 k_4} \right. \\
 & \left. + V_{l_3 k_1}^* U_{l_1 k_2} U_{l_2 k_3} V_{l_4 k_4} - U_{l_4 k_1}^* U_{l_1 k_2} U_{l_2 k_3} U_{l_3 k_4} \right) \right], \quad (C.3g)
 \end{aligned}$$

$$\begin{aligned}
 O_{k_1 k_2 k_3 k_4}^{40} = & \sum_{l_1 l_2 l_3 l_4} \left[\Theta_{l_1 l_2 l_3 l_4} \left(U_{l_1 k_1}^* U_{l_2 k_2}^* V_{l_4 k_3}^* V_{l_3 k_4}^* - U_{l_1 k_1}^* V_{l_4 k_2}^* U_{l_2 k_3}^* V_{l_3 k_4}^* - V_{l_4 k_1}^* U_{l_2 k_2}^* U_{l_1 k_3}^* V_{l_3 k_4}^* \right. \right. \\
 & \left. \left. + U_{l_1 k_1}^* V_{l_4 k_2}^* V_{l_3 k_3}^* U_{l_2 k_4}^* + V_{l_4 k_1}^* U_{l_2 k_2}^* V_{l_3 k_3}^* U_{l_1 k_4}^* + V_{l_4 k_1}^* V_{l_3 k_2}^* U_{l_1 k_3}^* U_{l_2 k_4}^* \right) \right. \\
 & + \Xi_{l_1 l_2 l_3 l_4} \left(U_{l_1 k_1}^* U_{l_2 k_2}^* U_{l_3 k_3}^* V_{l_4 k_4}^* - U_{l_1 k_1}^* U_{l_2 k_2}^* V_{l_4 k_3}^* U_{l_3 k_4}^* \right. \\
 & \left. + U_{l_1 k_1}^* V_{l_4 k_2}^* U_{l_2 k_3}^* U_{l_3 k_4}^* - V_{l_4 k_1}^* U_{l_1 k_2}^* U_{l_2 k_3}^* U_{l_3 k_4}^* \right) \\
 & + \Xi_{l_1 l_2 l_3 l_4}^* \left(V_{l_1 k_1}^* V_{l_2 k_2}^* V_{l_3 k_3}^* U_{l_4 k_4}^* - V_{l_1 k_1}^* V_{l_2 k_2}^* U_{l_4 k_3}^* V_{l_3 k_4}^* \right. \\
 & \left. + V_{l_1 k_1}^* U_{l_4 k_2}^* V_{l_2 k_3}^* V_{l_3 k_4}^* - U_{l_4 k_1}^* V_{l_1 k_2}^* V_{l_2 k_3}^* U_{l_3 k_4}^* \right) \right], \quad (C.3h)
 \end{aligned}$$

$$O_{k_1 k_2 k_3 k_4}^{04} = \sum_{l_1 l_2 l_3 l_4} \left[\Theta_{l_1 l_2 l_3 l_4} \left(U_{l_3 k_1} U_{l_4 k_2} V_{l_2 k_3} V_{l_1 k_4} - U_{l_3 k_1} V_{l_2 k_2} U_{l_4 k_3} V_{l_1 k_4} + U_{l_3 k_1} V_{l_2 k_2} V_{l_1 k_3} U_{l_4 k_4} \right. \right.$$

$$\begin{aligned}
 & - V_{l_2 k_1} U_{l_3 k_2} V_{l_1 k_3} U_{l_4 k_4} + V_{l_2 k_1} V_{l_1 k_2} U_{l_3 k_3} U_{l_4 k_4} + V_{l_2 k_1} U_{l_3 k_2} U_{l_4 k_3} V_{l_1 k_4}) \\
 + \Xi_{l_1 l_2 l_3 l_4} & \left(V_{l_1 k_1} V_{l_2 k_2} V_{l_3 k_3} U_{l_4 k_4} - V_{l_1 k_1} V_{l_2 k_2} U_{l_4 k_3} V_{l_3 k_4} \right. \\
 & \left. + V_{l_1 k_1} U_{l_4 k_2} V_{l_2 k_3} V_{l_3 k_4} - U_{l_4 k_1} V_{l_1 k_2} V_{l_2 k_3} V_{l_3 k_4} \right) \\
 + \Xi_{l_1 l_2 l_3 l_4}^* & \left(V_{l_4 k_1} U_{l_3 k_2} U_{l_2 k_3} U_{l_1 k_4} - U_{l_3 k_1} V_{l_4 k_2} U_{l_2 k_3} U_{l_1 k_4} \right. \\
 & \left. + U_{l_3 k_1} U_{l_2 k_2} V_{l_4 k_3} U_{l_1 k_4} - U_{l_3 k_1} U_{l_2 k_2} U_{l_1 k_3} V_{l_4 k_4} \right) \Big] . \tag{C.3i}
 \end{aligned}$$

The above expressions make use of four one- and two-body operators whose matrix elements are given in an arbitrary single-particle basis by

$$\Lambda_{pq} \equiv \Lambda_{pq}^{1N} + \Lambda_{pq}^{2N} + \Lambda_{pq}^{3N} \tag{C.4a}$$

$$= o_{pq}^{1N} + \sum_{rs} \bar{o}_{psqr}^{2N} \rho_{rs} + \frac{1}{2} \sum_{rstu} \bar{o}_{prsqtu}^{3N} \left(\rho_{us} \rho_{tr} + \frac{1}{2} \kappa_{rs}^* \kappa_{tu} \right) , \tag{C.4b}$$

$$\Upsilon_{pq} \equiv \Upsilon_{pq}^{2N} + \Upsilon_{pq}^{3N} \tag{C.4c}$$

$$= \frac{1}{2} \sum_{rs} \bar{o}_{pqrs}^{2N} \kappa_{rs} + \frac{1}{2} \sum_{rstu} \bar{o}_{rpqstu}^{3N} \rho_{sr} \kappa_{tu} , \tag{C.4d}$$

$$\Theta_{pqrs} \equiv \bar{o}_{pqrs}^{2N} + \sum_{tu} \bar{o}_{pqtrsu}^{3N} \rho_{ut} , \tag{C.4e}$$

$$\Xi_{pqrs} \equiv \frac{1}{2} \sum_{tu} \bar{o}_{pqrstu}^{3N} \kappa_{tu} . \tag{C.4f}$$

It is easy to verify the following properties

$$\Lambda_{pq}^{2N} = \Lambda_{qp}^{2N*} , \tag{C.5a}$$

$$\Lambda_{pq}^{3N} = \Lambda_{qp}^{3N*} , \tag{C.5b}$$

$$\Upsilon_{pq}^{2N} = -\Upsilon_{qp}^{2N} , \tag{C.5c}$$

$$\Upsilon_{pq}^{3N} = -\Upsilon_{qp}^{3N} , \tag{C.5d}$$

$$\Theta_{pqrs} = -\Theta_{pqsr} = \Theta_{qpsr} = -\Theta_{qprs} , \tag{C.5e}$$

$$\Theta_{pqrs} = \Theta_{rspq}^* , \tag{C.5f}$$

$$\Xi_{pqrs} = -\Xi_{qprs} = \Xi_{qrps} = -\Xi_{prqs} = \Xi_{rpqs} = -\Xi_{rqps} , \tag{C.5g}$$

as will be the case for the other operators to follow.

C.2 GRAND CANONICAL POTENTIAL $\hat{\Omega}$

In the particular case that O corresponds to the grand canonical potential Ω the matrix elements are given by

$$\Lambda_{pq} \equiv h_{pq} \quad (\text{C.6a})$$

$$\equiv t_{pq} - \lambda \delta_{pq} + \Gamma_{pq}^{2N} + \Gamma_{pq}^{3N} \quad (\text{C.6b})$$

$$= t_{pq} - \lambda \delta_{pq} + \sum_{rs} \bar{v}_{psqr} \rho_{rs} + \frac{1}{2} \sum_{rstu} \bar{w}_{prsqtu} \left(\rho_{us} \rho_{tr} + \frac{1}{2} \kappa_{rs}^* \kappa_{tu} \right), \quad (\text{C.6c})$$

$$\Upsilon_{pq} \equiv \Delta_{pq}^{2N} + \Delta_{pq}^{3N} \quad (\text{C.6d})$$

$$= \frac{1}{2} \sum_{rs} \bar{v}_{pqrs} \kappa_{rs} + \frac{1}{2} \sum_{rstu} \bar{w}_{rpqstu} \rho_{sr} \kappa_{tu}, \quad (\text{C.6e})$$

$$\Theta_{pqrs} \equiv \bar{v}_{pqrs} + \sum_{tu} \bar{w}_{pqtrsu} \rho_{ut}, \quad (\text{C.6f})$$

$$\Xi_{pqrs} \equiv \frac{1}{2} \sum_{tu} \bar{w}_{pqrstu} \kappa_{tu}. \quad (\text{C.6g})$$

C.3 HAMILTONIAN OPERATOR \hat{H}

Similarly to the grand potential case, one uses, along with the expressions in appendix C.1, four one- and two-body operators whose matrix elements are given in an arbitrary single-particle basis by

$$\Lambda_{pq} \equiv t_{pq} + \Gamma_{pq}^{2N} + \Gamma_{pq}^{3N} \quad (\text{C.7a})$$

$$= t_{pq} + \sum_{rs} \bar{v}_{psqr} \rho_{rs} + \frac{1}{2} \sum_{rstu} \bar{w}_{prsqtu} \left(\rho_{us} \rho_{tr} + \frac{1}{2} \kappa_{rs}^* \kappa_{tu} \right), \quad (\text{C.7b})$$

$$\Upsilon_{pq} \equiv \Delta_{pq}^{2N} + \Delta_{pq}^{3N} \quad (\text{C.7c})$$

$$= \frac{1}{2} \sum_{rs} \bar{v}_{pqrs} \kappa_{rs} + \frac{1}{2} \sum_{rstu} \bar{w}_{rpqstu} \rho_{sr} \kappa_{tu}, \quad (\text{C.7d})$$

$$\Theta_{pqrs} \equiv \bar{v}_{pqrs} + \sum_{tu} \bar{w}_{pqtrsu} \rho_{ut}, \quad (\text{C.7e})$$

$$\Xi_{pqrs} \equiv \frac{1}{2} \sum_{tu} \bar{w}_{pqrstu} \kappa_{tu}. \quad (\text{C.7f})$$

C.4 PARTICLE-NUMBER OPERATOR \hat{A}

Significant simplifications arise for the particle-number operator \hat{A} ,

$$\Lambda_{pq} \equiv a_{pq} \quad (\text{C.8a})$$

$$= \delta_{pq}, \quad (\text{C.8b})$$

$$\Upsilon_{pq} \equiv 0, \quad (\text{C.8c})$$

$$\Theta_{pqrs} \equiv 0, \quad (\text{C.8d})$$

$$\Xi_{pqrs} \equiv 0. \quad (\text{C.8e})$$

C.5 \hat{A}^2 OPERATOR

The \hat{A}^2 operator can be written using the work accomplished for a generic operator in appendix C.1, making use of one- and two-body operators whose matrix elements are given in an arbitrary single-particle basis by

$$\Lambda_{pq} \equiv a_{pq}^{(1)} + \sum_{rs} \bar{a}_{psqr}^{(2)} \rho_{rs} \quad (\text{C.9a})$$

$$= \delta_{pq} + \sum_{rs} 2(\delta_{pr}\delta_{qs} - \delta_{ps}\delta_{qr}) \rho_{rs} , \quad (\text{C.9b})$$

$$\Upsilon_{pq} \equiv \frac{1}{2} \sum_{rs} \bar{a}_{pqrs}^{(2)} \kappa_{rs} \quad (\text{C.9c})$$

$$= \sum_{rs} (\delta_{pr}\delta_{qs} - \delta_{ps}\delta_{qr}) \kappa_{rs} , \quad (\text{C.9d})$$

$$\Theta_{pqrs} \equiv \bar{a}_{pqrs}^{(2)} \quad (\text{C.9e})$$

$$= 2(\delta_{pr}\delta_{qs} - \delta_{ps}\delta_{qr}) , \quad (\text{C.9f})$$

$$\Xi_{pqrs} \equiv 0 . \quad (\text{C.9g})$$

D

Unperturbed Propagator

In the following we will derive the different unperturbed propagators present in BMBPT, i.e., all different components of the matrix propagator

$$\mathbf{G}^0 = \begin{pmatrix} G^{+- (0)} & G^{-- (0)} \\ G^{++ (0)} & G^{-+ (0)} \end{pmatrix}. \quad (\text{D.1})$$

Recall for the following derivation the definition of the generalized density matrix

$$\mathbf{R} = \begin{pmatrix} \frac{\langle \Phi | \beta_p^\dagger \beta_q | \Phi \rangle}{\langle \Phi | \Phi \rangle} & \frac{\langle \Phi | \beta_p \beta_q | \Phi \rangle}{\langle \Phi | \Phi \rangle} \\ \frac{\langle \Phi | \beta_p^\dagger \beta_q^\dagger | \Phi \rangle}{\langle \Phi | \Phi \rangle} & \frac{\langle \Phi | \beta_p \beta_q^\dagger | \Phi \rangle}{\langle \Phi | \Phi \rangle} \end{pmatrix} \equiv \begin{pmatrix} R_{pq}^{+-} & R_{pq}^{--} \\ R_{pq}^{++} & R_{pq}^{-+} \end{pmatrix} = \begin{pmatrix} 0 & 0 \\ 0 & 1 \end{pmatrix}, \quad (\text{D.2})$$

which will be used subsequently.

DERIVATION OF NORMAL PROPAGATORS $G^{+- (0)}$ AND $G^{-+ (0)}$

We start with the derivation of

$$\begin{aligned} G_{k_1 k_2}^{+- (0)}(\tau_1, \tau_2) &= \frac{\langle \Phi | \mathbb{T}[\beta_{k_1}^\dagger(\tau_1) \beta_{k_2}(\tau_2)] | \Phi \rangle}{\langle \Phi | \Phi \rangle} \\ &= +\theta(\tau_1 - \tau_2) \frac{\langle \Phi | \beta_{k_1}^\dagger(\tau_1) \beta_{k_2}(\tau_2) | \Phi \rangle}{\langle \Phi | \Phi \rangle} \\ &\quad - \theta(\tau_2 - \tau_1) \frac{\langle \Phi | \beta_{k_2}(\tau_2) \beta_{k_1}^\dagger(\tau_1) | \Phi \rangle}{\langle \Phi | \Phi \rangle} \\ &= +\theta(\tau_1 - \tau_2) e^{\tau_1 E_{k_1}} e^{-\tau_2 E_{k_2}} \frac{\langle \Phi | \beta_{k_1}^\dagger \beta_{k_2} | \Phi \rangle}{\langle \Phi | \Phi \rangle} \end{aligned}$$

$$\begin{aligned}
 & -\theta(\tau_2 - \tau_1)e^{\tau_1 E_{k_1}} e^{-\tau_2 E_{k_2}} \frac{\langle \Phi | \beta_{k_2} \beta_{k_1}^\dagger | \Phi \rangle}{\langle \Phi | \Phi \rangle} \\
 & = +\theta(\tau_1 - \tau_2)e^{\tau_1 E_{k_1}} e^{-\tau_2 E_{k_2}} R_{k_1 k_2}^{+-} - \theta(\tau_2 - \tau_1)e^{\tau_1 E_{k_1}} e^{-\tau_2 E_{k_2}} R_{k_2 k_1}^{-+} \\
 & = -\theta(\tau_2 - \tau_1)e^{\tau_1 E_{k_1}} e^{-\tau_2 E_{k_2}} \delta_{k_2 k_1} \\
 & = -\theta(\tau_2 - \tau_1)e^{-(\tau_2 - \tau_1)E_{k_1}} \delta_{k_1 k_2} .
 \end{aligned}$$

and similarly for the other normal propagator

$$\begin{aligned}
 G_{k_1 k_2}^{-+(0)}(\tau_1, \tau_2) & = \frac{\langle \Phi | \mathbb{T}[\beta_{k_1}(\tau_1) \beta_{k_2}^\dagger(\tau_2)]}{\langle \Phi | \Phi \rangle} \\
 & = +\theta(\tau_1 - \tau_2) \frac{\langle \Phi | \beta_{k_1}(\tau_1) \beta_{k_2}^\dagger(\tau_2) | \Phi \rangle}{\langle \Phi | \Phi \rangle} \\
 & \quad - \theta(\tau_2 - \tau_1) \frac{\langle \Phi | \beta_{k_2}^\dagger(\tau_2) \beta_{k_1}(\tau_1) | \Phi \rangle}{\langle \Phi | \Phi \rangle} \\
 & = +\theta(\tau_1 - \tau_2)e^{-\tau_1 E_{k_1}} e^{\tau_2 E_{k_2}} \frac{\langle \Phi | \beta_{k_1} \beta_{k_2}^\dagger | \Phi \rangle}{\langle \Phi | \Phi \rangle} \\
 & \quad - \theta(\tau_2 - \tau_1)e^{-\tau_1 E_{k_1}} e^{\tau_2 E_{k_2}} \frac{\langle \Phi | \beta_{k_2}^\dagger \beta_{k_1} | \Phi \rangle}{\langle \Phi | \Phi \rangle} \\
 & = +\theta(\tau_1 - \tau_2)e^{-\tau_1 E_{k_1}} e^{\tau_2 E_{k_2}} R_{k_1 k_2}^{-+} - \theta(\tau_2 - \tau_1)e^{\tau_1 E_{k_1}} e^{-\tau_2 E_{k_2}} R_{k_2 k_1}^{+-} \\
 & = -\theta(\tau_1 - \tau_2)e^{-\tau_1 E_{k_1}} e^{\tau_2 E_{k_2}} \delta_{k_1 k_2} \\
 & = -\theta(\tau_1 - \tau_2)e^{-(\tau_1 - \tau_2)E_{k_1}} \delta_{k_1 k_2} .
 \end{aligned}$$

DERIVATION OF ANOMALOUS PROPAGATORS $G^{--(0)}$ AND $G^{++(0)}$

Similarly, we derive the anomalous propagators

$$\begin{aligned}
 G_{k_1 k_2}^{--(0)}(\tau_1, \tau_2) & = \frac{\langle \Phi | \mathbb{T}[\beta_{k_1}(\tau_1) \beta_{k_2}(\tau_2)]}{\langle \Phi | \Phi \rangle} \\
 & = +\theta(\tau_1 - \tau_2) \frac{\langle \Phi | \beta_{k_1}(\tau_1) \beta_{k_2}(\tau_2) | \Phi \rangle}{\langle \Phi | \Phi \rangle} \\
 & \quad - \theta(\tau_2 - \tau_1) \frac{\langle \Phi | \beta_{k_2}(\tau_2) \beta_{k_1}(\tau_1) | \Phi \rangle}{\langle \Phi | \Phi \rangle} \\
 & = +\theta(\tau_1 - \tau_2)e^{-\tau_1 E_{k_1}} e^{-\tau_2 E_{k_2}} \frac{\langle \Phi | \beta_{k_1} \beta_{k_2} | \Phi \rangle}{\langle \Phi | \Phi \rangle} \\
 & \quad - \theta(\tau_2 - \tau_1)e^{-\tau_1 E_{k_1}} e^{-\tau_2 E_{k_2}} \frac{\langle \Phi | \beta_{k_2} \beta_{k_1} | \Phi \rangle}{\langle \Phi | \Phi \rangle} \\
 & = +\theta(\tau_1 - \tau_2)e^{-\tau_1 E_{k_1}} e^{-\tau_2 E_{k_2}} R_{k_1 k_2}^{--} - \theta(\tau_2 - \tau_1)e^{-\tau_1 E_{k_1}} e^{-\tau_2 E_{k_2}} R_{k_2 k_1}^{--} \\
 & = 0
 \end{aligned}$$

and

$$\begin{aligned}
G_{k_1 k_2}^{++(0)}(\tau_1, \tau_2) &= \frac{\langle \Phi | T[\beta_{k_1}^\dagger(\tau_1) \beta_{k_2}^\dagger(\tau_2)] | \Phi \rangle}{\langle \Phi | \Phi \rangle} \\
&= +\theta(\tau_1 - \tau_2) \frac{\langle \Phi | \beta_{k_1}^\dagger(\tau_1) \beta_{k_2}^\dagger(\tau_2) | \Phi \rangle}{\langle \Phi | \Phi \rangle} \\
&\quad - \theta(\tau_2 - \tau_1) \frac{\langle \Phi | \beta_{k_2}^\dagger(\tau_2) \beta_{k_1}^\dagger(\tau_1) | \Phi \rangle}{\langle \Phi | \Phi \rangle} \\
&= +\theta(\tau_1 - \tau_2) e^{\tau_1 E_{k_1}} e^{\tau_2 E_{k_2}} \frac{\langle \Phi | \beta_{k_1}^\dagger \beta_{k_2}^\dagger | \Phi \rangle}{\langle \Phi | \Phi \rangle} \\
&\quad - \theta(\tau_2 - \tau_1) e^{\tau_1 E_{k_1}} e^{\tau_2 E_{k_2}} \frac{\langle \Phi | \beta_{k_2}^\dagger \beta_{k_1}^\dagger | \Phi \rangle}{\langle \Phi | \Phi \rangle} \\
&= +\theta(\tau_1 - \tau_2) e^{\tau_1 E_{k_1}} e^{\tau_2 E_{k_2}} R_{k_1 k_2}^{++} - \theta(\tau_2 - \tau_1) e^{\tau_1 E_{k_1}} e^{\tau_2 E_{k_2}} R_{k_2 k_1}^{++} \\
&= 0.
\end{aligned}$$

which both vanish due to the appearance of $R^{qq'}$ with $q = q'$.

E

Spherical Bogoliubov Many-Body Perturbation Theory

In the following we discuss the angular-momentum coupling used in spherical BMBPT which is naturally formulated in quasiparticle space. The definitions of the relevant coupling symbols can be found in chapter 1 of this document.

E.1 SPHERICAL HARTREE-FOCK-BOGOLIUBOV THEORY

We start with a short discussion of spherical HFB theory and quote expressions of the reduced matrix elements of the quantities that enter BMBPT formulas.

The general Bogoliubov transformation has the form

$$\hat{\beta}_k^\dagger = \sum_a U_{ak} c_a^\dagger + V_{ak} \hat{c}_a. \quad (\text{E.1})$$

In the calculations the single-particle basis is taken as a harmonic oscillator (HO) basis carrying spherical symmetry, i.e., $a = (n, l, j, m, t)$. In the following we will equivalently describe single-particle states via $a = (n, \pi, j, m, t)$ where $\pi = (-1)^l$ defines the *parity* of a single-particle state.

Writing out the Bogoliubov transformation with respect to the quantum numbers leaves us with

$$\hat{\beta}_{n_k \pi_k j_k m_k t_k}^\dagger = \sum_{n \pi j m t} U_{n \pi j m t n_k \pi_k j_k m_k t_k} \hat{c}_{n \pi j m t}^\dagger + V_{n \pi j m t n_k \pi_k j_k m_k t_k} \hat{c}_{n \pi j m t} \quad (\text{E.2})$$

We will now derive the reduced matrix elements of the HFB quantities involved when using

a spherical formulation. In the following upper indices denote quantum numbers a given operator is diagonal in. In a spherical scheme any scalar operator is diagonal in the projection quantum number of total angular momentum m (and is independent of it). For the sake of brevity we suppress the m quantum number in the upper indices and, additionally, use the short-hand notation for the matrix elements of \hat{o}

$$\tilde{o}_{n_1 n_2}^{(\pi j t)_1} \equiv \tilde{o}_{n_1 n_2}^{(\pi_1 j_1 t_1)}. \quad (\text{E.3})$$

When the system under consideration is constrained to be in a 0^- state the transformation matrices U, V possess the following symmetries

$$U_{n_1 \pi_1 j_1 m_1 t_1; n_2 \pi_2 j_2 m_2 t_2} = \tilde{\delta}_{12} \delta_{m_1 m_2} \tilde{U}_{n_1 n_2}^{(\pi j t)_2} \quad (\text{E.4})$$

$$V_{n_1 \pi_1 j_1 m_1 t_1; n_2 \pi_2 j_2 m_2 t_2} = (-1)^{j_1 - m_1} \tilde{\delta}_{12} \delta_{m_1 - m_2} \tilde{V}_{n_1 n_2}^{(\pi j t)_2}, \quad (\text{E.5})$$

where we introduced the 'spherical' Kronecker delta

$$\tilde{\delta}_{12} \equiv \delta_{\pi_1 \pi_2} \delta_{j_1 j_2} \delta_{t_1 t_2}. \quad (\text{E.6})$$

The reduced HFB one-body densities, obtained from (13.9) and (13.10), are given by

$$\rho_{n_1 \pi_1 j_1 m_1 t_1; n_2 \pi_2 j_2 m_2 t_2} = \tilde{\delta}_{12} \delta_{m_1 m_2} \tilde{\rho}_{n_1 n_2}^{(\pi j t)_2}, \quad (\text{E.7})$$

$$\kappa_{n_1 \pi_1 j_1 m_1 t_1; n_2 \pi_2 j_2 m_2 t_2} = \tilde{\delta}_{12} \delta_{m_1 - m_2} (-1)^{j_1 - m_1} \tilde{\kappa}_{n_1 n_2}^{(\pi j t)_2}, \quad (\text{E.8})$$

which consequently leads to (cf. (13.19) and (13.20)),

$$\Gamma_{n_1 \pi_1 j_1 m_1 t_1; n_2 \pi_2 j_2 m_2 t_2} = \tilde{\delta}_{12} \delta_{m_1 m_2} \tilde{\Gamma}_{n_1 n_2}^{(\pi j t)_2}, \quad (\text{E.9})$$

$$\Delta_{n_1 \pi_1 j_1 m_1 t_1; n_2 \pi_2 j_2 m_2 t_2} = \tilde{\delta}_{12} \delta_{m_1 - m_2} (-1)^{j_1 - m_1} \tilde{\Delta}_{n_1 n_2}^{(\pi j t)_2}. \quad (\text{E.10})$$

Note the difference in diagonality of ρ and κ with respect to the magnetic quantum numbers.

From this the HF Hamiltonian reads as

$$\begin{aligned} h_{n_1 \pi_1 j_1 m_1 t_1; n_2 \pi_2 j_2 m_2 t_2} &= t_{n_1 \pi_1 j_1 m_1 t_1; n_2 \pi_2 j_2 m_2 t_2} + \Gamma_{n_1 \pi_1 j_1 m_1 t_1; n_2 \pi_2 j_2 m_2 t_2} - \lambda \mathbb{1} \\ &= \tilde{\delta}_{12} \delta_{m_1 m_2} \tilde{h}_{n_1 n_2}^{(\pi j t)_2}. \end{aligned} \quad (\text{E.11})$$

The above relations and their derivations with additional details on spherical formulas for the HFB energy can be found in Appendix B of [Her08].

E.2 ANGULAR-MOMENTUM COUPLING OF QUASIPARTICLE OPERATORS

Before proceeding with the angular-momentum coupling of the individual terms of a scalar operator \hat{O} , we briefly introduce the notion of tensor products of spherical tensor operators. For a thorough treatment of spherical tensor operators see Refs. [VMK88; Suh07].

COUPLING OF SPHERICAL TENSOR OPERATORS

In the following let \mathbf{T}_{L_1} and \mathbf{T}_{L_2} be two spherical tensors of rank L_1 and L_2 , respectively. We define the *tensor product* \mathbf{T}_{LM} by

$$\mathbf{T}_{LM} = \sum_{M_1 M_2} \begin{pmatrix} L_1 & L_2 & L \\ M_1 & M_2 & M \end{pmatrix} \mathbf{T}_{L_1 M_1} \mathbf{T}_{L_2 M_2} \equiv [T_{L_1} T_{L_2}]_{LM}. \quad (\text{E.12})$$

A particularly important case is given by the coupling of two spherical tensors of equal rank into a scalar

$$\begin{aligned} [\mathbf{T}_L \mathbf{S}_L]_{00} &= \sum_{M_1 M_2} \begin{pmatrix} L & L & 0 \\ M_1 & M_2 & 0 \end{pmatrix} \mathbf{T}_{L M_1} \mathbf{S}_{L M_2} \\ &= \sum_{M_1} \begin{pmatrix} L & L & 0 \\ M_1 & -M_1 & 0 \end{pmatrix} \mathbf{T}_{L M_1} \mathbf{S}_{L - M_1} \\ &= \sum_M (-1)^{L-M} \hat{L}^{-1} \mathbf{T}_{LM} \mathbf{S}_{L-M} \end{aligned} \quad (\text{E.13})$$

With this one conveniently defines the *scalar product* of two spherical tensors of equal rank by

$$\mathbf{T}_L \cdot \mathbf{S}_L \equiv (-1)^L \hat{L} [T_L S_L]_{00} = \sum_M (-1)^M \mathbf{T}_{LM} \mathbf{S}_{L-M}, \quad (\text{E.14})$$

where $\hat{J} = \sqrt{2J+1}$ denotes the 'hat symbol'.

SINGLE-PARTICLE CREATORS AND ANNIHILATORS

Consider now a single-particle state $|k\rangle$ labelled via $(n_k l_k j_k m_k t_k)$. The corresponding single-particle creation operator

$$\hat{c}_{n_k l_k j_k m_k t_k}^\dagger \equiv \mathcal{B}_{j_k m_k} \quad (\text{E.15})$$

is the m_k component of a spherical tensor of rank j_k . Similarly, the quantity ¹

¹We note that there is another convention for the definition of annihilators in proper tensor form using

$$(-1)^{m_k} \hat{c}_{n_k l_k j_k -m_k t_k} = \bar{\mathcal{B}}_{j_k m_k}.$$

$$(-1)^{j_k-m_k} \hat{c}_{n_k l_k j_k -m_k t_k} \equiv \bar{\mathcal{B}}_{j_k m_k}, \quad (\text{E.16})$$

defines a spherical tensor of rank m_k as well. With this the tensor product of a creation and annihilation operator is given by

$$\begin{aligned} \hat{c}_{n_{k_1} \pi_{k_1} j_{k_1} m_{k_1} t_{k_1}}^\dagger \hat{c}_{n_{k_2} \pi_{k_2} j_{k_2} m_{k_2} t_{k_2}} &= (-1)^{j_{k_2}-m_{k_2}} \mathcal{B}_{j_{k_1} m_{k_1}} \bar{\mathcal{B}}_{j_{k_2}-m_{k_2}} \\ &= (-1)^{j_{k_2}-m_{k_2}} \sum_{JM} \begin{pmatrix} j_{k_1} & j_{k_2} & J \\ m_{k_1} & -m_{k_2} & M \end{pmatrix} \left[\mathcal{B}_{j_{k_1}} \bar{\mathcal{B}}_{j_{k_2}} \right]_{JM}, \end{aligned} \quad (\text{E.17})$$

where $\left[\mathcal{B}_{j_{k_1}} \bar{\mathcal{B}}_{j_{k_2}} \right]_{JM}$ is the M component of a spherical tensor of rank J . Analogously, we get for the coupling of two creation operators

$$\begin{aligned} \hat{c}_{n_{k_1} \pi_{k_1} j_{k_1} m_{k_1} t_{k_1}}^\dagger \hat{c}_{n_{k_2} \pi_{k_2} j_{k_2} m_{k_2} t_{k_2}}^\dagger &= \mathcal{B}_{j_{k_1} m_{k_1}} \mathcal{B}_{j_{k_2} m_{k_2}} \\ &= \sum_{JM} \begin{pmatrix} j_{k_1} & j_{k_2} & J \\ m_{k_1} & m_{k_2} & M \end{pmatrix} \left[\mathcal{B}_{j_{k_1}} \mathcal{B}_{j_{k_2}} \right]_{JM}, \end{aligned} \quad (\text{E.18})$$

and of two annihilation operators

$$\begin{aligned} \hat{c}_{n_{k_1} \pi_{k_1} j_{k_1} m_{k_1} t_{k_1}} \hat{c}_{n_{k_2} \pi_{k_2} j_{k_2} m_{k_2} t_{k_2}} &= (-1)^{j_{k_1}+j_{k_2}-m_{k_1}-m_{k_2}} \bar{\mathcal{B}}_{j_{k_1}-m_{k_1}} \bar{\mathcal{B}}_{j_{k_2}-m_{k_2}} \\ &= (-1)^{j_{k_1}+j_{k_2}-m_{k_1}-m_{k_2}} \sum_{JM} \begin{pmatrix} j_{k_1} & j_{k_2} & J \\ -m_{k_1} & -m_{k_2} & M \end{pmatrix} \left[\bar{\mathcal{B}}_{j_{k_1}} \bar{\mathcal{B}}_{j_{k_2}} \right]_{JM}, \end{aligned} \quad (\text{E.19})$$

respectively.

USEFUL IDENTITIES

In the following we make extensive use of the following formula [Wol16]

$$\begin{aligned} &\sum_{m_1 m_2 m_3 m_4 M'} (-1)^{j_1+j_2+j_3+j_4+J'-m_1-m_2-m_3-m_4-M'} \begin{pmatrix} j_2 & J & j_1 \\ m_2 & -M & m_1 \end{pmatrix}_{\mathbf{3j}} \begin{pmatrix} j_1 & j_4 & J' \\ -m_1 & m_4 & M' \end{pmatrix}_{\mathbf{3j}} \\ &\times \begin{pmatrix} j_4 & J'' & j_3 \\ -m_4 & M'' & m_3 \end{pmatrix}_{\mathbf{3j}} \begin{pmatrix} j_3 & j_2 & J' \\ -m_3 & -m_2 & -M' \end{pmatrix}_{\mathbf{3j}} = (-1)^{J-M} \hat{j}^{-2} \delta_{JJ''} \delta_{MM''} \left\{ \begin{matrix} j_1 & j_2 & J \\ j_3 & j_4 & J' \end{matrix} \right\} \end{aligned} \quad (\text{E.20})$$

which relates Wigner $3j$ - and $6j$ -symbols as introduced in chapter 1.

However, since the derivations of the spherical HFB quantities were performed using the definition given in the main body of the text, we will stick to this convention.

E.3 CROSS COUPLING OF MATRIX ELEMENTS

From the definition of m -scheme matrix elements we see that there is no common block structure with respect to (M, Π) shared by all $\hat{O}^{[4]}$ matrix elements. While for example

$$m_{k_1} + m_{k_2} + m_{k_3} = m_{k_4} \quad \text{and} \quad \pi_{k_1}\pi_{k_2}\pi_{k_3} = \pi_{k_4} \quad (\text{E.21})$$

for $O_{k_1 k_2 k_3 k_4}^{31}$,

$$m_{k_1} + m_{k_2} = m_{k_3} + m_{k_4} \quad \text{and} \quad \pi_{k_1}\pi_{k_2} = \pi_{k_3}\pi_{k_4} \quad (\text{E.22})$$

holds for $O_{k_1 k_2 k_3 k_4}^{22}$. For the sake of simplicity and the efficiency of the numerical implementation it is desirable for all $\hat{O}^{[2]}$ and $\hat{O}^{[4]}$ matrix elements to share the same block structure.

Therefore, it is convenient to define *cross-coupled matrix elements* by [SHD14]

$$\tilde{O}_{k_1 k_2 k_3 k_4}^{40} \equiv O_{k_1 k_2 \bar{k}_3 \bar{k}_4}^{40}, \quad (\text{E.23a})$$

$$\tilde{O}_{k_1 k_2 k_3 k_4}^{04} \equiv O_{k_1 \bar{k}_2 k_3 k_4}^{04}, \quad (\text{E.23b})$$

$$\tilde{O}_{k_1 k_2 k_3 k_4}^{22} \equiv O_{k_1 k_2 k_3 k_4}^{22}, \quad (\text{E.23c})$$

$$\tilde{O}_{k_1 k_2 k_3 k_4}^{31} \equiv O_{k_1 k_2 \bar{k}_3 k_4}^{31}, \quad (\text{E.23d})$$

$$\tilde{O}_{k_1 k_2 k_3 k_4}^{13} \equiv O_{k_1 \bar{k}_2 k_3 k_4}^{13}, \quad (\text{E.23e})$$

$$\tilde{O}_{k_1 k_2}^{11} \equiv O_{k_1 k_2}^{11}, \quad (\text{E.23f})$$

$$\tilde{O}_{k_1 k_2}^{20} \equiv O_{k_1 \bar{k}_2}^{20}, \quad (\text{E.23g})$$

$$\tilde{O}_{k_1 k_2}^{02} \equiv O_{\bar{k}_1 k_2}^{02}, \quad (\text{E.23h})$$

where we introduced the notation,

$$\bar{k} \equiv (n_k, l_k, j_k, -m_k, t_k). \quad (\text{E.24})$$

By means of the above introduced matrix elements all quantities \tilde{O}^{ij} with $ij = 40, 04, 22, 31, 13$ carry the same (Π, M) block structure such that

$$M = m_{k_1} + m_{k_2} = m_{k_3} + m_{k_4}, \quad (\text{E.25})$$

$$\Pi = \pi_{k_1}\pi_{k_2} = \pi_{k_3}\pi_{k_4}. \quad (\text{E.26})$$

Furthermore, we get for \tilde{O}^{ij} with $ij = 20, 11, 02$ that

$$m_{k_1} = m_{k_2}, \quad (\text{E.27})$$

$$\pi_{k_1} = \pi_{k_2}. \quad (\text{E.28})$$

We note that the introduction of cross-coupled matrix elements for $O_{k_1 k_2 k_3 k_4}^{22}$ and $O_{k_1 k_2}^{11}$ is trivial since the operator already possesses the desired diagonality with respect to M and Π .

In the following we perform the angular-momentum coupling of cross-coupled matrix elements of an arbitrary *scalar* operator with anti-symmetrized two-body matrix elements denoted by $\bar{o}_{l_1 l_2 l_3 l_4}$.²

E.3.1 ANGULAR-MOMENTUM COUPLING OF $\hat{O}^{[22]}$

The m -scheme matrix element of $\hat{O}^{[22]}$ is given by

$$\begin{aligned} \tilde{O}_{k_1 k_2 k_3 k_4}^{22} = \sum_{l_1 l_2 l_3 l_4} \bar{o}_{l_1 l_2 l_3 l_4} & \left(U_{l_1 k_1}^* U_{l_2 k_2}^* U_{l_3 k_3} U_{l_4 k_4} + V_{l_3 k_1}^* V_{l_4 k_2}^* V_{l_1 k_3} V_{l_2 k_4} + U_{l_1 k_1}^* V_{l_4 k_2}^* V_{l_2 k_3} U_{l_3 k_4} \right. \\ & \left. - V_{l_4 k_1}^* U_{l_1 k_2}^* V_{l_2 k_3} U_{l_3 k_4} - U_{l_1 k_1}^* V_{l_4 k_2}^* U_{l_3 k_3} V_{l_2 k_4} + V_{l_4 k_1}^* U_{l_1 k_2}^* U_{l_3 k_3} V_{l_2 k_4} \right). \end{aligned} \quad (\text{E.29})$$

We start with transforming the creation and annihilation operators to a spherical basis. For a generic operator O this yields the following expression

$$\begin{aligned} \hat{O}^{[22]} &= \frac{1}{4} \sum_{k_1 k_2 k_3 k_4} O_{k_1 k_2 k_3 k_4}^{[22]} \hat{\beta}_{k_1}^\dagger \hat{\beta}_{k_2}^\dagger \hat{\beta}_{k_4} \hat{\beta}_{k_3} \\ &= -\frac{1}{4} \sum_{\tilde{k}_1 \tilde{k}_2 \tilde{k}_3 \tilde{k}_4} \sum_{\substack{m_{k_1} m_{k_2} \\ m_{k_3} m_{k_4}}} (-1)^{j_{k_3} - m_{k_3} + j_{k_4} - m_{k_4}} O_{k_1 k_2 k_3 k_4}^{[22]} \mathcal{B}_{k_1 m_{k_1}} \mathcal{B}_{k_2 m_{k_2}} \bar{\mathcal{B}}_{j_{k_3} - m_{k_3}} \bar{\mathcal{B}}_{j_{k_4} - m_{k_4}} \\ &= -\frac{1}{4} \sum_{\tilde{k}_1 \tilde{k}_2 \tilde{k}_3 \tilde{k}_4} \sum_{\substack{m_{k_1} m_{k_2} \\ m_{k_3} m_{k_4}}} \sum_{J J' M M'} (-1)^{j_{k_3} - m_{k_3} + j_{k_4} - m_{k_4}} O_{k_1 k_2 k_3 k_4}^{[22]} \\ &\quad \times \begin{pmatrix} j_{k_1} & j_{k_2} & J \\ m_{k_1} & m_{k_2} & M \end{pmatrix} \begin{pmatrix} j_{k_3} & j_{k_4} & J' \\ -m_{k_3} & -m_{k_4} & M' \end{pmatrix} [\mathcal{B}_{k_1} \mathcal{B}_{k_2}]_{JM} [\bar{\mathcal{B}}_{k_3} \bar{\mathcal{B}}_{k_4}]_{J'M'} \\ &= -\frac{1}{4} \sum_{\tilde{k}_1 \tilde{k}_2 \tilde{k}_3 \tilde{k}_4} \sum_{\substack{m_{k_1} m_{k_2} \\ m_{k_3} m_{k_4}}} \sum_{\substack{J J' \\ M M'}} \tilde{O}_{k_1 k_2 k_3 k_4}^{[22]} \begin{pmatrix} j_{k_1} & j_{k_2} & J \\ m_{k_1} & m_{k_2} & M \end{pmatrix} \begin{pmatrix} j_{k_3} & j_{k_4} & J' \\ m_{k_3} & m_{k_4} & -M' \end{pmatrix} \\ &\quad \times (-1)^{J'+M'} [\mathcal{B}_{k_1} \mathcal{B}_{k_2}]_{JM} [\bar{\mathcal{B}}_{k_3} \bar{\mathcal{B}}_{k_4}]_{J'M'} \\ &= -\frac{1}{4} \sum_{\tilde{k}_1 \tilde{k}_2 \tilde{k}_3 \tilde{k}_4} \sum_{\substack{m_{k_1} m_{k_2} \\ m_{k_3} m_{k_4}}} \sum_{\substack{J J' \\ M M'}} \tilde{O}_{k_1 k_2 k_3 k_4}^{[22]} \begin{pmatrix} j_{k_1} & j_{k_2} & J \\ m_{k_1} & m_{k_2} & M \end{pmatrix} \begin{pmatrix} j_{k_3} & j_{k_4} & J' \\ m_{k_3} & m_{k_4} & M' \end{pmatrix} \\ &\quad \times (-1)^{J'+M'} [\mathcal{B}_{j_{k_1}} \mathcal{B}_{j_{k_2}}]_{JM} [\bar{\mathcal{B}}_{k_3} \bar{\mathcal{B}}_{k_4}]_{J'-M'}, \end{aligned} \quad (\text{E.30})$$

²One can cut loose the restriction of scalar operators in the following derivation by allowing bra and ket indices of m -scheme matrix elements $o_{l_1 l_2 l_3 l_4}$ in single-particle space to couple to different total angular momenta. Since the many-body formalism at play, however, is restricted to scalar observables from the beginning we restrict ourselves to the coupling of scalar operators as well.

from which we define

$$\tilde{O}_{\tilde{k}_1\tilde{k}_2JM;\tilde{k}_3\tilde{k}_4J''M''}^{[22]} \equiv \sum_{\substack{m_{k_1}m_{k_2} \\ m_{k_3}m_{k_4}}} (-1)^{J''+M''+1} \tilde{O}_{k_1k_2k_3k_4}^{[22]} \begin{pmatrix} j_{k_1} & j_{k_2} & J \\ m_{k_1} & m_{k_2} & M \end{pmatrix} \begin{pmatrix} j_{k_3} & j_{k_4} & J'' \\ m_{k_3} & m_{k_4} & M'' \end{pmatrix}. \quad (\text{E.31})$$

We split the fully anti-symmetrized matrix elements into its six parts and perform the angular-momentum coupling individually,

$$\begin{aligned} {}^1\tilde{O}_{k_1k_2JM;k_3k_4J''M''}^{[22]} &= (-1)^{J''+M''+1} \sum_{\substack{m_{k_1}m_{k_2} \\ m_{k_3}m_{k_4}}} \sum_{l_1l_2l_3l_4} \bar{o}_{l_1l_2l_3l_4} U_{l_1k_1}^* U_{l_2k_2}^* U_{l_3k_3}^* U_{l_4k_4}^* \\ &\quad \begin{pmatrix} j_{k_1} & j_{k_2} & J \\ m_{k_1} & m_{k_2} & M \end{pmatrix} \begin{pmatrix} j_{k_3} & j_{k_4} & J'' \\ m_{k_3} & m_{k_4} & M'' \end{pmatrix} \\ &= (-1)^{J''+M''+1} \sum_{\substack{m_{k_1}m_{k_2} \\ m_{k_3}m_{k_4}}} \sum_{J'M'} \sum_{n_1n_2n_3n_4} \bar{o}_{n_1l_1j_{k_1}n_2l_2j_{k_2}n_3l_3j_{k_3}n_4l_4j_{k_4}}^{J'} \\ &\quad \times \tilde{U}_{n_1n_{k_1}}^{(\pi jt)_{k_1}} \tilde{U}_{n_2n_{k_2}}^{(\pi jt)_{k_2}} \tilde{U}_{n_3n_{k_3}}^{(\pi jt)_{k_3}} \tilde{U}_{n_4n_{k_4}}^{(\pi jt)_{k_4}} \\ &\quad \times \begin{pmatrix} j_{k_1} & j_{k_2} & J \\ m_{k_1} & m_{k_2} & M \end{pmatrix} \begin{pmatrix} j_{k_3} & j_{k_4} & J'' \\ m_{k_3} & m_{k_4} & -M'' \end{pmatrix} \begin{pmatrix} j_{k_1} & j_{k_2} & J' \\ m_{k_1} & m_{k_2} & M' \end{pmatrix} \begin{pmatrix} j_{k_3} & j_{k_4} & J' \\ m_{k_3} & m_{k_4} & M' \end{pmatrix} \\ &= (-1)^{J+M+1} \sum_{n_1n_2n_3n_4} \bar{o}_{n_1l_1j_{k_1}n_2l_2j_{k_2}n_3l_3j_{k_3}n_4l_4j_{k_4}}^J \\ &\quad \times \tilde{U}_{n_1n_{k_1}}^{(\pi jt)_{k_1}} \tilde{U}_{n_2n_{k_2}}^{(\pi jt)_{k_2}} \tilde{U}_{n_3n_{k_3}}^{(\pi jt)_{k_3}} \tilde{U}_{n_4n_{k_4}}^{(\pi jt)_{k_4}} \delta_{JJ''} \delta_{MM''}, \end{aligned} \quad (\text{E.32})$$

$$\begin{aligned} {}^2\tilde{O}_{k_1k_2JM;k_3k_4J''M''}^{[22]} &= (-1)^{J''+M''+1} \sum_{\substack{m_{k_1}m_{k_2} \\ m_{k_3}m_{k_4}}} \sum_{l_1l_2l_3l_4} \bar{o}_{l_1l_2l_3l_4} V_{l_3k_1} V_{l_4k_2} V_{l_1k_3} V_{l_2k_4} \\ &\quad \times \begin{pmatrix} j_{k_1} & j_{k_2} & J \\ m_{k_1} & m_{k_2} & M \end{pmatrix} \begin{pmatrix} j_{k_3} & j_{k_4} & J'' \\ m_{k_3} & m_{k_4} & -M'' \end{pmatrix} \\ &= \sum_{\substack{m_{k_1}m_{k_2} \\ m_{k_3}m_{k_4}}} \sum_{J'M'} \sum_{n_1n_2n_3n_4} \bar{o}_{n_1l_1j_{k_3}n_2l_2j_{k_4}n_3l_3j_{k_1}n_4l_4j_{k_2}}^{J'} \\ &\quad \times (-1)^{J''+M+1+j_{k_1}+j_{k_2}+j_{k_3}+j_{k_4}+M'+M''} \tilde{V}_{n_1n_{k_3}}^{(\pi jt)_{k_3}} \tilde{V}_{n_2n_{k_4}}^{(\pi jt)_{k_4}} \tilde{V}_{n_3n_{k_1}}^{(\pi jt)_{k_1}} \tilde{V}_{n_4n_{k_2}}^{(\pi jt)_{k_2}} \\ &\quad \times \begin{pmatrix} j_{k_1} & j_{k_2} & J \\ m_{k_1} & m_{k_2} & M \end{pmatrix} \begin{pmatrix} j_{k_3} & j_{k_4} & J'' \\ m_{k_3} & m_{k_4} & M'' \end{pmatrix} \begin{pmatrix} j_{k_3} & j_{k_4} & J' \\ -m_{k_3} & -m_{k_4} & M' \end{pmatrix} \begin{pmatrix} j_{k_1} & j_{k_2} & J' \\ -m_{k_1} & -m_{k_2} & M' \end{pmatrix} \\ &= \sum_{n_1n_2n_3n_4} \bar{o}_{n_1l_1j_{k_3}n_2l_2j_{k_4}n_3l_3j_{k_1}n_4l_4j_{k_2}}^{J'} \tilde{V}_{n_1n_{k_3}}^{(\pi jt)_{k_3}} \tilde{V}_{n_2n_{k_4}}^{(\pi jt)_{k_4}} \tilde{V}_{n_3n_{k_1}}^{(\pi jt)_{k_1}} \tilde{V}_{n_4n_{k_2}}^{(\pi jt)_{k_2}} \\ &\quad \times \delta_{JJ''} \delta_{MM''} (-1)^{J+M+1}, \end{aligned} \quad (\text{E.33})$$

$$\begin{aligned}
 {}^3\tilde{O}_{k_1 k_2 J M; k_3 k_4 J'' M''}^{[22]} &= (-1)^{J''+M''+1} \sum_{\substack{m_{k_1} m_{k_2} \\ m_{k_3} m_{k_4}}} \sum_{l_1 l_2 l_3 l_4} \bar{o}_{l_1 l_2 l_3 l_4} U_{l_1 k_1} V_{l_4 k_2} V_{l_2 k_3} U_{l_3 k_4} \\
 &\times \begin{pmatrix} j_{k_1} & j_{k_2} \\ m_{k_1} & m_{k_2} \end{pmatrix} \begin{pmatrix} j_{k_3} & j_{k_4} \\ m_{k_3} & m_{k_4} \end{pmatrix} \begin{pmatrix} J \\ M \end{pmatrix} \begin{pmatrix} J'' \\ -M'' \end{pmatrix} \\
 &= \sum_{\substack{m_{k_1} m_{k_2} \\ m_{k_3} m_{k_4}}} \sum_{J' M'} \sum_{n_1 n_2 n_3 n_4} \bar{o}_{n_1 l_1 j t_{k_1} n_2 l_2 j t_{k_3} n_3 l_3 j t_{k_4} n_4 l_4 j t_{k_2}}^{J'} \\
 &\times (-1)^{J''+M''+1+j_{k_2}+j_{k_3}-m_{k_2}-m_{k_3}} \tilde{U}_{n_1 n_{k_1}}^{(\pi j t)_{k_1}} \tilde{V}_{n_4 n_{k_2}}^{(\pi j t)_{k_2}} \tilde{V}_{n_2 n_{k_3}}^{(\pi j t)_{k_3}} \tilde{U}_{n_3 n_{k_4}}^{(\pi j t)_{k_4}} \\
 &\times \begin{pmatrix} j_{k_1} & j_{k_2} \\ m_{k_1} & m_{k_2} \end{pmatrix} \begin{pmatrix} j_{k_3} & j_{k_4} \\ m_{k_3} & m_{k_4} \end{pmatrix} \begin{pmatrix} J \\ M \end{pmatrix} \begin{pmatrix} J'' \\ -M'' \end{pmatrix} \begin{pmatrix} j_{k_1} & j_{k_3} \\ m_{k_1} & -m_{k_3} \end{pmatrix} \begin{pmatrix} J' \\ M' \end{pmatrix} \begin{pmatrix} j_{k_4} & j_{k_2} \\ m_{k_4} & -m_{k_2} \end{pmatrix} \begin{pmatrix} J' \\ M' \end{pmatrix} \\
 &= (-1)^{j_{k_3}+j_{k_4}+1+M} \sum_{J'} \sum_{n_1 n_2 n_3 n_4} \bar{o}_{n_1 l_1 j t_{k_1} n_2 l_2 j t_{k_3} n_3 l_3 j t_{k_4} n_4 l_4 j t_{k_2}}^{J'} \\
 &\times \tilde{U}_{n_1 n_{k_1}}^{(\pi j t)_{k_1}} \tilde{V}_{n_4 n_{k_2}}^{(\pi j t)_{k_2}} \tilde{V}_{n_2 n_{k_3}}^{(\pi j t)_{k_3}} \tilde{U}_{n_3 n_{k_4}}^{(\pi j t)_{k_4}} \hat{j}^2 \begin{Bmatrix} j_{k_1} & j_{k_2} & J \\ j_{k_4} & j_{k_3} & J' \end{Bmatrix} \delta_{J J''} \delta_{M M''}, \quad (\text{E.34})
 \end{aligned}$$

$$\begin{aligned}
 {}^4\tilde{O}_{k_1 k_2 J M; k_3 k_4 J'' M''}^{[22]} &= (-1)^{J''+M''+1} \sum_{\substack{m_{k_1} m_{k_2} \\ m_{k_3} m_{k_4}}} \sum_{l_1 l_2 l_3 l_4} \bar{o}_{l_1 l_2 l_3 l_4} V_{l_4 k_1} U_{l_1 k_2} V_{l_2 k_3} \bar{U}_{l_3 k_4} \\
 &\times \begin{pmatrix} j_{k_1} & j_{k_2} \\ m_{k_1} & m_{k_2} \end{pmatrix} \begin{pmatrix} j_{k_3} & j_{k_4} \\ m_{k_3} & m_{k_4} \end{pmatrix} \begin{pmatrix} J \\ M \end{pmatrix} \begin{pmatrix} J'' \\ M'' \end{pmatrix} \\
 &= \sum_{\substack{m_{k_1} m_{k_2} \\ m_{k_3} m_{k_4}}} \sum_{J' M'} \sum_{n_1 n_2 n_3 n_4} \bar{o}_{n_1 l_1 j t_{k_2} n_2 l_2 j t_{k_3} n_3 l_3 j t_{k_4} n_4 l_4 j t_{k_1}}^{J'} \\
 &\times (-1)^{J''+M''+1+j_{k_1}+j_{k_3}-m_{k_1}-m_{k_3}} \tilde{V}_{n_4 n_{k_1}}^{(\pi j t)_{k_1}} \tilde{U}_{n_1 n_{k_2}}^{(\pi j t)_{k_2}} \tilde{V}_{n_2 n_{k_3}}^{(\pi j t)_{k_3}} \tilde{U}_{n_3 n_{k_4}}^{(\pi j t)_{k_4}} \\
 &\times \begin{pmatrix} j_{k_1} & j_{k_2} \\ m_{k_1} & m_{k_2} \end{pmatrix} \begin{pmatrix} j_{k_3} & j_{k_4} \\ m_{k_3} & m_{k_4} \end{pmatrix} \begin{pmatrix} J \\ M \end{pmatrix} \begin{pmatrix} J'' \\ M'' \end{pmatrix} \begin{pmatrix} j_{k_2} & j_{k_3} \\ m_{k_2} & -m_{k_3} \end{pmatrix} \begin{pmatrix} J' \\ M' \end{pmatrix} \begin{pmatrix} j_{k_4} & j_{k_1} \\ m_{k_4} & -m_{k_1} \end{pmatrix} \begin{pmatrix} J' \\ M' \end{pmatrix} \\
 &= \sum_{J'} \sum_{n_1 n_2 n_3 n_4} \bar{o}_{n_1 l_1 j t_{k_2} n_2 l_2 j t_{k_3} n_3 l_3 j t_{k_4} n_4 l_4 j t_{k_1}}^{J'} \tilde{V}_{n_4 n_{k_1}}^{(\pi j t)_{k_1}} \tilde{U}_{n_1 n_{k_2}}^{(\pi j t)_{k_2}} \tilde{V}_{n_2 n_{k_3}}^{(\pi j t)_{k_3}} \tilde{U}_{n_3 n_{k_4}}^{(\pi j t)_{k_4}} \\
 &\times \hat{j}^2 \begin{Bmatrix} j_{k_1} & j_{k_2} & J \\ j_{k_3} & j_{k_4} & J' \end{Bmatrix} (-1)^{J+M+1+j_{k_1}+j_{k_2}+j_{k_3}+j_{k_4}} \delta_{J J''} \delta_{M M''}, \quad (\text{E.35})
 \end{aligned}$$

$$\begin{aligned}
 {}^5\tilde{O}_{k_1 k_2 J M; k_3 k_4 J'' M''}^{[22]} &= (-1)^{J''+M''+1} \sum_{\substack{m_{k_1} m_{k_2} \\ m_{k_3} m_{k_4}}} \sum_{l_1 l_2 l_3 l_4} \bar{o}_{l_1 l_2 l_3 l_4} U_{l_1 k_1} V_{l_4 k_2} U_{l_3 k_3} V_{l_2 k_4} \\
 &\times \begin{pmatrix} j_{k_1} & j_{k_2} \\ m_{k_1} & m_{k_2} \end{pmatrix} \begin{pmatrix} j_{k_3} & j_{k_4} \\ m_{k_3} & m_{k_4} \end{pmatrix} \begin{pmatrix} J \\ M \end{pmatrix} \begin{pmatrix} J'' \\ M'' \end{pmatrix} \\
 &= \sum_{\substack{m_{k_1} m_{k_2} \\ m_{k_3} m_{k_4}}} \sum_{J' M'} \sum_{n_1 n_2 n_3 n_4} \bar{o}_{n_1 l_1 j t_{k_1} n_2 l_2 j t_{k_4} n_3 l_3 j t_{k_3} n_4 l_4 j t_{k_2}}^{J'}
 \end{aligned}$$

$$\begin{aligned}
 & \times (-1)^{J''+M''+1+j_{k_2}+j_{k_4}-m_{k_2}-m_{k_4}} \tilde{U}_{n_{l_1}n_{k_1}}^{(\pi jt)_{k_1}} \tilde{V}_{n_{l_4}n_{k_2}}^{(\pi jt)_{k_2}} \tilde{U}_{n_{l_3}n_{k_3}}^{(\pi jt)_{k_3}} \tilde{V}_{n_{l_2}n_{k_4}}^{(\pi jt)_{k_4}} \\
 & \times \begin{pmatrix} j_{k_1} & j_{k_2} & | & J \\ m_{k_1} & m_{k_2} & | & M \end{pmatrix} \begin{pmatrix} j_{k_3} & j_{k_4} & | & J'' \\ m_{k_3} & m_{k_4} & | & M'' \end{pmatrix} \begin{pmatrix} j_{k_1} & j_{k_4} & | & J' \\ m_{k_1} & -m_{k_4} & | & M' \end{pmatrix} \begin{pmatrix} j_{k_3} & j_{k_2} & | & J' \\ m_{k_3} & -m_{k_2} & | & M' \end{pmatrix} \\
 & = (-1)^{J+M+1} \sum_{J'} \sum_{n_{l_1}n_{l_2}n_{l_3}n_{l_4}} o_{n_{l_1}l_{j_{k_1}}n_{l_2}l_{j_{k_4}}n_{l_3}l_{j_{k_3}}n_{l_4}l_{j_{k_2}}}^{J'} \\
 & \times \tilde{U}_{n_{l_1}n_{k_1}}^{(\pi jt)_{k_1}} \tilde{V}_{n_{l_4}n_{k_2}}^{(\pi jt)_{k_2}} \tilde{U}_{n_{l_3}n_{k_3}}^{(\pi jt)_{k_3}} \tilde{V}_{n_{l_2}n_{k_4}}^{(\pi jt)_{k_4}} \hat{J}'^2 \begin{Bmatrix} j_{k_1} & j_{k_2} & J \\ j_{k_3} & j_{k_4} & J' \end{Bmatrix} \delta_{JJ''} \delta_{MM''}, \quad (\text{E.36})
 \end{aligned}$$

$$\begin{aligned}
 {}^6\tilde{O}_{k_1k_2JM;k_3k_4J''M''}^{[22]} & = (-1)^{J''+M''+1} \sum_{\substack{m_{k_1}m_{k_2} \\ m_{k_3}m_{k_4}}} \sum_{l_1l_2l_3l_4} \bar{o}_{l_1l_2l_3l_4} V_{l_4k_1} U_{l_1k_2} U_{l_3k_3} V_{l_2k_4} \\
 & \times \begin{pmatrix} j_{k_1} & j_{k_2} & | & J \\ m_{k_1} & m_{k_2} & | & M \end{pmatrix} \begin{pmatrix} j_{k_3} & j_{k_4} & | & J'' \\ m_{k_3} & m_{k_4} & | & M'' \end{pmatrix} \\
 & = \sum_{\substack{m_{k_1}m_{k_2} \\ m_{k_3}m_{k_4}}} \sum_{J'M'} \sum_{n_{l_1}n_{l_2}n_{l_3}n_{l_4}} \bar{o}_{n_{l_1}l_{j_{k_2}}n_{l_2}l_{j_{k_4}}n_{l_3}l_{j_{k_3}}n_{l_4}l_{j_{k_1}}}^{J'} \\
 & \times (-1)^{J''+M''+1+j_{k_1}+j_{k_4}-m_{k_1}-m_{k_4}} \tilde{V}_{n_{l_4}n_{k_1}}^{(\pi jt)_{k_1}} \tilde{U}_{n_{l_1}n_{k_2}}^{(\pi jt)_{k_2}} \tilde{U}_{n_{l_3}n_{k_3}}^{(\pi jt)_{k_3}} \tilde{V}_{n_{l_2}n_{k_4}}^{(\pi jt)_{k_4}} \\
 & \times \begin{pmatrix} j_{k_1} & j_{k_2} & | & J \\ m_{k_1} & m_{k_2} & | & M \end{pmatrix} \begin{pmatrix} j_{k_3} & j_{k_4} & | & J'' \\ m_{k_3} & m_{k_4} & | & M'' \end{pmatrix} \begin{pmatrix} j_{k_2} & j_{k_4} & | & J' \\ m_{k_2} & -m_{k_4} & | & M' \end{pmatrix} \begin{pmatrix} j_{k_3} & j_{k_1} & | & J' \\ m_{k_3} & -m_{k_1} & | & M' \end{pmatrix} \\
 & = \sum_{J'} \sum_{n_{l_1}n_{l_2}n_{l_3}n_{l_4}} \bar{o}_{n_{l_1}l_{j_{k_2}}n_{l_2}l_{j_{k_4}}n_{l_3}l_{j_{k_3}}n_{l_4}l_{j_{k_1}}}^{J'} \tilde{V}_{n_{l_4}n_{k_1}}^{(\pi jt)_{k_1}} \tilde{U}_{n_{l_1}n_{k_2}}^{(\pi jt)_{k_2}} \tilde{U}_{n_{l_3}n_{k_3}}^{(\pi jt)_{k_3}} \tilde{V}_{n_{l_2}n_{k_4}}^{(\pi jt)_{k_4}} \\
 & \times \hat{J}'^2 (-1)^{j_{k_1}+j_{k_2}+1+M} \begin{Bmatrix} j_{k_1} & j_{k_2} & J \\ j_{k_4} & j_{k_3} & J' \end{Bmatrix} \delta_{JJ''} \delta_{MM''}, \quad (\text{E.37})
 \end{aligned}$$

With this we define the J -coupled matrix element by

$$\tilde{O}_{\tilde{k}_1\tilde{k}_2JM;\tilde{k}_3\tilde{k}_4J''M''}^{[22]} \equiv (-1)^M \delta_{JJ''} \delta_{MM''} {}^J\tilde{O}_{\tilde{k}_1\tilde{k}_2\tilde{k}_3\tilde{k}_4}^{[22]} \quad (\text{E.38})$$

and thus finally arrive at

$$\begin{aligned}
 \hat{O}^{[22]} & = -\frac{1}{4} \sum_{\tilde{k}_1\tilde{k}_2\tilde{k}_3\tilde{k}_4} \sum_{JM} {}^J\tilde{O}_{\tilde{k}_1\tilde{k}_2\tilde{k}_3\tilde{k}_4}^{[22]} (-1)^M [\mathcal{B}_{j_{k_1}} \mathcal{B}_{j_{k_2}}]_{JM} [\bar{\mathcal{B}}_{j_{k_3}} \bar{\mathcal{B}}_{j_{k_4}}]_{J-M}, \\
 & = -\frac{1}{4} \sum_{\tilde{k}_1\tilde{k}_2\tilde{k}_3\tilde{k}_4} \sum_J {}^J\tilde{O}_{\tilde{k}_1\tilde{k}_2\tilde{k}_3\tilde{k}_4}^{[22]} [\mathcal{B}_{j_{k_1}} \mathcal{B}_{j_{k_2}}]_J \cdot [\bar{\mathcal{B}}_{j_{k_3}} \bar{\mathcal{B}}_{j_{k_4}}]_J, \quad (\text{E.39})
 \end{aligned}$$

which is the spherical representation of $\hat{O}^{[22]}$.

ANGULAR-MOMENTUM COUPLING OF \hat{O}^{40}

The m -scheme matrix element is given by

$$\begin{aligned}\tilde{O}_{k_1 k_2 k_3 k_4}^{40} &= O_{k_1 k_2 \bar{k}_3 \bar{k}_4}^{40} \\ &= \sum_{l_1 l_2 l_3 l_4} \Theta_{l_1 l_2 l_3 l_4} \left(U_{l_1 k_1}^* U_{l_2 k_2}^* V_{l_4 \bar{k}_3}^* V_{l_3 \bar{k}_4}^* - U_{l_1 k_1}^* V_{l_4 k_2}^* U_{l_2 \bar{k}_3}^* V_{l_3 \bar{k}_4}^* - V_{l_4 k_1}^* U_{l_2 k_2}^* U_{l_1 \bar{k}_3}^* V_{l_3 \bar{k}_4}^* \right. \\ &\quad \left. + U_{l_1 k_1}^* V_{l_4 k_2}^* V_{l_3 \bar{k}_3}^* U_{l_2 \bar{k}_4}^* + V_{l_4 k_1}^* U_{l_2 k_2}^* V_{l_3 \bar{k}_3}^* U_{l_1 \bar{k}_4}^* + V_{l_4 k_1}^* V_{l_3 k_2}^* U_{l_1 \bar{k}_3}^* U_{l_2 \bar{k}_4}^* \right). \quad (\text{E.40})\end{aligned}$$

The coupling of the operator yields

$$\begin{aligned}\hat{O}^{[40]} &= \frac{1}{24} \sum_{k_1 k_2 k_3 k_4} O_{k_1 k_2 k_3 k_4}^{[40]} \hat{\beta}_{k_1}^\dagger \hat{\beta}_{k_2}^\dagger \hat{\beta}_{k_3}^\dagger \hat{\beta}_{k_4}^\dagger \\ &= \frac{1}{24} \sum_{\tilde{k}_1 \tilde{k}_2 \tilde{k}_3 \tilde{k}_4} \sum_{\substack{m_{k_1} m_{k_2} \\ m_{k_3} m_{k_4}}} \sum_{\substack{J J' \\ M M'}} O_{k_1 k_2 k_3 k_4}^{[40]} \begin{pmatrix} j_{k_1} & j_{k_2} \\ m_{k_1} & m_{k_2} \end{pmatrix} \begin{pmatrix} j_{k_3} & j_{k_4} \\ m_{k_3} & m_{k_4} \end{pmatrix} \\ &\quad \times [\mathcal{B}_{j_{k_1}} \mathcal{B}_{j_{k_2}}]_{JM} [\mathcal{B}_{j_{k_3}} \mathcal{B}_{j_{k_4}}]_{J'M'} \\ &= \frac{1}{24} \sum_{\tilde{k}_1 \tilde{k}_2 \tilde{k}_3 \tilde{k}_4} \sum_{\substack{m_{k_1} m_{k_2} \\ m_{k_3} m_{k_4}}} \sum_{\substack{J J' \\ M M'}} \tilde{O}_{k_1 k_2 \bar{k}_3 \bar{k}_4}^{[40]} \begin{pmatrix} j_{k_1} & j_{k_2} \\ m_{k_1} & m_{k_2} \end{pmatrix} \begin{pmatrix} j_{k_3} & j_{k_4} \\ m_{k_3} & m_{k_4} \end{pmatrix} \\ &\quad \times [\mathcal{B}_{j_{k_1}} \mathcal{B}_{j_{k_2}}]_{JM} [\mathcal{B}_{j_{k_3}} \mathcal{B}_{j_{k_4}}]_{J'M'} \\ &= \frac{1}{24} \sum_{\tilde{k}_1 \tilde{k}_2 \tilde{k}_3 \tilde{k}_4} \sum_{\substack{m_{k_1} m_{k_2} \\ m_{k_3} m_{k_4}}} \sum_{\substack{J J' \\ M M'}} \tilde{O}_{k_1 k_2 k_3 k_4}^{[40]} \begin{pmatrix} j_{k_1} & j_{k_2} \\ m_{k_1} & m_{k_2} \end{pmatrix} \begin{pmatrix} j_{k_3} & j_{k_4} \\ -m_{k_3} & -m_{k_4} \end{pmatrix} \\ &\quad \times [\mathcal{B}_{j_{k_1}} \mathcal{B}_{j_{k_2}}]_{JM} [\mathcal{B}_{j_{k_3}} \mathcal{B}_{j_{k_4}}]_{J'M'} \\ &= \frac{1}{24} \sum_{\tilde{k}_1 \tilde{k}_2 \tilde{k}_3 \tilde{k}_4} \sum_{\substack{m_{k_1} m_{k_2} \\ m_{k_3} m_{k_4}}} \sum_{\substack{J J' \\ M M'}} \tilde{O}_{k_1 k_2 k_3 k_4}^{[40]} \begin{pmatrix} j_{k_1} & j_{k_2} \\ m_{k_1} & m_{k_2} \end{pmatrix} \begin{pmatrix} j_{k_3} & j_{k_4} \\ m_{k_3} & m_{k_4} \end{pmatrix} \\ &\quad \times (-1)^{j_{k_3} + j_{k_4} + J'} [\mathcal{B}_{j_{k_1}} \mathcal{B}_{j_{k_2}}]_{JM} [\mathcal{B}_{j_{k_3}} \mathcal{B}_{j_{k_4}}]_{J'M'} \quad (\text{E.41})\end{aligned}$$

and we define

$$\tilde{O}_{k_1 \bar{k}_2 JM; \bar{k}_3 \bar{k}_4 J' M'}^{[40]} \equiv \sum_{\substack{m_{k_1} m_{k_2} \\ m_{k_3} m_{k_4}}} (-1)^{j_{k_3} + j_{k_4} + J'} \tilde{O}_{k_1 k_2 k_3 k_4}^{[40]} \begin{pmatrix} j_{k_1} & j_{k_2} \\ m_{k_1} & m_{k_2} \end{pmatrix} \begin{pmatrix} j_{k_3} & j_{k_4} \\ m_{k_3} & m_{k_4} \end{pmatrix} \begin{pmatrix} J' \\ -M' \end{pmatrix}. \quad (\text{E.42})$$

Again we perform the coupling of the six terms individually.

$${}^1 \tilde{O}_{k_1 k_2 JM; k_3 k_4 J' M''}^{[40]} = (-1)^{j_{k_3} + j_{k_4} + J''} \sum_{\substack{m_{k_1} m_{k_2} \\ m_{k_3} m_{k_4}}} \sum_{l_1 l_2 l_3 l_4} \bar{o}_{l_1 l_2 l_3 l_4} U_{l_1 k_1}^* U_{l_2 k_2}^* V_{l_4 \bar{k}_3}^* V_{l_3 \bar{k}_4}^*$$

$$\begin{aligned}
 & \times \begin{pmatrix} j_{k_1} & j_{k_2} & | & J \\ m_{k_1} & m_{k_2} & | & M \end{pmatrix} \begin{pmatrix} j_{k_3} & j_{k_4} & | & J'' \\ m_{k_3} & m_{k_4} & | & -M'' \end{pmatrix} \\
 = & \sum_{\substack{m_{k_1} m_{k_2} \\ m_{k_3} m_{k_4}}} \sum_{J' M'} \sum_{n_1 n_2 n_3 n_4} \bar{o}_{n_1 l j t_{k_1} n_2 l j t_{k_2} n_3 l j t_{k_4} n_4 l j t_{k_3}}^{J'} (-1)^{m_{k_3} + m_{k_4} + J''} \\
 & \times \tilde{U}_{n_1 n_{k_1}}^{(\pi j t)_{k_1}} \tilde{U}_{n_2 n_{k_2}}^{(\pi j t)_{k_2}} \tilde{V}_{n_4 n_{k_3}}^{(\pi j t)_{k_3}} \tilde{V}_{n_3 n_{k_4}}^{(\pi j t)_{k_4}} \\
 & \times \begin{pmatrix} j_{k_1} & j_{k_2} & | & J \\ m_{k_1} & m_{k_2} & | & M \end{pmatrix} \begin{pmatrix} j_{k_3} & j_{k_4} & | & J'' \\ m_{k_3} & m_{k_4} & | & -M'' \end{pmatrix} \begin{pmatrix} j_{k_1} & j_{k_2} & | & J' \\ m_{k_1} & m_{k_2} & | & M' \end{pmatrix} \begin{pmatrix} j_{k_4} & j_{k_3} & | & J' \\ m_{k_4} & m_{k_3} & | & M' \end{pmatrix} \\
 = & \sum_{n_1 n_2 n_3 n_4} \bar{o}_{n_1 l j t_{k_1} n_2 l j t_{k_2} n_3 l j t_{k_4} n_4 l j t_{k_3}}^{J'} \tilde{U}_{n_1 n_{k_1}}^{(\pi j t)_{k_1}} \tilde{U}_{n_2 n_{k_2}}^{(\pi j t)_{k_2}} \tilde{V}_{n_4 n_{k_3}}^{(\pi j t)_{k_3}} \tilde{V}_{n_3 n_{k_4}}^{(\pi j t)_{k_4}} \\
 & \times (-1)^{j_{k_3} + j_{k_4} + M} \delta_{J J''} \delta_{M - M''}, \tag{E.43}
 \end{aligned}$$

$$\begin{aligned}
 {}^2\tilde{O}_{k_1 k_2 J M; k_3 k_4 J'' M''}^{[40]} & = (-1)^{j_{k_3} + j_{k_4} + J''} \sum_{\substack{m_{k_1} m_{k_2} \\ m_{k_3} m_{k_4}}} \sum_{l_1 l_2 l_3 l_4} \bar{o}_{l_1 l_2 l_3 l_4} U_{l_1 k_1}^* V_{l_4 k_2}^* U_{l_2 \bar{k}_3}^* V_{l_3 \bar{k}_4}^* \\
 & \times \begin{pmatrix} j_{k_1} & j_{k_2} & | & J \\ m_{k_1} & m_{k_2} & | & M \end{pmatrix} \begin{pmatrix} j_{k_3} & j_{k_4} & | & J'' \\ m_{k_3} & m_{k_4} & | & -M'' \end{pmatrix} \\
 = & \sum_{\substack{m_{k_1} m_{k_2} \\ m_{k_3} m_{k_4}}} \sum_{J' M'} \sum_{n_1 n_2 n_3 n_4} \bar{o}_{n_1 l j t_{k_1} n_2 l j t_{k_3} n_3 l j t_{k_4} n_4 l j t_{k_2}}^{J'} \\
 & \times (-1)^{j_{k_2} + j_{k_3} + m_{k_2} - m_{k_4} + 1 + J''} \tilde{U}_{n_1 n_{k_1}}^{(\pi j t)_{k_1}} \tilde{V}_{n_4 n_{k_2}}^{(\pi j t)_{k_2}} \tilde{U}_{n_2 n_{k_3}}^{(\pi j t)_{k_3}} \tilde{V}_{n_3 n_{k_4}}^{(\pi j t)_{k_4}} \\
 & \times \begin{pmatrix} j_{k_1} & j_{k_2} & | & J \\ m_{k_1} & m_{k_2} & | & M \end{pmatrix} \begin{pmatrix} j_{k_3} & j_{k_4} & | & J'' \\ m_{k_3} & m_{k_4} & | & -M'' \end{pmatrix} \begin{pmatrix} j_{k_1} & j_{k_3} & | & J' \\ m_{k_1} & -m_{k_3} & | & M' \end{pmatrix} \begin{pmatrix} j_{k_4} & j_{k_2} & | & J' \\ m_{k_4} & -m_{k_2} & | & M' \end{pmatrix} \\
 = & \sum_{n_1 n_2 n_3 n_4} \bar{o}_{n_1 l j t_{k_1} n_2 l j t_{k_3} n_3 l j t_{k_4} n_4 l j t_{k_2}}^{J'} \tilde{U}_{n_1 n_{k_1}}^{(\pi j t)_{k_1}} \tilde{V}_{n_4 n_{k_2}}^{(\pi j t)_{k_2}} \tilde{U}_{n_2 n_{k_3}}^{(\pi j t)_{k_3}} \tilde{V}_{n_3 n_{k_4}}^{(\pi j t)_{k_4}} \\
 & \times (-1)^{j_{k_3} + j_{k_4} + M + 1} \hat{j}^2 \begin{Bmatrix} j_{k_1} & j_{k_2} & J \\ j_{k_4} & j_{k_3} & J' \end{Bmatrix} \delta_{J J''} \delta_{M - M''}, \tag{E.44}
 \end{aligned}$$

$$\begin{aligned}
 {}^3\tilde{O}_{k_1 k_2 J M; k_3 k_4 J'' M''}^{[40]} & = (-1)^{j_{k_3} + j_{k_4} + J''} \sum_{\substack{m_{k_1} m_{k_2} \\ m_{k_3} m_{k_4}}} \sum_{l_1 l_2 l_3 l_4} \bar{o}_{l_1 l_2 l_3 l_4} V_{l_4 k_1}^* U_{l_2 k_2}^* U_{l_1 \bar{k}_3}^* V_{l_3 \bar{k}_4}^* \\
 & \times \begin{pmatrix} j_{k_1} & j_{k_2} & | & J \\ m_{k_1} & m_{k_2} & | & M \end{pmatrix} \begin{pmatrix} j_{k_3} & j_{k_4} & | & J'' \\ m_{k_3} & m_{k_4} & | & -M'' \end{pmatrix} \\
 = & \sum_{\substack{m_{k_1} m_{k_2} \\ m_{k_3} m_{k_4}}} \sum_{J' M'} \sum_{n_1 n_2 n_3 n_4} \bar{o}_{n_1 l j t_{k_3} n_2 l j t_{k_2} n_3 l j t_{k_4} n_4 l j t_{k_1}}^{J'} \\
 & \times (-1)^{j_{k_1} + j_{k_3} + m_{k_1} - m_{k_4} + J'' + 1} \tilde{V}_{n_4 n_{k_1}}^{(\pi j t)_{k_1}} \tilde{U}_{n_2 n_{k_2}}^{(\pi j t)_{k_2}} \tilde{U}_{n_1 n_{k_3}}^{(\pi j t)_{k_3}} \tilde{V}_{n_3 n_{k_4}}^{(\pi j t)_{k_4}}
 \end{aligned}$$

$$\begin{aligned}
 & \times \begin{pmatrix} j_{k_1} & j_{k_2} & J \\ m_{k_1} & m_{k_2} & M \end{pmatrix} \begin{pmatrix} j_{k_3} & j_{k_4} & J'' \\ m_{k_3} & m_{k_4} & -M'' \end{pmatrix} \begin{pmatrix} j_{k_3} & j_{k_2} & J' \\ -m_{k_3} & m_{k_2} & M' \end{pmatrix} \begin{pmatrix} j_{k_4} & j_{k_1} & J' \\ m_{k_4} & -m_{k_1} & M' \end{pmatrix} \\
 = & \sum_{n_1 n_2 n_3 n_4} \sum_{J'} \bar{o}_{n_1 l j t_{k_3} n_2 l j t_{k_2} n_3 l j t_{k_4} n_4 l j t_{k_1}}^{\bar{J}'} \tilde{V}_{n_4 n_{k_1}}^{(\pi j t)_{k_1}} \tilde{U}_{n_2 n_{k_2}}^{(\pi j t)_{k_2}} \tilde{U}_{n_1 n_{k_3}}^{(\pi j t)_{k_3}} \tilde{V}_{n_3 n_{k_4}}^{(\pi j t)_{k_4}} \\
 & \times (-1)^{j_{k_1} + j_{k_4} + J' + J'' + M + 1} \delta_{J J''} \delta_{M - M''} \hat{J}'^2 \begin{Bmatrix} j_{k_1} & j_{k_2} & J \\ j_{k_3} & j_{k_4} & J' \end{Bmatrix} \\
 = & \sum_{n_1 n_2 n_3 n_4} \sum_{J'} \bar{o}_{n_1 l j t_{k_3} n_2 l j t_{k_2} n_4 l j t_{k_1} n_3 l j t_{k_4}}^{\bar{J}'} \tilde{V}_{n_4 n_{k_1}}^{(\pi j t)_{k_1}} \tilde{U}_{n_2 n_{k_2}}^{(\pi j t)_{k_2}} \tilde{U}_{n_1 n_{k_3}}^{(\pi j t)_{k_3}} \tilde{V}_{n_3 n_{k_4}}^{(\pi j t)_{k_4}} \\
 & \times (-1)^{J + M} \hat{J}'^2 \begin{Bmatrix} j_{k_1} & j_{k_2} & J \\ j_{k_3} & j_{k_4} & J' \end{Bmatrix} \delta_{J J''} \delta_{M - M''}, \tag{E.45}
 \end{aligned}$$

$$\begin{aligned}
 {}^4\tilde{O}_{k_1 k_2 J M; k_3 k_4 J'' M''}^{[40]} & = (-1)^{j_{k_3} + j_{k_4} + J''} \sum_{\substack{m_{k_1} m_{k_2} \\ m_{k_3} m_{k_4}}} \sum_{l_1 l_2 l_3 l_4} \bar{o}_{l_1 l_2 l_3 l_4} U_{l_1 k_1}^* V_{l_4 k_2}^* V_{l_3 k_3}^* U_{l_2 k_4}^* \\
 & \times \begin{pmatrix} j_{k_1} & j_{k_2} & J \\ m_{k_1} & m_{k_2} & M \end{pmatrix} \begin{pmatrix} j_{k_3} & j_{k_4} & J'' \\ m_{k_3} & m_{k_4} & -M'' \end{pmatrix} \\
 = & \sum_{\substack{m_{k_1} m_{k_2} \\ m_{k_3} m_{k_4}}} \sum_{J' M'} \sum_{n_1 n_2 n_3 n_4} \bar{o}_{n_1 l j t_{k_1} n_2 l j t_{k_4} n_3 l j t_{k_3} n_4 l j t_{k_2}}^{\bar{J}'} \\
 & \times (-1)^{j_{k_2} + j_{k_4} + m_{k_2} - m_{k_3} + J'' + 1} \tilde{U}_{n_1 n_{k_1}}^{(\pi j t)_{k_1}} \tilde{V}_{n_4 n_{k_2}}^{(\pi j t)_{k_2}} \tilde{V}_{n_3 n_{k_3}}^{(\pi j t)_{k_3}} \tilde{U}_{n_2 n_{k_4}}^{(\pi j t)_{k_4}} \\
 & \times \begin{pmatrix} j_{k_1} & j_{k_2} & J \\ m_{k_1} & m_{k_2} & M \end{pmatrix} \begin{pmatrix} j_{k_3} & j_{k_4} & J'' \\ m_{k_3} & m_{k_4} & -M'' \end{pmatrix} \begin{pmatrix} j_{k_1} & j_{k_4} & J' \\ m_{k_1} & -m_{k_4} & M' \end{pmatrix} \begin{pmatrix} j_{k_3} & j_{k_2} & J' \\ m_{k_3} & -m_{k_2} & M' \end{pmatrix} \\
 = & \sum_{n_1 n_2 n_3 n_4} \sum_{J'} \bar{o}_{n_1 l j t_{k_1} n_2 l j t_{k_4} n_3 l j t_{k_3} n_4 l j t_{k_2}}^{\bar{J}'} \tilde{U}_{n_1 n_{k_1}}^{(\pi j t)_{k_1}} \tilde{V}_{n_4 n_{k_2}}^{(\pi j t)_{k_2}} \tilde{V}_{n_3 n_{k_3}}^{(\pi j t)_{k_3}} \tilde{U}_{n_2 n_{k_4}}^{(\pi j t)_{k_4}} \\
 & \times (-1)^{J + M + 1} \hat{J}'^2 \begin{Bmatrix} j_{k_1} & j_{k_2} & J \\ j_{k_3} & j_{k_4} & J' \end{Bmatrix} \delta_{J J''} \delta_{M - M''}, \tag{E.46}
 \end{aligned}$$

$$\begin{aligned}
 {}^5\tilde{O}_{k_1 k_2 J M; k_3 k_4 J'' M''}^{[40]} & = (-1)^{j_{k_3} + j_{k_4} + J''} \sum_{\substack{m_{k_1} m_{k_2} \\ m_{k_3} m_{k_4}}} \sum_{l_1 l_2 l_3 l_4} \bar{o}_{l_1 l_2 l_3 l_4} V_{l_4 k_1}^* U_{l_2 k_2}^* V_{l_3 k_3}^* U_{l_1 k_4}^* \\
 & \times \begin{pmatrix} j_{k_1} & j_{k_2} & J \\ m_{k_1} & m_{k_2} & M \end{pmatrix} \begin{pmatrix} j_{k_3} & j_{k_4} & J'' \\ m_{k_3} & m_{k_4} & -M'' \end{pmatrix} \\
 = & \sum_{\substack{m_{k_1} m_{k_2} \\ m_{k_3} m_{k_4}}} \sum_{J' M'} \sum_{n_1 n_2 n_3 n_4} \bar{o}_{n_1 l j t_{k_4} n_2 l j t_{k_2} n_3 l j t_{k_3} n_4 l j t_{k_1}}^{\bar{J}'} \\
 & \times (-1)^{j_{k_1} + j_{k_4} + m_{k_1} - m_{k_3} + J'' + 1} \tilde{V}_{n_4 n_{k_1}}^{(\pi j t)_{k_1}} \tilde{U}_{n_2 n_{k_2}}^{(\pi j t)_{k_2}} \tilde{V}_{n_3 n_{k_3}}^{(\pi j t)_{k_3}} \tilde{U}_{n_1 n_{k_4}}^{(\pi j t)_{k_4}} \\
 & \times \begin{pmatrix} j_{k_1} & j_{k_2} & J \\ m_{k_1} & m_{k_2} & M \end{pmatrix} \begin{pmatrix} j_{k_3} & j_{k_4} & J'' \\ m_{k_3} & m_{k_4} & -M'' \end{pmatrix} \begin{pmatrix} j_{k_4} & j_{k_2} & J' \\ -m_{k_4} & m_{k_2} & M' \end{pmatrix} \begin{pmatrix} j_{k_3} & j_{k_1} & J' \\ m_{k_3} & -m_{k_1} & M' \end{pmatrix}
 \end{aligned}$$

$$\begin{aligned}
 &= \sum_{n_1 n_2 n_3 n_4} \sum_{J'} \bar{o}_{n_1 l j t_{k_4} n_2 l j t_{k_2} n_3 l j t_{k_3} n_4 l j t_{k_1}}^{J'} \tilde{V}_{n_4 n_{k_1}}^{(\pi j t)_{k_1}} \tilde{U}_{n_2 n_{k_2}}^{(\pi j t)_{k_2}} \tilde{V}_{n_3 n_{k_3}}^{(\pi j t)_{k_3}} \tilde{U}_{n_1 n_{k_4}}^{(\pi j t)_{k_4}} \\
 &\quad \times (-1)^{j_{k_1} + j_{k_4} + J' + M} \delta_{JJ''} \delta_{M-M''} \hat{J}'^2 \begin{Bmatrix} j_{k_1} & j_{k_2} & J \\ j_{k_4} & j_{k_3} & J' \end{Bmatrix} \\
 &= \sum_{n_1 n_2 n_3 n_4} \sum_{J'} \bar{o}_{n_1 l j t_{k_4} n_2 l j t_{k_2} n_4 l j t_{k_1} n_3 l j t_{k_3}}^{J'} \tilde{V}_{n_4 n_{k_1}}^{(\pi j t)_{k_1}} \tilde{U}_{n_2 n_{k_2}}^{(\pi j t)_{k_2}} \tilde{V}_{n_3 n_{k_3}}^{(\pi j t)_{k_3}} \tilde{U}_{n_1 n_{k_4}}^{(\pi j t)_{k_4}} \\
 &\quad \times (-1)^{j_{k_3} + j_{k_4} + M} \hat{J}'^2 \begin{Bmatrix} j_{k_1} & j_{k_2} & J \\ j_{k_4} & j_{k_3} & J' \end{Bmatrix} \delta_{JJ''} \delta_{M-M''}, \tag{E.47}
 \end{aligned}$$

$$\begin{aligned}
 {}^6 \tilde{O}_{k_1 k_2 J M; k_3 k_4 J'' M''}^{[40]} &= (-1)^{j_{k_3} + j_{k_4} + J''} \sum_{\substack{m_{k_1} m_{k_2} \\ m_{k_3} m_{k_4}}} \sum_{l_1 l_2 l_3 l_4} \bar{o}_{l_1 l_2 l_3 l_4} V_{l_4 k_1}^* V_{l_3 k_2}^* U_{l_1 k_3}^* U_{l_2 k_4}^* \\
 &\quad \times \begin{pmatrix} j_{k_1} & j_{k_2} & J \\ m_{k_1} & m_{k_2} & M \end{pmatrix} \begin{pmatrix} j_{k_3} & j_{k_4} & J'' \\ m_{k_3} & m_{k_4} & -M'' \end{pmatrix} \\
 &= \sum_{\substack{m_{k_1} m_{k_2} \\ m_{k_3} m_{k_4}}} \sum_{J' M'} \sum_{n_1 n_2 n_3 n_4} \bar{o}_{n_1 l j t_{k_3} n_2 l j t_{k_4} n_3 l j t_{k_2} n_4 l j t_{k_1}}^{J'} \\
 &\quad \times (-1)^{j_{k_1} + j_{k_2} + j_{k_3} + j_{k_4} + m_{k_1} + m_{k_2} + J'' + 1} \tilde{V}_{n_4 n_{k_1}}^{(\pi j t)_{k_1}} \tilde{V}_{n_3 n_{k_2}}^{(\pi j t)_{k_2}} \tilde{U}_{n_1 n_{k_3}}^{(\pi j t)_{k_3}} \tilde{U}_{n_2 n_{k_4}}^{(\pi j t)_{k_4}} \\
 &\quad \times \begin{pmatrix} j_{k_1} & j_{k_2} & J \\ m_{k_1} & m_{k_2} & M \end{pmatrix} \begin{pmatrix} j_{k_3} & j_{k_4} & J'' \\ m_{k_3} & m_{k_4} & -M'' \end{pmatrix} \begin{pmatrix} j_{k_3} & j_{k_4} & J' \\ -m_{k_3} & -m_{k_4} & M' \end{pmatrix} \begin{pmatrix} j_{k_2} & j_{k_1} & J' \\ -m_{k_2} & -m_{k_1} & M' \end{pmatrix} \\
 &= \sum_{n_1 n_2 n_3 n_4} \bar{o}_{n_1 l j t_{k_3} n_2 l j t_{k_4} n_3 l j t_{k_2} n_4 l j t_{k_1}}^{J'} \tilde{V}_{n_4 n_{k_1}}^{(\pi j t)_{k_1}} \tilde{V}_{n_3 n_{k_2}}^{(\pi j t)_{k_2}} \tilde{U}_{n_1 n_{k_3}}^{(\pi j t)_{k_3}} \tilde{U}_{n_2 n_{k_4}}^{(\pi j t)_{k_4}} \\
 &\quad \times (-1)^{j_{k_1} + j_{k_2} + M} \delta_{JJ''} \delta_{M-M''}. \tag{E.48}
 \end{aligned}$$

We again get for the coupled matrix element

$$\tilde{O}_{k_1 k_2 J M; k_3 k_4 J'' M''}^{[40]} \equiv (-1)^M \delta_{JJ''} \delta_{M-M''} {}^J \tilde{O}_{\tilde{k}_1 \tilde{k}_2 \tilde{k}_3 \tilde{k}_4}^{[40]}, \tag{E.49}$$

such that we can write

$$\begin{aligned}
 O^{[40]} &= \frac{1}{24} \sum_{\tilde{k}_1 \tilde{k}_2 \tilde{k}_3 \tilde{k}_4} \sum_{JM} {}^J \tilde{O}_{\tilde{k}_1 \tilde{k}_2 \tilde{k}_3 \tilde{k}_4}^{[40]} (-1)^M [\mathcal{B}_{j_{k_1}} \mathcal{B}_{j_{k_2}}]_{JM} [\mathcal{B}_{j_{k_3}} \mathcal{B}_{j_{k_4}}]_{J-M} \\
 &= \frac{1}{24} \sum_{\tilde{k}_1 \tilde{k}_2 \tilde{k}_3 \tilde{k}_4} \sum_J {}^J \tilde{O}_{\tilde{k}_1 \tilde{k}_2 \tilde{k}_3 \tilde{k}_4}^{[40]} [\mathcal{B}_{j_{k_1}} \mathcal{B}_{j_{k_2}}]_J \cdot [\mathcal{B}_{j_{k_3}} \mathcal{B}_{j_{k_4}}]_J. \tag{E.50}
 \end{aligned}$$

For the transformation from m-scheme to J -scheme we have

$${}^J \tilde{O}_{\tilde{k}_1 \tilde{k}_2 \tilde{k}_3 \tilde{k}_4}^{[40]} = \sum_{\substack{m_{k_1} m_{k_2} \\ m_{k_3} m_{k_4}}} \tilde{O}_{k_1 k_2 k_3 k_4}^{[40]} (-1)^{j_{k_3} + j_{k_4} + J + M} \begin{pmatrix} j_{k_1} & j_{k_2} & J \\ m_{k_1} & m_{k_2} & M \end{pmatrix} \begin{pmatrix} j_{k_3} & j_{k_4} & J \\ m_{k_3} & m_{k_4} & M \end{pmatrix}, \tag{E.51}$$

and conversely,

$$\tilde{O}_{k_1 k_2 k_3 k_4}^{[40]} = \sum_{JM}^J \tilde{O}_{\tilde{k}_1 \tilde{k}_2 \tilde{k}_3 \tilde{k}_4}^{[40]} (-1)^{j_{k_3} + j_{k_4} + J + M} \begin{pmatrix} j_{k_1} & j_{k_2} & J \\ m_{k_1} & m_{k_2} & M \end{pmatrix} \begin{pmatrix} j_{k_3} & j_{k_4} & J \\ m_{k_3} & m_{k_4} & M \end{pmatrix}. \quad (\text{E.52})$$

ANGULAR-MOMENTUM COUPLING OF \hat{O}^{31}

The m-scheme expressions of the cross-coupled matrix element is given by

$$\begin{aligned} \tilde{O}_{k_1 k_2 k_3 k_4}^{31} = & \sum_{l_1 l_2 l_3 l_4} \Theta_{l_1 l_2 l_3 l_4} \left(U_{l_1 k_1}^* V_{l_4 k_2}^* V_{l_3 \bar{k}_3}^* V_{l_2 k_4} - V_{l_4 k_1}^* U_{l_1 k_2}^* V_{l_3 \bar{k}_3}^* V_{l_2 k_4} - V_{l_3 k_1}^* V_{l_4 k_2}^* U_{l_1 \bar{k}_3}^* V_{l_2 k_4} \right. \\ & \left. + V_{l_3 k_1}^* U_{l_2 k_2}^* U_{l_1 \bar{k}_3}^* U_{l_4 k_4} - U_{l_2 k_1}^* V_{l_3 k_2}^* U_{l_1 \bar{k}_3}^* U_{l_4 k_4} - U_{l_1 k_1}^* U_{l_2 k_2}^* V_{l_3 \bar{k}_3}^* U_{l_4 k_4} \right). \quad (\text{E.53}) \end{aligned}$$

The coupling of the operator reads as

$$\begin{aligned} \hat{O}^{[31]} = & \frac{1}{6} \sum_{k_1 k_2 k_3 k_4} O_{k_1 k_2 k_3 k_4}^{[31]} \hat{\beta}_{k_1}^\dagger \hat{\beta}_{k_2}^\dagger \hat{\beta}_{k_3}^\dagger \hat{\beta}_{k_4} \\ = & \frac{1}{6} \sum_{\tilde{k}_1 \tilde{k}_2 \tilde{k}_3 \tilde{k}_4} \sum_{\substack{m_{k_1} m_{k_2} \\ m_{k_3} m_{k_4}}} (-1)^{j_{k_4} - m_{k_4}} O_{k_1 k_2 k_3 k_4}^{[31]} \mathcal{B}_{k_1 m_{k_1}} \mathcal{B}_{k_2 m_{k_2}} \mathcal{B}_{k_3 m_{k_3}} \bar{\mathcal{B}}_{j_{k_4} - m_{k_4}} \\ = & \frac{1}{6} \sum_{\tilde{k}_1 \tilde{k}_2 \tilde{k}_3 \tilde{k}_4} \sum_{\substack{m_{k_1} m_{k_2} \\ m_{k_3} m_{k_4}}} \sum_{JJ'MM'} (-1)^{j_{k_4} - m_{k_4}} O_{k_1 k_2 k_3 k_4}^{[31]} \\ & \times \begin{pmatrix} j_{k_1} & j_{k_2} & J \\ m_{k_1} & m_{k_2} & M \end{pmatrix} \begin{pmatrix} j_{k_3} & j_{k_4} & J' \\ m_{k_3} & -m_{k_4} & M' \end{pmatrix} [\mathcal{B}_{j_{k_1}} \mathcal{B}_{j_{k_2}}]_{JM} \cdot [\mathcal{B}_{j_{k_3}} \bar{\mathcal{B}}_{j_{k_4}}]_{J'M'}, \\ = & \frac{1}{6} \sum_{\tilde{k}_1 \tilde{k}_2 \tilde{k}_3 \tilde{k}_4} \sum_{\substack{m_{k_1} m_{k_2} \\ m_{k_3} m_{k_4}}} \sum_{JJ'MM'} (-1)^{j_{k_4} - m_{k_4}} \tilde{O}_{k_1 k_2 \bar{k}_3 k_4}^{[31]} \\ & \times \begin{pmatrix} j_{k_1} & j_{k_2} & J \\ m_{k_1} & m_{k_2} & M \end{pmatrix} \begin{pmatrix} j_{k_3} & j_{k_4} & J' \\ m_{k_3} & -m_{k_4} & M' \end{pmatrix} [\mathcal{B}_{j_{k_1}} \mathcal{B}_{j_{k_2}}]_{JM} \cdot [\mathcal{B}_{j_{k_3}} \bar{\mathcal{B}}_{j_{k_4}}]_{J'M'}, \\ = & \frac{1}{6} \sum_{\tilde{k}_1 \tilde{k}_2 \tilde{k}_3 \tilde{k}_4} \sum_{\substack{m_{k_1} m_{k_2} \\ m_{k_3} m_{k_4}}} \sum_{JJ'MM'} (-1)^{j_{k_4} - m_{k_4}} \tilde{O}_{k_1 k_2 k_3 k_4}^{[31]} \\ & \times \begin{pmatrix} j_{k_1} & j_{k_2} & J \\ m_{k_1} & m_{k_2} & M \end{pmatrix} \begin{pmatrix} j_{k_3} & j_{k_4} & J' \\ -m_{k_3} & -m_{k_4} & M' \end{pmatrix} [\mathcal{B}_{j_{k_1}} \mathcal{B}_{j_{k_2}}]_J \cdot [\mathcal{B}_{j_{k_3}} \bar{\mathcal{B}}_{j_{k_4}}]_{J'M'} \quad (\text{E.54}) \end{aligned}$$

and define

$$\tilde{O}_{\tilde{k}_1 \tilde{k}_2 JM; \tilde{k}_3 \tilde{k}_4 J'M'}^{[31]} = \sum_{\substack{m_{k_1} m_{k_2} \\ m_{k_3} m_{k_4}}} (-1)^{j_{k_4} - m_{k_4}} \tilde{O}_{k_1 k_2 k_3 k_4}^{[31]} \begin{pmatrix} j_{k_1} & j_{k_2} & J \\ m_{k_1} & m_{k_2} & M \end{pmatrix} \begin{pmatrix} j_{k_3} & j_{k_4} & J' \\ -m_{k_3} & -m_{k_4} & M' \end{pmatrix}. \quad (\text{E.55})$$

The corresponding six terms are given by

$$\begin{aligned}
 {}^1\tilde{O}_{k_1 k_2 J M; k_3 k_4 J'' M''}^{[31]} &= (-1)^{j_{k_4} - m_{k_4}} \sum_{\substack{m_{k_1} m_{k_2} \\ m_{k_3} m_{k_4}}} \sum_{l_1 l_2 l_3 l_4} \bar{o}_{l_1 l_2 l_3 l_4} U_{l_1 k_1}^* V_{l_4 k_2}^* V_{l_3 \bar{k}_3}^* V_{l_2 k_4} \\
 &\times \begin{pmatrix} j_{k_1} & j_{k_2} & J \\ m_{k_1} & m_{k_2} & M \end{pmatrix} \begin{pmatrix} j_{k_3} & j_{k_4} & J'' \\ -m_{k_3} & -m_{k_4} & M'' \end{pmatrix} \\
 &= \sum_{\substack{m_{k_1} m_{k_2} \\ m_{k_3} m_{k_4}}} \sum_{J' M'} \sum_{n_1 n_2 n_3 n_4} \bar{o}_{n_1 l j t_{k_1} n_2 l j t_{k_4} n_3 l j t_{k_3} n_4 l j t_{k_2}}^{J'} \\
 &\times (-1)^{j_{k_2} + j_{k_3} + m_{k_2} - m_{k_3} + 1} \tilde{U}_{n_1 n_{k_1}}^{(\pi j t)_{k_1}} \tilde{V}_{n_4 n_{k_2}}^{(\pi j t)_{k_2}} \tilde{V}_{n_3 n_{k_3}}^{(\pi j t)_{k_3}} \tilde{V}_{n_2 n_{k_4}}^{(\pi j t)_{k_4}} \\
 &\times \begin{pmatrix} j_{k_1} & j_{k_2} & J \\ m_{k_1} & m_{k_2} & M \end{pmatrix} \begin{pmatrix} j_{k_3} & j_{k_4} & J'' \\ -m_{k_3} & -m_{k_4} & M'' \end{pmatrix} \begin{pmatrix} j_{k_1} & j_{k_4} & J' \\ m_{k_1} & -m_{k_4} & M' \end{pmatrix} \begin{pmatrix} j_{k_3} & j_{k_2} & J' \\ m_{k_3} & -m_{k_2} & M' \end{pmatrix} \\
 &= \sum_{n_1 n_2 n_3 n_4} \sum_{J'} \bar{o}_{n_1 l j t_{k_1} n_2 l j t_{k_4} n_3 l j t_{k_3} n_4 l j t_{k_2}}^{J'} \tilde{U}_{n_1 n_{k_1}}^{(\pi j t)_{k_1}} \tilde{V}_{n_4 n_{k_2}}^{(\pi j t)_{k_2}} \tilde{V}_{n_3 n_{k_3}}^{(\pi j t)_{k_3}} \tilde{V}_{n_2 n_{k_4}}^{(\pi j t)_{k_4}} \\
 &\times (-1)^{J+M} \hat{j}'^2 \begin{Bmatrix} j_{k_1} & j_{k_2} & J \\ j_{k_3} & j_{k_4} & J' \end{Bmatrix} \delta_{J J''} \delta_{M M''}, \tag{E.56}
 \end{aligned}$$

$$\begin{aligned}
 {}^2\tilde{O}_{k_1 k_2 J M; k_3 k_4 J'' M''}^{[31]} &= (-1)^{j_{k_4} - m_{k_4}} \sum_{\substack{m_{k_1} m_{k_2} \\ m_{k_3} m_{k_4}}} \sum_{l_1 l_2 l_3 l_4} \bar{o}_{l_1 l_2 l_3 l_4} V_{l_4 k_1} U_{l_1 k_2} V_{l_3 \bar{k}_3} V_{l_2 k_4} \\
 &\times \begin{pmatrix} j_{k_1} & j_{k_2} & J \\ m_{k_1} & m_{k_2} & M \end{pmatrix} \begin{pmatrix} j_{k_3} & j_{k_4} & J'' \\ -m_{k_3} & -m_{k_4} & M'' \end{pmatrix} \\
 &= \sum_{\substack{m_{k_1} m_{k_2} \\ m_{k_3} m_{k_4}}} \sum_{J' M'} \sum_{n_1 n_2 n_3 n_4} \bar{o}_{n_1 l j t_{k_2} n_2 l j t_{k_4} n_3 l j t_{k_3} n_4 l j t_{k_1}}^{J'} \\
 &\times (-1)^{j_{k_1} + j_{k_3} + m_{k_1} - m_{k_3} + 1} \tilde{V}_{n_4 n_{k_1}}^{(\pi j t)_{k_1}} \tilde{U}_{n_1 n_{k_2}}^{(\pi j t)_{k_2}} \tilde{V}_{n_3 n_{k_3}}^{(\pi j t)_{k_3}} \tilde{V}_{n_2 n_{k_4}}^{(\pi j t)_{k_4}} \\
 &\times \begin{pmatrix} j_{k_1} & j_{k_2} & J \\ m_{k_1} & m_{k_2} & M \end{pmatrix} \begin{pmatrix} j_{k_3} & j_{k_4} & J'' \\ -m_{k_3} & -m_{k_4} & M'' \end{pmatrix} \begin{pmatrix} j_{k_2} & j_{k_4} & J' \\ m_{k_2} & -m_{k_4} & M' \end{pmatrix} \begin{pmatrix} j_{k_3} & j_{k_1} & J' \\ m_{k_3} & -m_{k_1} & M' \end{pmatrix} \\
 &= (-1)^{j_{k_1} + j_{k_2} + M} \sum_{n_1 n_2 n_3 n_4} \sum_{J'} \bar{o}_{n_1 l j t_{k_2} n_2 l j t_{k_4} n_3 l j t_{k_3} n_4 l j t_{k_1}}^{J'} \\
 &\times \tilde{V}_{n_4 n_{k_1}}^{(\pi j t)_{k_1}} \tilde{U}_{n_1 n_{k_2}}^{(\pi j t)_{k_2}} \tilde{V}_{n_3 n_{k_3}}^{(\pi j t)_{k_3}} \tilde{V}_{n_2 n_{k_4}}^{(\pi j t)_{k_4}} \hat{j}'^2 \begin{Bmatrix} j_{k_1} & j_{k_2} & J \\ j_{k_4} & j_{k_3} & J' \end{Bmatrix} \delta_{J J''} \delta_{M - M''}, \tag{E.57}
 \end{aligned}$$

$$\begin{aligned}
 {}^3\bar{O}_{k_1 k_2 J M; k_3 k_4 J'' M''}^{[31]} &= (-1)^{j_{k_4} - m_{k_4}} \sum_{\substack{m_{k_1} m_{k_2} \\ m_{k_3} m_{k_4}}} \sum_{l_1 l_2 l_3 l_4} \bar{o}_{l_1 l_2 l_3 l_4} V_{l_3 k_1} V_{l_4 k_2} U_{l_1 \bar{k}_3} V_{l_2 k_4} \\
 &\times \begin{pmatrix} j_{k_1} & j_{k_2} & J \\ m_{k_1} & m_{k_2} & M \end{pmatrix} \begin{pmatrix} j_{k_3} & j_{k_4} & J'' \\ -m_{k_3} & -m_{k_4} & M'' \end{pmatrix} \\
 &= \sum_{\substack{m_{k_1} m_{k_2} \\ m_{k_3} m_{k_4}}} \sum_{J' M'} \sum_{n_1 n_2 n_3 n_4} \bar{o}_{n_1 l j t_{k_3} n_2 l j t_{k_4} n_3 l j t_{k_1} n_4 l j t_{k_2}}^{J'}
 \end{aligned}$$

$$\begin{aligned}
 & \times (-1)^{j_{k_1}+j_{k_2}-m_{k_1}-m_{k_2}+1} \tilde{V}_{n_{l_3}n_{k_1}}^{(\pi jt)_{k_1}} \tilde{V}_{n_{l_4}n_{k_2}}^{(\pi jt)_{k_2}} \tilde{U}_{n_{l_1}n_{k_3}}^{(\pi jt)_{k_3}} \tilde{V}_{n_{l_2}n_{k_4}}^{(\pi jt)_{k_4}} \\
 & \times \begin{pmatrix} j_{k_1} & j_{k_2} \\ m_{k_1} & m_{k_2} \end{pmatrix} \begin{pmatrix} J \\ M \end{pmatrix} \begin{pmatrix} j_{k_3} & j_{k_4} \\ -m_{k_3} & -m_{k_4} \end{pmatrix} \begin{pmatrix} J'' \\ M'' \end{pmatrix} \begin{pmatrix} j_{k_3} & j_{k_4} \\ -m_{k_3} & -m_{k_4} \end{pmatrix} \begin{pmatrix} J' \\ M' \end{pmatrix} \begin{pmatrix} j_{k_1} & j_{k_2} \\ -m_{k_1} & -m_{k_2} \end{pmatrix} \begin{pmatrix} J' \\ M' \end{pmatrix} \\
 & = (-1)^{J+M+1} \delta_{JJ''} \delta_{M-M''} \sum_{n_{l_1}n_{l_2}n_{l_3}n_{l_4}} \bar{o}_{n_{l_1}l_{j_{k_3}n_{l_2}l_{j_{k_4}n_{l_3}l_{j_{k_1}n_{l_4}l_{j_{k_2}}}}^{J'}} \\
 & \times \tilde{V}_{n_{k_3}n_{k_1}}^{(\pi jt)_{k_1}} \tilde{V}_{n_{l_4}n_{k_2}}^{(\pi jt)_{k_2}} \tilde{U}_{n_{l_1}n_{k_3}}^{(\pi jt)_{k_3}} \tilde{V}_{n_{l_2}n_{k_4}}^{(\pi jt)_{k_4}} \delta_{JJ''} \delta_{M-M''}, \tag{E.58}
 \end{aligned}$$

$$\begin{aligned}
 {}^4\tilde{O}_{k_1k_2JM;k_3k_4J''M''}^{[31]} & = (-1)^{j_{k_4}-m_{k_4}} \sum_{\substack{m_{k_1}m_{k_2} \\ m_{k_3}m_{k_4}}} \sum_{l_1l_2l_3l_4} \bar{o}_{l_1l_2l_3l_4} V_{l_3k_1} U_{l_2k_2} U_{l_1\bar{k}_3} U_{l_4k_4} \\
 & \times \begin{pmatrix} j_{k_1} & j_{k_2} \\ m_{k_1} & m_{k_2} \end{pmatrix} \begin{pmatrix} J \\ M \end{pmatrix} \begin{pmatrix} j_{k_3} & j_{k_4} \\ -m_{k_3} & -m_{k_4} \end{pmatrix} \begin{pmatrix} J'' \\ M'' \end{pmatrix} \\
 & = \sum_{\substack{m_{k_1}m_{k_2} \\ m_{k_3}m_{k_4}}} \sum_{J'M'} \sum_{n_{l_1}n_{l_2}n_{l_3}n_{l_4}} \bar{o}_{n_{l_1}l_{j_{k_3}n_{l_2}l_{j_{k_2}n_{l_3}l_{j_{k_1}n_{l_4}l_{j_{k_4}}}}^{J'}} \\
 & \times (-1)^{j_{k_1}+j_{k_4}+m_{k_1}-m_{k_4}} \tilde{V}_{n_{l_3}n_{k_1}}^{(\pi jt)_{k_1}} \tilde{U}_{n_{l_2}n_{k_2}}^{(\pi jt)_{k_2}} \tilde{U}_{n_{l_1}n_{k_3}}^{(\pi jt)_{k_3}} \tilde{U}_{n_{l_4}n_{k_4}}^{(\pi jt)_{k_4}} \\
 & \times \begin{pmatrix} j_{k_1} & j_{k_2} \\ m_{k_1} & m_{k_2} \end{pmatrix} \begin{pmatrix} J \\ M \end{pmatrix} \begin{pmatrix} j_{k_3} & j_{k_4} \\ -m_{k_3} & -m_{k_4} \end{pmatrix} \begin{pmatrix} J'' \\ M'' \end{pmatrix} \begin{pmatrix} j_{k_3} & j_{k_2} \\ -m_{k_3} & m_{k_2} \end{pmatrix} \begin{pmatrix} J' \\ M' \end{pmatrix} \begin{pmatrix} j_{k_1} & j_{k_4} \\ -m_{k_1} & m_{k_4} \end{pmatrix} \begin{pmatrix} J' \\ M' \end{pmatrix} \\
 & = (-1)^{M+J+1} \sum_{n_{l_1}n_{l_2}n_{l_3}n_{l_4}} \bar{o}_{n_{l_1}l_{j_{k_3}n_{l_2}l_{j_{k_2}n_{l_3}l_{j_{k_1}n_{l_4}l_{j_{k_4}}}}^{J'}} \\
 & \times \tilde{V}_{n_{l_3}n_{k_1}}^{(\pi jt)_{k_1}} \tilde{U}_{n_{l_2}n_{k_2}}^{(\pi jt)_{k_2}} \tilde{U}_{n_{l_1}n_{k_3}}^{(\pi jt)_{k_3}} \tilde{U}_{n_{l_4}n_{k_4}}^{(\pi jt)_{k_4}} \hat{J}'^2 \begin{Bmatrix} j_{k_1} & j_{k_2} & J \\ j_{k_3} & j_{k_4} & J' \end{Bmatrix} \delta_{JJ''} \delta_{M-M''}, \tag{E.59}
 \end{aligned}$$

$$\begin{aligned}
 {}^5\tilde{O}_{k_1k_2JM;k_3k_4J''M''}^{[31]} & = (-1)^{j_{k_4}-m_{k_4}} \sum_{\substack{m_{k_1}m_{k_2} \\ m_{k_3}m_{k_4}}} \sum_{l_1l_2l_3l_4} \bar{o}_{l_1l_2l_3l_4} U_{l_2k_1} V_{l_3k_2} U_{l_1\bar{k}_3} U_{l_4k_4} \\
 & \times \begin{pmatrix} j_{k_1} & j_{k_2} \\ m_{k_1} & m_{k_2} \end{pmatrix} \begin{pmatrix} J \\ M \end{pmatrix} \begin{pmatrix} j_{k_3} & j_{k_4} \\ m_{k_3} & -m_{k_4} \end{pmatrix} \begin{pmatrix} J'' \\ M'' \end{pmatrix} \\
 & = \sum_{\substack{m_{k_1}m_{k_2} \\ m_{k_3}m_{k_4}}} \sum_{J'M'} \sum_{n_{l_1}n_{l_2}n_{l_3}n_{l_4}} \bar{o}_{n_{l_1}l_{j_{k_3}n_{l_2}l_{j_{k_1}n_{l_3}l_{j_{k_2}n_{l_4}l_{j_{k_4}}}}^{J'}} \\
 & \times (-1)^{j_{k_2}+j_{k_4}+m_{k_2}-m_{k_4}} \tilde{U}_{n_{l_2}n_{k_1}}^{(\pi jt)_{k_1}} \tilde{V}_{n_{l_3}n_{k_2}}^{(\pi jt)_{k_2}} \tilde{U}_{n_{l_1}n_{k_3}}^{(\pi jt)_{k_3}} \tilde{U}_{n_{l_4}n_{k_4}}^{(\pi jt)_{k_4}} \\
 & \times \begin{pmatrix} j_{k_1} & j_{k_2} \\ m_{k_1} & m_{k_2} \end{pmatrix} \begin{pmatrix} J \\ M \end{pmatrix} \begin{pmatrix} j_{k_3} & j_{k_4} \\ -m_{k_3} & -m_{k_4} \end{pmatrix} \begin{pmatrix} J'' \\ M'' \end{pmatrix} \begin{pmatrix} j_{k_3} & j_{k_1} \\ -m_{k_3} & m_{k_1} \end{pmatrix} \begin{pmatrix} J' \\ M' \end{pmatrix} \begin{pmatrix} j_{k_2} & j_{k_4} \\ -m_{k_2} & m_{k_4} \end{pmatrix} \begin{pmatrix} J' \\ M' \end{pmatrix} \\
 & = (-1)^{j_{k_1}+j_{k_2}+M+1} \sum_{n_{l_1}n_{l_2}n_{l_3}n_{l_4}} \bar{o}_{n_{l_1}l_{j_{k_3}n_{l_2}l_{j_{k_1}n_{l_3}l_{j_{k_2}n_{l_4}l_{j_{k_4}}}}^{J'}}
 \end{aligned}$$

$$\times \tilde{V}_{n_{l_3} n_{k_1}}^{(\pi j t)_{k_1}} \tilde{U}_{n_{l_2} n_{k_1}}^{(\pi j t)_{k_1}} \tilde{V}_{n_{l_3} n_{k_2}}^{(\pi j t)_{k_2}} \tilde{U}_{n_{l_1} n_{k_3}}^{(\pi j t)_{k_3}} \tilde{U}_{n_{l_4} n_{k_4}}^{(\pi j t)_{k_4}} \hat{J}'^2 \begin{Bmatrix} j_{k_1} & j_{k_2} & J \\ j_{k_4} & j_{k_3} & J' \end{Bmatrix} \delta_{JJ''} \delta_{M-M''}, \quad (\text{E.60})$$

$$\begin{aligned} {}^6 \tilde{O}_{k_1 k_2 J M; k_3 k_4 J'' M''}^{[31]} &= (-1)^{j_{k_4} - m_{k_4}} \sum_{\substack{m_{k_1} m_{k_2} \\ m_{k_3} m_{k_4}}} \sum_{l_1 l_2 l_3 l_4} \bar{o}_{l_1 l_2 l_3 l_4} U_{l_1 k_1} U_{l_2 k_2} V_{l_3 \bar{k}_3} U_{l_4 k_4} \\ &\times \begin{pmatrix} j_{k_1} & j_{k_2} & J \\ m_{k_1} & m_{k_2} & M \end{pmatrix} \begin{pmatrix} j_{k_3} & j_{k_4} & J'' \\ -m_{k_3} & -m_{k_4} & M'' \end{pmatrix} \\ &= \sum_{\substack{m_{k_1} m_{k_2} \\ m_{k_3} m_{k_4}}} \sum_{J' M'} \sum_{n_{l_1} n_{l_2} n_{l_3} n_{l_4}} \bar{o}_{n_{l_1} l j t_{k_1} n_{l_2} l j t_{k_2} n_{l_3} l j t_{k_3} n_{l_4} l j t_{k_4}}^{J'} \\ &\times (-1)^{j_{k_3} - m_{k_3} + j_{k_4} - m_{k_4}} \tilde{U}_{n_{l_1} n_{k_1}}^{(\pi j t)_{k_1}} \tilde{U}_{n_{l_2} n_{k_2}}^{(\pi j t)_{k_2}} \tilde{V}_{n_{l_3} n_{k_3}}^{(\pi j t)_{k_3}} \tilde{U}_{n_{l_4} n_{k_4}}^{(\pi j t)_{k_4}} \\ &\times \begin{pmatrix} j_{k_1} & j_{k_2} & J \\ m_{k_1} & m_{k_2} & M \end{pmatrix} \begin{pmatrix} j_{k_3} & j_{k_4} & J'' \\ -m_{k_3} & -m_{k_4} & M'' \end{pmatrix} \begin{pmatrix} j_{k_1} & j_{k_2} & J' \\ m_{k_1} & m_{k_2} & M' \end{pmatrix} \begin{pmatrix} j_{k_3} & j_{k_4} & J' \\ m_{k_3} & m_{k_4} & M' \end{pmatrix} \\ &= (-1)^{J+M} \sum_{n_{l_1} n_{l_2} n_{l_3} n_{l_4}} \bar{o}_{n_{l_1} l j t_{k_1} n_{l_2} l j t_{k_2} n_{l_3} l j t_{k_3} n_{l_4} l j t_{k_4}}^{J'} \\ &\times \tilde{U}_{n_{l_1} n_{k_1}}^{(\pi j t)_{k_1}} \tilde{U}_{n_{l_2} n_{k_2}}^{(\pi j t)_{k_2}} \tilde{V}_{n_{l_3} n_{k_3}}^{(\pi j t)_{k_3}} \tilde{U}_{n_{l_4} n_{k_4}}^{(\pi j t)_{k_4}} \delta_{JJ''} \delta_{M-M''}. \quad (\text{E.61}) \end{aligned}$$

Therefore, we finally arrive at

$$O_{k_1 k_2 J M; k_3 k_4 J'' M''}^{[31]} \equiv (-1)^M \delta_{JJ''} \delta_{M-M''} {}^J \tilde{O}_{k_1 k_2 \bar{k}_3 \bar{k}_4}^{[31]}, \quad (\text{E.62})$$

leading to the spherical form of the operator

$$\begin{aligned} \tilde{O}_{k_1 k_2 \bar{k}_3 \bar{k}_4}^{[31]} &= \frac{1}{6} \sum_{\bar{k}_1 \bar{k}_2 \bar{k}_3 \bar{k}_4} \sum_{J J' M M'} {}^J \tilde{O}_{k_1 \bar{k}_2 \bar{k}_3 \bar{k}_4}^{[31]} (-1)^M [\mathcal{B}_{j_{k_1}} \mathcal{B}_{j_{k_2}}]_{JM} [\mathcal{B}_{j_{k_3}} \bar{\mathcal{B}}_{j_{k_4}}]_{J-M} \\ &= \frac{1}{6} \sum_{\bar{k}_1 \bar{k}_2 \bar{k}_3 \bar{k}_4} \sum_J {}^J \tilde{O}_{k_1 \bar{k}_2 \bar{k}_3 \bar{k}_4}^{[31]} [\mathcal{B}_{j_{k_1}} \mathcal{B}_{j_{k_2}}]_J \cdot [\mathcal{B}_{j_{k_3}} \bar{\mathcal{B}}_{j_{k_4}}]_J. \quad (\text{E.63}) \end{aligned}$$

We finally write the matrix element as

$$\begin{aligned} {}^J \tilde{O}_{k_1 \bar{k}_2 \bar{k}_3 \bar{k}_4}^{[31]} &= \sum_{\substack{m_{k_1} m_{k_2} \\ m_{k_3} m_{k_4}}} (-1)^{j_{k_4} - m_{k_4} + M} \tilde{O}_{k_1 k_2 k_3 k_4}^{[31]} \begin{pmatrix} j_{k_1} & j_{k_2} & J \\ m_{k_1} & m_{k_2} & M \end{pmatrix} \begin{pmatrix} j_{k_3} & j_{k_4} & J \\ -m_{k_3} & -m_{k_4} & -M \end{pmatrix} \\ &= \sum_{\substack{m_{k_1} m_{k_2} \\ m_{k_3} m_{k_4}}} (-1)^{j_{k_3} - m_{k_4} - J + M + 1} \tilde{O}_{k_1 k_2 k_3 k_4}^{[31]} \begin{pmatrix} j_{k_1} & j_{k_2} & J \\ m_{k_1} & m_{k_2} & M \end{pmatrix} \begin{pmatrix} j_{k_3} & j_{k_4} & J \\ m_{k_3} & m_{k_4} & M \end{pmatrix} \quad (\text{E.64}) \end{aligned}$$

and conversely

$$\tilde{O}_{k_1 k_2 k_3 k_4}^{[31]} = \sum_{JM} (-1)^{j_{k_3} - m_{k_4} - J + M + 1} \times J \tilde{O}_{\tilde{k}_1 \tilde{k}_2 \tilde{k}_3 \tilde{k}_4}^{[31]} \begin{pmatrix} j_{k_1} & j_{k_2} & | & J \\ m_{k_1} & m_{k_2} & | & M \end{pmatrix} \begin{pmatrix} j_{k_3} & j_{k_4} & | & J \\ m_{k_3} & m_{k_4} & | & M \end{pmatrix}. \quad (\text{E.65})$$

ANGULAR-MOMENTUM COUPLING OF \hat{O}^{13}

Analogously, we start from the m -scheme expression of the cross-coupled matrix element:

$$\begin{aligned} \tilde{O}_{k_1 k_2 k_3 k_4}^{13} = & \sum_{l_1 l_2 l_3 l_4} \Theta_{l_1 l_2 l_3 l_4} \left(V_{l_4 k_1}^* U_{l_3 \bar{k}_2} V_{l_2 k_3} V_{l_1 k_4} - V_{l_4 k_1}^* V_{l_2 \bar{k}_2} U_{l_3 k_3} V_{l_1 k_4} - V_{l_4 k_1}^* V_{l_1 \bar{k}_2} V_{l_2 k_3} U_{l_3 k_4} \right. \\ & \left. + U_{l_1 k_1}^* V_{l_2 \bar{k}_2} U_{l_3 k_3} U_{l_4 k_4} - U_{l_1 k_1}^* U_{l_3 \bar{k}_2} V_{l_2 k_3} U_{l_4 k_4} + U_{l_1 k_1}^* U_{l_3 \bar{k}_2} U_{l_4 k_3} V_{l_2 k_4} \right). \quad (\text{E.66}) \end{aligned}$$

Coupling of the operator yields

$$\begin{aligned} \hat{O}^{[13]} = & \frac{1}{6} \sum_{k_1 k_2 k_3 k_4} O_{k_1 k_2 k_3 k_4}^{[13]} \hat{\beta}_{k_1}^\dagger \hat{\beta}_{k_4} \hat{\beta}_{k_3} \hat{\beta}_{k_2} \\ = & -\frac{1}{6} \sum_{\tilde{k}_1 \tilde{k}_2 \tilde{k}_3 \tilde{k}_4} \sum_{\substack{m_{k_1} m_{k_2} \\ m_{k_3} m_{k_4}}} (-1)^{j_{k_2} - m_{k_2} + j_{k_3} - m_{k_3} + j_{k_4} - m_{k_4}} O_{k_1 k_2 k_3 k_4}^{[13]} \\ & \times \mathcal{B}_{k_1 m_{k_1}} \bar{\mathcal{B}}_{j_{k_2} - m_{k_2}} \bar{\mathcal{B}}_{j_{k_3} - m_{k_3}} \bar{\mathcal{B}}_{j_{k_4} - m_{k_4}} \\ = & -\frac{1}{6} \sum_{\tilde{k}_1 \tilde{k}_2 \tilde{k}_3 \tilde{k}_4} \sum_{\substack{m_{k_1} m_{k_2} \\ m_{k_3} m_{k_4}}} \sum_{JJ'MM'} (-1)^{j_{k_2} - m_{k_2} + j_{k_3} - m_{k_3} + j_{k_4} - m_{k_4}} \tilde{O}_{k_1 k_2 k_3 k_4}^{[13]} \\ & \times \begin{pmatrix} j_{k_1} & j_{k_2} & | & J \\ m_{k_1} & -m_{k_2} & | & M \end{pmatrix} \begin{pmatrix} j_{k_3} & j_{k_4} & | & J' \\ -m_{k_3} & -m_{k_4} & | & M' \end{pmatrix} [\mathcal{B}_{j_{k_1}} \bar{\mathcal{B}}_{j_{k_2}}]_{JM} [\bar{\mathcal{B}}_{j_{k_3}} \bar{\mathcal{B}}_{j_{k_4}}]_{J'M'} \\ = & -\frac{1}{6} \sum_{\tilde{k}_1 \tilde{k}_2 \tilde{k}_3 \tilde{k}_4} \sum_{\substack{m_{k_1} m_{k_2} \\ m_{k_3} m_{k_4}}} \sum_{JJ'MM'} (-1)^{j_{k_2} - m_{k_2} + J' + M'} \tilde{O}_{k_1 \tilde{k}_2 k_3 k_4}^{[13]} \\ & \times \begin{pmatrix} j_{k_1} & j_{k_2} & | & J \\ m_{k_1} & -m_{k_2} & | & M \end{pmatrix} \begin{pmatrix} j_{k_3} & j_{k_4} & | & J' \\ m_{k_3} & m_{k_4} & | & -M' \end{pmatrix} [\mathcal{B}_{j_{k_1}} \bar{\mathcal{B}}_{j_{k_2}}]_{JM} [\bar{\mathcal{B}}_{j_{k_3}} \bar{\mathcal{B}}_{j_{k_4}}]_{J'M'} \\ = & -\frac{1}{6} \sum_{\tilde{k}_1 \tilde{k}_2 \tilde{k}_3 \tilde{k}_4} \sum_{\substack{m_{k_1} m_{k_2} \\ m_{k_3} m_{k_4}}} \sum_{JJ'MM'} (-1)^{j_{k_2} + m_{k_2} + J' + M'} \tilde{O}_{k_1 k_2 k_3 k_4}^{[13]} \\ & \times \begin{pmatrix} j_{k_1} & j_{k_2} & | & J \\ m_{k_1} & m_{k_2} & | & M \end{pmatrix} \begin{pmatrix} j_{k_3} & j_{k_4} & | & J' \\ m_{k_3} & m_{k_4} & | & -M' \end{pmatrix} [\mathcal{B}_{j_{k_1}} \bar{\mathcal{B}}_{j_{k_2}}]_{JM} [\bar{\mathcal{B}}_{j_{k_3}} \bar{\mathcal{B}}_{j_{k_4}}]_{J'M'} \quad (\text{E.67}) \end{aligned}$$

and we define the cross-coupled matrix element in J -scheme by

$$\tilde{O}_{\tilde{k}_1 \tilde{k}_2 JM; \tilde{k}_3 \tilde{k}_4 J'M'}^{[13]} = \sum_{\substack{m_{k_1} m_{k_2} \\ m_{k_3} m_{k_4}}} (-1)^{j_{k_2} + m_{k_2} + J' + M' + 1} \tilde{O}_{k_1 k_2 k_3 k_4}^{[13]} \begin{pmatrix} j_{k_1} & j_{k_2} & | & J \\ m_{k_1} & m_{k_2} & | & M \end{pmatrix} \begin{pmatrix} j_{k_3} & j_{k_4} & | & J' \\ m_{k_3} & m_{k_4} & | & -M' \end{pmatrix}. \quad (\text{E.68})$$

The corresponding six terms are given by

$$\begin{aligned}
 {}^1\tilde{O}_{k_1 k_2 J M; k_3 k_4 J'' M''}^{[13]} &= (-1)^{j_{k_2} + m_{k_2} + J + M' + 1} \sum_{\substack{m_{k_1} m_{k_2} \\ m_{k_3} m_{k_4}}} \sum_{l_1 l_2 l_3 l_4} \bar{o}_{l_1 l_2 l_3 l_4} V_{l_4 k_1}^* U_{l_3 \bar{k}_2} V_{l_2 k_3} V_{l_1 k_4} \\
 &\quad \times \begin{pmatrix} j_{k_1} & j_{k_2} \\ m_{k_1} & m_{k_2} \end{pmatrix} \begin{pmatrix} J \\ M \end{pmatrix} \begin{pmatrix} j_{k_3} & j_{k_4} \\ m_{k_3} & m_{k_4} \end{pmatrix} \begin{pmatrix} J'' \\ -M'' \end{pmatrix} \\
 &= \sum_{\substack{m_{k_1} m_{k_2} \\ m_{k_3} m_{k_4}}} \sum_{J' M'} \sum_{n_1 n_2 n_3 n_4} \bar{o}_{n_1 l j t_{k_4} n_2 l j t_{k_3} n_3 l j t_{\bar{k}_2} n_4 l j t_{k_1}}^{J'} \\
 &\quad \times (-1)^{j_{k_2} + j_{k_3} + j_{k_4} + m_{k_2} + m_{k_3} - m_{k_4}} \tilde{V}_{n_4 n_{k_1}}^{(\pi j t)_{k_1}} \tilde{U}_{n_3 n_{\bar{k}_2}}^{(\pi j t)_{\bar{k}_2}} \tilde{V}_{n_2 n_{k_3}}^{(\pi j t)_{k_3}} \tilde{V}_{n_1 n_{k_4}}^{(\pi j t)_{k_4}} \\
 &\quad \times \begin{pmatrix} j_{k_1} & j_{k_2} \\ m_{k_1} & m_{k_2} \end{pmatrix} \begin{pmatrix} J \\ M \end{pmatrix} \begin{pmatrix} j_{k_3} & j_{k_4} \\ m_{k_3} & m_{k_4} \end{pmatrix} \begin{pmatrix} J'' \\ -M'' \end{pmatrix} \begin{pmatrix} j_{k_4} & j_{k_3} \\ -m_{k_4} & -m_{k_3} \end{pmatrix} \begin{pmatrix} J' \\ M' \end{pmatrix} \begin{pmatrix} j_{k_2} & j_{k_1} \\ -m_{k_2} & -m_{k_1} \end{pmatrix} \begin{pmatrix} J' \\ M' \end{pmatrix} \\
 &= (-1)^{j_{k_3} + j_{k_4} + M_{J''}} \sum_{n_1 n_2 n_3 n_4} \bar{o}_{n_1 l j t_{k_4} n_2 l j t_{k_3} n_3 l j t_{\bar{k}_1} n_4 l j t_{\bar{k}_2}}^{J'} \\
 &\quad \times \tilde{V}_{n_4 n_{k_1}}^{(\pi j t)_{k_1}} \tilde{U}_{n_3 n_{\bar{k}_2}}^{(\pi j t)_{\bar{k}_2}} \tilde{V}_{n_2 n_{k_3}}^{(\pi j t)_{k_3}} \tilde{V}_{n_1 n_{k_4}}^{(\pi j t)_{k_4}} \delta_{J J''} \delta_{M - M''}, \tag{E.69}
 \end{aligned}$$

$$\begin{aligned}
 {}^2\tilde{O}_{k_1 k_2 J M; k_3 k_4 J'' M''}^{[13]} &= (-1)^{j_{k_2} + m_{j_{k_2}} + J' + M' + 1} \sum_{\substack{m_{k_1} m_{k_2} \\ m_{k_3} m_{k_4}}} \sum_{l_1 l_2 l_3 l_4} o_{l_1 l_2 l_3 l_4} V_{l_4 k_1}^* V_{l_2 \bar{k}_2} U_{l_3 k_3} V_{l_1 k_4} \\
 &\quad \times \begin{pmatrix} j_{k_1} & j_{k_2} \\ m_{k_1} & m_{k_2} \end{pmatrix} \begin{pmatrix} J \\ M \end{pmatrix} \begin{pmatrix} j_{k_3} & j_{k_4} \\ m_{k_3} & m_{k_4} \end{pmatrix} \begin{pmatrix} J'' \\ -M'' \end{pmatrix} \\
 &= \sum_{\substack{m_{k_1} m_{k_2} \\ m_{k_3} m_{k_4}}} \sum_{n_1 n_2 n_3 n_4} \sum_{J' M'} \bar{o}_{n_1 l j t_{k_4} n_2 l j t_{k_2} n_3 l j t_{k_1} n_4 l j t_{k_3}}^{J'} \\
 &\quad \times (-1)^{j_{k_1} + j_{k_4} + m_{k_2} - m_{k_4} - M + M'' + J'' + 1} \tilde{V}_{n_4 n_{k_1}}^{(\pi j t)_{k_1}} \tilde{V}_{n_2 n_{\bar{k}_2}}^{(\pi j t)_{\bar{k}_2}} \tilde{U}_{n_3 n_{k_3}}^{(\pi j t)_{k_3}} \tilde{V}_{n_1 n_{k_4}}^{(\pi j t)_{k_4}} \\
 &\quad \times \begin{pmatrix} j_{k_1} & j_{k_2} \\ m_{k_1} & m_{k_2} \end{pmatrix} \begin{pmatrix} J \\ M \end{pmatrix} \begin{pmatrix} j_{k_3} & j_{k_4} \\ m_{k_3} & m_{k_4} \end{pmatrix} \begin{pmatrix} J'' \\ -M'' \end{pmatrix} \begin{pmatrix} j_{k_4} & j_{k_2} \\ -m_{k_4} & m_{k_2} \end{pmatrix} \begin{pmatrix} J' \\ M' \end{pmatrix} \begin{pmatrix} j_{k_1} & j_{k_3} \\ -m_{k_1} & m_{k_3} \end{pmatrix} \begin{pmatrix} J' \\ M' \end{pmatrix} \\
 &= (-1)^{j_{k_3} + j_{k_4} + M + 1} \sum_{n_1 n_2 n_3 n_4} \sum_{J'} \bar{o}_{n_1 l j t_{k_4} n_2 l j t_{k_2} n_3 l j t_{k_1} n_4 l j t_{k_3}}^{J'} \\
 &\quad \times \tilde{V}_{n_4 n_{k_1}}^{(\pi j t)_{k_1}} \tilde{V}_{n_2 n_{k_2}}^{(\pi j t)_{k_2}} \tilde{U}_{n_3 n_{k_3}}^{(\pi j t)_{k_3}} \tilde{V}_{n_1 n_{k_4}}^{(\pi j t)_{k_4}} \hat{J}'^2 \left\{ \begin{matrix} j_{k_1} & j_{k_2} & J \\ j_{k_4} & j_{k_3} & J' \end{matrix} \right\} \delta_{J J''} \delta_{M - M''}, \tag{E.70}
 \end{aligned}$$

$$\begin{aligned}
 {}^3\tilde{O}_{k_1 k_2 J M; k_3 k_4 J'' M''}^{[13]} &= (-1)^{j_{k_2} + m_{j_{k_2}} + J' + M' + 1} \sum_{\substack{m_{k_1} m_{k_2} \\ m_{k_3} m_{k_4}}} \sum_{l_1 l_2 l_3 l_4} o_{l_1 l_2 l_3 l_4} V_{l_4 k_1} V_{l_1 \bar{k}_2} V_{l_2 k_3} U_{l_3 k_4} \\
 &\quad \times \begin{pmatrix} j_{k_1} & j_{k_2} \\ m_{k_1} & m_{k_2} \end{pmatrix} \begin{pmatrix} J \\ M \end{pmatrix} \begin{pmatrix} j_{k_3} & j_{k_4} \\ m_{k_3} & m_{k_4} \end{pmatrix} \begin{pmatrix} J'' \\ -M'' \end{pmatrix}
 \end{aligned}$$

$$\begin{aligned}
 &= \sum_{\substack{m_{k_1} m_{k_2} \\ m_{k_3} m_{k_4}}} \sum_{n_1 n_2 n_3 n_4} \sum_{J' M'} \bar{o}_{n_1 l j t_{k_3} n_2 l j t_{k_2} n_3 l j t_{k_1} n_4 l j t_{k_4}}^{J'} \\
 &\times (-1)^{j_{k_1} + j_{k_3} + m_{k_2} - m_{k_3} + J'' - M + M'' + 1} \tilde{V}_{n_4 n_{k_1}}^{(\pi j t)_{k_1}} \tilde{V}_{n_1 n_{k_2}}^{(\pi j t)_{k_2}} \tilde{V}_{n_2 n_{k_3}}^{(\pi j t)_{k_3}} \tilde{U}_{n_3 n_{k_4}}^{(\pi j t)_{k_4}} \\
 &\times \begin{pmatrix} j_{k_1} & j_{k_2} \\ m_{k_1} & m_{k_2} \end{pmatrix} \begin{pmatrix} j_{k_3} & j_{k_4} \\ m_{k_3} & m_{k_4} \end{pmatrix} \begin{pmatrix} j_{k_3} & j_{k_2} \\ -m_{k_3} & m_{k_2} \end{pmatrix} \begin{pmatrix} j_{k_1} & j_{k_4} \\ -m_{k_1} & m_{k_4} \end{pmatrix} \\
 &= (-1)^{J+M+1} \sum_{n_1 n_2 n_3 n_4} \sum_{J'} \bar{o}_{n_1 l j t_{k_3} n_2 l j t_{k_2} n_3 l j t_{k_1} n_4 l j t_{k_4}}^{J'} \\
 &\times \tilde{U}_{n_3 n_{k_1}}^{(\pi j t)_{k_1}} \tilde{V}_{n_4 n_{k_1}}^{(\pi j t)_{k_1}} \tilde{V}_{n_1 n_{k_2}}^{(\pi j t)_{k_2}} \tilde{V}_{n_2 n_{k_3}}^{(\pi j t)_{k_3}} \tilde{U}_{n_3 n_{k_4}}^{(\pi j t)_{k_4}} \hat{J}'^2 \begin{Bmatrix} j_{k_1} & j_{k_2} & J \\ j_{k_3} & j_{k_4} & J' \end{Bmatrix} \delta_{J J''} \delta_{M - M''}, \tag{E.71}
 \end{aligned}$$

$$\begin{aligned}
 {}^4 \tilde{O}_{k_1 k_2 J M; k_3 k_4 J'' M''}^{[13]} &= (-1)^{j_{k_2} + m_{j_{k_2}} + J' + M' + 1} \sum_{\substack{m_{k_1} m_{k_2} \\ m_{k_3} m_{k_4}}} \sum_{l_1 l_2 l_3 l_4} o_{l_1 l_2 l_3 l_4} U_{l_1 k_1} V_{l_2 \bar{k}_2} U_{l_3 k_3} U_{l_4 k_4} \\
 &\times \begin{pmatrix} j_{k_1} & j_{k_2} \\ m_{k_1} & m_{k_2} \end{pmatrix} \begin{pmatrix} j_{k_3} & j_{k_4} \\ m_{k_3} & m_{k_4} \end{pmatrix} \\
 &= \sum_{\substack{m_{k_1} m_{k_2} \\ m_{k_3} m_{k_4}}} \sum_{n_1 n_2 n_3 n_4} \sum_{J' M'} \bar{o}_{n_1 l j t_{k_3} n_2 l j t_{k_1} n_3 l j t_{k_2} n_4 l j t_{k_4}}^{J'} \\
 &\times (-1)^{j_{k_2} + j_{k_3} + M'' + J'' + 1} \tilde{U}_{n_1 n_{k_1}}^{(\pi j t)_{k_1}} \tilde{V}_{n_2 n_{k_2}}^{(\pi j t)_{k_2}} \tilde{U}_{n_3 n_{k_3}}^{(\pi j t)_{k_3}} \tilde{U}_{n_4 n_{k_4}}^{(\pi j t)_{k_4}} \\
 &\times \begin{pmatrix} j_{k_1} & j_{k_2} \\ m_{k_1} & m_{k_2} \end{pmatrix} \begin{pmatrix} j_{k_3} & j_{k_4} \\ m_{k_3} & m_{k_4} \end{pmatrix} \begin{pmatrix} j_{k_3} & j_{k_1} \\ -m_{k_3} & m_{k_1} \end{pmatrix} \begin{pmatrix} j_{k_2} & j_{k_4} \\ -m_{k_2} & m_{k_4} \end{pmatrix} \\
 &= (-1)^{j_{k_1} + j_{k_2} + M + 1} \sum_{n_1 n_2 n_3 n_4} \sum_{J'} \bar{o}_{n_1 l j t_{k_3} n_2 l j t_{k_1} n_3 l j t_{k_2} n_4 l j t_{k_4}}^{J'} \\
 &\times \tilde{U}_{n_1 n_{k_1}}^{(\pi j t)_{k_1}} \tilde{V}_{n_2 n_{k_2}}^{(\pi j t)_{k_2}} \tilde{U}_{n_3 n_{k_3}}^{(\pi j t)_{k_3}} \tilde{U}_{n_4 n_{k_4}}^{(\pi j t)_{k_4}} \hat{J}'^2 \begin{Bmatrix} j_{k_1} & j_{k_2} & J \\ j_{k_4} & j_{k_3} & J' \end{Bmatrix} \delta_{J J''} \delta_{M - M''}, \tag{E.72}
 \end{aligned}$$

$$\begin{aligned}
 {}^5 \tilde{O}_{k_1 k_2 J M; k_3 k_4 J'' M''}^{[13]} &= (-1)^{j_{k_2} + m_{j_{k_2}} + J' + M' + 1} \sum_{\substack{m_{k_1} m_{k_2} \\ m_{k_3} m_{k_4}}} \sum_{l_1 l_2 l_3 l_4} o_{l_1 l_2 l_3 l_4} U_{l_1 k_1} U_{l_3 \bar{k}_2} V_{l_2 k_3} U_{l_4 k_4} \\
 &\times \begin{pmatrix} j_{k_1} & j_{k_2} \\ m_{k_1} & m_{k_2} \end{pmatrix} \begin{pmatrix} j_{k_3} & j_{k_4} \\ m_{k_3} & m_{k_4} \end{pmatrix} \\
 &= \sum_{\substack{m_{k_1} m_{k_2} \\ m_{k_3} m_{k_4}}} \sum_{n_1 n_2 n_3 n_4} \sum_{J' M'} \bar{o}_{n_1 l j t_{k_2} n_2 l j t_{k_1} n_3 l j t_{k_3} n_4 l j t_{k_4}}^{J'} \\
 &\times \tilde{U}_{n_1 n_{k_1}}^{(\pi j t)_{k_1}} \tilde{U}_{n_3 n_{k_2}}^{(\pi j t)_{k_2}} \tilde{V}_{n_2 n_{k_3}}^{(\pi j t)_{k_3}} \tilde{U}_{n_4 n_{k_4}}^{(\pi j t)_{k_4}} (-1)^{J'' + M''} \\
 &\times \begin{pmatrix} j_{k_1} & j_{k_2} \\ m_{k_1} & m_{k_2} \end{pmatrix} \begin{pmatrix} j_{k_3} & j_{k_4} \\ m_{k_3} & m_{k_4} \end{pmatrix} \begin{pmatrix} j_{k_2} & j_{k_1} \\ m_{k_2} & m_{k_1} \end{pmatrix} \begin{pmatrix} j_{k_3} & j_{k_4} \\ m_{k_3} & m_{k_4} \end{pmatrix}
 \end{aligned}$$

$$\begin{aligned}
 &= (-1)^{j_{k_1}+j_{k_2}+M} \sum_{n_1 n_2 n_3 n_4} \bar{o}_{n_1 l j t_{k_3} n_2 l j t_{k_1} n_3 l j t_{k_2} n_4 l j t_{k_4}}^{J'} \\
 &\quad \times \tilde{U}_{n_1 n_{k_1}}^{(\pi j t)_{k_1}} \tilde{U}_{n_3 n_{k_2}}^{(\pi j t)_{k_2}} \tilde{V}_{n_2 n_{k_3}}^{(\pi j t)_{k_3}} \tilde{U}_{n_4 n_{k_4}}^{(\pi j t)_{k_4}} \delta_{JJ''} \delta_{M-M''}, \tag{E.73}
 \end{aligned}$$

$$\begin{aligned}
 {}^6\tilde{O}_{k_1 k_2 JM; k_3 k_4 J'' M''}^{[13]} &= (-1)^{j_{k_2}+m_{j_{k_2}}+J'+M'+1} \sum_{\substack{m_{k_1} m_{k_2} \\ m_{k_3} m_{k_4}}} \sum_{l_1 l_2 l_3 l_4} o_{l_1 l_2 l_3 l_4} U_{l_1 k_1} U_{l_3 \bar{k}_2} U_{l_4 k_3} V_{l_2 k_4} \\
 &\quad \times \begin{pmatrix} j_{k_1} & j_{k_2} \\ m_{k_1} & m_{k_2} \end{pmatrix} \begin{pmatrix} j_{k_3} & j_{k_4} \\ m_{k_3} & m_{k_4} \end{pmatrix} \begin{pmatrix} J \\ -M'' \end{pmatrix} \\
 &= \sum_{\substack{m_{k_1} m_{k_2} \\ m_{k_3} m_{k_4}}} \sum_{n_1 n_2 n_3 n_4} \sum_{J' M'} \bar{o}_{n_1 l j t_{k_4} n_2 l j t_{k_1} n_3 l j t_{k_2} n_4 l j t_{k_3}}^{J'} \\
 &\quad \times \tilde{U}_{n_1 n_{k_1}}^{(\pi j t)_{k_1}} \tilde{U}_{n_3 n_{k_2}}^{(\pi j t)_{k_2}} \tilde{U}_{n_4 n_{k_3}}^{(\pi j t)_{k_3}} \tilde{V}_{n_2 n_{k_4}}^{(\pi j t)_{k_4}} (-1)^{j_{k_2}+j_{k_4}+M+M'+M''+J''} \\
 &\quad \times \begin{pmatrix} j_{k_1} & j_{k_2} \\ m_{k_1} & m_{k_2} \end{pmatrix} \begin{pmatrix} j_{k_3} & j_{k_4} \\ m_{k_3} & m_{k_4} \end{pmatrix} \begin{pmatrix} J \\ -M'' \end{pmatrix} \begin{pmatrix} j_{k_4} & j_{k_1} \\ -m_{k_4} & m_{k_1} \end{pmatrix} \begin{pmatrix} J' \\ -M \end{pmatrix} \\
 &= (-1)^{j_{k_1}+j_{k_2}+j_{k_3}+j_{k_4}+J+M+1} \sum_{n_1 n_2 n_3 n_4} \sum_{J'} \bar{o}_{n_1 l j t_{k_4} n_2 l j t_{k_1} n_3 l j t_{k_2} n_4 l j t_{k_3}}^{J'} \\
 &\quad \times \tilde{U}_{n_1 n_{k_1}}^{(\pi j t)_{k_1}} \tilde{U}_{n_3 n_{k_2}}^{(\pi j t)_{k_2}} \tilde{U}_{n_4 n_{k_3}}^{(\pi j t)_{k_3}} \tilde{V}_{n_2 n_{k_4}}^{(\pi j t)_{k_4}} \hat{J}'^2 \begin{Bmatrix} j_{k_1} & j_{k_2} & J \\ j_{k_3} & j_{k_4} & J' \end{Bmatrix} \delta_{JJ''} \delta_{M-M''}. \tag{E.74}
 \end{aligned}$$

Therefore, we finally arrive at

$$O_{k_1 k_2 JM; k_3 k_4 J'' M''}^{[13]} \equiv (-1)^M \delta_{JJ''} \delta_{M-M''} J \tilde{O}_{\bar{k}_1 \bar{k}_2 \bar{k}_3 \bar{k}_4}^{[13]}, \tag{E.75}$$

leading to the spherical form of the operator

$$\begin{aligned}
 \tilde{O}^{[13]} &= \frac{1}{6} \sum_{\bar{k}_1 \bar{k}_2 \bar{k}_3 \bar{k}_4} \sum_{JJ'MM'} J \tilde{O}_{\bar{k}_1 \bar{k}_2 \bar{k}_3 \bar{k}_4}^{[13]} (-1)^M [\mathcal{B}_{j_{k_1}} \bar{\mathcal{B}}_{j_{k_2}}]_{JM} [\bar{\mathcal{B}}_{j_{k_3}} \mathcal{B}_{j_{k_4}}]_{J-M} \\
 &= \frac{1}{6} \sum_{\bar{k}_1 \bar{k}_2 \bar{k}_3 \bar{k}_4} \sum_J J \tilde{O}_{\bar{k}_1 \bar{k}_2 \bar{k}_3 \bar{k}_4}^{[13]} [\mathcal{B}_{j_{k_1}} \bar{\mathcal{B}}_{j_{k_2}}]_J \cdot [\bar{\mathcal{B}}_{j_{k_3}} \mathcal{B}_{j_{k_4}}]_J. \tag{E.76}
 \end{aligned}$$

By diagonality in J and M we can write

$$J \tilde{O}_{\bar{k}_1 \bar{k}_2 \bar{k}_3 \bar{k}_4}^{[13]} \equiv \sum_{\substack{m_{k_1} m_{k_2} \\ m_{k_3} m_{k_4}}} (-1)^{j_{k_2}+m_{k_2}+J+1} \times \tilde{O}_{k_1 k_2 k_3 k_4}^{[13]} \begin{pmatrix} j_{k_1} & j_{k_2} \\ m_{k_1} & m_{k_2} \end{pmatrix} \begin{pmatrix} j_{k_3} & j_{k_4} \\ m_{k_3} & m_{k_4} \end{pmatrix} \begin{pmatrix} J \\ M \end{pmatrix} \tag{E.77}$$

as well as the converse transformation

$$\tilde{O}_{k_1 k_2 k_3 k_4}^{[13]} \equiv \sum_{JM} (-1)^{j_{k_2}+m_{k_2}+J+1} \times J \tilde{O}_{\bar{k}_1 \bar{k}_2 \bar{k}_3 \bar{k}_4}^{[13]} \begin{pmatrix} j_{k_1} & j_{k_2} \\ m_{k_1} & m_{k_2} \end{pmatrix} \begin{pmatrix} j_{k_3} & j_{k_4} \\ m_{k_3} & m_{k_4} \end{pmatrix} \begin{pmatrix} J \\ M \end{pmatrix}. \tag{E.78}$$

ANGULAR-MOMENTUM COUPLING OF \hat{O}^{04}

The m -scheme expression of the cross-coupled matrix element is

$$\begin{aligned} \tilde{O}_{k_1 k_2 k_3 k_4}^{04} = & \sum_{l_1 l_2 l_3 l_4} \Theta_{l_1 l_2 l_3 l_4} \left(U_{l_3 \bar{k}_1} U_{l_4 \bar{k}_2} V_{l_2 k_3} V_{l_1 k_4} - U_{l_3 \bar{k}_1} V_{l_2 \bar{k}_2} U_{l_4 k_3} V_{l_1 k_4} + U_{l_3 \bar{k}_1} V_{l_2 \bar{k}_2} V_{l_1 k_3} U_{l_4 k_4} \right. \\ & \left. - V_{l_2 k_1} U_{l_3 k_2} V_{l_1 k_3} U_{l_4 k_4} + V_{l_2 \bar{k}_1} V_{l_1 \bar{k}_2} U_{l_3 k_3} U_{l_4 k_4} + V_{l_2 \bar{k}_1} U_{l_3 \bar{k}_2} U_{l_4 k_3} V_{l_1 k_4} \right). \end{aligned} \quad (\text{E.79})$$

The coupling of the operator yields

$$\begin{aligned} \hat{O}^{[04]} = & \frac{1}{24} \sum_{k_1 k_2 k_3 k_4} O_{k_1 k_2 k_3 k_4}^{[04]} \hat{\beta}_{k_1} \hat{\beta}_{k_2} \hat{\beta}_{k_3} \hat{\beta}_{k_4} \\ = & \sum_{\tilde{k}_1 \tilde{k}_2 \tilde{k}_3 \tilde{k}_4} \sum_{\substack{m_{k_1} m_{k_2} \\ m_{k_3} m_{k_4}}} (-1)^{j_{k_1} - m_{k_1} + j_{k_2} - m_{k_2} + j_{k_3} - m_{k_3} + j_{k_4} - m_{k_4}} O_{k_1 k_2 k_3 k_4}^{[04]} \\ & \times \bar{\mathcal{B}}_{j_{k_1} - m_{k_1}} \bar{\mathcal{B}}_{j_{k_2} - m_{k_2}} \bar{\mathcal{B}}_{j_{k_3} - m_{k_3}} \bar{\mathcal{B}}_{j_{k_4} - m_{k_4}} \\ = & \frac{1}{24} \sum_{\tilde{k}_1 \tilde{k}_2 \tilde{k}_3 \tilde{k}_4} \sum_{\substack{m_{k_1} m_{k_2} \\ m_{k_3} m_{k_4}}} \sum_{J J' M M'} (-1)^{j_{k_1} + j_{k_2} + j_{k_3} + j_{k_4} + M + M'} O_{k_1 k_2 k_3 k_4}^{[04]} \\ & \times \begin{pmatrix} j_{k_1} & j_{k_2} & | & J \\ -m_{k_1} & -m_{k_2} & | & M \end{pmatrix} \begin{pmatrix} j_{k_3} & j_{k_4} & | & J' \\ -m_{k_3} & -m_{k_4} & | & M' \end{pmatrix} [\bar{\mathcal{B}}_{j_{k_1}} \bar{\mathcal{B}}_{j_{k_2}}]_{JM} [\bar{\mathcal{B}}_{j_{k_3}} \bar{\mathcal{B}}_{j_{k_4}}]_{J'M'} \\ = & \frac{1}{24} \sum_{\tilde{k}_1 \tilde{k}_2 \tilde{k}_3 \tilde{k}_4} \sum_{\substack{m_{k_1} m_{k_2} \\ m_{k_3} m_{k_4}}} \sum_{J J' M M'} (-1)^{j_{k_1} + j_{k_2} + J + M + M'} O_{k_1 k_2 k_3 k_4}^{[04]} \\ & \times \begin{pmatrix} j_{k_1} & j_{k_2} & | & J \\ -m_{k_1} & -m_{k_2} & | & M \end{pmatrix} \begin{pmatrix} j_{k_3} & j_{k_4} & | & J' \\ m_{k_3} & m_{k_4} & | & -M' \end{pmatrix} [\bar{\mathcal{B}}_{j_{k_1}} \bar{\mathcal{B}}_{j_{k_2}}]_{JM} [\bar{\mathcal{B}}_{j_{k_3}} \bar{\mathcal{B}}_{j_{k_4}}]_{J'M'} \\ = & \frac{1}{24} \sum_{\tilde{k}_1 \tilde{k}_2 \tilde{k}_3 \tilde{k}_4} \sum_{\substack{m_{k_1} m_{k_2} \\ m_{k_3} m_{k_4}}} \sum_{J J' M M'} (-1)^{j_{k_1} + j_{k_2} + J - m_{k_1} - m_{k_2} - m_{k_3} - m_{k_4}} \tilde{O}_{k_1 k_2 k_3 k_4}^{[04]} \\ & \times \begin{pmatrix} j_{k_1} & j_{k_2} & | & J \\ -m_{k_1} & -m_{k_2} & | & M \end{pmatrix} \begin{pmatrix} j_{k_3} & j_{k_4} & | & J' \\ m_{k_3} & m_{k_4} & | & -M' \end{pmatrix} [\bar{\mathcal{B}}_{j_{k_1}} \bar{\mathcal{B}}_{j_{k_2}}]_{JM} [\bar{\mathcal{B}}_{j_{k_3}} \bar{\mathcal{B}}_{j_{k_4}}]_{J'M'} \\ = & \frac{1}{24} \sum_{\tilde{k}_1 \tilde{k}_2 \tilde{k}_3 \tilde{k}_4} \sum_{\substack{m_{k_1} m_{k_2} \\ m_{k_3} m_{k_4}}} \sum_{J J' M M'} (-1)^{j_{k_1} + j_{k_2} + J + m_{k_1} + m_{k_2} - m_{k_3} - m_{k_4}} \tilde{O}_{k_1 k_2 k_3 k_4}^{[04]} \\ & \times \begin{pmatrix} j_{k_1} & j_{k_2} & | & J \\ m_{k_1} & m_{k_2} & | & M \end{pmatrix} \begin{pmatrix} j_{k_3} & j_{k_4} & | & J' \\ m_{k_3} & m_{k_4} & | & -M' \end{pmatrix} [\bar{\mathcal{B}}_{j_{k_1}} \bar{\mathcal{B}}_{j_{k_2}}]_{JM} [\bar{\mathcal{B}}_{j_{k_3}} \bar{\mathcal{B}}_{j_{k_4}}]_{J'M'} \\ = & \frac{1}{24} \sum_{\tilde{k}_1 \tilde{k}_2 \tilde{k}_3 \tilde{k}_4} \sum_{\substack{m_{k_1} m_{k_2} \\ m_{k_3} m_{k_4}}} \sum_{J J' M M'} (-1)^{j_{k_1} + j_{k_2} + J - M + M'} \tilde{O}_{k_1 k_2 k_3 k_4}^{[04]} \\ & \times \begin{pmatrix} j_{k_1} & j_{k_2} & | & J \\ m_{k_1} & m_{k_2} & | & M \end{pmatrix} \begin{pmatrix} j_{k_3} & j_{k_4} & | & J' \\ m_{k_3} & m_{k_4} & | & -M' \end{pmatrix} [\bar{\mathcal{B}}_{j_{k_1}} \bar{\mathcal{B}}_{j_{k_2}}]_{JM} [\bar{\mathcal{B}}_{j_{k_3}} \bar{\mathcal{B}}_{j_{k_4}}]_{J'M'} \end{aligned} \quad (\text{E.80})$$

and we define the cross-coupled matrix element in J -scheme by

$$\tilde{O}_{k_1 k_2 J M; k_3 k_4 J' M'}^{[04]} = \sum_{\tilde{k}_1 \tilde{k}_2 \tilde{k}_3 \tilde{k}_4} (-1)^{j_{k_1} + j_{k_2} + J' - M + M'} \tilde{O}_{k_1 k_2 k_3 k_4}^{[04]} \begin{pmatrix} j_{k_1} & j_{k_2} & J \\ m_{k_1} & m_{k_2} & M \end{pmatrix} \begin{pmatrix} j_{k_3} & j_{k_4} & J' \\ m_{k_3} & m_{k_4} & -M' \end{pmatrix}. \quad (\text{E.81})$$

The corresponding six terms are given by

$$\begin{aligned} {}^1 \tilde{O}_{k_1 k_2 J M; k_3 k_4 J'' M''}^{[04]} &= (-1)^{j_{k_1} + j_{k_2} + J'' - M + M''} \sum_{\substack{m_{k_1} m_{k_2} \\ m_{k_3} m_{k_4}}} \sum_{l_1 l_2 l_3 l_4} \bar{o}_{l_1 l_2 l_3 l_4} U_{l_3 \bar{k}_1} U_{l_4 \bar{k}_2} V_{l_2 k_3} V_{l_1 k_4} \\ &\times \begin{pmatrix} j_{k_1} & j_{k_2} & J \\ m_{k_1} & m_{k_2} & M \end{pmatrix} \begin{pmatrix} j_{k_3} & j_{k_4} & J'' \\ m_{k_3} & m_{k_4} & -M'' \end{pmatrix} \\ &= \sum_{\substack{m_{k_1} m_{k_2} \\ m_{k_3} m_{k_4}}} \sum_{J' M'} \sum_{n_1 n_2 n_3 n_4} \bar{o}_{n_1 l j t_{k_4} n_2 l j t_{k_3} n_3 l j t_{\bar{k}_1} n_4 l j t_{\bar{k}_2}} \bar{o}_{n_1 l j t_{k_4} n_2 l j t_{k_3} n_3 l j t_{\bar{k}_1} n_4 l j t_{\bar{k}_2}} \\ &\times (-1)^{j_{k_2} + j_{k_3} + j_{k_4} + m_{k_2} + m_{k_3} - m_{k_4}} \tilde{U}_{n_3 n_{k_1}}^{(\pi j t)_{k_1}} \tilde{U}_{n_4 n_{k_2}}^{(\pi j t)_{k_2}} \tilde{V}_{n_2 n_{k_3}}^{(\pi j t)_{k_3}} \tilde{V}_{n_1 n_{k_4}}^{(\pi j t)_{k_4}} \\ &\times \begin{pmatrix} j_{k_1} & j_{k_2} & J \\ m_{k_1} & m_{k_2} & M \end{pmatrix} \begin{pmatrix} j_{k_3} & j_{k_4} & J'' \\ m_{k_3} & m_{k_4} & -M'' \end{pmatrix} \begin{pmatrix} j_{k_4} & j_{k_3} & J' \\ -m_{k_4} & -m_{k_3} & M' \end{pmatrix} \begin{pmatrix} j_{k_1} & j_{k_2} & J' \\ -m_{k_1} & -m_{k_2} & M' \end{pmatrix} \\ &= (-1)^{j_{k_3} + j_{k_4} + M''} \sum_{J'} \sum_{n_1 n_2 n_3 n_4} \bar{o}_{n_1 l j t_{k_4} n_2 l j t_{k_3} n_3 l j t_{\bar{k}_1} n_4 l j t_{\bar{k}_2}} \bar{o}_{n_1 l j t_{k_4} n_2 l j t_{k_3} n_3 l j t_{\bar{k}_1} n_4 l j t_{\bar{k}_2}} \\ &\times \tilde{U}_{n_3 n_{k_1}}^{(\pi j t)_{k_1}} \tilde{U}_{n_4 n_{k_2}}^{(\pi j t)_{k_2}} \tilde{V}_{n_2 n_{k_3}}^{(\pi j t)_{k_3}} \tilde{V}_{n_1 n_{k_4}}^{(\pi j t)_{k_4}} \delta_{J J''} \delta_{M - M''}, \quad (\text{E.82}) \end{aligned}$$

$$\begin{aligned} {}^2 \tilde{O}_{k_1 k_2 J M; k_3 k_4 J'' M''}^{[04]} &= (-1)^{j_{k_1} + j_{k_2} + J'' - M + M''} \sum_{\substack{m_{k_1} m_{k_2} \\ m_{k_3} m_{k_4}}} \sum_{l_1 l_2 l_3 l_4} o_{l_1 l_2 l_3 l_4} U_{l_3 \bar{k}_1} V_{l_2 \bar{k}_2} U_{l_4 k_3} V_{l_1 k_4} \\ &\times \begin{pmatrix} j_{k_1} & j_{k_2} & J \\ m_{k_1} & m_{k_2} & M \end{pmatrix} \begin{pmatrix} j_{k_3} & j_{k_4} & J'' \\ m_{k_3} & m_{k_4} & -M'' \end{pmatrix} \\ &= \sum_{\substack{m_{k_1} m_{k_2} \\ m_{k_3} m_{k_4}}} \sum_{n_1 n_2 n_3 n_4} \sum_{J' M'} \bar{o}_{n_1 l j t_{k_4} n_2 l j t_{k_2} n_3 l j t_{k_1} n_4 l j t_{k_3}} \bar{o}_{n_1 l j t_{k_4} n_2 l j t_{k_2} n_3 l j t_{k_1} n_4 l j t_{k_3}} \\ &\times (-1)^{j_{k_1} + j_{k_4} + m_{k_2} - m_{k_4} - M + M'' + J'' + 1} \tilde{U}_{n_3 n_{k_1}}^{(\pi j t)_{k_1}} \tilde{V}_{n_2 n_{k_2}}^{(\pi j t)_{k_2}} \tilde{U}_{n_4 n_{k_3}}^{(\pi j t)_{k_3}} \tilde{V}_{n_1 n_{k_4}}^{(\pi j t)_{k_4}} \\ &\times \begin{pmatrix} j_{k_1} & j_{k_2} & J \\ m_{k_1} & m_{k_2} & M \end{pmatrix} \begin{pmatrix} j_{k_3} & j_{k_4} & J'' \\ m_{k_3} & m_{k_4} & -M'' \end{pmatrix} \begin{pmatrix} j_{k_4} & j_{k_2} & J' \\ -m_{k_4} & m_{k_2} & M' \end{pmatrix} \begin{pmatrix} j_{k_1} & j_{k_3} & J' \\ -m_{k_1} & m_{k_3} & M' \end{pmatrix} \\ &= (-1)^{j_{k_3} + j_{k_4} + M + 1} \sum_{n_1 n_2 n_3 n_4} \sum_{J'} \bar{o}_{n_1 l j t_{k_4} n_2 l j t_{k_2} n_3 l j t_{k_1} n_4 l j t_{k_3}} \bar{o}_{n_1 l j t_{k_4} n_2 l j t_{k_2} n_3 l j t_{k_1} n_4 l j t_{k_3}} \\ &\times \tilde{U}_{n_3 n_{k_1}}^{(\pi j t)_{k_1}} \tilde{V}_{n_2 n_{k_2}}^{(\pi j t)_{k_2}} \tilde{U}_{n_4 n_{k_3}}^{(\pi j t)_{k_3}} \tilde{V}_{n_1 n_{k_4}}^{(\pi j t)_{k_4}} \hat{J}' \begin{Bmatrix} j_{k_1} & j_{k_2} & J \\ j_{k_4} & j_{k_3} & J' \end{Bmatrix} \delta_{J J''} \delta_{M - M''}, \quad (\text{E.83}) \end{aligned}$$

$$\begin{aligned}
 {}^3\tilde{O}_{k_1 k_2 J M; k_3 k_4 J'' M''}^{[04]} &= (-1)^{j_{k_1} + j_{k_2} + J'' - M + M''} \sum_{\substack{m_{k_1} m_{k_2} \\ m_{k_3} m_{k_4}}} \sum_{l_1 l_2 l_3 l_4} o_{l_1 l_2 l_3 l_4} U_{l_3 \bar{k}_1} V_{l_2 \bar{k}_2} V_{l_1 k_3} U_{l_4 k_4} \\
 &\times \begin{pmatrix} j_{k_1} & j_{k_2} & | & J \\ m_{k_1} & m_{k_2} & | & M \end{pmatrix} \begin{pmatrix} j_{k_3} & j_{k_4} & | & J'' \\ m_{k_3} & m_{k_4} & | & -M'' \end{pmatrix} \\
 &= \sum_{\substack{m_{k_1} m_{k_2} \\ m_{k_3} m_{k_4}}} \sum_{n_{l_1} n_{l_2} n_{l_3} n_{l_4}} \sum_{J' M'} \bar{o}_{n_{l_1} l_1 j t_{k_3} n_{l_2} l_2 j t_{k_2} n_{l_3} l_3 j t_{k_1} n_{l_4} l_4 j t_{k_4}}^{J'} \\
 &\times (-1)^{j_{k_1} + j_{k_3} + m_{k_2} - m_{k_3} + J'' - M + M'' + 1} \tilde{U}_{n_{l_3} n_{k_1}}^{(\pi j t)_{k_1}} \tilde{V}_{n_{l_2} n_{k_2}}^{(\pi j t)_{k_2}} \tilde{V}_{n_{l_1} n_{k_3}}^{(\pi j t)_{k_3}} \tilde{U}_{n_{l_4} n_{k_4}}^{(\pi j t)_{k_4}} \\
 &\times \begin{pmatrix} j_{k_1} & j_{k_2} & | & J \\ m_{k_1} & m_{k_2} & | & -M \end{pmatrix} \begin{pmatrix} j_{k_3} & j_{k_4} & | & J'' \\ m_{k_3} & m_{k_4} & | & -M'' \end{pmatrix} \begin{pmatrix} j_{k_3} & j_{k_2} & | & J' \\ -m_{k_3} & m_{k_2} & | & M' \end{pmatrix} \begin{pmatrix} j_{k_1} & j_{k_4} & | & J' \\ -m_{k_1} & m_{k_4} & | & M \end{pmatrix} \\
 &= (-1)^{J + M + 1} \sum_{n_{l_1} n_{l_2} n_{l_3} n_{l_4}} \sum_{J'} \bar{o}_{n_{l_1} l_1 j t_{k_3} n_{l_2} l_2 j t_{k_2} n_{l_3} l_3 j t_{k_1} n_{l_4} l_4 j t_{k_4}}^{J'} \\
 &\times \tilde{U}_{n_{l_3} n_{k_1}}^{(\pi j t)_{k_1}} \tilde{V}_{n_{l_2} n_{k_2}}^{(\pi j t)_{k_2}} \tilde{V}_{n_{l_1} n_{k_3}}^{(\pi j t)_{k_3}} \tilde{U}_{n_{l_4} n_{k_4}}^{(\pi j t)_{k_4}} \hat{J}' \begin{Bmatrix} j_{k_1} & j_{k_2} & J \\ j_{k_3} & j_{k_4} & J' \end{Bmatrix} \delta_{J J''} \delta_{M - M''}, \quad (\text{E.84})
 \end{aligned}$$

$$\begin{aligned}
 {}^4\tilde{O}_{k_1 k_2 J M; k_3 k_4 J'' M''}^{[04]} &= (-1)^{j_{k_1} + j_{k_2} + J'' - M + M''} \sum_{\substack{m_{k_1} m_{k_2} \\ m_{k_3} m_{k_4}}} \sum_{l_1 l_2 l_3 l_4} o_{l_1 l_2 l_3 l_4} V_{l_2 \bar{k}_1} U_{l_3 \bar{k}_2} V_{l_1 k_3} U_{l_4 k_4} \\
 &\times \begin{pmatrix} j_{k_1} & j_{k_2} & | & J \\ m_{k_1} & m_{k_2} & | & M \end{pmatrix} \begin{pmatrix} j_{k_3} & j_{k_4} & | & J'' \\ m_{k_3} & m_{k_4} & | & -M'' \end{pmatrix} \\
 &= \sum_{\substack{m_{k_1} m_{k_2} \\ m_{k_3} m_{k_4}}} \sum_{n_{l_1} n_{l_2} n_{l_3} n_{l_4}} \sum_{J' M'} \bar{o}_{n_{l_1} l_1 j t_{k_3} n_{l_2} l_2 j t_{k_1} n_{l_3} l_3 j t_{k_2} n_{l_4} l_4 j t_{k_4}}^{J'} \\
 &\times (-1)^{j_{k_2} + j_{k_3} + M'' + J'' + 1} \tilde{V}_{n_{l_2} n_{k_1}}^{(\pi j t)_{k_1}} \tilde{U}_{n_{l_3} n_{k_2}}^{(\pi j t)_{k_2}} \tilde{V}_{n_{l_1} n_{k_3}}^{(\pi j t)_{k_3}} \tilde{U}_{n_{l_4} n_{k_4}}^{(\pi j t)_{k_4}} \\
 &\times \begin{pmatrix} j_{k_1} & j_{k_2} & | & J \\ m_{k_1} & m_{k_2} & | & M \end{pmatrix} \begin{pmatrix} j_{k_3} & j_{k_4} & | & J'' \\ m_{k_3} & m_{k_4} & | & -M'' \end{pmatrix} \begin{pmatrix} j_{k_3} & j_{k_1} & | & J' \\ -m_{k_3} & m_{k_1} & | & M' \end{pmatrix} \begin{pmatrix} j_{k_2} & j_{k_4} & | & J' \\ -m_{k_2} & m_{k_4} & | & M \end{pmatrix} \\
 &= (-1)^{j_{k_1} + j_{k_2} + M + 1} \sum_{n_{l_1} n_{l_2} n_{l_3} n_{l_4}} \sum_{J'} \bar{o}_{n_{l_1} l_1 j t_{k_3} n_{l_2} l_2 j t_{k_1} n_{l_3} l_3 j t_{k_2} n_{l_4} l_4 j t_{k_4}}^{J'} \\
 &\times \tilde{V}_{n_{l_2} n_{k_1}}^{(\pi j t)_{k_1}} \tilde{U}_{n_{l_3} n_{k_2}}^{(\pi j t)_{k_2}} \tilde{V}_{n_{l_1} n_{k_3}}^{(\pi j t)_{k_3}} \tilde{U}_{n_{l_4} n_{k_4}}^{(\pi j t)_{k_4}} \hat{J}' \begin{Bmatrix} j_{k_1} & j_{k_2} & J \\ j_{k_4} & j_{k_3} & J' \end{Bmatrix} \delta_{J J''} \delta_{M - M''}, \quad (\text{E.85})
 \end{aligned}$$

$$\begin{aligned}
 {}^5\tilde{O}_{k_1 k_2 J M; k_3 k_4 J'' M''}^{[04]} &= (-1)^{j_{k_1} + j_{k_2} + J'' - M + M''} \sum_{\substack{m_{k_1} m_{k_2} \\ m_{k_3} m_{k_4}}} \sum_{l_1 l_2 l_3 l_4} o_{l_1 l_2 l_3 l_4} V_{l_2 \bar{k}_1} V_{l_1 \bar{k}_2} U_{l_3 k_3} U_{l_4 k_4} \\
 &\times \begin{pmatrix} j_{k_1} & j_{k_2} & | & J \\ m_{k_1} & m_{k_2} & | & M \end{pmatrix} \begin{pmatrix} j_{k_3} & j_{k_4} & | & J'' \\ m_{k_3} & m_{k_4} & | & -M'' \end{pmatrix} \\
 &= \sum_{\substack{m_{k_1} m_{k_2} \\ m_{k_3} m_{k_4}}} \sum_{n_{l_1} n_{l_2} n_{l_3} n_{l_4}} \sum_{J' M'} \bar{o}_{n_{l_1} l_1 j t_{k_2} n_{l_2} l_2 j t_{k_1} n_{l_3} l_3 j t_{k_3} n_{l_4} l_4 j t_{k_4}}^{J'}
 \end{aligned}$$

$$\begin{aligned}
 & \times \tilde{V}_{n_{l_2} n_{k_1}}^{(\pi j t)_{k_1}} \tilde{V}_{n_{l_1} n_{k_2}}^{(\pi j t)_{k_2}} \tilde{U}_{n_{l_3} n_{k_3}}^{(\pi j t)_{k_3}} \tilde{U}_{n_{l_4} n_{k_4}}^{(\pi j t)_{k_4}} (-1)^{J''+M''} \\
 & \times \begin{pmatrix} j_{k_1} & j_{k_2} & | & J \\ m_{k_1} & m_{k_2} & | & M \end{pmatrix} \begin{pmatrix} j_{k_3} & j_{k_4} & | & J'' \\ m_{k_3} & m_{k_4} & | & -M'' \end{pmatrix} \begin{pmatrix} j_{k_2} & j_{k_1} & | & J' \\ m_{k_2} & m_{k_1} & | & M' \end{pmatrix} \begin{pmatrix} j_{k_3} & j_{k_4} & | & J' \\ m_{k_3} & m_{k_4} & | & M \end{pmatrix} \\
 & = (-1)^{j_{k_1}+j_{k_2}+M} \sum_{n_{l_1} n_{l_2} n_{l_3} n_{l_4}} \bar{o}_{n_{l_1} l j t_{k_3} n_{l_2} l j t_{k_1} n_{l_3} l j t_{k_2} n_{l_4} l j t_{k_4}}^{J'} \\
 & \times \tilde{V}_{n_{l_2} n_{k_1}}^{(\pi j t)_{k_1}} \tilde{V}_{n_{l_1} n_{k_2}}^{(\pi j t)_{k_2}} \tilde{U}_{n_{l_3} n_{k_3}}^{(\pi j t)_{k_3}} \tilde{U}_{n_{l_4} n_{k_4}}^{(\pi j t)_{k_4}} \delta_{JJ''} \delta_{M-M''}, \tag{E.86}
 \end{aligned}$$

$$\begin{aligned}
 {}^6 \tilde{O}_{k_1 k_2 J M; k_3 k_4 J'' M''}^{[04]} & = (-1)^{j_{k_1}+j_{k_2}+J''-M+M''} \sum_{\substack{m_{k_1} m_{k_2} \\ m_{k_3} m_{k_4}}} \sum_{l_1 l_2 l_3 l_4} o_{l_1 l_2 l_3 l_4} V_{l_2 \bar{k}_1} U_{l_3 \bar{k}_2} U_{l_4 k_3} V_{l_1 k_4} \\
 & \times \begin{pmatrix} j_{k_1} & j_{k_2} & | & J \\ m_{k_1} & m_{k_2} & | & M \end{pmatrix} \begin{pmatrix} j_{k_3} & j_{k_4} & | & J'' \\ m_{k_3} & m_{k_4} & | & -M'' \end{pmatrix} \\
 & = \sum_{\substack{m_{k_1} m_{k_2} \\ m_{k_3} m_{k_4}}} \sum_{n_{l_1} n_{l_2} n_{l_3} n_{l_4}} \sum_{J' M'} \bar{o}_{n_{l_1} l j t_{k_4} n_{l_2} l j t_{k_1} n_{l_3} l j t_{k_2} n_{l_4} l j t_{k_3}}^{J'} \\
 & \times \tilde{V}_{n_{l_2} n_{k_1}}^{(\pi j t)_{k_1}} \tilde{U}_{n_{l_3} n_{k_2}}^{(\pi j t)_{k_2}} \tilde{U}_{n_{l_4} n_{k_3}}^{(\pi j t)_{k_3}} \tilde{V}_{n_{l_1} n_{k_4}}^{(\pi j t)_{k_4}} (-1)^{j_{k_2}+j_{k_4}+M+M'+M''+J''} \\
 & \times \begin{pmatrix} j_{k_1} & j_{k_2} & | & J \\ m_{k_1} & m_{k_2} & | & M \end{pmatrix} \begin{pmatrix} j_{k_3} & j_{k_4} & | & J'' \\ m_{k_3} & m_{k_4} & | & -M'' \end{pmatrix} \begin{pmatrix} j_{k_4} & j_{k_1} & | & J' \\ -m_{k_4} & m_{k_1} & | & M' \end{pmatrix} \begin{pmatrix} j_{k_2} & j_{k_3} & | & J' \\ -m_{k_2} & m_{k_3} & | & M \end{pmatrix} \\
 & = (-1)^{j_{k_1}+j_{k_2}+j_{k_3}+j_{k_4}+J+M+1} \sum_{n_{l_1} n_{l_2} n_{l_3} n_{l_4}} \sum_{J'} \bar{o}_{n_{l_1} l j t_{k_4} n_{l_2} l j t_{k_1} n_{l_3} l j t_{k_2} n_{l_4} l j t_{k_3}}^{J'} \\
 & \times \tilde{V}_{n_{l_2} n_{k_1}}^{(\pi j t)_{k_1}} \tilde{U}_{n_{l_3} n_{k_2}}^{(\pi j t)_{k_2}} \tilde{V}_{n_{l_1} n_{k_3}}^{(\pi j t)_{k_3}} \tilde{U}_{n_{l_4} n_{k_4}}^{(\pi j t)_{k_4}} \hat{J}' \begin{Bmatrix} j_{k_1} & j_{k_2} & J \\ j_{k_3} & j_{k_4} & J' \end{Bmatrix} \delta_{JJ''} \delta_{M-M''}. \tag{E.87}
 \end{aligned}$$

Therefore, we finally arrive at

$$O_{k_1 k_2 J M; k_3 k_4 J'' M''}^{[04]} \equiv (-1)^M \delta_{JJ''} \delta_{M-M''} {}^J \tilde{O}_{\bar{k}_1 \bar{k}_2 \bar{k}_3 \bar{k}_4}^{[04]}, \tag{E.88}$$

leading to the spherical form of the operator

$$\begin{aligned}
 \tilde{O}^{[04]} & = \frac{1}{24} \sum_{\bar{k}_1 \bar{k}_2 \bar{k}_3 \bar{k}_4} \sum_{JJ'MM'} {}^J \tilde{O}_{\bar{k}_1 \bar{k}_2 \bar{k}_3 \bar{k}_4}^{[04]} (-1)^M [\bar{\mathcal{B}}_{j_{k_1}} \bar{\mathcal{B}}_{j_{k_2}}]_{JM} [\bar{\mathcal{B}}_{j_{k_3}} \bar{\mathcal{B}}_{j_{k_4}}]_{J-M} \\
 & = \frac{1}{24} \sum_{\bar{k}_1 \bar{k}_2 \bar{k}_3 \bar{k}_4} \sum_J {}^J \tilde{O}_{\bar{k}_1 \bar{k}_2 \bar{k}_3 \bar{k}_4}^{[04]} [\bar{\mathcal{B}}_{j_{k_1}} \bar{\mathcal{B}}_{j_{k_2}}]_J \cdot [\bar{\mathcal{B}}_{j_{k_3}} \bar{\mathcal{B}}_{j_{k_4}}]_J. \tag{E.89}
 \end{aligned}$$

By diagonality in J and M we can write

$${}^J \tilde{O}_{\bar{k}_1 \bar{k}_2; \bar{k}_3 \bar{k}_4}^{[04]} \equiv \sum_{\substack{m_{k_1} m_{k_2} \\ m_{k_3} m_{k_4}}} (-1)^{j_{k_1}+j_{k_2}+J} \times \tilde{O}_{k_1 k_2 k_3 k_4}^{[04]} \begin{pmatrix} j_{k_1} & j_{k_2} & | & J \\ m_{k_1} & m_{k_2} & | & M \end{pmatrix} \begin{pmatrix} j_{k_3} & j_{k_4} & | & J \\ m_{k_3} & m_{k_4} & | & M \end{pmatrix} \tag{E.90}$$

as well as the converse transformation

$$\tilde{O}_{k_1 k_2 k_3 k_4}^{[04]} \equiv \sum_{JM} (-1)^{j_{k_1} + j_{k_2} + J} \times {}^J \tilde{O}_{\tilde{k}_1 \tilde{k}_2 \tilde{k}_3 \tilde{k}_4}^{[04]} \begin{pmatrix} j_{k_1} & j_{k_2} & J \\ m_{k_1} & m_{k_2} & M \end{pmatrix} \begin{pmatrix} j_{k_3} & j_{k_4} & J \\ m_{k_3} & m_{k_4} & M \end{pmatrix}. \quad (\text{E.91})$$

COMPILATION OF RESULTS

For the derivation of low-order BMBPT formulas we will make extensive use of angular-momentum coupling of cross-coupled matrix elements. Therefore, we gather all relevant expressions necessary for deriving the angular-momentum coupled counterparts of their m -scheme expressions.

Transformation of Matrix Elements in Quasiparticle Space

$$\tilde{O}_{k_1 k_2 k_3 k_4}^{[04]} = \sum_{JM} (-1)^{j_{k_1} + j_{k_2} + J + M} \times {}^J \tilde{O}_{\tilde{k}_1 \tilde{k}_2 \tilde{k}_3 \tilde{k}_4}^{[04]} \begin{pmatrix} j_{k_1} & j_{k_2} & J \\ m_{k_1} & m_{k_2} & M \end{pmatrix} \begin{pmatrix} j_{k_3} & j_{k_4} & J \\ m_{k_3} & m_{k_4} & M \end{pmatrix} \quad (\text{E.92})$$

$$\tilde{O}_{k_1 k_2 k_3 k_4}^{[13]} = \sum_{JM} (-1)^{j_{k_2} + m_{k_2} + J + 1} \times {}^J \tilde{O}_{\tilde{k}_1 \tilde{k}_2 \tilde{k}_3 \tilde{k}_4}^{[04]} \begin{pmatrix} j_{k_1} & j_{k_2} & J \\ m_{k_1} & m_{k_2} & M \end{pmatrix} \begin{pmatrix} j_{k_3} & j_{k_4} & J \\ m_{k_3} & m_{k_4} & -M \end{pmatrix} \quad (\text{E.93})$$

$$\tilde{O}_{k_1 k_2 k_3 k_4}^{[22]} = \sum_{JM} {}^J \tilde{O}_{\tilde{k}_1 \tilde{k}_2 \tilde{k}_3 \tilde{k}_4}^{[22]} \begin{pmatrix} j_{k_1} & j_{k_2} & J \\ m_{k_1} & m_{k_2} & M \end{pmatrix} \begin{pmatrix} j_{k_3} & j_{k_4} & J' \\ m_{k_3} & m_{k_4} & M' \end{pmatrix} \quad (\text{E.94})$$

$$\tilde{O}_{k_1 k_2 k_3 k_4}^{[31]} = \sum_{JM} (-1)^{j_{k_4} - m_{k_4} + M} \times {}^J \tilde{O}_{\tilde{k}_1 \tilde{k}_2 \tilde{k}_3 \tilde{k}_4}^{[31]} \begin{pmatrix} j_{k_1} & j_{k_2} & J \\ m_{k_1} & m_{k_2} & M \end{pmatrix} \begin{pmatrix} j_{k_3} & j_{k_4} & J \\ -m_{k_3} & -m_{k_4} & -M \end{pmatrix} \quad (\text{E.95})$$

$$\tilde{O}_{k_1 k_2 k_3 k_4}^{[40]} = \sum_{JM} (-1)^{j_{k_3} + j_{k_4} + J + M} \times {}^J \tilde{O}_{\tilde{k}_1 \tilde{k}_2 \tilde{k}_3 \tilde{k}_4}^{[40]} \begin{pmatrix} j_{k_1} & j_{k_2} & J \\ m_{k_1} & m_{k_2} & M \end{pmatrix} \begin{pmatrix} j_{k_3} & j_{k_4} & J \\ m_{k_3} & m_{k_4} & M \end{pmatrix} \quad (\text{E.96})$$

E.4 PARTICLE-NUMBER OPERATOR

Of particular importance in BMPT is the derivation of particle-number corrections. The reduced matrix element of the cross-coupled particle number operator in quasiparticle space is given by

$$\begin{aligned} \tilde{A}_{k_1 k_2}^{[20]} &= \sum_{l_1 l_2} U_{k_1 l_1}^\dagger V_{l_1 \bar{k}_2} - V_{k_1 l_1}^\dagger U_{l_1 \bar{k}_2}^* \\ &= \sum_{l_1} U_{l_1 k_1} V_{l_1 \bar{k}_2} - V_{l_1 k_1} U_{l_1 \bar{k}_2} \\ &= \sum_{n_{l_1}} \left((-1)^{j_{l_1} - m_{l_1}} \tilde{\delta}_{l_1 k_1} \tilde{U}_{n_{l_1} n_{k_1}}^{(\pi j t)_{k_1}} \tilde{\delta}_{l_1 k_2} \tilde{V}_{n_{l_1} n_{k_2}}^{(\pi j t)_{k_2}} \delta_{m_{k_1} m_{k_2}} \right. \\ &\quad \left. - (-1)^{j_{l_1} - m_{l_1}} \tilde{\delta}_{l_1 k_1} \tilde{V}_{n_{l_1} n_{k_1}}^{(\pi j t)_{k_1}} \tilde{\delta}_{l_1 k_2} \tilde{U}_{n_{l_1} n_{k_2}}^{(\pi j t)_{k_2}} \delta_{m_{k_1} m_{k_2}} \right) \end{aligned}$$

$$= (-1)^{j_{k_1} - m_{k_1}} \tilde{\delta}_{k_1 k_2} \delta_{m_{k_1} m_{k_2}} \sum_{n_{l_1}} \left(\tilde{U}_{n_{l_1} n_{k_1}}^{(\pi j t)_{k_1}} \tilde{V}_{n_{l_1} n_{k_2}}^{(\pi j t)_{k_2}} + \tilde{V}_{n_{l_1} n_{k_1}}^{(\pi j t)_{k_1}} \tilde{U}_{n_{l_1} n_{k_2}}^{(\pi j t)_{k_2}} \right), \quad (\text{E.97})$$

which is diagonal with respect to all quantum numbers other than n .

E.5 PARTICLE-NUMBER VARIANCE OPERATOR

As already seen, the anti-symmetrized matrix elements of the two-body part of the particle-number variance operator in single-particle space are given by

$$\bar{a}_{pqrs}^{(2)} = 2(\delta_{pr}\delta_{qs} - \delta_{ps}\delta_{qr}). \quad (\text{E.98})$$

We define

$$\begin{aligned} \bar{a}_{\tilde{p}\tilde{q}JM;\tilde{r}\tilde{s}J''M''}^{(2)} &\equiv \sum_{m_p m_q m_r m_s} \bar{a}_{pqrs}^{(2)} \begin{pmatrix} j_p & j_q & J \\ m_p & m_q & M \end{pmatrix} \begin{pmatrix} j_r & j_s & J'' \\ m_r & m_s & M'' \end{pmatrix} \\ &= 2 \sum_{m_p m_q} \left\{ \begin{pmatrix} j_p & j_q & J \\ m_p & m_q & M \end{pmatrix} \begin{pmatrix} j_p & j_q & J'' \\ m_p & m_q & M'' \end{pmatrix} - \begin{pmatrix} j_p & j_q & J \\ m_p & m_q & M \end{pmatrix} \begin{pmatrix} j_q & j_p & J'' \\ m_q & m_p & M'' \end{pmatrix} \right\} \\ &= 2 \sum_{m_p m_q} \left\{ \delta_{pr}\delta_{qs} \begin{pmatrix} j_p & j_q & J \\ m_p & m_q & M \end{pmatrix} \begin{pmatrix} j_p & j_q & J'' \\ m_p & m_q & M'' \end{pmatrix} \right. \\ &\quad \left. - (-1)^{j_p+j_q-J} \delta_{ps}\delta_{qr} \begin{pmatrix} j_p & j_q & J \\ m_p & m_q & M \end{pmatrix} \begin{pmatrix} j_p & j_q & J'' \\ m_p & m_q & M'' \end{pmatrix} \right\} \\ &= \delta_{JJ''} \delta_{MM''} 2 \left(\delta_{\tilde{p}\tilde{r}} \delta_{\tilde{q}\tilde{s}} - (-1)^{j_p+j_q-J} \delta_{\tilde{p}\tilde{s}} \delta_{\tilde{q}\tilde{r}} \right), \quad (\text{E.99}) \end{aligned}$$

and, therefore, for the J -coupled matrix element we get

$$J \bar{a}_{\tilde{p}\tilde{q}\tilde{r}\tilde{s}}^{(2)} \equiv 2 \left(\delta_{\tilde{p}\tilde{r}} \delta_{\tilde{q}\tilde{s}} - (-1)^{j_p+j_q-J} \delta_{\tilde{p}\tilde{s}} \delta_{\tilde{q}\tilde{r}} \right). \quad (\text{E.100})$$

The J -coupled matrix elements from (E.100) are then used as input for the angular-momentum coupled form in quasiparticle space.

E.6 SECOND-ORDER CORRECTIONS FOR OPERATORS

The angular-momentum coupled form of the second-order BMBPT correction of an arbitrary (scalar) two-body operator \hat{O} is given by

$$\begin{aligned} PO1.2 &= -\frac{1}{24} \sum_{k_1 k_2 k_3 k_4} \frac{O_{k_1 k_2 k_3 k_4}^{04} O_{k_1 k_2 k_3 k_4}^{40}}{E_{k_1} + E_{k_2} + E_{k_3} + E_{k_4}} \\ &= -\frac{1}{24} \sum_{k_1 k_2 k_3 k_4} \frac{O_{k_1 k_2 k_3 k_4}^{04} O_{k_3 k_4 k_1 k_2}^{40}}{E_{k_1} + E_{k_2} + E_{k_3} + E_{k_4}} \end{aligned}$$

$$\begin{aligned}
 &= -\frac{1}{24} \sum_{k_1 k_2 k_3 k_4} \frac{\tilde{\Omega}_{\bar{k}_1 \bar{k}_2 k_3 k_4}^{04} \tilde{O}_{k_3 k_4 \bar{k}_1 \bar{k}_2}^{40}}{E_{k_1} + E_{k_2} + E_{k_3} + E_{k_4}} \\
 &= -\frac{1}{24} \sum_{k_1 k_2 k_3 k_4} \frac{\tilde{\Omega}_{k_1 k_2 k_3 k_4}^{04} \tilde{O}_{k_3 k_4 k_1 k_2}^{40}}{E_{k_1} + E_{k_2} + E_{k_3} + E_{k_4}} \\
 &= -\frac{1}{24} \sum_{k_1 k_2 k_3 k_4} \sum_{\substack{JJ' \\ MM'}} \begin{pmatrix} j_{k_1} & j_{k_2} \\ m_{k_1} & m_{k_2} \end{pmatrix} \begin{pmatrix} J \\ M \end{pmatrix} \begin{pmatrix} j_{k_3} & j_{k_4} \\ m_{k_3} & m_{k_4} \end{pmatrix} \begin{pmatrix} J \\ M \end{pmatrix} \begin{pmatrix} j_{k_1} & j_{k_2} \\ m_{k_1} & m_{k_2} \end{pmatrix} \begin{pmatrix} J' \\ M' \end{pmatrix} \begin{pmatrix} j_{k_3} & j_{k_4} \\ m_{k_3} & m_{k_4} \end{pmatrix} \begin{pmatrix} J' \\ M' \end{pmatrix} \\
 &\quad \times (-1)^{2j_{k_1} + 2j_{k_2} + J + J'} \frac{J \tilde{\Omega}_{\bar{k}_1 \bar{k}_2 \bar{k}_3 \bar{k}_4}^{04} J' \tilde{O}_{\bar{k}_3 \bar{k}_4 \bar{k}_1 \bar{k}_2}^{40}}{E_{k_1} + E_{k_2} + E_{k_3} + E_{k_4}} \\
 &= -\frac{1}{24} \sum_{\bar{k}_1 \bar{k}_2 \bar{k}_3 \bar{k}_4} \sum_J \hat{j}^2 \frac{J \tilde{\Omega}_{\bar{k}_1 \bar{k}_2 \bar{k}_3 \bar{k}_4}^{04} J \tilde{O}_{\bar{k}_3 \bar{k}_4 \bar{k}_1 \bar{k}_2}^{40}}{E_{\bar{k}_1} + E_{\bar{k}_2} + E_{\bar{k}_3} + E_{\bar{k}_4}}, \tag{E.101}
 \end{aligned}$$

where we have used the definition of cross-coupled matrix elements as well as orthogonality relations of the Clebsch-Gordan coefficients. The energy correction is obtained as the particular case where $\hat{O} = \hat{O}$. Note that when using a spherical HFB reference the quasiparticle energies are independent of m_k , i.e., $E_k = E_{\bar{k}}$.

E.7 THIRD-ORDER PARTICLE-NUMBER CORRECTION

The third-order particle-number correction in cross-coupled scheme is given by

$$\begin{aligned}
 PA2.1 &= \frac{1}{6} \sum_{k_1 k_2 k_3 k_4 k_5} \frac{A_{k_1 k_2}^{[20]} \Omega_{k_3 k_4 k_5 k_1}^{[31]} \Omega_{k_3 k_4 k_5 k_2}^{[04]}}{(E_{k_1} + E_{k_2})(E_{k_2} + E_{k_3} + E_{k_4} + E_{k_5})} \\
 &= \frac{1}{6} \sum_{k_1 k_2 k_3 k_4 k_5} \frac{\tilde{A}_{k_1 \bar{k}_2}^{[20]} \tilde{\Omega}_{k_3 k_4 \bar{k}_5 k_1}^{[31]} \tilde{\Omega}_{\bar{k}_5 \bar{k}_2 k_3 k_4}^{[04]}}{(E_{k_1} + E_{k_2})(E_{k_2} + E_{k_3} + E_{k_4} + E_{k_5})} \\
 &= \frac{1}{6} \sum_{k_1 k_2 k_3 k_4 k_5} \frac{\tilde{A}_{k_1 k_2}^{[20]} \tilde{\Omega}_{k_3 k_4 k_5 k_1}^{[31]} \tilde{\Omega}_{k_5 k_2 k_3 k_4}^{[04]}}{(E_{k_1} + E_{k_2})(E_{k_2} + E_{k_3} + E_{k_4} + E_{k_5})} \\
 &= \frac{1}{6} \sum_{k_1 k_2 k_3 k_4 k_5} \sum_{\substack{JJ' \\ MM'}} \begin{pmatrix} j_{k_3} & j_{k_4} \\ m_{k_3} & m_{k_4} \end{pmatrix} \begin{pmatrix} J \\ M \end{pmatrix} \begin{pmatrix} j_{k_5} & j_{k_1} \\ -m_{k_5} & -m_{k_1} \end{pmatrix} \begin{pmatrix} J \\ -M \end{pmatrix} \begin{pmatrix} j_{k_5} & j_{k_1} \\ m_{k_5} & m_{k_1} \end{pmatrix} \begin{pmatrix} J' \\ M' \end{pmatrix} \begin{pmatrix} j_{k_3} & j_{k_4} \\ m_{k_3} & m_{k_4} \end{pmatrix} \begin{pmatrix} J' \\ M' \end{pmatrix} \\
 &\quad \times (-1)^{j_{k_1} - m_{k_1}} (-1)^{j_{k_5} + j_{k_2} + J'} (-1)^{j_{k_1} - m_{k_1}} \frac{A_{n_{k_1} n_{k_2}}^{[20] (\pi j t)_{k_2} J} \tilde{\Omega}_{k_3 k_4 k_5 k_1}^{[31]} J' \tilde{\Omega}_{k_3 k_4 k_5 k_2}^{[04]}}{(E_{k_1} + E_{k_2})(E_{k_2} + E_{k_3} + E_{k_4} + E_{k_5})} \\
 &= \frac{1}{6} \sum_{\bar{k}_1 \bar{k}_2 \bar{k}_3 \bar{k}_4 \bar{k}_5} \sum_J \hat{j}^2 \frac{A_{n_{k_1} n_{k_2}}^{[20] (\pi j t)_{k_2} J} \tilde{\Omega}_{k_3 k_4 k_5 k_1}^{[31]} J \tilde{\Omega}_{k_3 k_4 k_5 k_2}^{[04]}}{(E_{k_1} + E_{k_2})(E_{k_2} + E_{k_3} + E_{k_4} + E_{k_5})}. \tag{E.102}
 \end{aligned}$$

For a more efficient evaluation we define an auxiliary quantity

$$B_{k_1 k_2 k_3 k_4} \equiv \sum_u \frac{\tilde{A}_{uk_1}^{[20]}}{(E_u + E_{k_1})} \tilde{\Omega}_{k_3 k_4 k_2 u}^{[31]} \quad (\text{E.103})$$

and we, additionally, define the anti-symmetrized matrix element by

$$\bar{B}_{k_1 k_2 k_3 k_4} \equiv \frac{1}{2} \sum_u \left(\frac{\tilde{A}_{uk_1}^{[20]}}{(E_u + E_{k_1})} \tilde{\Omega}_{k_3 k_4 k_2 u}^{[31]} - \frac{\tilde{A}_{uk_2}^{[20]}}{(E_u + E_{k_2})} \tilde{\Omega}_{k_3 k_4 k_1 u}^{[31]} \right) \quad (\text{E.104})$$

such that

$$\bar{B}_{k_1 k_2 k_3 k_4} = -\bar{B}_{k_2 k_1 k_3 k_4} = -\bar{B}_{k_1 k_2 k_4 k_3} = \bar{B}_{k_2 k_1 k_4 k_3}. \quad (\text{E.105})$$

We further define auxiliary matrix elements

$$C_{uk_1} \equiv \frac{\tilde{A}_{uk_1}^{[20]}}{(E_u + E_{k_1})}. \quad (\text{E.106})$$

The m -scheme particle-number correction can now be written as

$$PA2.1 = \frac{1}{6} \sum_{k_1 k_2 k_3 k_4} \bar{B}_{k_1 k_2 k_3 k_4} \frac{\tilde{\Omega}_{k_1 k_2 k_3 k_4}^{[04]}}{(E_{k_1} + E_{k_2} + E_{k_3} + E_{k_4})}. \quad (\text{E.107})$$

We define the angular-momentum-coupled quantity by

$$\begin{aligned} B_{\tilde{k}_1 \tilde{k}_2 J M; \tilde{k}_3 \tilde{k}_4 J'' M''} &\equiv \sum_{\substack{m_{k_1} m_{k_2} \\ m_{k_3} m_{k_4}}} \bar{B}_{k_1 k_2 k_3 k_4} \begin{pmatrix} j_{k_1} & j_{k_2} & J \\ m_{k_1} & m_{k_2} & M \end{pmatrix} \begin{pmatrix} j_{k_3} & j_{k_4} & J'' \\ m_{k_3} & m_{k_4} & M'' \end{pmatrix} \\ &= \sum_{\substack{m_{k_1} m_{k_2} \\ m_{k_3} m_{k_4}}} \sum_{J' M'} \sum_u \begin{pmatrix} j_{k_1} & j_{k_2} & J \\ m_{k_1} & m_{k_2} & M \end{pmatrix} \begin{pmatrix} j_{k_3} & j_{k_4} & J'' \\ m_{k_3} & m_{k_4} & M'' \end{pmatrix} (-1)^M \\ &\quad \times \left(C_{uk_1}^{[20] J'} \Omega_{\tilde{k}_3 \tilde{k}_4 \tilde{k}_2 \tilde{u}}^{[31]} \begin{pmatrix} j_{k_3} & j_{k_4} & J' \\ m_{k_3} & m_{k_4} & M' \end{pmatrix} \begin{pmatrix} j_{k_2} & j_u & J' \\ -m_{k_2} & -m_u & -M' \end{pmatrix} (-1)^{j_{k_1} - m_{k_1}} \right. \\ &\quad \left. - C_{uk_2}^{[20] J'} \Omega_{\tilde{k}_3 \tilde{k}_4 \tilde{k}_1 \tilde{u}}^{[31]} \begin{pmatrix} j_{k_3} & j_{k_4} & J' \\ m_{k_3} & m_{k_4} & M' \end{pmatrix} \begin{pmatrix} j_{k_1} & j_u & J' \\ -m_{k_1} & -m_u & -M' \end{pmatrix} (-1)^{j_{k_2} - m_{k_2}} \right) \\ &= \sum_{m_{k_1} m_{k_2}} \sum_u \begin{pmatrix} j_{k_1} & j_{k_2} & J \\ m_{k_1} & m_{k_2} & M \end{pmatrix} (-1)^M \\ &\quad \times \left(C_{uk_1}^{[20] J'} \Omega_{\tilde{k}_3 \tilde{k}_4 \tilde{k}_2 \tilde{u}}^{[31]} \begin{pmatrix} j_{k_2} & j_u & J'' \\ -m_{k_2} & -m_u & -M'' \end{pmatrix} (-1)^{j_{k_1} - m_{k_1}} \right. \\ &\quad \left. - C_{uk_2}^{[20] J'} \Omega_{\tilde{k}_3 \tilde{k}_4 \tilde{k}_1 \tilde{u}}^{[31]} \begin{pmatrix} j_{k_1} & j_u & J'' \\ -m_{k_1} & -m_u & -M'' \end{pmatrix} (-1)^{j_{k_2} - m_{k_2}} \right) \end{aligned}$$

$$\begin{aligned}
 &= \sum_{m_{k_1} m_{k_2}} \sum_{n_u} \left(\begin{array}{cc|c} j_{k_1} & j_{k_2} & J \\ m_{k_1} & m_{k_2} & M \end{array} \right) (-1)^M \\
 &\times \left(\mathcal{C}_{\tilde{u}\tilde{k}_1}^{(ljt)[20]J'} \Omega_{\tilde{k}_3\tilde{k}_4\tilde{k}_2\tilde{u}}^{[31]} \left(\begin{array}{cc|c} j_{k_2} & j_{k_1} & J'' \\ -m_{k_2} & -m_{k_1} & -M'' \end{array} \right) (-1)^{j_{k_1}+j_u-m_{k_1}-m_u} \right. \\
 &\quad \left. - \mathcal{C}_{\tilde{u}\tilde{k}_2}^{(ljt)[20]J'} \Omega_{\tilde{k}_3\tilde{k}_4\tilde{k}_1\tilde{u}}^{[31]} \left(\begin{array}{cc|c} j_{k_1} & j_{k_2} & J'' \\ -m_{k_1} & -m_{k_2} & -M'' \end{array} \right) (-1)^{j_{k_2}+j_u-m_{k_2}-m_u} \right) \\
 &= (-1)^M \sum_{n_u} \left((-1)^{j_{k_1}-j_{k_2}+J} \mathcal{C}_{\tilde{u}\tilde{k}_1}^{(ljt)[20]J} \Omega_{\tilde{k}_3\tilde{k}_4\tilde{k}_2\tilde{u}}^{[31]} - \mathcal{C}_{\tilde{u}\tilde{k}_2}^{(ljt)[20]J} \Omega_{\tilde{k}_3\tilde{k}_4\tilde{k}_1\tilde{u}}^{[31]} \right) \delta_{JJ''} \delta_{MM''}
 \end{aligned} \tag{E.108}$$

such that we can write

$$PA2.1 = \frac{1}{6} \sum_{\tilde{k}_1\tilde{k}_2\tilde{k}_3\tilde{k}_4} \sum_J \hat{J}^2 \times {}^J \bar{B}_{\tilde{k}_1\tilde{k}_2\tilde{k}_3\tilde{k}_4} \frac{{}^J \tilde{\Omega}_{\tilde{k}_1\tilde{k}_2\tilde{k}_3\tilde{k}_4}^{[04]}}{(E_{\tilde{k}_1} + E_{\tilde{k}_2} + E_{\tilde{k}_3} + E_{\tilde{k}_4})}. \tag{E.109}$$

List of Acronyms

ASG	Anti-symmetrized Goldstone (diagram)
BCC	Bogoliubov Coupled Cluster
BCH	Baker-Campbell-Hausdorff
BMBPT	Bogoliubov Many-Body Perturbation Theory
BMZ	Bloch-Messiah-Zumino (theorem)
CC	Coupled-Cluster method
CG	Clebsch-Gordan (coefficient)
CI	Configuration Interaction
EDF	Energy Density Functional
EFT	Effective Field Theory
EN	Epstein-Nesbet (partitioning)
EOM	Equation of Motion
GFMC	Green's Function Monte Carlo
HF	Hartree-Fock
HF-MBPT	Hartree-Fock Many-Body Perturbation Theory
HFB	Hartree-Fock-Bogoliubov
HO	Harmonic Oscillator
IM-SRG	In-Medium Similarity Renormalization Group
IRREP	Irreducible Representation of a symmetry group
IT-NCSM	Importance-Truncated No-Core Shell Model
LEC	Low-Energy Constant
MBPT	Many-Body Perturbation Theory

MCPT	Multi-Configurational Perturbation Theory
MP	Møller-Plesset (partitioning)
NCSM	No-Core Shell Model
NCSM-PT	No-Core Shell Model Perturbation Theory
NO2B	Normal-Ordered Two-Body Approximation
ODE	Ordinary Differential Equation
PNR	Particle-Number Restoration
PT	Perturbation Theory
SCGF	Self-Consistent Green's Function
SD	Slater Determinant
SRG	Similarity Renormalization Group
UCOM	Unitary Correlation Operator Method

Bibliography

- [Agr06] B. K. Agrawal. “Exploring the extended density-dependent Skyrme effective forces for normal and isospin-rich nuclei to neutron stars”. In: *Physical Review C* 73.3 (2006). DOI: [10.1103/PhysRevC.73.034319](https://doi.org/10.1103/PhysRevC.73.034319) (cit. on p. 172).
- [ALP03] F. Andreozzi, N. Lo Iudice, and A. Porrino. “An importance sampling algorithm for generating exact eigenstates of the nuclear Hamiltonian”. In: *J. Phys. G: Nucl. Part. Phys.* 10 (2003), p. 2319. URL: <http://stacks.iop.org/0954-3899/29/2319> (cit. on p. 87).
- [BB69] R. Balian and E. Brezin. “Nonunitary bogoliubov transformations and extension of Wick’s theorem”. In: *Il Nuovo Cimento B* 64.1 (1969), pp. 37–55 (cit. on pp. 11, 145).
- [BDL09] M. Bender, T. Duguet, and D. Lacroix. “Particle-number restoration within the energy density functional formalism”. In: *Physical Review C* 79.4 (2009), p. 044319. DOI: [10.1103/PhysRevC.79.044319](https://doi.org/10.1103/PhysRevC.79.044319) (cit. on pp. 171, 172).
- [Ben08] M. Bender. “Configuration mixing of angular-momentum and particle-number projected triaxial Hartree-Fock-Bogoliubov states using the Skyrme energy density functional”. In: *Physical Review C* 78.2 (2008). DOI: [10.1103/PhysRevC.78.024309](https://doi.org/10.1103/PhysRevC.78.024309) (cit. on p. 171).
- [BFP07] S. K. Bogner, R. J. Furnstahl, and R. J. Perry. “Similarity renormalization group for nucleon-nucleon interactions”. In: *Physical Review C* 75 (2007), 061001(R) (cit. on pp. vii, 19, 21).
- [Bin⁺13] S. Binder, P. Piecuch, A. Calci, et al. “Extension of coupled-cluster theory with a noniterative treatment of connected triply excited clusters to three-body Hamiltonians”. In: *Physical Review C* 88.5 (2013), pp. 054319– (cit. on p. 185).
- [Bin⁺14] S. Binder, J. Langhammer, A. Calci, et al. “Ab Initio Path to Heavy Nuclei”. In: *Physics Letters B* 736 (2014), pp. 119–123 (cit. on pp. viii, 61).
- [Bin10] S. Binder. “Angular Momentum Projection and Three-Body Forces in the No-Core Shell Model”. MA thesis. TU Darmstadt, 2010 (cit. on p. 83).
- [Bin14] S. Binder. “Coupled-Cluster Theory for Nuclear Structure”. PhD thesis. TU Darmstadt, 2014 (cit. on pp. viii, 22, 61, 185).
- [BM07] R. J. Bartlett and M. Musial. “Coupled-cluster theory in quantum chemistry”. In: *Reviews of Modern Physics* 79.1 (2007), pp. 291–352 (cit. on pp. viii, 61).

- [BNV13] B. R. Barrett, P. Navrátil, and J. P. Vary. “Ab initio no core shell model”. In: *Progress in Particle and Nuclear Physics* 69 (2013), pp. 131–181. DOI: [10.1016/j.pnpnp.2012.10.003](https://doi.org/10.1016/j.pnpnp.2012.10.003) (cit. on pp. vii, 83, 87).
- [Bog⁺08] S. K. Bogner, R. J. Furnstahl, P. Maris, et al. “Convergence in the no-core shell model with low-momentum two-nucleon interactions”. In: *Nucl. Phys. A* 801 (2008), p. 21 (cit. on p. 83).
- [Bog⁺14] S. K. Bogner, H. Hergert, J. D. Holt, et al. “Nonperturbative Shell-Model Interactions from the In-Medium Similarity Renormalization Group”. In: *Physical Review Letters* 113.14 (2014), p. 142501. DOI: [10.1103/PhysRevLett.113.142501](https://doi.org/10.1103/PhysRevLett.113.142501) (cit. on p. ix).
- [Bru55] K. A. Brueckner. “Many-Body Problem for Strongly Interacting Particles. II. Linked Cluster Expansion”. In: *Physical Review* 100.1 (1955), pp. 36–45. DOI: [10.1103/PhysRev.100.36](https://doi.org/10.1103/PhysRev.100.36) (cit. on p. 49).
- [Cal14] A. Calci. “Evolved Chiral Hamiltonians at the Three-Body Level and Beyond”. PhD thesis. Technische Universität Darmstadt, 2014 (cit. on p. 23).
- [CBN13] A. Cipollone, C. Barbieri, and P. Navrátil. “Isotopic Chains Around Oxygen from Evolved Chiral Two- and Three-Nucleon Interactions”. In: *Physical Review Letters* 111.6 (2013), pp. 062501– (cit. on pp. viii, 118).
- [Cha⁺16] S. Chattopadhyay, R. K. Chaudhuri, U. S. Mahapatra, et al. “State-specific multireference perturbation theory: development and present status”. In: *Computational Molecular Science* 6.266–291 (2016) (cit. on p. 49).
- [Číž66] J. Čížek. “On the Correlation Problem in Atomic and Molecular Systems. Calculation of Wavefunction Components in Ursell-Type Expansion Using Quantum-Field Theoretical Methods”. In: *The Journal of Chemical Physics* 45.11 (1966), pp. 4256–4266 (cit. on pp. 61, 85).
- [CK60] F. Coester and H. Kümmel. “Short-range correlations in nuclear wave functions”. In: *Nuclear Physics* 17 (1960), pp. 477–485 (cit. on pp. 61, 85).
- [Coe58] F. Coester. “Bound states of a many-particle system”. In: *Nuclear Physics* 7 (1958), pp. 421–424 (cit. on p. 85).
- [Con30] E. U. Condon. “The Theory of Complex Spectra”. In: *Physical Review* 36.7 (1930), pp. 1121–1133. DOI: [10.1103/PhysRev.36.1121](https://doi.org/10.1103/PhysRev.36.1121) (cit. on p. 45).
- [ČP69] J. Čížek and J. Paldus. “On the Use of the Cluster Expansion and the Technique of Diagrams in Calculations of Correlation Effects in Atoms and Molecules”. In: *Advances in Chemical Physics: Correlation Effects in Atoms and Molecules* 14 (1969) (cit. on pp. 61, 85).

-
- [DB04] W. Dickhoff and C. Barbieri. “Self-consistent Green’s function method for nuclei and nuclear matter”. In: *Progress in Particle and Nuclear Physics* 52.2 (2004), pp. 377–496. ISSN: 0146-6410. DOI: [10.1016/j.ppnp.2004.02.038](https://doi.org/10.1016/j.ppnp.2004.02.038) (cit. on p. viii).
- [DD94] W. Duch and G. H. F. Diercksen. “Size-extensivity corrections in configuration interaction methods”. In: *The Journal of Chemical Physics* 101.4 (1994), pp. 3018–3030. DOI: [10.1063/1.467615](https://doi.org/10.1063/1.467615) (cit. on p. 85).
- [DH04] D. J. Dean and M. Hjorth-Jensen. “Coupled-cluster approach to nuclear physics”. In: *Physical Review C* 69 (2004), p. 054320 (cit. on pp. viii, 61).
- [DHS16] C. Drischler, K. Hebeler, and A. Schwenk. “Asymmetric nuclear matter based on chiral two- and three-nucleon interactions”. In: *Physical Review C* 93.5 (2016). DOI: [10.1103/PhysRevC.93.054314](https://doi.org/10.1103/PhysRevC.93.054314) (cit. on p. 77).
- [Dob⁺07] J. Dobaczewski, M. V. Stoitsov, W. Nazarewicz, et al. “Particle-number projection and the density functional theory”. In: *Physical Review C* 76.5 (2007), p. 054315 (cit. on p. 171).
- [Dör15] B. Dörig. “Ladder Summations in Many-Body Perturbation Theory”. Bsc. Thesis. TU Darmstadt, 2015 (cit. on p. 78).
- [DS16] T. Duguet and A. Signoracci. “Symmetry broken and restored coupled-cluster theory: II. Global gauge symmetry and particle number”. In: *Journal of Physics G: Nuclear and Particle Physics* 44.1 (2016) (cit. on pp. xi, 65, 131, 139, 188, 189).
- [Dug⁺15] T. Duguet, M. Bender, J.-P. Ebran, et al. “Ab initio-driven nuclear energy density functional method”. In: *The European Physical Journal A* 51.12 (2015), p. 162. ISSN: 1434-601X. DOI: [10.1140/epja/i2015-15162-4](https://doi.org/10.1140/epja/i2015-15162-4) (cit. on pp. 165, 173).
- [Dug14] T. Duguet. “The Nuclear Energy Density Functional Formalism”. In: *The Euroschool on Exotic Beams, Vol. IV*. Ed. by C. Scheidenberger and M. Pfützner. Berlin, Heidelberg: Springer Berlin Heidelberg, 2014, pp. 293–350. ISBN: 978-3-642-45141-6. DOI: [10.1007/978-3-642-45141-6_7](https://doi.org/10.1007/978-3-642-45141-6_7) (cit. on pp. xi, 165).
- [Dug15] T. Duguet. “Symmetry broken and restored coupled-cluster theory: I. Rotational symmetry and angular momentum”. In: *Journal of Physics G: Nuclear and Particle Physics* G42.2 (2015), p. 025107. DOI: [10.1088/0954-3899/42/2/025107](https://doi.org/10.1088/0954-3899/42/2/025107) (cit. on pp. 65, 139).
- [EHM09] E. Epelbaum, H.-W. Hammer, and U.-G. Meißner. “Modern theory of nuclear forces”. In: *Reviews of Modern Physics* 81 (2009), p. 1773. DOI: [10.1103/RevModPhys.81.1773](https://doi.org/10.1103/RevModPhys.81.1773) (cit. on p. vii).
-

- [Eks⁺13] A. Ekström, G. Baardsen, C. Forssén, et al. “Optimized Chiral Nucleon-Nucleon Interaction at Next-to-Next-to-Leading Order”. In: *Physical Review Letters* 110.19 (2013), p. 192502 (cit. on p. 17).
- [EM03] D. R. Entem and R. Machleidt. “Accurate charge-dependent nucleon-nucleon potential at fourth order of chiral perturbation theory”. In: *Physical Review C* 68 (2003), 041001(R) (cit. on pp. vii, 17).
- [Epe⁺02] E. Epelbaum, A. Nogga, W. Glöckle, et al. “Three-nucleon forces from chiral effective field theory”. In: *Physical Review C* 66.6 (2002), pp. 064001–. URL: <http://link.aps.org/doi/10.1103/PhysRevC.66.064001> (cit. on p. 17).
- [Epe06] E. Epelbaum. “Four-nucleon force in chiral effective field theory”. In: *Physics Letters B* 639.5 (2006), pp. 456–461. ISSN: 0370-2693. DOI: [10.1016/j.physletb.2006.06.046](https://doi.org/10.1016/j.physletb.2006.06.046) (cit. on p. 17).
- [Epe09] E. Epelbaum. “Nuclear forces from chiral effective field theory: a primer”. In: *Lectures given at the 2009 Joliot-Curie School, Lacanau, France, 27 September - 3 October* (2009) (cit. on p. 17).
- [Fel⁺98] H. Feldmeier, T. Neff, R. Roth, et al. “A Unitary Correlation Operator Method”. In: *Nuclear Physics A* 632 (1998), p. 61 (cit. on p. 21).
- [GCR16] E. Gebrerufael, A. Calci, and R. Roth. “Open-shell nuclei and excited states from multireference normal-ordered Hamiltonians”. In: *Physical Review C* 93.3 (2016) (cit. on pp. 14, 118).
- [Geb⁺16] E. Gebrerufael, K. Vobig, H. Hergert, et al. “Ab Initio Description of Open-Shell Nuclei: Merging No-Core Shell Model and In-Medium Similarity Renormalization Group”. In: *arXiv:1610.05254* (2016). eprint: [1610.05254](https://arxiv.org/abs/1610.05254) (cit. on p. 81).
- [Geb13] E. Gebrerufael. “Multi-Reference Normal Ordering for 3N Interactions”. MA thesis. TU Darmstadt, 2013 (cit. on p. 14).
- [Geo99] H. Georgie. *Lie Algebras in Particle Physics*. Perseus Books Group, 1999 (cit. on p. 165).
- [Gol57] J. Goldstone. “Derivation of the Brueckner many-body theory”. In: *Proceedings of the Royal Society of London A* 239 (1957), pp. 267–279 (cit. on p. 49).
- [GS17] J. Golak and R. Skibiński, eds. *Workshop on Chiral Forces in Low Energy Nuclear Physics - the LENPIC Meeting*. 2017 (cit. on p. 17).
- [Hag⁺09] G. Hagen, T. Papenbrock, D. J. Dean, et al. “Ab initio computation of neutron-rich oxygen isotopes”. In: *Phys. Rev. C* 80 (2009), p. 021306. DOI: [10.1103/PhysRevC.80.021306](https://doi.org/10.1103/PhysRevC.80.021306) (cit. on p. 118).

-
- [Hag⁺10] G. Hagen, T. Papenbrock, D. J. Dean, et al. “Ab initio coupled-cluster approach to nuclear structure with modern nucleon-nucleon interactions”. In: *Physical Review C* 82 (2010), p. 034330. DOI: [10.1103/PhysRevC.82.034330](https://doi.org/10.1103/PhysRevC.82.034330) (cit. on pp. viii, 61).
- [Hag⁺12] G. Hagen, M. Hjorth-Jensen, G. R. Jansen, et al. “Continuum Effects and Three-Nucleon Forces in Neutron-Rich Oxygen Isotopes”. In: *Physical Review Letters* 108.24 (2012), pp. 242501– (cit. on pp. 16, 118).
- [Heb⁺10] K. Hebeler, J. M. Lattimer, C. J. Pethick, et al. “Constraints on Neutron Star Radii Based on Chiral Effective Field Theory Interactions”. In: *Phys. Rev. Lett.* 105.16 (2010), p. 161102 (cit. on p. 77).
- [Heb12] K. Hebeler. “Momentum-space evolution of chiral three-nucleon forces”. In: *Physical Review C* 85.2 (2012), pp. 021002– (cit. on p. 17).
- [Hen⁺14] T. M. Henderson, J. Dukelsky, G. E. Scuseria, et al. “Quasiparticle Coupled Cluster Theory for Pairing Interactions”. In: *Phys. Rev.* C89.5 (2014), p. 054305. DOI: [10.1103/PhysRevC.89.054305](https://doi.org/10.1103/PhysRevC.89.054305) (cit. on pp. 132, 139).
- [Her⁺13] H. Hergert, S. K. Bogner, S. Binder, et al. “In-medium similarity renormalization group with chiral two- plus three-nucleon interactions”. In: *Physical Review C* 87.3 (2013), p. 034307 (cit. on pp. viii, 118).
- [Her⁺16] H. Hergert, S. K. Bogner, T. D. Morris, et al. “The In-Medium Similarity Renormalization Group: A Novel Ab Initio Method for Nuclei”. In: *Physics Reports* 621 (2016), pp. 165–222. DOI: [10.1016/j.physrep.2015.12.007](https://doi.org/10.1016/j.physrep.2015.12.007) (cit. on pp. viii, 81).
- [Her08] H. Hergert. “An Ab-Initio Approach to Pairing Phenomena Using Modern Effective Interactions”. PhD thesis. Darmstadt: Technische Universität, 2008. URL: <http://tuprints.ulb.tu-darmstadt.de/959/> (cit. on pp. 133, 212).
- [Her14] H. Hergert. “Ab Initio Multi-Reference In-Medium Similarity Renormalization Group Calculations of Even Calcium and Nickel Isotopes”. In: *Physical Review C* 90.041302 (2014) (cit. on pp. viii, x, 175).
- [Hir03] S. Hirata. “Tensor Contraction Engine: Abstraction and Automated Parallel Implementation of Configuration-Interaction, Coupled-Cluster, and Many-Body Perturbation Theories”. In: *The Journal of Physical Chemistry A* 107.46 (2003), pp. 9887–9897. DOI: [10.1021/jp034596z](https://doi.org/10.1021/jp034596z) (cit. on p. 114).
- [Hol⁺12] J. D. Holt, T. Otsuka, A. Schwenk, et al. “Three-body forces and shell structure in calcium isotopes”. In: *Journal of Physics G: Nuclear and Particle Physics* 39.8 (2012) (cit. on pp. 16, 48).
-

- [HR07] H. Hergert and R. Roth. “The Unitary Correlation Operator Method from a Similarity Renormalization Group Perspective”. In: *Physical Review C* 75 (2007), 051001(R) (cit. on pp. vii, 19, 21).
- [HR09a] H. Hergert and R. Roth. “Pairing in the framework of the unitary correlation operator method (UCOM): Hartree-Fock-Bogoliubov calculations”. In: *Phys. Rev. C* 80 (2009), p. 024312. DOI: [10.1103/PhysRevC.80.024312](https://doi.org/10.1103/PhysRevC.80.024312) (cit. on p. 133).
- [HR09b] H. Hergert and R. Roth. “Treatment of the intrinsic Hamiltonian in particle-number nonconserving theories”. In: *Physics Letters B* 682.1 (2009), pp. 27–32. ISSN: 0370-2693. DOI: [10.1016/j.physletb.2009.10.100](https://doi.org/10.1016/j.physletb.2009.10.100) (cit. on p. 138).
- [HS10] K. Hebeler and A. Schwenk. “Chiral three-nucleon forces and neutron matter”. In: *Phys. Rev. C* 82 (2010), p. 014314. DOI: [10.1103/PhysRevC.82.014314](https://doi.org/10.1103/PhysRevC.82.014314) (cit. on p. 17).
- [Hum72] J. E. Humphreys. *Introduction to Lie Algebras and Representation Theory*. Springer, 1972 (cit. on p. 165).
- [HW10] I. Hubac and S. Wilson. *Brillouin-Wigner Methods for Many-Body Systems*. Dordrecht: Springer Netherlands, 2010, pp. 133–189. URL: http://dx.doi.org/10.1007/978-90-481-3373-4_4 (cit. on p. 48).
- [HW53] D. L. Hill and J. A. Wheeler. “The Method of Generator Coordinates”. In: *Phys. Rev* 89 (1953), p. 1103 (cit. on p. 171).
- [Jan⁺14] G. R. Jansen, J. Engel, G. Hagen, et al. “Ab Initio Coupled-Cluster Effective Interactions for the Shell Model: Application to Neutron-Rich Oxygen and Carbon Isotopes”. In: *Physical Review Letters* 113.14 (2014), p. 142502. DOI: [10.1103/PhysRevLett.113.142502](https://doi.org/10.1103/PhysRevLett.113.142502) (cit. on pp. ix, 65).
- [JNF09] E. D. Jurgenson, P. Navrátil, and R. J. Furnstahl. “Evolution of Nuclear Many-Body Forces with the Similarity Renormalization Group”. In: *Physical Review Letters* 103 (2009), p. 082501. DOI: [10.1103/PhysRevLett.103.082501](https://doi.org/10.1103/PhysRevLett.103.082501) (cit. on p. 21).
- [JS91] C. L. Janssen and H. F. Schaefer. “The automated solution of second quantization equations with applications to the coupled cluster approach”. In: *Theoretica chimica acta* 79.1 (1991), pp. 1–42. ISSN: 1432-2234. DOI: [10.1007/BF01113327](https://doi.org/10.1007/BF01113327) (cit. on p. 114).
- [Jur⁺13] E. D. Jurgenson, P. Maris, R. J. Furnstahl, et al. “Structure of p-shell nuclei using three-nucleon interactions evolved with the similarity renormalization group”. In: *Physical Review C* 87.5 (2013), p. 054312 (cit. on p. 19).
- [Kac08] V. G. Kac. *Infinite Dimensional Lie Algebras*. Cambridge University Press, 2008 (cit. on p. 165).

-
- [Kal76] U. Kaldor. “An algorithm for generating Goldstone and Bloch-Brandow diagrams”. In: *Journal of Computational Physics* 20.4 (1976), pp. 432–441. ISSN: 0021-9991. DOI: [10.1016/0021-9991\(76\)90092-9](https://doi.org/10.1016/0021-9991(76)90092-9) (cit. on p. 105).
- [KM97] W. Kutzelnigg and D. Mukherjee. “Normal order and extended Wick theorem for a multiconfiguration reference wave function”. In: *Journal of Chemical Physics* 107 (1997), p. 432. DOI: [10.1063/1.474405](https://doi.org/10.1063/1.474405) (cit. on pp. 12, 14, 65).
- [Kow⁺04] K. Kowalski, D. J. Dean, M. Hjorth-Jensen, et al. “Coupled Cluster Calculations of Ground and Excited States of Nuclei”. In: *Physical Review Letters* 92.13 (2004), p. 132501 (cit. on pp. viii, 61).
- [Krü⁺13] T. Krüger, I. Tews, K. Hebeler, et al. “Neutron matter from chiral effective field theory interactions”. In: *Phys. Rev. C* 88.2 (2013), p. 025801 (cit. on p. 77).
- [LD74] S. R. Langhoff and E. R. Davidson. “Configuration interaction calculations on the nitrogen molecule”. In: *International Journal of Quantum Chemistry* 8.1 (1974), pp. 61–72. ISSN: 1097-461X. DOI: [10.1002/qua.560080106](https://doi.org/10.1002/qua.560080106) (cit. on p. 85).
- [LDB09] D. Lacroix, T. Duguet, and M. Bender. “Configuration mixing within the energy density functional formalism: Removing spurious contributions from nondiagonal energy kernels”. In: *Physical Review C* 79.4 (2009), p. 044318. DOI: [10.1103/PhysRevC.79.044318](https://doi.org/10.1103/PhysRevC.79.044318) (cit. on p. 171).
- [LG12] D. Lacroix and D. Gambacurta. “Projected quasiparticle perturbation theory”. In: *Phys. Rev. C* 86 (2012), p. 014306 (cit. on p. 139).
- [LIA05] D. I. Lyakh, V. V. Ivanov, and L. Adamowicz. “Automated generation of coupled-cluster diagrams: Implementation in the multireference state-specific coupled-cluster approach with the complete-active-space reference”. In: *The Journal of Chemical Physics* 122.2 (2005), p. 024108 (cit. on p. 114).
- [LRS12] J. Langhammer, R. Roth, and C. Stumpf. “Spectra of open-shell nuclei with Padé-resummed degenerate perturbation theory”. In: *Physical Review C* 86.5 (2012), p. 054315 (cit. on p. 69).
- [Mac89] R. Machleidt. “The Meson Theory of Nuclear Forces and Nuclear Structure”. In: *Adv. Nucl. Phys.* 19 (1989), p. 189 (cit. on p. 16).
- [Mah⁺98] U. S. Mahapatra, B. Datta, B. Bandyopadhyay, et al. “State-Specific Multi-Reference Coupled Cluster Formulations: Two Paradigms”. In: *Advances in Quantum Chemistry* 30 (1998), pp. 163–193. ISSN: 0065-3276. DOI: [10.1016/S0065-3276\(08\)60507-9](https://doi.org/10.1016/S0065-3276(08)60507-9) (cit. on p. 65).
- [ME11] R. Machleidt and D. R. Entem. “Chiral effective field theory and nuclear forces”. In: *Physics Reports* 503 (2011), p. 1. DOI: [10.1016/j.physrep.2011.02.001](https://doi.org/10.1016/j.physrep.2011.02.001) (cit. on p. 17).
-

- [MPB15] T. D. Morris, N. Parzuchowski, and S. K. Bogner. “Magnus expansion and in-medium similarity renormalization group”. In: *Physical Review C* 92.3 (2015), p. 034331. DOI: [10.1103/PhysRevC.92.034331](https://doi.org/10.1103/PhysRevC.92.034331) (cit. on p. viii).
- [Nak93] H. Nakano. “Quasidegenerate perturbation theory with multiconfigurational self-consistent-field reference functions”. In: *The Journal of Chemical Physics* 99.10 (1993), pp. 7983–7992 (cit. on p. 49).
- [Nav⁺09] P. Navrátil, S. Quaglioni, I. Stetcu, et al. “Recent developments in no-core shell-model calculations”. In: *Journal of Physics G: Nuclear and Particle Physics* 36 (2009), p. 083101. DOI: [10.1088/0954-3899/36/8/083101](https://doi.org/10.1088/0954-3899/36/8/083101) (cit. on p. vii).
- [Nav07] P. Navrátil. “Local three-nucleon interaction from chiral effective field theory”. In: *Few Body Systems* 41 (2007), pp. 117–140. DOI: [10.1007/s00601-007-0193-3](https://doi.org/10.1007/s00601-007-0193-3) (cit. on p. 17).
- [NF04] T. Neff and H. Feldmeier. “Cluster Structures within Fermionic Molecular Dynamics”. In: *Nucl. Phys.* A738 (2004), p. 357 (cit. on p. 21).
- [NVB00] P. Navrátil, J. P. Vary, and B. R. Barrett. “Large-basis ab initio no-core shell model and its application to ^{12}C ”. In: *Physical Review C* 62 (2000), p. 054311 (cit. on p. 83).
- [Ots⁺10] T. Otsuka, T. Suzuki, J. D. Holt, et al. “Three-Body Forces and the Limit of Oxygen Isotopes”. In: *Physical Review Letters* 105 (2010), p. 032501. DOI: [10.1103/PhysRevLett.105.032501](https://doi.org/10.1103/PhysRevLett.105.032501) (cit. on p. 118).
- [PG90] W. N. Polyzou and W. Glöckle. “Three-body interactions and on-shell equivalent two-body interactions”. In: *Few-Body Systems* 9.2 (1990), pp. 97–121. ISSN: 1432-5411. DOI: [10.1007/BF01091701](https://doi.org/10.1007/BF01091701) (cit. on p. 16).
- [PGW09] P. Piecuch, J. R. Gour, and M. Wloch. “Left-eigenstate completely renormalized equation-of-motion coupled-cluster methods: Review of key concepts, extension to excited states of open-shell systems, and comparison with electron-attached and ionized approaches”. In: *International Journal of Quantum Chemistry* 109.14 (2009), pp. 3268–3304. DOI: [10.1002/qua.22367](https://doi.org/10.1002/qua.22367) (cit. on pp. viii, ix, 61, 65).
- [PMB16] N. M. Parzuchowski, T. D. Morris, and S. K. Bogner. “Ab Initio Excited States from the In-Medium Similarity Renormalization Group”. In: *arXiv:1611.00661* (2016). eprint: [1611.00661](https://arxiv.org/abs/1611.00661) (cit. on p. ix).
- [Pud⁺97] B. S. Pudliner, V. R. Pandharipande, J. Carlson, et al. “Quantum Monte Carlo calculations of nuclei with $A < 7$ ”. In: *Physical Review C* 56 (1997), p. 1720 (cit. on p. viii).
- [PW01] S. C. Pieper and R. B. Wiringa. “Quantum Monte Carlo Calculations of Light Nuclei”. In: *Ann. Rev. Nucl. Part. Sci.* 51 (2001), p. 53 (cit. on p. viii).

-
- [PW73] J. Paldus and H. Wong. “Computer generation of Feynman diagrams for perturbation theory I. General algorithm”. In: *Computer Physics Communications* 6.1 (1973), pp. 1–7. ISSN: 0010-4655. DOI: [10.1016/0010-4655\(73\)90016-7](https://doi.org/10.1016/0010-4655(73)90016-7) (cit. on p. 105).
- [Rei68] R. V. Reid Jr. “Local phenomenological nucleon-nucleon potentials”. In: *Annals of Physics* 50 (1968), pp. 411–448. DOI: [10.1016/0003-4916\(68\)90126-7](https://doi.org/10.1016/0003-4916(68)90126-7) (cit. on p. 16).
- [RL10] R. Roth and J. Langhammer. “Padé-resummed high-order perturbation theory for nuclear structure calculations”. In: *Physics Letters B* 683.272 (2010) (cit. on p. 69).
- [RN07] R. Roth and P. Navrátil. “Ab Initio Study of ^{40}Ca with an Importance-Truncated No-Core Shell Model”. In: *Physical Review Letters* 99 (2007), p. 092501 (cit. on pp. 83, 87).
- [Rod10] T. R. Rodríguez. “Triaxial angular momentum projection and configuration mixing calculations with the Gogny force”. In: *Physical Review C* 81.6 (2010). DOI: [10.1103/PhysRevC.81.064323](https://doi.org/10.1103/PhysRevC.81.064323) (cit. on p. 171).
- [Rot⁺11] R. Roth, J. Langhammer, A. Calci, et al. “Similarity-Transformed Chiral NN+3N Interactions for the Ab Initio Description of 12-C and 16-O”. In: *Physical Review Letters* 107 (2011), p. 072501. DOI: [10.1103/PhysRevLett.107.072501](https://doi.org/10.1103/PhysRevLett.107.072501) (cit. on pp. vii, 16, 19).
- [Rot08] R. Roth. “Importance truncation in ab-initio configuration interaction approaches”. in preparation. 2008 (cit. on pp. 85, 87, 88).
- [Rot09] R. Roth. “Importance Truncation for Large-Scale Configuration Interaction Approaches”. In: *Physical Review C* 79 (2009), p. 064324. DOI: [10.1103/PhysRevC.79.064324](https://doi.org/10.1103/PhysRevC.79.064324) (cit. on pp. 87, 88).
- [RRH08] R. Roth, S. Reinhardt, and H. Hergert. “Unitary correlation operator method and similarity renormalization group: Connections and differences”. In: *Physical Review C* 77 (2008), p. 064003 (cit. on pp. vii, 19, 21).
- [RS80] P. Ring and P. Schuck. *The Nuclear Many-Body Problem*. Springer Verlag, New York, 1980 (cit. on pp. 133, 136).
- [RSS03] Z. Rolik, A. Szabados, and P. R. Surján. “On the perturbation of multi-configuration wave functions”. In: *Journal of Chemical Physics* 119.1922 (2003) (cit. on pp. x, 81, 89).
- [SB09] I. Shavitt and R. J. Bartlett. *Many-body methods in chemistry and physics*. Cambridge University Press, 2009 (cit. on pp. viii, 8, 9, 11, 35, 45, 52, 57, 61, 85).
-

- [Sch13] S. Schulz. “SRG-Induced Four-Body Forces in Ab Initio Nuclear Structure”. MA thesis. Technische Universität Darmstadt, 2013 (cit. on p. 23).
- [Sch26] E. Schrödinger. “Quantisierung als Eigenwertproblem”. In: *Annalen der Physik* 385.13 (1926), pp. 437–490 (cit. on pp. viii, 35).
- [SDB11] V. Somà, T. Duguet, and C. Barbieri. “Ab initio self-consistent Gorkov-Green’s function calculations of semimagic nuclei: Formalism at second order with a two-nucleon interaction”. In: *Physical Review C* 84.6 (2011), p. 064317 (cit. on pp. 131, 139).
- [SHD14] A. Signoracci, G. Hagen, and T. Duguet. “Bogoliubov coupled cluster theory”. Unpublished. 2014 (cit. on p. 215).
- [Sig⁺15] A. Signoracci, T. Duguet, G. Hagen, et al. “Ab initio Bogoliubov coupled cluster theory for open-shell nuclei”. In: *Physical Review C* 91.6 (2015), p. 064320. DOI: [10.1103/PhysRevC.91.064320](https://doi.org/10.1103/PhysRevC.91.064320) (cit. on pp. 65, 131, 188, 201).
- [Sla29] J. C. Slater. “The Theory of Complex Spectra”. In: *Physical Review* 34.10 (1929), pp. 1293–1322. DOI: [10.1103/PhysRev.34.1293](https://doi.org/10.1103/PhysRev.34.1293) (cit. on p. 45).
- [SO82] A. Szabo and N. S. Ostlund. *Modern Quantum Chemistry*. Dover Publications Inc., 1982 (cit. on pp. viii, 8, 29, 35).
- [Som⁺14] V. Somà, A. Cipollone, C. Barbieri, et al. “Leading chiral three-nucleon forces along isotope chains in the calcium region”. In: *Physical Review C* 89 (2014), p. 061301 (cit. on pp. 131, 139).
- [SP00] S. Szpigel and R. J. Perry. “The Similarity Renormalization Group”. In: *Quantum Field Theory. A 20th Century Profile*. Ed. by A. N. Mitra. 2000, Hindustan Publishing Co., New Delhi (cit. on p. 19).
- [SSK04] P. R. Surján, A. Szabados, and D. Köhalmi. “Partitioning in multiconfigurational perturbation theory”. In: *Annalen der Physik* 13.223 (2004) (cit. on pp. x, 81, 89).
- [Suh07] J. Suhonen. *From Nucleons to Nucleus*. Theoretical and Mathematical Physics. Berlin, Germany: Springer, 2007. ISBN: 9783540488613, 9783540488590. DOI: [10.1007/978-3-540-48861-3](https://doi.org/10.1007/978-3-540-48861-3) (cit. on pp. 55, 213).
- [TBS11] K. Tsukiyama, S. K. Bogner, and A. Schwenk. “In-Medium Similarity Renormalization Group For Nuclei”. In: *Physical Review Letters* 106 (2011), p. 222502. DOI: [10.1103/PhysRevLett.106.222502](https://doi.org/10.1103/PhysRevLett.106.222502) (cit. on p. viii).
- [TGR17] A. Tichai, E. Gebrerufael, and R. Roth. “Open-Shell Nuclei from No-Core Shell Model with Perturbative Improvement”. (submitted to Physical Review Letters). 2017 (cit. on p. x).

-
- [Tic⁺16] A. Tichai, J. Langhammer, S. Binder, et al. “Hartree-Fock many-body perturbation theory for nuclear ground-states”. In: *Physics Letters B* 756 (2016), pp. 283–288. ISSN: 0370-2693. DOI: [10.1016/j.physletb.2016.03.029](https://doi.org/10.1016/j.physletb.2016.03.029) (cit. on p. 59).
- [Tic14] A. Tichai. “Convergence Behavior of Many-Body Perturbation Series”. MA thesis. TU Darmstadt, 2014 (cit. on p. 70).
- [Vee11] S. Veerasamy”. “Momentum-space Argonne V18 interaction”. In: *Physical Review C* 84.3 (2011). DOI: [10.1103/PhysRevC.84.034003](https://doi.org/10.1103/PhysRevC.84.034003) (cit. on p. 16).
- [VMK88] D. A. Varshalovich, A. N. Moskalev, and V. K. Khersonskii. *Quantum Theory of Angular Momentum*. World Scientific Publishing Company, 1988 (cit. on pp. 7, 196, 213).
- [Wan⁺12] M. Wang, G. Audi, A. H. Wapstra, et al. “The AME 2012 atomic mass evaluation”. In: *Chinese Physics C* 36.12 (2012), p. 1603 (cit. on pp. 74, 76, 117, 176, 178–180).
- [Wei90] S. Weinberg. “Nuclear forces from chiral Lagrangians”. In: *Physics Letters B* 251.2 (1990), pp. 288–292. DOI: [10.1016/0370-2693\(90\)90938-3](https://doi.org/10.1016/0370-2693(90)90938-3) (cit. on p. 17).
- [Wei91] S. Weinberg. “Effective chiral Lagrangians for nucleon-pion interactions and nuclear forces”. In: *Nuclear Physics B* 363.1 (1991), pp. 3–18. DOI: [10.1016/0550-3213\(91\)90231-L](https://doi.org/10.1016/0550-3213(91)90231-L) (cit. on p. 17).
- [Wei92] S. Weinberg. “Three-body interactions among nucleons and pions”. In: *Physics Letters B* 295.1–2 (1992), pp. 114–121. DOI: [10.1016/0370-2693\(92\)90099-P](https://doi.org/10.1016/0370-2693(92)90099-P) (cit. on p. 17).
- [Wic50] G. C. Wick. “The Evaluation of the Collision Matrix”. In: *Physical Review* 80.2 (1950), pp. 268–272. DOI: [10.1103/PhysRev.80.268](https://doi.org/10.1103/PhysRev.80.268) (cit. on p. 9).
- [Wol16] Wolfram Alpha. *ThreeJSymbol*. 2016. URL: <http://functions.wolfram.com/HypergeometricFunctions/ThreeJSymbol/23/01/04/0001/> (cit. on p. 214).
- [WP73] H. Wong and J. Paldus. “Computer generation of Feynman diagrams for perturbation theory II. Program description”. In: *Computer Physics Communications* 6.1 (1973), pp. 9–16. ISSN: 0010-4655. DOI: [10.1016/0010-4655\(73\)90017-9](https://doi.org/10.1016/0010-4655(73)90017-9) (cit. on p. 105).
- [WSA84] R. Wiringa, R. Smith, and T. Ainsworth. “Nucleon-Nucleon Potentials with and without $\Delta(1232)$ Degrees of Freedom”. In: *Phys. Rev. C* 29 (1984), p. 1207 (cit. on p. 16).
-

- [Yao10] J. M. Yao. “Configuration mixing of angular-momentum-projected triaxial relativistic mean-field wave functions”. In: *Physical Review C* 81.4 (2010). DOI: [10.1103/PhysRevC.81.044311](https://doi.org/10.1103/PhysRevC.81.044311) (cit. on p. 171).

Erklärung zur Dissertation

Hiermit versichere ich, die vorliegende Dissertation ohne Hilfe Dritter nur mit den angegebenen Quellen und Hilfsmitteln angefertigt zu haben. Alle Stellen, die aus Quellen entnommen wurden, sind als solche kenntlich gemacht. Diese Arbeit hat in gleicher oder ähnlicher Form noch keiner Prüfungsbehörde vorgelegen. Eine Promotion wurde bisher noch nicht versucht.

Darmstadt, den 18.07.2017

Alexander Tichai

Acknowledgments

First of all I want to thank my supervisor Prof. Robert Roth for giving me the opportunity of working on this very interesting topic and becoming part of the tnp++ group.

Second I thank Prof. Jens Braun for the second advisory of my thesis and being my co-supervisor over the last three years.

I further thank all people of the tnp++ group, in particular Eskendr Gebrerufael, Christina Stumpf, Roland Wirth, Thomas Hüther, Stefan Schulz and Klaus Vobig for all the great discussions and nice atmosphere in the past years.

In particular I thank Roland Wirth for countless times where he helped with IT problems of every kind.

Moreover, I would like to thank Prof. Thomas Duguet and Pierre Arthuis from CEA, Saclay, France, for many fruitful discussions regarding the BMBPT project.

Additionally, I thank Prof. Heiko Hergert from Michigan State University, East Lansing, USA, for valuable support regarding the HFB code and further for his hospitality during my two-month stay in 2016.

I am very grateful for the financial support provided by HGS-HIRe over the last three and a half years. Furthermore, the travel support gave me the opportunity to participate at many interesting conferences and foster international contacts during my studies.

Last I would like to thank my family for their never-ending support, in particular over the last months of writing up this document.

After thanking my partners in physics, I most importantly thank my partner in life, Larissa Heckler, for her patience, tolerance and love that helped me to endure the pain of finding bugs and phase factors.

Lebenslauf

Zur Person

Name	Alexander Tichai
Geburstag	13. Dezember 1987
Geburtsort	Darmstadt
Nationalität	deutsch

Schulischer Bildungsweg

1993 - 1998	Grundschule , Geiersberg-Schule, Groß-Umstadt
1998 - 2006	Gymnasium , Max-Planck-Gymnasium, Groß-Umstadt
2007 - 2011	Bachelorstudium Physik , TU Darmstadt
2010 - 2013	Bachelorstudium Mathematik , TU Darmstadt
2011 - 2014	Masterstudium Physik , TU Darmstadt
2013 - 2016	Masterstudium Mathematik , TU Darmstadt
2014 - 2017	Promotionsstudium Physik , TU Darmstadt